Neural Stem Cell Grafts and the Influence of Apolipoprotein E in a Mouse Model of Global Ischaemia

Andrew M-S Wong B.Sc. (Hons)

Doctor of Philosophy

The University of Edinburgh

2007

Declaration

In accordance with the regulations of the University of Edinburgh I declare that this dissertation in its entirety is not substantially the same as any that the author has previously submitted for a degree or diploma or any other qualification at any other university. The work is solely that of the author, except where and if indicated.

Andrew Ming-Shang Wong

Acknowledgements

This PhD project would not have been possible without the generous funding provided by Research Into Ageing, to whom I am extremely grateful.

I was fortunate to undertake my PhD studies under the supervision of Dr Karen Horsburgh, who provided valuable advice, support and technical input over the course of my PhD. My second supervisor, Professor Helen Hodges, was a constant source of guidance and suggestions and I am thankful to both my supervisors for their role in designing this PhD project.

I would also like to thank all the other members of the lab, Dr Sandra Magnoni, Dr Jill Fowler and Dr Laura Kennedy for their constructive input and assistance.

I was lucky to start my PhD at the same time as three other students, namely Graeme Jordan, Tom Wishart and Emma Perkins (with a special mention to Oliver Voss). Our office in 1.4, 1 George Square was a constantly educational and entertaining location. The other long-term resident of 1.4 was Dr Philip Chen, who was a font of information and counsel for all of us.

Finally, I must thank my parents for all their encouragement and confidence throughout my PhD.

Contents

Chapter 1: Introduction

Chapter 2: Materials and Methods

Chapter 3: Characterisation of neural stem cell grafts in a mouse model of global ischaemia

Chapter 5: Influence of *APOE* genotype on neural stem cell grafts in a mouse model of global ischaemia

Chapter 6: General discussion

List of figures

Chapter 4

Chapter 5

List of tables

Abbreviations

4-HNE	4-Hydroxynonenal
Aβ	Beta-amyloid
AMPA	α-amino-3-hydroxy-5-methyl-4-isoxazoleproprionic acid
APOE	Apolipoprotein E (gene)
ApoE	Apolipoprotein E (protein)
APP	Amyloid precursor protein
BBB	Blood-brain barrier
BCCAo	Bilateral common carotid artery occlusion
BDNF	Brain-derived neurotrophic factor
BrdU	5-bromo-2-deoxyuridine
BSA	Bovine serum albumin
Ca^{2+}	Calcium
CAA	Cerebral amyloid angiopathy
CBF	Cerebral blood flow
Cdk5	Cyclin-dependent kinase 5
CNS	Central nervous system
CREB	cAMP response element binding protein

CsA	Cyclosporin A
CSF	Cerebrospinal fluid
CXCR4	Chemokine (C-X-C motif) receptor 4
DAB	Diaminobenzine
Dab1	Disabled 1 (gene)
DMEM	Dulbecco's modified Eagle's medium
DNA	Deoxyribonucleic acid
ECL	Enhanced chemiluminescence
EGF	Epidermal growth factor
EGTA	Ethylene glycol tetraacetic acid
ERK	Extracellular signal-regulated kinase
ES cell	Embryonic Stem cell
FGF	Fibroblast growth factor
GABA	Gamma-aminobutyric acid
GDNF	Glial cell line-derived neurotrophic factor
GFAP	Glial fibrillary acidic protein
GSK-3B	Glycogen synthase kinase-3β
H & E	Haematoxylin and Eosin
HBSS	Hank's balanced salt solution
HRP	Horseradish peroxidase
IFN-γ	Interferon-γ
IL-1β	Interleukin-1β
IL-2	Interleukin-2
iNOS	Inducible nitric oxide synthase
JNK	c-jun N-terminal kinase
LIF	Leukaemia inhibitory factor
LTP	Long-term potentiation
MAP2	Microtubule associated protein 2
MCAo	Middle cerebral artery occlusion
MHC	Major histocompatibility complex
MK-801	Dizocilpine malonate
MRI	Magnetic resonance imaging

mRNA	Messenger ribonucleic acid
NAC	N-acetyl cysteine
NBQX	6-nitro-7-sulfamoylbenzo(*f*)quinoxaline-2,3-dione
NeuN	Neuronal nuclei
NGF	Nerve growth factor
NMDA	N-methyl-D-aspartate
NSE	Neuron specific enolase
OCT	Optimal cutting temperature embedding medium
PBS	Phosphate buffered saline
PCR	Polymerase chain reaction
PET	Positron emission tomography
PI3K	Phosphatidylinositol-3-kinase
PNS	Peripheral nervous system
PSD-95	Post-synaptic density protein 95
PVDF	Polyvinylidene fluoride
R.O.D.	Relative optical density
RIPA	Radioimmunoprecipitation buffer
SCF	Stem cell factor
SDF-1	Stromal cell-derived factor 1
SDS-PAGE	Sodium-dodecyl-sulphate polyacrylamide gel electropheresis
SGZ	Sub-granular zone
SVZ	Sub-ventricular zone
TBI	Traumatic brain injury
TNF-α	Tumour necrosis factor
WT	Wild-type

Abstract

Neural stem cell (NSC) transplantation is a promising therapy for the treatment of brain damage. Although the "proof of principle" for NSC transplantation therapy has been demonstrated in a variety of animal models of brain injury (stroke, traumatic brain injury, ageing) and in a clinical setting (Parkinson's disease), the mechanisms by which grafted stem cells survive, migrate and differentiate in host brain are yet to be elucidated. Initial studies have demonstrated that, after transplantation of the MHP36 neural stem cell line in a focal ischaemia model, the lipid transport protein apolipoprotein E (apoE) is upregulated and co-localised to differentiated cells in parallel with functional recovery. ApoE has been shown to have a critical role in the response to brain injury and repair processes. Furthermore, in humans, three different forms of apoE exist (E2, E3, E4 encoded by the alleles ε2, ε3, ε4) and each of these has a different ability to promote repair, with the E4 form associated with an impaired capacity. This thesis tests the hypothesis that apoE is critical in stem cell integration and investigates whether this effect is *APOE* genotype dependent, in a mouse model of global cerebral ischaemia. This model was chosen as it produces diffuse selective neuronal damage in the striatum and hippocampus, which also occurs in other conditions such as ageing and Alzheimer's disease. The studies described in this thesis were designed to test the hypothesis and are outlined as follows:

I. Characterisation of neural stem cell grafts in a mouse model of global ischaemia

In order to investigate the potential influence of apoE on stem cell grafts, it was first essential to characterise stem cells grafts in mouse brain. Thus, the initial aim of the thesis was to characterise MHP36 grafts in a mouse model of ischaemic neuronal injury. The effect of cyclosporin A (CsA) immunosuppression was also investigated. C57Bl/6J mice underwent an episode of transient global ischaemia induced by bilateral common carotid artery occlusion. Three days following ischaemia, mice received a unilateral striatal graft of fluorescently labelled MHP36 neural stem cells or vehicle; the mice also received CsA or saline. The mice were terminated at either

1 or 4 weeks post-transplantation. This study determined that MHP36 grafts survived and migrated robustly in host ischaemic brain at both 1 week and 4 weeks post-transplantation. Grafted MHP36 cells differentiated into neurons and were able to reduce the extent of ischaemic neuronal damage. An acute host inflammatory response was evoked following MHP36 grafting, but this decreased dramatically by 4 weeks post-transplantation. CsA immunosuppression did not affect MHP36 survival and migration or reduce the host inflammatory response. The successful transplantation and characterisation of MHP36 grafts in mouse brain allowed for future investigation into the genetic factors underlying stem cell graft integration via the use of apoE transgenic mice.

II. Influence of apoE on neural stem cell grafts in a mouse model of global ischaemia

The aim of this study was to investigate whether endogenous apoE influenced MHP36 survival, migration and differentiation and then to determine potential signalling pathways that may be involved. ApoE deficient mice on a C57Bl/6J background (*APOE*-KO) and control wildtype C57Bl/6J (WT) mice were subjected to an episode of transient global ischaemia, as in Experiment 1. Two weeks following ischaemia, all mice received unilateral striatal and hippocampal grafts of MHP36 cells. All mice received CsA immunosuppression. Mice were terminated 4 weeks post-transplantation. MHP36 survival and migration was significantly increased in WT as compared to *APOE*-KO mice. In addition, neuronal differentiation was significantly increased in WT as compared to *APOE*-KO mice. Increased astrocytic differentiation was observed in the hippocampus, but not striatum of WT as compared to *APOE*-KO mice. Measurement of the levels of signalling proteins associated with cell survival, extracellular signal-regulated kinase (ERKs) and c-Jun amino-terminal kinase (JNKs) and their phosphorylated forms (pERK and pJNK), indicated selective alterations in JNK with no change in ERK in *APOE*-KO as compared to WT mice, suggesting that JNK may underlie the apoE effects in stem cell integration. This study demonstrated that apoE strongly influences the survival, migration and differentiation of grafted MHP36 cells and provides initial evidence for the signalling pathways involved.

III. Influence of *APOE* genotype on neural stem cell grafts in a mouse model of global ischaemia

Following the demonstration that endogenous mouse apoE has a critical role in MHP36 graft survival, migration and differentiation, this study sought to investigate whether these effects are influenced by human *APOE* genotype. Transgenic mice expressing human *APOE*-ε3 or ε4, (on an *APOE*-KO background) and a control group of *APOE*-KO mice underwent transient global ischaemia and two weeks later MHP36 cells were transplanted unilaterally into the striatum and hippocampus. 1 week after grafting the mice were started on a series of tests for motor balance and coordination using the rotarod, and taken for histology 4 weeks post-transplantation. MHP36 graft survival was significantly improved in *APOE*-ε3 mice compared to *APOE*-KO and *APOE*-ε4 mice. However, the migration and differentiation of MHP36 cells and motor performance of grafted mice were similar in all three *APOE* groups, indicating a comparable fate and functional activity within a 4 week survival time. Thus the data indicate that *APOE* genotype may influence cell survival with minimal effect on stem cell migration and differentiation.

The data presented in this thesis demonstrate that endogenous apoE strongly influences MHP36 graft survival, migration and differentiation. Although there was minimal evidence that human *APOE* genotype influences cell migration and differentiation, stem cell survival was markedly improved in a human *APOE*-ε3 allelic environment, which may affect the effectiveness of stem cells in *APOE*-ε4 individuals.

Chapter 1
Introduction

1.1 Regenerative Strategies

1.1.1 The changing perception of CNS regeneration

In the last 20 years there has been a dramatic shift in the perception of central nervous system (CNS) damage and repair. Classically, the CNS was regarded as a non-renewable environment, where growth and plasticity of new neurons and glia ceased at the end of development. As recent as a decade ago, neuroscience textbooks maintained that damage to neurons in adult human brain and spinal cord was irreparable. This prevailing opinion was famously stated by Santiago Ramon y Cajal, "*In adult centres the nerve paths are something fixed, ended, immutable. Everything may die, nothing may be regenerated. It is for the science of the future to change, if possible, this harsh decree."* (Ramon y Cajal, 1928). This historical viewpoint of a fixed and immutable mature CNS led to the acceptance that loss of CNS cells to ageing or brain injury was an inevitable, inexorable outcome. This is in contrast to the haematopoietic system, where self-renewal and repair is a continuous and well-defined process. Therefore, therapies for neurological disorders focused on prevention and restriction of further damage. For example, starting in the mid-1980s, there was a great deal of research into the use of calcium channel antagonists and glutamate receptor antagonists as neuroprotective agents against excitotoxic damage (Simon et al., 1984, Lipton and Rosenberg, 1994). However, whilst these compounds have been successful in animal models of brain injury, they have failed in all clinical trials to date (Ikonomidou and Turski, 2002, Hoyte et al., 2004, Birmingham, 2002). However, the discovery of neural stem cells in the adult and foetal brain has led to subsequent findings that the mature CNS undergoes dynamic remodelling and exhibits regeneration. This was coupled with advances in the understanding of the mechanisms involved in neurological disorders, leading to radical, new therapeutic approaches for treatment of CNS damage in the field of regenerative medicine.

1.1.2 Principles of regenerative medicine

Neurodegenerative disorders comprising diseases such as Alzheimer's, Creutzfeldt-Jakob's, Huntington's, Parkinson's and conditions including global ischaemia, stroke, traumatic brain injury differ in cause of onset, brain regions affected and

subsequent damage. However, they all share a common factor, specifically the loss of neural cells. While neuroprotection strategies have been successful in the laboratory, this has not translated through to the clinic. In the past decade, there has been a switch away from neuroprotection towards strategies aimed at repair and regeneration of the CNS. The goal of regenerative medicine is to restore and replace tissue in order to achieve functional regeneration. In the CNS there are two broad strategies: induction of endogenous neurogenesis *in vivo*, and transplantation of exogenous neural stem cells. To date, the strategy of transplantation has shown greater evidence for repair and induction of functional recovery. Therefore, this thesis will focus on the transplantation of neural stem cells and its therapeutic use in a mouse model of global ischaemia.

1.2 Ischaemic Models to Investigate Regenerative Strategies

1.2.1 Cerebral ischaemia

In order to investigate regeneration, it is necessary to find a model of reproducible degeneration in the CNS. One method of inducing CNS damage is via disruption of brain homeostasis. The brain has a high metabolic requirement, dependent on energy supplied via the aerobic oxidation of glucose. While an average adult brain represents around 2% of the total body weight, it accounts for approximately 20% of the oxygen used by the body (Clark & Sokoloff, 1999). Cerebral blood flow (CBF) is the sole route for delivery of oxygen and glucose to the brain and for the removal of metabolic waste, therefore any interruption to this supply can have significant consequences. The lack of an adequate blood flow to the brain is referred to as cerebral ischaemia. This may be a result of a blood clot, blood vessel constriction or a haemorrhage. Cerebral ischaemia can be subdivided into global and focal ischaemia, depending on the localisation of the loss of CBF. Global ischaemia is characterised by reduction of CBF throughout most or all of the brain, whereas focal ischaemia is characterised by a reduction in CBF to a specific, localised brain region. Cerebral ischaemia instigates a cascade of pathophysiological processes which contribute to ischaemia cell damage (Figure 1.1). The restriction of glucose and oxygen supply in ischaemia impairs the ability of cells to maintain ionic gradients.

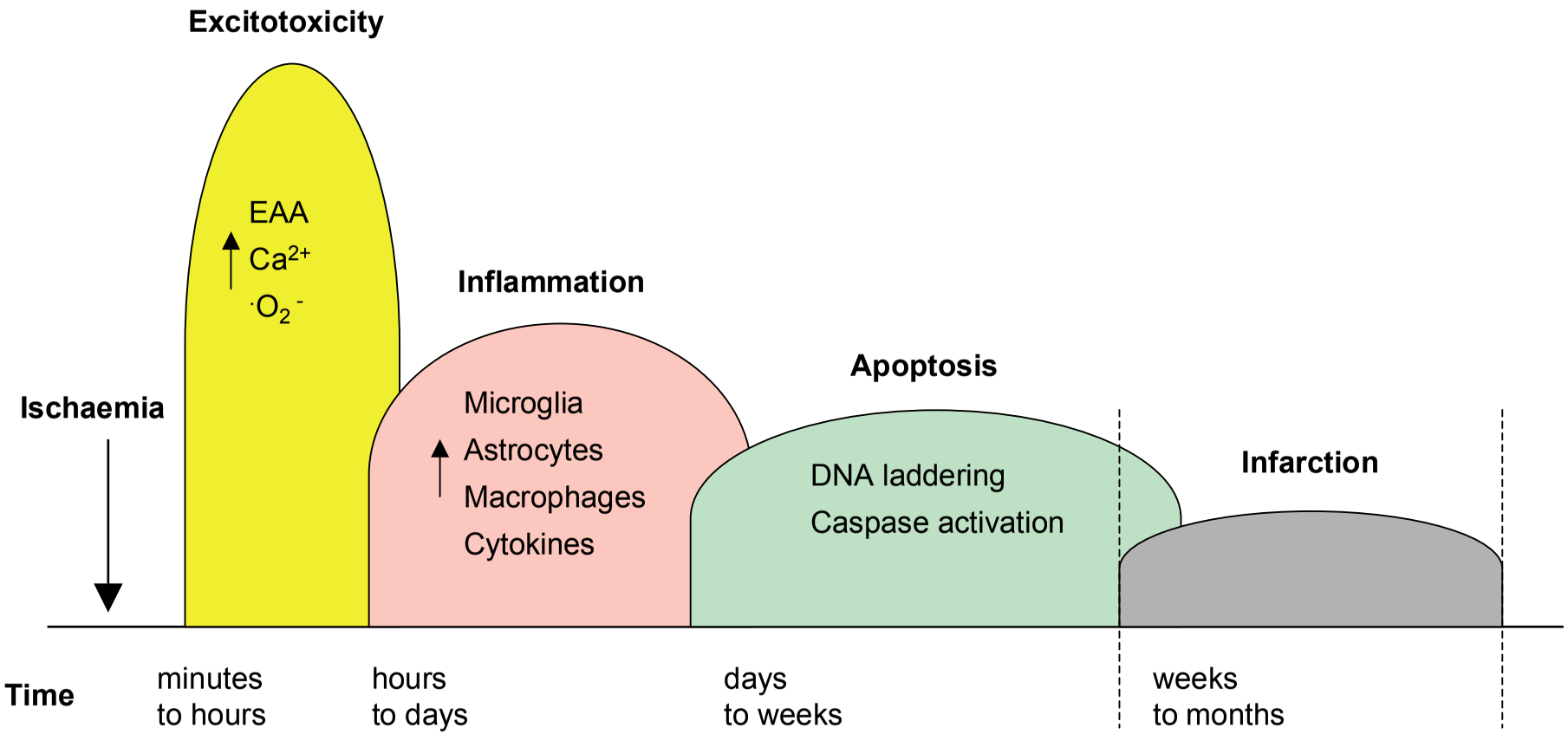

Figure 1.1 Pathophysiological cascade after cerebral ischaemia
Following an ischaemic event, a cascade of pathophysiological processes occur. Rapid membrane depolarisation instigates a sudden excitotoxic period. This is followed by inflammation and apoptosis of damaged neurons. If the damage sustained is extreme, the ischaemic region may eventually undergo infarction.

The loss of membrane potential causes neurons and glia to depolarise and release of massive quantities of excitatory amino acids, in particular glutamate (Martin et al., 1994, Katsura et al., 1994) Coupled with an inhibition of glutamate reuptake mechanisms, there is a net increase of glutamate in the extracellular environment. The free glutamate activates NMDA and metabotropic glutamate receptors and an influx of Ca^{2+} into cells via receptor and voltage gated Ca^{2+} channels. Some stores of intracellular Ca^{2+} are also released into the cytosol. This increase in free Ca^{2+} activates a number of enzymes, such as proteases, endonucleases and nitric oxide synthase, which damage the membrane, nucleus and other organelles (Kristian and Siesjo, 1998). Ca^{2+} mediated activation of phospholipases and cyclooxygenase generates free radical species, which overwhelm endogenous free radical scavenging mechanisms. These free radical species subsequently trigger lipid peroxidation and later effects such as inflammation and apoptosis. This excitotoxic period is followed by a phase of inflammation. There is a migration of neutrophil leukocytes, followed by macrophages and monocytes to the ischaemic tissue (Clark et al., 1995). Astrocytes and microglia are rapidly activated after ischaemia (Petito et al., 1990). Activated astroglia secrete inflammatory cytokines such as interleukin-1β (IL-1β), tumour necrosis factor (TNF-α) and inducible nitric oxide synthase (iNOS) which can all exert neurotoxic effects (Saito et al., 1996, Sairanen et al., 1997, Barone et al., 1997, Endoh et al., 1994). Expression of these cytokines starts a few days after ischaemia and lasts for up to 1 month. Overlapping and extending past this phase of inflammation are apoptotic changes in damaged neurons. The classical markers of apoptosis, DNA laddering (Kihara et al., 1994) and caspase activation (Namura et al., 1998) are upregulated following ischaemia. In the case of a focal ischaemic insult, or a particularly severe episode of global ischaemia, the time course of damage may be extended through formation of an infarct and atrophy of damaged tissue.

1.2.2 Global cerebral ischaemia

Global cerebral ischaemia predominantly occurs as a result of cardiac arrest. The clinical syndrome associated with global ischaemia is termed hypoxic-ischaemic encephalopathy. It is estimated that approximately 220,000 people die from cardiovascular related causes annually in the UK, of which a sizeable proportion

suffer from a cardiac arrest (British Heart Foundation). Other causes of global ischaemia include severe hypotension, cerebral hyperthermia and head trauma. Carbon monoxide poisoning or near drowning can also induce hypoxia, although in these situations there is no impairment of blood flow. The pathological consequences of global ischaemia range from selective neuronal death to infarction (pan-necrosis of all tissue elements) in the case of increased severity or prolonged duration. Global ischaemia can be either transient or permanent, depending on whether the blood flow to the brain is restored. Permanent global ischaemia usually results in death. Transient global ischaemia is associated with characteristic pathology of selective and delayed neuronal damage in vulnerable regions of the brain. In both animals and man, selectively vulnerable regions include the hippocampus, caudate nucleus, cerebral cortex and thalamus (Auer and Sutherland, Greenfield's Neuropathology, 7th Edition).

1.2.3 Pathophysiology of global ischaemia

Depending on the species and model of ischaemia, there is a subsequent hierarchy of vulnerability in selectively vulnerable brain. In gerbils, transient bilateral occlusion of the carotid arteries results in selective death of hippocampal CA1 neurons (Kirino, 1982, Kirino and Sano, 1984), whereas in mouse, using a similar model of ischaemia results in selective damage of the hippocampal CA2 neurons and caudate nucleus (Horsburgh et al., 1999, Gillingwater et al., 2004). Extending the duration of the ischaemic episode furthers the extent of damage. In the rat two-vessel occlusion (2-VO) model, a brief 2 minute episode of ischaemia damages the hippocampus, while a 4 minute episode extends the damage to the neocortex and a longer 10 minute episode causes damage to the caudate nucleus (Smith et al., 1984). The mechanisms which underlie selective vulnerability have yet to be elucidated.

It has been suggested that neuronal vulnerability may occur as a result of increased susceptibility to excitotoxicity due to the presence of differing glutamate receptors on neurons (Rothman and Olney, 1986). For example, vulnerable CA1 hippocampal neurons have an abundance of NMDA receptors in contrast to other subfields of the hippocampus (Greenamyre et al., 1985, Monaghan & Cotman, 1985). However, this

is not conclusive, as demonstrated by granule cells in the dentate gyrus, which are rich in NMDA receptors but do not suffer from the same vulnerability as CA1 neurons. In other vulnerable regions, there is a different neuronal susceptibility to ischaemia. There is selective loss of GABAergic neurons in the caudate nucleus (Francis & Pulsinelli, 1982), and thalamus (Ross & Duhaime, 1989), yet GABAergic interneurons in the hippocampus appear to be resistant to global ischaemia (Johansen et al., 1983). Vascular factors affecting the restoration of CBF may also influence selective vulnerability (Hossmann, 1993, Hossmann, 1997). Increased blood viscosity, oedema, and post-ischaemia hypotension can all disturb the rate of CBF reflow, leading to an increased ischaemic period. A recent study has demonstrated that selectively vulnerable regions exhibit a gradual decrease in the apparent diffusion coefficient of water, suggestive of impaired energy metabolism and oedema (Lythgoe et al., 2005).

The pathology of delayed neuronal damage was first discovered in the hippocampus of gerbils and rats subjected to a brief episode of ischaemia (Kirino et al., 1982, Pulsinelli et al., 1982, Kirino et al., 1984). CA1 neurons were morphologically viable 24 hours following ischaemia, but over the next 72 hours, there was a slow and progressive deterioration of the neurons towards an ischaemic phenotype. In rodent models of global ischaemia, there is a classical maturation of ischaemic damage to a maximal point roughly 72 hours after the initial insult (Pulsinelli, 1985). Human pathological studies have shown that this phenomenon also manifests after an episode of cardiac arrest (Petito et al., 1987, Horn and Scholte, 1992, Collins et al., 1989). Delayed neuronal damage occurs as the result of deleterious secondary processes, although the exact mechanisms responsible are incompletely understood. Possible candidates include neuronal hyperactivity (Suzuki et al., 1983), inhibition of protein synthesis (Thilmann et al., 1986), changes in mitochondrial gene expression (Abe et al., 1995), free radical generation (Siesjo et al., 1989) and continuing excitotoxicity (Siesjo, 1992). Importantly, delayed neuronal death does not occur solely as a result of apoptotic mechanisms. These neurons are not committed to death following the initial ischaemic insult and remain viable for a post-ischaemic "window", during which it may be possible to therapeutically intervene and rescue

these neurons. Therefore, the time course of the pathophysiological cascade has implications for therapeutic strategies (transplantation and neuroprotective approaches). Early intervention has the potential to prevent further damage, although this has to be balanced against the hostile pathophysiological environment. Conversely, stem cell grafts and neuroprotective agents may be able to exert a stronger therapeutic effect at a later time point, but the damage may have progressed beyond the stage where therapeutic intervention would be beneficial.

1.2.4 Animal models of global ischaemia

Models of cerebral ischaemia have been performed in large (cats, dogs, pigs, sheep, primates) and small animals (gerbils, rats, mice). The initial models of cerebral ischaemia were developed in large animals, due to the similarity of their brains to humans. However, there are a number of problematic factors associated with large animals, namely the financial and technical costs associated with these models, and the public animal welfare concerns regarding the use of large animals. Therefore, small animal models are the commonly utilised by researchers. The costs to acquire and maintain small animals are significantly reduced compared to large animals. Small animals can be bred to genetic homogeneity and in the case of mice, it is relatively easy to produce transgenic mice in order to investigate the influence of genetic components on the model.

1.2.4.1 Gerbil model

The gerbil has been commonly used for models of global ischaemia due to their unique vasculature. Gerbils lack a posterior communicating artery, which connects the anterior circulation (carotid system) to the posterior circulation (vertebrobasilar system), resulting in an incomplete circle of Willis (Levine and Sohn,. 1969). Therefore, induction of global ischaemia via bilateral common carotid artery occlusion (BCCAo) in gerbils results in near total interruption of CBF (Crockard et al., 1980), allowing for easily reproducible and reliable induction of global ischaemic damage. A BCCAo time of five minutes causes selective and delayed damage to the CA1 region (Kirino et al., 1982).

1.2.4.2 Rat models

The four vessel occlusion model (4-VO) was developed by Pulsinelli and Brierley (1979). This model is a two-stage procedure commencing with permanent occlusion of the vertebral arteries on the first day followed by occlusion of the bilateral common carotid arteries on the second day. While the 4-VO model has been well validated and utilised since its inception, it typically has a success rate of 50-75%, due to the surgical complexities of a two-stage process. Therefore the simpler two-vessel occlusion model (2-VO) (Eklof and Siesjo, 1972) was investigated by researchers. However, in the rat, occlusion of the bilateral common carotid arteries does not reduce CBF below the ischaemic threshold (Eklof and Siesjo, 1973). In order to produce an ischaemic insult, it is necessary to reduce CBF at the same time as the carotid vessels are occluded. The 2-VO model couples BCCAo with a reduction in CBF via systemic hypotension. Hypotension can be induced via exsanguination, administration of peripheral vasodilators or a combination of the two approaches. Both the 2-VO and 4-VO models produce selective and delayed damage in CA1 pyramidal neurons, caudate nucleus and the neocortex (Smith et al., 1984, Pulsinelli et al., 1982).

1.2.4.3 Mouse models

The BCCAo model of global ischaemia has also been used in mice, although technical aspects of the model result in high mortality and preponderance towards seizures. Part of this disparity is due to the strain of mice and the variability of the circle of Willis development. The C57Bl/6J strain of mice is the most susceptible to BCCAo compared to several other common mouse strains, including ICR, BALB/c, C3H, CBA, ddY, DBA/2, SV-129 and MF1 (Yang et al., 2000, Fujii et al., 1997) which is linked to poor development of the circle of Willis and variations in arterial blood pressure (Kelly et al., 2001). The pattern of ischaemia damage in mouse is also different to that produced in rat and gerbil. In rat and gerbil models, hippocampal neurons in the CA1 region are more vulnerable than the CA2/3 region, the caudate nucleus and the cerebral cortex. In comparison, BCCAo in the mouse preferentially damages the caudate nucleus and the CA2/3 region of the hippocampus (Yang et al., 2000, Gillingwater et al., 2004).

These animal models of global ischaemia have been extensively used for screening of pharmacological neuroprotective agents (Weigl et al., 2005). However, as described previously, the promise of pharmacological intervention has not been translated from the laboratory to the clinic. Unexpected side effects, inconsistent results and diminished efficacy are some of the issues pertaining to clinical trials of neuroprotective drugs. It is therefore of interest to investigate the alternative strategies provided via regenerative medicine. The intrinsic neurogenic capacity of the brain is now accepted as fact. Although this self-reparative capability is modest, it may be possible to utilise and enhance endogenous neurogenesis for repair of ischaemic brain damage.

1.3 Endogenous Neurogenesis for Repair of Ischaemic Brain Damage

1.3.1 Evidence for adult neurogenesis

For over a century, neuroscientific dogma held that that neurogenesis only occurred during embryogenesis, and was not possible in adult mammalian brain. During the late 1950s, the introduction of [^{3}H]-thymidine autoradiography allowed labelling of the DNA of dividing cells. When Altman and colleagues applied this technique to adult rats, they found evidence for new neurons in the neocortex, dentate gyrus (Altman, 1963) and olfactory bulb (Altman, 1969). However, a lack of cell specific markers made it difficult to comprehensively identify the new cells as neurons. Altman's claims for neurogenesis in the adult brain were supported by a series of electron microscopy studies carried out by Kaplan and colleagues (1984). Cells that incorporated [^{3}H]-thymidine had ultrastructural characteristics of neurons as opposed to astrocytes or oligodendrocytes (Kaplan and Bell, 1984, Kaplan, 1985). Kaplan was also able to observe mitosis in the subventricular zone of adult macaque monkeys using the same techniques (Kaplan, 1983).

A series of experiments carried out by Nottebohm and colleagues on the neural basis of song learning in birds led to the discovery of avian neurogenesis. Experiments

with tritiated thymidine showed the production of new cells in the avian brain (Goldman and Nottebohm, 1983) and ultrastructural observation indicated that these new cells were neurons receiving synapses (Burd and Nottebohm, 1985). Finally, these new neurons were able to evoke action potentials in response to sound, demonstrating that they were functionally integrated into the avian brain. (Paton and Nottebohm, 1984) At the time, these studies were viewed as an artefact specialised to the avian brain and had little effect in overturning the belief that adult mammalian brain was incapable of generating new neurons.

Over the last 20 years, an advent of new techniques has provided increasing evidence for adult mammalian neurogenesis. The synthetic thymidine analogue, BrdU (5-bromo-2-deoxyuridine) allows labelling of proliferating cells and their progeny. Unlike [^{3}H]-thymidine autoradiography, detection of BrdU can be carried out using immunocytochemistry. The ability to visualise individual cells containing BrdU allowed stereological estimation of the total number of cells. This was used in conjunction with cell-specific antibody markers for neurons, astrocytes and oligodendrocytes such as NeuN, GFAP and O4 respectively, providing a definitive identification of BrdU incorporating cells along with phenotype, and confirmed the reality of neurogenesis in the adult mammalian brain. Further evidence for neurogenesis in higher mammals came with studies that proved the existence of new neurons in the dentate gyrus of adult primate and human brains. The human studies utilised the fact that BrdU is administered to some cancer patients for clinical diagnosis. Post-mortem examination of hippocampal tissue revealed the presence of many BrdU-incorporating neurons, which had to have been generated following BrdU adminstration and prior to death (Eriksson et al., 1998). Further investigation confirmed previous indications that neurogenesis in the adult mammalian brain occurs in two specific regions, the sub-ventricular zone (SVZ) which lines the lateral ventricles and the sub-granular zone (SGZ) in the dentate gyrus (Figure 1.2). Neurogenesis can be modulated by a variety of factors, genetic (Kempermann et al., 1997), pharmacological (Raballo et al., 2000), physiological (Kuhn et al., 1996, van Praag et al., 1999, Gould et al., 1999) or neuropathological (Parent et al., 1997,

Parent et al., 2002, Gould and Tanapat, 1999). Ischaemic damage has also been shown to influence neurogenesis.

1.3.2 Neurogenesis following global ischaemia

Global ischaemia also stimulates enhanced SGZ neurogenesis in gerbil (Liu et al., 1998,); rat (Kee et al., 2001); mouse (Takagi et al., 1999) and primate brain (Tonchev et al., 2005). These studies suggest that the majority of BrdU positive, newly generated cells post-ischaemia eventually adopt a neuronal phenotype and migrate from the SGZ to the granule cell layer, although there is no direct evidence that the new neurons replace those lost following the ischaemic insult. There is also evidence that global ischaemia is able to potentiate SVZ neurogenesis (Iwai et al., 2003) although this has been more thoroughly demonstrated following focal ischaemia (Jin et al., 2001, Zhang et al., 2001, Arvidsson et al., 2002).

The mechanisms involved in ischaemia induced neurogenesis are still poorly understood. A variety of growth factors, signalling molecules and transcription factors may be involved. Administration of exogenous growth factors (e.g. EGF, FGF, BDNF, SCF) has been shown to modulate the neurogenic response following ischaemia (Larsson et al., 2002, Jin et al., 2002, Teramoto et al., 2003, Matsuoka et al., 2003, Nakatomi et al., 2002). The glutamatergic system is also able to regulate neurogenesis following global ischaemia (Bernabeu and Sharp, 2000). Adminstration of the glutamate receptor antagonists (MK-801 and NBQX) dramatically increased in number of BrdU positive cells in non-ischaemic gerbils. However, injections of these antagonists at the time of ischaemia prevented the ischaemia-mediated increase in neurogenesis but also prevent death of the vulnerable CA1 neurons. Investigation into the mechanisms of ischaemia induced neurogenesis and subsequent migration may also provide further insight into the ability of transplanted stem cells to survive and migrate in damaged brain.

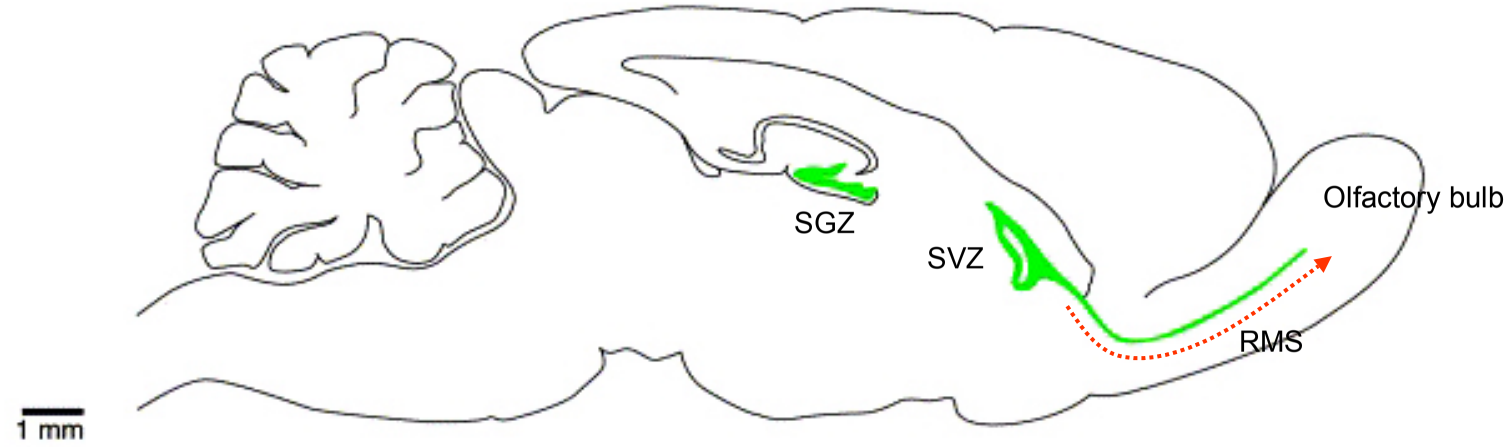

Figure 1.2 Schematic sagittal section of rodent brain illustrating the regions of neurogenesis
There are two regions of neurogenesis in adult mammalian brain, the subgranular zone (SGZ) of the dentate gyrus and the subventricular zone (SVZ). Neural stem cells from the SGZ differentiate into hippocampal neurons. SVZ neurogenesis occurs at a much higher rate than in the SGZ. Neural stem cells from the SVZ follow the rostral migratory stream (RMS) in order to repopulate the olfactory bulb. Adapted from Peterson, 2002.

1.3.3 Neurogenesis as a regenerative strategy

Recruitment of endogenous NSCs is an elegant approach to treating damaged neural tissue. The use of endogenous NSCs bypasses the ethical problems associated with the use and manipulation of foetal tissue and embryonic stem cells. However, there are a number of restrictions to endogenous neurogenesis which must be overcome in order to fulfil the regenerative potential. The number of endogenous NSCs in the adult brain is a fraction of number of cells typically lost through injury. Endogenous NSCs were only able to replace 0.2 % of the lost striatal neuron population after a model of stroke (Arvidsson et al., 2002). It is unlikely that this degree of replacement would significantly influence functional recovery. The population of endogenous NSCs is simply too small to effect any significant replacement. Another pertinent point is that even with enhancement of the neurogenic response through growth factors, neurotrophins or environmental enrichment, it remains to be demonstrated that new neurons are able to functionally integrate and promote recovery. Therefore, neural transplantation is currently the only regenerative strategy which has shown functional effectiveness.

1.4 Neural Transplantation for Repair of Ischaemic Brain Damage

1.4.1 History of neural transplantation

With all the increased media and public interest in stem cell transplantation, it is interesting to note that the rationale for transplantation into the brain is not a new concept. The first recorded attempt at transplanting neural tissue was carried out by Walter Thompson at the end of the 19th century, who transplanted cortical tissue from adult cats into the brain of adult dogs (Thompson, 1890). The first published instance of successful neural transplantation came around 30 years later, from the work of Elizabeth Dunn, who reported the results of transplantation of neonatal rat cortical tissue into the brains of adult rats (Dunn, 1917). This was followed by the first successful transplantation of foetal neuronal tissue into a neonatal host brain (Le Gros Clark, 1940). Over the next thirty years, there were scattered reports of successful neural transplantation, mostly using neonatal and embryonic tissue for

transplantation. It is clear that the theoretical use of exogenous tissue in neural transplantation was apparent to these early researchers. A number of discoveries heralded the beginning of 'modern' era of neural transplantation in the 1970s. The first of these discoveries were a series of experiments confirming the presence of neurogenesis, and by definition, adult neural stem cells, in the adult brain.

1.4.2 The modern era of neural transplantation

The proof of principle behind cell transplantation therapy was demonstrated by the first human bone marrow transplant for treatment of leukaemia at the beginning of the 1970s (Buckner et al., 1970). Around the same time, the first evidence that regenerative regrowth of axons was capable in the adult mammalian CNS came from Raisman (1969) who studied synaptic rearrangement following the severing of individual inputs to the septum in rodents. The medial septum receives two major inputs from the brainstem, one via the medial forebrain bundle and the other from the fimbria. Severing of one input leads to degeneration of the nerve terminals and loss of synapses onto the septum, but over the following weeks the number of synapses returns to normal, and are of the type associated with the uncut input. The fimbrial input sprouts new terminals to replace those lost after the medial forebrain bundle is cut, and vice versa.

These findings were quickly followed by a number of seminal experiments in the latter half of the decade. A systematic characterisation study on the conditions for favourable survival and development of transplanted brain tissue provided a framework for standardised transplantation techniques (Stenevi et al., 1976). Transplanted neural tissue was able to form synapses and connections to host tissue (Lund and Hauschka, 1976), and subsequently followed by demonstration of behavioural recovery following transplantation of foetal dopaminergic tissue in a rat model of Parkinson's disease (Perlow et al., 1979). Another breakthrough came in 1981, when embryonic stem (ES) cells were first isolated from the inner cell mass of mouse blastocysts (Evans and Kaufman, 1981, Martin, 1981). ES cells are pluripotent, meaning that they have the capacity to differentiate into any cell type of the three germ layers (ectoderm, mesoderm and endoderm). The isolation of human

ES cells arrived nearly 20 years later (Thomson et al., 1998). ES cells revolutionised the field of stem cell research, allowing for investigation into the events that occur during development (cell division and differentiation), screening for new drugs, and most importantly for the purposes of this thesis, application in stem cell therapy.

1.4.3 Embryonic stem cells

The therapeutic promise of ES cells in the field of tissue replacement and regenerative medicine arises from their capacity to differentiate into every type of cell and tissue in the body. As described above, all ES cells are initially derived from the inner cell mass of the blastocyst. They can be maintained *in vitro* culture either in the presence of leukaemia inhibitory factor (LIF) or on a feeder layer of embryonic fibroblasts. Under these conditions, ES cells are capable of undergoing an unlimited number of symmetrical divisions without undergoing differentiation. ES cells are karyotypically stable, in that they maintain a full, diploid complement of chromosomes following division. Pluripotent ES cells can be induced to differentiate into cells from all three embryonic germ layers. For the purposes of this thesis, the focus is on the differentiation of ES cells into neurons, astrocytes and oligodendrocytes. However, as an example of ES cell pluripotency, reports have described differentiation *in vitro* into adipocytes, cardiomyocytes, chondrocytes, mast cells, osteoblasts, pancreatic islets and striated muscle (Dani, 1999, Maltsev et al., 1994, Kramer et al., 2006, Wiles and Keller, 1991, Buttery et al., 2001, Kahan et al., 2003, Dinsmore et al., 1996).

1.4.4 Sources of tissue for neural transplantation

There are three general sources of tissue for neural transplantation therapy – primary foetal tissue, embryonic stem cells and neural stem cells. Each of these sources has associated advantages and disadvantages. Primary foetal tissue still represents the highest standard for functional recovery after brain damage. Transplants of embryonic dopaminergic tissue for patients afflicted with Parkinson's disease reinnervate the striatum, integrate into the patient's brain and release dopamine, inducing a substantial and lasting clinical improvement (Lindvall, 2000). Foetal grafts therefore illustrate the 'proof of principle' behind neural transplantation as a

therapy. However, there are major caveats blocking the widespread use of foetal tissue for neural transplantation. Primary foetal tissue is heterogenous, containing a mix of differentiated and undifferentiated tissue. Therefore, the number of disorders which could potentially be treated is limited. The choice of Parkinson's disease for demonstrating the utility of foetal grafts stems, in part, from the fact that Parkinson's disease pathology is a highly selective degeneration of the nigrostriatal dopamine system. This dopaminergic deficit is an easy target for treatment, as opposed to the widespread, diffuse damage present in Alzheimer's disease and global ischaemia. The heterogenous nature of foetal grafts also means that the results of grafts will be variable from patient to patient. In contrast, embryonic and neural stem cells are undifferentiated, with the ability to undergo pluripotent or multipotent differentiation. As such, stem cells could theoretically be used to treat the majority of neurological disorders. The generation of clonal cell lines from embryonic and neural stem cell sources also ensure homogeneity and uniform results between patients. Foetal grafts also present ethical and technical problems. In the aforementioned Parkinson's disease trial, each patient required tissue from 6-8 embryos (Lindvall, 2000). Acquisition of this volume of tissue is a technical hurdle and limits foetal use to small-scale experimental studies. In contrast, stem cell lines can be expanded *in vitro* in order to generate near-unlimited quantities for large-scale therapeutic application. However, the proliferative capacity of stem cells (particularly embryonic stem cells) does raise the risk of tumorigenicity, which is less of a factor with differentiated foetal tissue. Transplants of incorrectly directed ES cells may end up differentiating into a wholly unsuitable cell type, or give rise to teratomas, as has been shown in rodents (Arnhold et al., 2004, Fujikawa et al., 2005). However, stem cells can be genetically modified in order to conditionally control cell division. This capacity for genetic modification also allows for the incorporation of beneficial genes (e.g. neurotrophic factors) into stem cell lines, which is not possible with foetal tissue. The regulatory steps involved in the derivation of stem cell lines are highly stringent and incorporate appropriate safety checks, whereas the primary nature of foetal tissue raises numerous safety issues. Therefore, although primary foetal grafts have been invaluable for validating the theory of neural transplantation, it is clear that stem cell lines, either from embryonic or neural origins, represent the more

viable therapeutic option. The choice between using embryonic stem cells or neural stem cells also involves various pros and cons. Embryonic stem cells derived from the blastocyst are pluripotent and capable of unlimited self-renewal. However, ES cells also raise ethical questions, along with the possible tumorigenicity describe earlier. It may also be necessary to restrict these cells to a neural lineage prior to transplantation. Neural stem cells (derived from either the embryonic CNS or adult neurogenic regions) are committed to a neural lineage. This multipotent capacity reduces the risk of tumourigenesis. However, these cells are still capable of self-proliferation, although their intrinsic capacity for long-term maintenance *in vitro* is less extensive than ES cells. These neural stem cells may also display a certain degree of restricted differentiation, depending on the developmental stage and region from which they were derived. The reduced ethical issues associated with the use of neural stem cells have led to increased investigation into their clinical potential (Pollock et al., 2006).

1.4.5 Neural stem cells

Investigation into regions of neurogenesis led to the discovery of neural stem cells in adult mammalian brain. It is now accepted that there are two sites of constitutive neurogenesis in the adult mammalian brain: the subventricular zone (SVZ) and the subgranular zone (SGZ) of the hippocampal dentate gyrus (Figure 1.2). Neural stem cells (NSCs) can be defined by the following characteristics.

NSCs are:

a) undifferentiated,
b) able to proliferate and self-renew,
c) able to generate all three lineages of cells in the CNS: neurons, astrocytes and oligodendrocytes.

In the two primary neurogenic regions described previously, NSCs from the SVZ follow the rostral migratory stream to the olfactory bulb to become interneurons, whereas NSCs from the SGZ differentiate into hippocampal granule neurons (Garcia-Verdugo et al., 1998). NSCs generate intermediate neural progenitor cells. These neural progenitors undergo further restriction which determines the lineage of

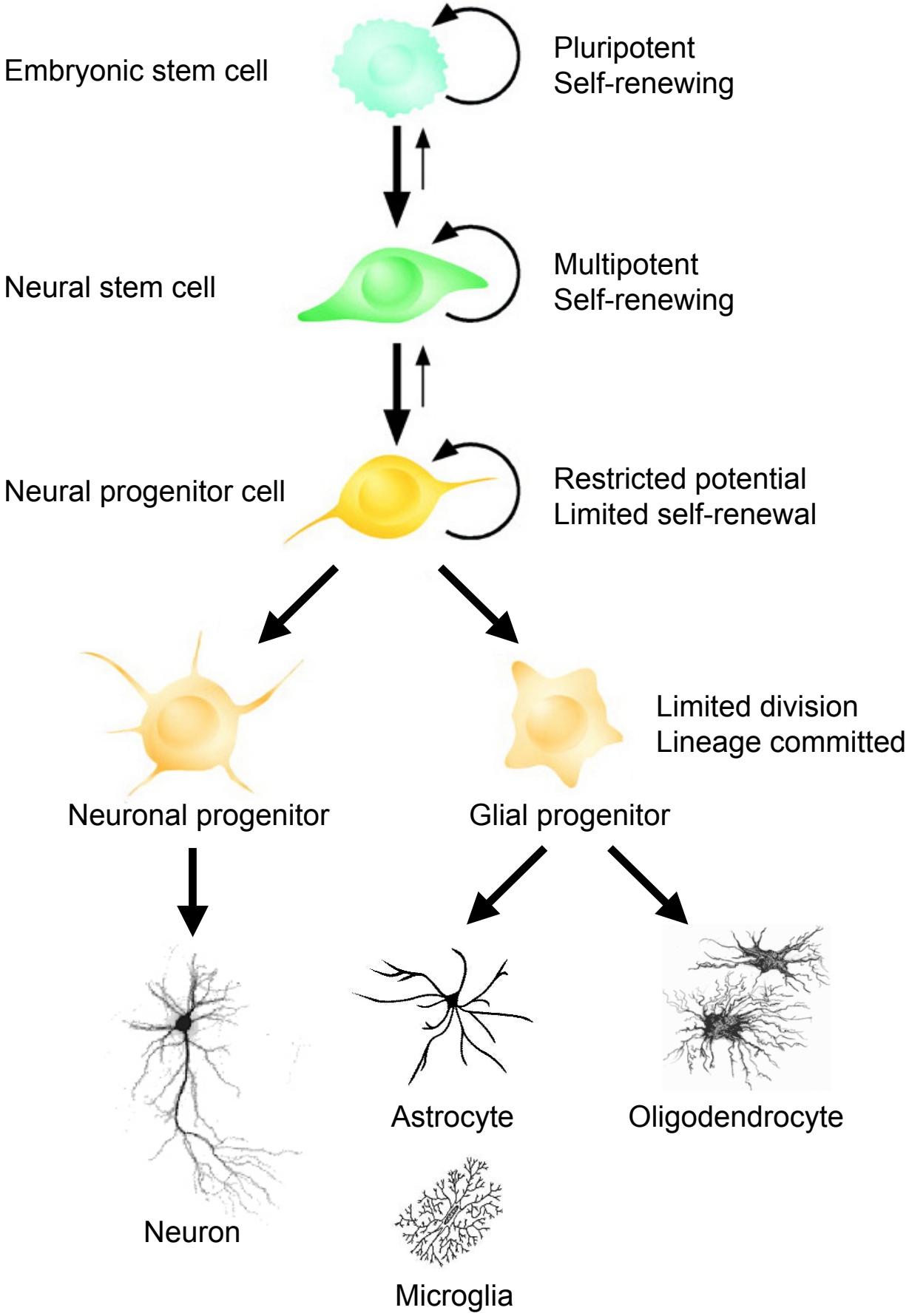

Figure 1.3 An illustration of stem cells with potential capability for neural differentiation

The classes of cells are displayed in a hierarchy of developmental potency and ability for self-renewal. Adapted from Gage, 2000.

subsequent cells; neuronal progenitor cells generate only neurons, and glial progenitor cells generate only glia. These progenitor cells may also have some capacity for self-renewal (Figure 1.3). The discovery of neural stem cells has led to the possibility of their use in clinical treatment of CNS damage. Regenerative therapies using NSCs typically focus on:

I) the recruitment of endogenous NSCs

II) exogenous transplantation of NSCs.

1.5 Neural Stem Cell Transplantation Therapy

Neural replacement via endogenous neurogenesis is suitable for turnover replacement of neurons in specific regions, but it cannot restore the extent of loss associated with the aforementioned disorders. The capacity of the endogenous centres of neurogenesis is insufficient to cope with massive loss of neural tissue. Neural stem cell therapy is the treatment of neurological disorders by administration of neural stem cells that have been selected, expanded and pharmacologically or genetically altered *ex vivo*.

1.5.1 Neurospheres

A variety of culturing techniques have been developed for the selection and large-scale expansion of neural stem cells from both embryonic and adult mouse brain. The neurosphere assay is the standard assay for detection and isolation of NSCs. Tissue from the embryonic brain is a combination of stem, precursor and differentiated cells. In order to isolate the stem and precursor cells, the tissue has to be cultured in specific conditions; 1) free-floating, in the absence of a substrate for the cells to settle on, and 2) with medium supplemented with high levels of epidermal and/or fibroblast growth factors (EGF/FGF). Under these conditions, differentiated cells die whilst stem and precursor cells survive and proliferate. The free-floating stem/precursor cells aggregate to form growing spheres of dividing cells, termed ‘neurospheres’ (Reynolds and Weiss, 1992). The population of stem/precursor cells can be expanded under these conditions, and induced to differentiate by the provision of a substrate in the culture media to which the stem/precursor cells can attach. The neurosphere assay can be applied to adult NSCs

isolated from the SVZ of adult rodents. Neurospheres dissociated into single cells will frequently start to form a new neurosphere. This property of neurosphere formation allows experimental, although retroactive, identification of NSCs.

1.5.2 Immortalised neural stem cell lines

Although the functional efficacy and integration of foetal tissue in neural transplantation has been well documented, the ethical and logistical hurdles surrounding their use limit widespread therapeutic use (Hoffer and Olson, 1991, Widner and Brundin, 1988). An alternative to expansion through neurospheres is to use a neural stem cell line. In order for a cell to become the clonal progenitor of a cell line, it must bypass the barrier to continued cell division. The property of uncontrolled and continual cell division is common to tumours and therefore these were one of the original sources examined for neural cell lines. There are a number of spontaneously arising neural cell lines, either neuroblastomas or glioblastomas. While these are useful for *in vitro* investigation of differentiation, the inherent tumorigenicity of these cells precludes their use in transplantation experiments. Another spontaneously arising source is teratocarcinomas, from which it is possible to derive embryonal carcinoma (EC) clones. These cells are totipotent, and can differentiate into non-neural and neural lineages. However, the uncharacterised origins these spontaneously arising cells lines raise issues of safety. Therefore, a number of neural cell lines have been transformed by researchers in order to establish an immortalised neural cell line. The advantages of these lines is that they are derived from a chosen region of the CNS, via a normally occurring source of NSCs, maintain the capacity for multipotential differentiation and are now able to withstand continued passage *in vitro*. Whilst the mechanisms responsible for continued cell division in tumour-derived cells are unknown, it is possible to exploit oncogenes in order to derive specific cell lines. Immortalised NSC lines can be derived by infecting the desired NSC population with a retrovirus encoding the immortalising oncogene. Individual clones are then isolated, characterised and expanded *in vitro*. Transforming proteins, such as SV40 large T antigen (T-ag) or myc, are constitutively expressed, even during cell differentiation. As the therapeutic endpoint of these cell lines is neural transplantation, this constitutive expression raises the

potential problem of carcinoma formation. It is possible to avoid this problem using a conditionally immortalising oncogene, such as the temperature sensitive (ts) mutants of SV40 large T antigen (ts-T-ag) or the Rous sarcoma virus (ts-RSV). These mutants drive proliferation of the immortalised cells at the permissive temperature (33^{o}C), but following a shift to the non-permissive temperature (>37^{o}C), the oncogene product is rapidly degraded and unable to promote cell division.

1.5.2.1 The NT-2 stem cell line

One well-characterised example of a teratocarcinoma derived line is the human NTera-2 (NT-2) cell line, (Andrews et al., 1984). Treatment of NT-2 cells with retinoic acid and mitotic inhibitor results in an enriched population of differentiated neurons (Pleasure et al., 1992). These are referred to as NT2N or hNT cells, and have been commercially optioned by Layton Bioscience (LBS-Neurons). NT2N cells transplanted into non-lesioned rat brain are able to survive for up to a year and express mature neuronal markers (Kleppner et al., 1995, Miyazono et al., 1996). However, the transplanted cells did not appear to fully integrate with host tissue. Although NT2N cells formed synapse-like structures and developed axo-dendritic architecture, these axons remained unmyelinated and no synaptic connections were formed with host neurons. NT2N cells have also been transplanted in a rat model of traumatic brain injury (Philips et al., 1999, Muir et al., 1999) where they survived but did not improve deficits. However, NT2N cells incorporating an eGFP label were able to attenuate cognitive dysfunction (Watson et al., 2003) following traumatic brain injury in mice. Similarly, NT2N cells survive in a rat model of Parkinson's disease but did not aid functional recovery (Baker et al., 2000, Fricker-Gates et al., 2004). However, functional improvements were observed following transplantation of NT2N cells in rats subjected to quinolic acid lesions in the striatum, with grafted rats displaying partial recovery on the skilled forelimb task (Hurlbert et al., 1999). In a focal ischaemia model of MCAo, transplanted NT2N cells were able to ameliorate behavioural deficits in passive avoidance and motor function (Borlongan et al., 1998, Saporta et al., 1999). The promising results of the NT2N cells in animal models of stroke have led to their use in clinical trials in patients with basal ganglia stroke (Kondziolka et al., Neurology, 2000). These phase I clinical trials are still ongoing,

and initial reports have been promising (Meltzer et al., 2001, Nelson et al., 2002, Kondziolka et al., 2005). Importantly, these initial results have underlined the safety and feasibility of neural transplantation in the clinical setting, although the lack of synaptic integration of NT2N grafts into host tissue raises the possibility that these cells exert their therapeutic influence through release of neuroprotective or trophic factors, rather than through functional replacement (Whittemore and Onifer, 2000, Kleppner et al., 1995, Miyazono et al., 1996). Although the NT2 cell line has advantages, namely their human origin and therapeutic effects, there are corresponding disadvantages, such as the potential for tumorigenesis, uncharacterised origins and the lack of functional integration. Conditionally immortalised neural stem cell lines have the advantage of full characterisation during construction, whilst displaying the functional integration and differentiation of spontaneously arising neural stem cell lines.

1.5.2.2 The C17.2 stem cell line

The C17.2 cell line was obtained from transformation of neonatal P4 mouse cerebellar cells with the avian v-myc oncogene (Ryder et al., 1990). At this stage of development, neurons and glia are generated from the external germinal layer of the cerebellum. Hence, immortalised C17.2 cells derived from this region are multipotent, differentiating into neurons and glia both *in vitro* and *in vivo*. Following transplantation into the cerebellum of neo-natal mice, the C17.2 cells integrate into the developing cerebellum in the correct anatomical location, and differentiate into neurons or glia appropriately depending on the region of engraftment. Electron microscopy revealed that transplanted cells establish and receive synaptic connections (Snyder et al., 1992). Similar to primary neural tissue, FGF and EGF act as potent mitogens for C17.2 cells (Kitchens et al., 1994). The C17.2 line has been investigated for therapeutic uses in various models of neurodegenerative disease. Following transplantation in a rodent model of traumatic brain injury, C17.2 cells survive, differentiate into neurons and astrocytes, and improve the performance of the animals on behavioural tests of motor function (Riess et al., 2002). These therapeutic effects can be further improved by genetic modification of the C17.2 cells to secrete glial cell line-derived neurotrophic factor (GDNF) (Bakshi et al.,

2006). In both intact and 6-hydroxydopamine lesioned rats, C17.2 cells transplanted into the striatum express dopaminergic and neuronal markers, suggesting that these cells undergo site-appropriate differentiation, irrespective of damage (Yang et al., 2002). C17.2 cells modified to express firefly luciferase migrate to the infarct region following middle cerebral artery occlusion, where they differentiate into neurons and astrocytes (Kim et al., 2004). In a similar model of focal hypoxic-ischaemic injury, C17.2 cells migrate to the infarct and penumbra, where they engraft and differentiate into all three neural cell types (Park, 2000, Park et al., 2002). This study also demonstrated that modifying the time of transplantation markedly affect the outcome of transplanted cells. No engraftment was observed when C17.2 cells were transplanted 5 weeks after the hypoxic-ischaemic injury. Conversely, optimal engraftment was observed when transplanting 3-7 days following the insult, suggesting that there is a therapeutic window for optimal stem cell transplantation.

1.5.2.3 The RN33B stem cell line

Another well-characterised example of an immortalised neural cell line is the RN33B line established by Whittemore and White (1993). This was derived from E12.5 embryonic rat medullary raphe nucleus cells infected with a retrovirus encoding the temperature sensitive SV40 large T-antigen (ts-T-ag). Unlike the v-myc oncogene used for immortalisation of the C17.2 line, the oncogene in the ts-T-ag system is linked to a temperature sensitive promoter. This added level of regulation allows for greater control over the tumourigenic potential of the oncogene. *In vitro*, differentiated RN33B cells express neuron specific markers but do not express any astrocytic or oligodendrocyte specific protein markers. Differentiated RN33B cells will express T-antigen when returned to 33^{o}C, but do not de-differentiate and recommence mitosis (Whittemore and White, 1993). Following transplantation into undamaged adult and neonatal cortex, RN33B cells stably integrate and differentiate into morphologically site-appropriate neurons, i.e. in the cerebral cortex; RN33B cells displayed morphologies similar to pyramidal neurons and stellate cells, whilst in the hippocampus; RN33B cells assumed morphologies similar to CA1 and CA3 pyramidal neurons (Shihabuddin et al., 1995). Immunohistochemical evidence also supports the notion that differentiation of RN33B cells is region specific, from the

expression of site-appropriate markers following transplantation (Shihabuddin et al., 1996). Transplanted RN33B cells can integrate in lesioned neonatal or adult rat brain (Lundberg et al., 1996, Shihabuddin et al., 1996). Functional integration of RN33B neurons was verified by electrophysiological recordings of action potentials (Englund et al., 2002).

1.5.2.4 The MHP36 stem cell line

The MHP36 neural stem cell line used in this thesis is an immortalised cell line. However, in contrast to the previous two lines described, the MHP36 cell line was immortalised prior to derivation. Neuroepithelial tissue was dissected from the hippocampus of embryonic day 14 H-2K^b-tsA58 transgenic mice (Sinden et al., 1997). This 'immortomouse' already stably expresses the temperature sensitive SV40 large T-antigen described previously, and incorporates a further level of regulation by linking control of the ts-T-ag to the inducible promoter of the mouse *H-2K^b* gene (Jat et al., 1991). The *H-2K^b* gene is present at low levels in a wide variety of tissues, and its expression can be upregulated above basal levels by exposure to gamma interferon (IFN-γ). Therefore, cell lines isolated from this transgenic mouse are conditionally proliferative depending on both temperature and application of IFN-γ. The optimal conditions for growth are maintenance at 33^{o}C and presence of IFN-γ. Single cell suspensions from the dissected hippocampal tissue were plated out, and then transduced with a *lac-Z* reporter and neomycin-resistance selectable genes. 32 clonal cell lines arose from neomycin-resistance selection, from which nine were selected for further investigation. Two of these nine lines displayed a proliferative response to fibroblast growth factor 2. One of the FGF2 responsive cell lines (MHP36) also expressed the neural stem cell marker, nestin, as well as the SV40 antigen in permissive conditions. Following transfer to non-permissive conditions, these MHP36 cells could be induced to differentiate into PGP 9.5 positive neurons and GFAP positive astrocytes after treatment with retinoic acid. These PGP 9.5 positive neurons also exhibited suitable morphology, with long neuritic processes. Although MHP36 cells are nestin positive when in an undifferentiated state, once the cells start to undergo differentiation, nestin expression is rapidly downregulated (Mellodew et al., 2004). In an *in vitro* co-culture

system, MHP36 cells seeded onto organotypic hippocampal slices stop expressing nestin 4 hours after seeding. This loss of expression is controlled by the targeting of nestin to the proteasome for ubiqutin-mediated degradation.

1.6 Therapeutic Transplantation of the MHP36 Stem Cell Line

Neural transplantation of MHP36 cells has been shown to be therapeutic in a variety of animal models (primarily rodent) of neurological disorders.

1.6.1 Global ischaemia

The rodent 4-VO model of transient global ischaemia (Pulsinelli et al., 1982) produces selective loss of hippocampal CA1 pyramidal neurons, in addition to functional deficits in spatial navigation and working memory (Nunn and Hodges, 1994). Control rats displayed spatial learning capabilities on a water maze task, while ischaemic rats receiving sham grafts showed clear deficits in the same task. Ischaemic rats grafted with MHP36 cells or foetal CA1 tissue showed similar performance to the control group. This improvement in spatial learning was attributed to extensive repopulation of the lesioned CA1 region by the grafted MHP36 cells (Sinden et al., 1997).

1.6.2 Focal ischaemia

MHP36 grafts also promote functional recovery in a rat model of focal ischaemia (Veizovic et al., 2001). Rodents subjected to transient middle cerebral artery occlusion received grafts of MHP36 cells in the hemisphere contralateral to the focal infarct. MHP36 cells were observed to migrate towards the lesioned hemisphere. The infarct volume was significantly reduced in grafted rats compared to the sham-grafted MCAo controls. Behavioural tests showed that the MHP36 grafts ameliorated sensorimotor deficits associated with MCAo, but did not rescue spatial learning deficits. Further studies showed that the behavioural effects of MHP36 grafts varied depending on the site of implantation (Modo et al., 2002). Interestingly, grafts delivered via the intraparenchymal route functionally improved bilateral asymmetry deficits but did not improve spatial learning. However, the converse was observed

were seen following intraventricular grafts, namely an improvement in spatial learning but persistent defects in bilateral asymmetry.

1.6.3 Alzheimer's disease

MHP36 grafts have been investigated in a model of cognitive deficits associated with Alzheimer's disease (Grigoryan et al., 2000). Rats received bilateral infusions of AMPA into the nucleus basalis magnocellularis and medial septum. Lesioning of these regions induced discrete, area-specific loss of cholinergic projection neurons, similar to that observed in Alzheimer's disease. These lesions resulted in spatial deficits on the water maze task which were reversed by grafts of MHP36 cells. Grafted cells displayed both neuronal and glial morphologies and migrated away from the injection site towards the lesioned areas.

1.6.4 Ageing

The process of ageing brings with it progressive cognitive decline, as evidenced by a loss of cholinergic neurons and subsequent age-associated memory impairments such as memory storage deficits, decline in neurotransmitter function and delayed speed of mental processing (Abdulla et al., 1995, Luine and Hearns, 1990). Gross changes manifest as a loss in brain weight (Miller et al., 1980), paralleled by histopathological changes including neuronal atrophy, synaptic loss and gliosis. MHP36 grafts were able to halt this decline as assessed by a spatial learning and memory task (Hodges et al., 2000). A group of aged rats (22 months) was trained to find a hidden platform in the water maze. The aged rats were subdivided into two groups, 'impaired' and 'unimpaired', based on their performance during training. The unimpaired group did not differ in latency times from a group of young (3 months) controls. The impaired group was further subdivided into MHP36 graft or vehicle groups. The unimpaired group and young controls also received vehicle grafts. Upon further behavioural testing six to eight weeks post-transplantation, the impaired group that received MHP36 grafts now performed at the same level as the unimpaired group on latency to find the platform and distance swum. Both these groups were significantly better than the impaired group with vehicle grafts, although the young controls performed better on the task overall. A parallel study

investigating whether aged, non-grafted rats improve over the six to eight week period demonstrated no improvement in the task, suggesting that the MHP36 grafts do not merely retard age-associated memory impairments, but actually reverse them.

1.6.5 Primate models of damage

The efficacy of MHP36 grafts was also demonstrated in primates (Virley et al., 1999). Common marmosets were trained using the Wisconsin General Test Apparatus to discriminate between rewarded and non-rewarded objects (simple discrimination) and to discriminate between two different pairs of identical objects (conditional discrimination). Following training and establishment of a baseline, the marmosets were selectively lesioned in the CA1 field of the hippocampus by administration of NMDA. As in the rodent study, MHP36 cells appeared to reconstruct the lesioned CA1 region. MHP36 grafted primates showed an improvement on conditional discrimination tasks to the levels of non-lesioned controls and were substantially improved compared to the lesioned group.

1.6.6 Understanding mechanisms for MHP36 graft effects

Although the regenerative properties of NSC transplantation have been demonstrated with a variety of NSC lines, there is still very little known about the host cues which serve to inform the transplanted NSCs regarding migration and differentiation. In the case of the MHP36 stem cell line, the results of two initial studies implicate various mechanisms for MHP36 survival, migration and differentiation.

1.6.6.1 Immunogenic properties of MHP36 stem cells

Survival of transplanted NSCs is particularly dependent on the immunogenic response. Foreign grafted tissue may provoke an acute response from the immune system, which can lead to rejection and extensive upregulation of immune system mediators. The immunogenic properties of MHP36 cells were investigated in a rat model of stroke (Modo et al., 2002). MHP36 grafts were either delivered ipsi- or contralateral in MCAo lesioned mice or sham controls. The animals were also divided into a cyclosporin A treated group or non-immunosuppressed controls. MHP36 grafts did not alter the proliferative response to lymphocytes. There was an

increase in the immune markers MHC class I, CD45 and CD11b in the vicinity of the injection tract, but this was due to the trauma of injection, not the delivery of vehicle or MHP36 cells. The use of immunosuppression did not alter the lymphocyte response and surprisingly, greater graft survival was achieved in the absence of immunosuppression than the presence. *In vitro* experiments on the expression of MHC class I and II by MHP36 cells shows that when maintained in an undifferentiated, proliferating state (33^{o}C), over 90% of MHP36 cells express both MHC class I and II antigens (Modo et al., 2003). However, upon switching to the non-proliferative temperature of 37^{o}C, there was a marked downregulation of MHC class I and II antigens, with approximately 25-30% of MHP36 cells expressing both antigens, demonstrating the low immunogenic properties of these cells. This study suggests that MHP36 stem cells manifest an intrinsic ability to escape detection by the immune system *in vivo*, which would improve the likelihood of survival, particularly in the hostile, highly immunogenic environment of damaged brain.

1.6.6.2 The role of apolipoprotein E in MHP36 integration

A recent study suggested a link between the lipid transport protein, apolipoprotein E (apoE) and MHP36 graft survival and integration into host tissue (Modo et al., 2003). ApoE has been associated with neurodegeneration, regeneration and development (see following sections), and has been shown to be upregulated following global and focal ischaemia (Horsburgh et al., 2000, Laskowitz et al., 1997, Virley et al., 2000). This study investigated the expression and localisation of apoE after MCAo and grafts of MHP36 cells into the ipsi- and contralateral hemispheres and ventricles. MCAo damage alone induced upregulation of apoE in the ipsilateral somatosensory cortex, striatum, corpus callosum and thalamus. Parenchymal MHP36 grafts further increased upregulation of apoE, particularly in the contralateral hemisphere, whilst this was not observed with intraventricular grafts. Interestingly, this dissociation between the sites of grafting paralleled an earlier study in which parenchymal grafts promoted sensorimotor recovery, whereas ventricular grafts improved spatial learning after focal ischaemia (Modo et al., 2002). This was hypothesized to represent a remodelling process which would allow the contralateral hemisphere to take over some of the functions of the lesioned hemisphere. The majority of apoE

immunostaining was localised to astrocytes, although neuronal expression was observed in the lesioned somatosensory cortex. However, only around 15% of grafted MHP36 cells were apoE-positive. The expression of apoE on both host and grafted cells raises the possibility that apoE may facilitate interaction and integration between the cells after ischaemic damage. It remains to the seen whether the increase in apoE following MHP36 grafting is from the host or grafted cells. Host astrocytes might secrete apoE in response to the grafted stem cells as an attractant, directing the MHP36 cells to the regions of damage. Alternatively, the grafted cells could be secreting apoE in order to reduce the extent of damage, based on the neuroprotective action of apoE. Whilst these initial findings do suggest that apoE does affect the fate of transplanted stem cells, it is clear that much more work is required in order to elucidate the role of apoE on stem cell integration.

1.7 Apolipoprotein E as a Mediator for the Effects of MHP36 Stem Cell Grafts

1.7.1 Background

1.7.1.1 Lipoproteins

Plasma lipoproteins are assemblies of lipid and protein which facilitate transport of insoluble lipids throughout the body. The lipoprotein core consists of insoluble triacylglycerides and cholesterol esters. This is surrounded by a phospholipid shell which imparts solubility to the particle. Apolipoproteins attach to the surface of the lipoprotein and are responsible for stability, directing transport and receptor binding of the lipoprotein particle to its target (Figure 1.4). Classification of lipoproteins is done by size and density. Listed in order from large, less dense to small, high dense are chylomicrons, (transport of dietary triglycerides to the liver), very low density lipoproteins (VLDL; transport of freshly synthesised triglycerides from the liver), low density lipoproteins (LDL), intermediate density lipoprotein (IDL; transport of cholesterol) and high density lipoproteins (HDL; transport of cholesterol from tissue to the liver)

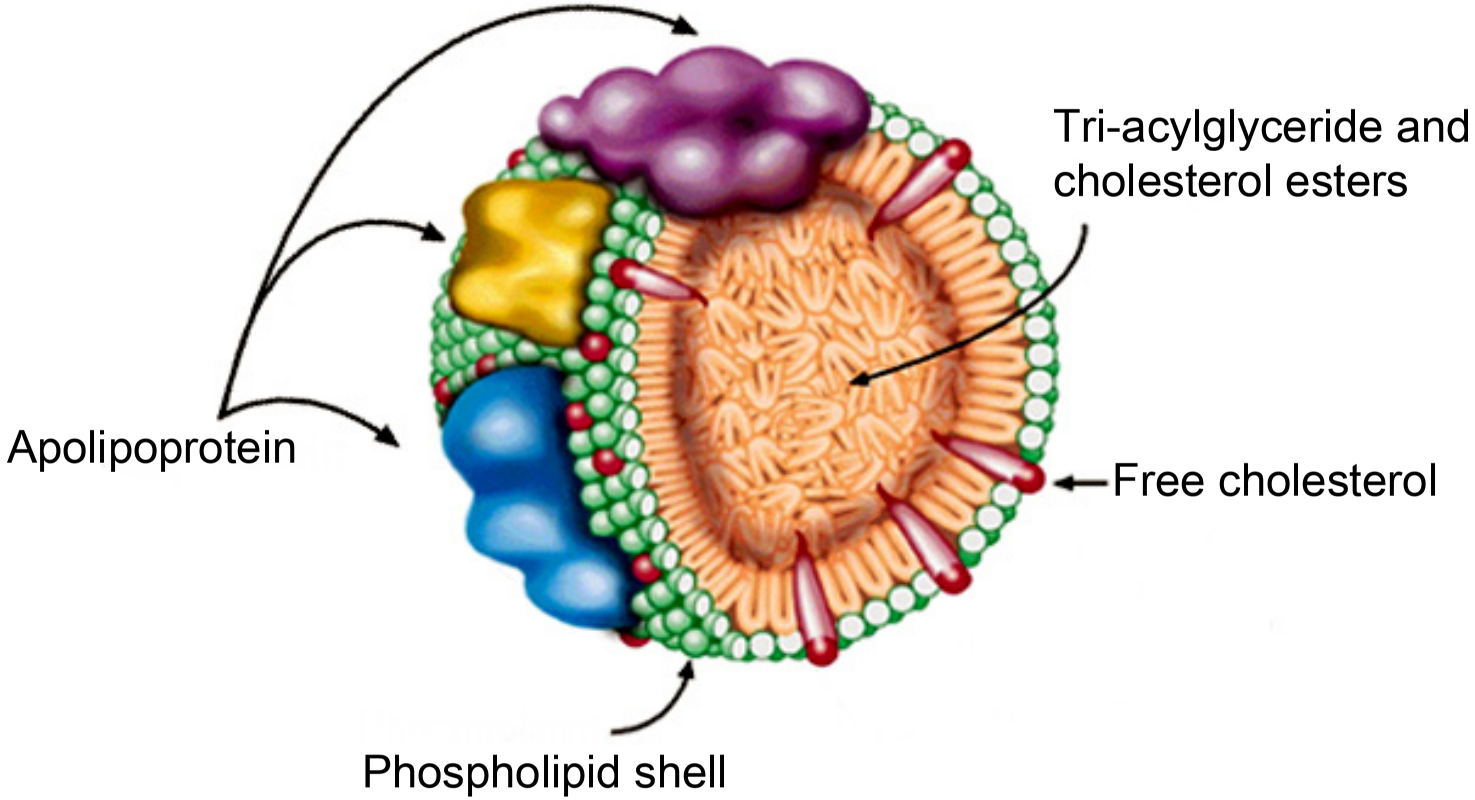

Figure 1.4 Schematic illustration of a lipoprotein particle
A phospholipid shell surrounds a core composed of triglycerides and cholesterol esters. Apolipoproteins and free cholesterol associate on the surface of the particle. Image modified from Peprotech.

1.7.1.2 History

Apolipoprotein E (apoE: protein, *APOE:* gene) is a protein constituent of plasma lipoproteins that has a major role in cholesterol transport. It was originally identified in 1973 by Shore and Shore (1973) as a component of VLDL and was later discovered as a constituent of chylomicrons and HDL, where it mediates the lipoprotein-specific function described above. In order to mediate this, apoE has three binding regions, allowing binding to lipids, receptors and heparin.

1.7.1.3 Structure of apoE

ApoE consists of 299 amino acids and has a molecular weight of approximately 34 kDa. The primary structure shows a region increased in basic amino acids, residues 136-150. This region is responsible for two functions of apoE, receptor binding and heparin binding. The secondary structure predicts that apoE has two domains separated by a hinge region, which was confirmed by physical and biochemical studies (Wetterau et al., 1988, Aggerbeck et al., 1988). The amino-terminal domain (residues 20-165) contains the receptor and heparin binding domain, as predicted from primary structure, whilst the carboxy-terminal domain (residues 225-299) consists of amphipathic α-helices, responsible for the third function of apoE, lipoprotein binding. The three-dimensional tertiary structure of apoE was elucidated by x-ray crystallography and circular dichroism (Wilson et al., 1991, Barbier et al., 2006, Clement-Collin et al., 2006). The N-terminal domain arranges as a four-helix bundle, with the isoform difference resulting in small structural and functional changes.

Human apoE has three isoforms, referred to as apoE2, E3 and E4, which differ from each other by single amino acid substitutions at position 112 and 158. The most common isoform, apoE3, has a cysteine at residue 112 and an arginine at residue 158 with a net charge of +1. ApoE2 has cysteine at both positions and a net charge of 0, with apoE4 containing arginine at both positions with a net charge of +2. This genetically determined polymorphism was discovered via iso-electric focusing (Utermann et al., 1977) and two-dimensional electrophoresis (Zannis and Breslow, 1981, Zannis et al., 1981) based on the charge difference between the three isoforms.

The isoform specific functional changes differ according to the binding property of apoE. There are no isoform specific differences to heparin binding. ApoE3 and E4 isoforms have a similar affinity for binding to the LDL receptor, whilst apoE2 has only 2% of the affinity of the other two isoforms. Homozygosity for the apoE2 isoform is a causal molecular defect for type III hyperlipoproteinemia, a genetic disorder characterised by enrichment of the abnormal lipoprotein β-VLDL (Mahley et al., 1999). However, regarding lipid binding, apoE2 and E3 have a preferred affinity for HDL, whilst apoE4 has a preferential affinity for VLDL.

1.7.1.4 The role of apoE in plasma

The major function of apoE is the transport and redistribution of lipids among cells within the body (Mahley, 1988). The liver is the integral organ for lipid metabolism, and therefore the bulk of apoE in the body is synthesized in the liver (Elshourbagy et al., 1985). ApoE is involved in the transport of dietary lipids from the intestine to the liver. Chylomicrons are synthesized and secreted by the small intestine in response to dietary fat intake. Upon secretion into plasma, these chylomicrons associate with apoE. As these apoE-chylomicron lipoproteins circulate through the capillaries, lipoprotein lipase hydrolyses the triglyceride group of the chylomicrons in order to generate free fatty acids for metabolic requirements. The chylomicron remnants are highly enriched in cholesterol and are eventually cleared from the plasma by the liver through LDL receptor uptake (Mahley, 1988). ApoE also redistributes VLDL from the liver to peripheral tissues. ApoE is a component of VLDL particles as they are synthesized and secreted from the liver. These particles also undergo lipoprotein lipase hydrolysis in the plasma, and progress from VLDL remnants to IDL and finally LDL. ApoE mediates uptake of these LDL particles into peripheral tissues via LDL receptors. ApoE also associates with HDL in order to eliminate excess cholesterol from cells. This process is termed reverse cholesterol transport. Cholesterol enriched cells release cholesterol into the interstitial fluid. HDL particles have a high affinity for cholesterol, and as they become enriched in cholesterol, apoE associates with the particle. ApoE then acts as a ligand for delivery to the liver, where the cholesterol is eliminated from the body through bile formation.

1.7.1.5 The role of apoE in the nervous system

Although the liver synthesises the largest quantity of apoE in the body, the brain is the second largest producer of apoE (Elshourbagy et al., 1985). It is the predominant lipid transport protein in the CNS, where astrocytes are the major cell type that produce and secrete apoE (Boyles et al., 1985). This localised abundance suggested to researchers that apoE may have an important role in neurobiology. Initial evidence for the role of apoE in the nervous system came from investigations into peripheral nerve system damage. Following peripheral nerve injury to the sciatic or optic nerve, apoE is significantly upregulated around the site of injury (Stoll and Muller, 1986, Snipes et al., 1986) to the degree that apoE represents 2-5% of extracellular protein in the regenerating sciatic nerve sheath three weeks after injury (Ignatius et al., 1986). ApoE also redistributes lipids among cells within a tissue, such as in peripheral nerves following injury (Ignatius et al., 1986, Boyles et al., 1989). ApoE is upregulated 100- to 200- fold in rat sciatic nerve following a crush or a cut injury. Resident macrophages are responsible for this increase in the production and secretion of apoE. ApoE scavenges cholesterol from the damaged environment and transports it to the macrophage for storage. Later, apoE mediates redistribution of cholesterol to the regenerating axons for use in membrane synthesis and also for remyelinization of the axons by Schwann cells (Boyles et al., 1989). A similar regenerative role for apoE has been demonstrated in the CNS. In models of hippocampal denervation and reinnervation, upregulation of apoE has been associated with cholesterol transport for synaptic synthesis and increased mossy fibre sprouting (Poirier et al., 1993, Teter et al., 1999, White et al., 2001).

1.7.2 Association of apoE with disease

1.7.2.1 Alzheimer's disease

Just under a century ago, Alois Alzheimer published the clinical and neuropathological observations of the disease which bears his name (Alzheimer, 1907). Alzheimer's disease (AD) is a debilitating neurodegenerative disorder characterised by irreversible, progressive loss of cognitive function. It is the most common form of dementia and a major public heath challenge in industrialized

countries. The flurry of investigation into the role of apoE in the CNS during the early 1990s led to the discovery that possession of the ε4 allele was linked to the pathogenesis of AD (Saunders et al., 1993, Strittmatter et al., 1993). Initially, this association was determined for late-onset familial AD, with the age of onset directly linked to the gene dose of *APOE*-ε4 (Corder et al., 1993). The mean age of onset for non ε4 possessing individuals was 84 years, compared to 68 years for individuals homozygous for the ε4 allele. These homozygous ε4 carriers were also predominantly fated to develop AD by the age of 80. Subsequently, an association between apoE polymorphism and sporadic AD was determined, with the ε4 allele exhibiting an increased prevalence in AD individuals (Rebeck et al., 1993, Poirier et al., 1993). In contrast, the *APOE*-ε2 allele has been shown to confer a degree of protection against late-onset AD (Corder et al., 1994). There are three other risk factor genes for AD, namely amyloid precursor protein, presenilin-1 and presenilin-2. Mutations in these three genes results in an increase in the production of amyloid-beta (Aβ) peptides and have been linked to early-onset familial AD, which accounts for around 5% of all AD cases (Selkoe, 2002). This illustrates the importance of apoE in AD, as the two forms associated with apoE, late-onset familial and sporadic, therefore account for 95% of all AD cases. ApoE associates with the neuropathological markers of AD, namely neuritic amyloid plaques, neurofibrillary tangles and amyloid deposits (Benzing and Mufson, 1995, Namba et al., 1991, Strittmatter et al., 1993, Wisniewski and Frangione, 1992). *APOE*-ε4 exerts a dose-dependent increase in plaque and neurofibrillary tangle formation.

1.7.2.2 Ischaemic stroke

Ischaemic strokes accounts for approximately 80% of stroke cases and arise from blockage of an artery supplying the brain with blood. This blockage usually arises as the result of a blood clot. The role of apoE in plasma directly impacts on cardiovascular function and has a potent anti-atherogenic effect. The apoE-deficient mouse was originally created in order to investigate the effect of apoE on atherosclerosis (Piedrahita et al., 1992, Plump et al., 1992). These mice are severely hypercholesterolaemic and susceptible to atherosclerotic lesions, even when maintained on a low fat diet (Zhang et al., 1994). As atherosclerosis is the underlying

cause of heart attacks and strokes in the Western world, a large number of studies have sought to determine whether apoE polymorphisms affect cardiovascular diseases. Possession of an *APOE-ε4* allele has been linked to increased risk of ischaemic stroke (Couderc et al., 1993, Margaglione et al., 1998, Peng et al., 1999, McCarron et al., 1999, Sudlow et al., 2006). However, this association is still controversial, with other studies failing to observe any correlation (Kuusisto et al., 1995, Basun et al., 1996, Ferrucci et al., 1997, MacLeod et al., 2001, Slooter et al., 2004). Subsequent meta-analyses have suggested the discrepancy between these studies is due to variations in cohort selection, ethnic background, age of subjects as the main selection biases (Sudlow et al., 2006). There is also accumulating evidence for association between apoE genotype and the outcome from ischaemic stroke, although this is still inconclusive. No apoE genotype difference in functional recovery after stroke was observed in a number of studies (McCarron et al., 1998, Catto et al., 2000, McCarron et al., 2000). However, in-depth analysis of particular events following ischemic stroke have linked the *APOE*-ε4 allele with increased risk of dementia after stroke (Slooter et al., 1997), declines in information processing and recall (Dik et al., 2000), increased progression and expansion of the infarct (Liu et al., 2002) and increased prevalence of aphasia after ischaemic stroke (Treger et al., 2003).

1.7.2.3 Haemorrhagic stroke

ApoE genotype has also been reported to influence outcome following haemorrhagic stroke. An association has been reported between the ε4 allele and a poorer neurological outcome after intracerebral haemorrhage (Alberts et al., 1995, McCarron et al., 1998). Later studies have revealed that ε4 carriers also suffer from increased mortality after a haemorrhagic stroke, although this association is independent of haematoma and oedema volumes (McCarron et al., 1999, McCarron et al., 2003). A recent case-control study suggested that the ε4 allele is also a risk factor for lobar intracerebral haemorrhage (Woo et al., 2005) and also increases likelihood of recurrence (O'Donnell et al., 2000). Interestingly, meta-analysis carried out on eight studies investigating *APOE* genotype association with intracerebral hemorrhage did not confirm any increased risk associated with the ε4 allele, but did

reveal an association with the ε2 allele (Sudlow et al., 2006). Cerebral amyloid angiopathy (CAA) is a major cause of lobar intracerebral hemorrhage. CAA is characterised by amyloid beta peptide deposition in the cerebral vasculature, which accumulate over time and in severe cases, lead to rupture of the blood vessels. Investigation into the role of apoE polymorphisms and Alzheimer's disease pathology led to the discovery that the ε4 allele was strongly associated with increased vascular deposits of amyloid (Schmechel et al., 1993). Later studies have confirmed the association of the ε4 allele with CAA and CAA-related intracerebral hemorrhage (Greenberg et al., 1995, Olichney et al., 1996, Kalaria et al., 1996, Premkumar et al., 1996). However, it has also been shown that the *APOE*-ε2 allele is also over-represented in cases of CAA-related hemorrhage (Nicoll et al., 1997, Greenberg et al., 1998, McCarron et al., 1998. Pathological examinations suggest that whilst the ε4 allele promote CAA-related hemorrhage through increased deposition of amyloid, the ε2 allele increases the susceptibility of amyloid-laden blood vessels to rupture, possibly through increased fibrinoid necrosis (Greenberg et al., 1998, McCarrron et al., 1999). Consistent with this hypothesis, individuals with a heterozygous ε2/ε4 genotype are particularly predisposed to onset of CAA at a young age (Greenberg et al., 1998, McCarron et al., 1998). An association of apoE with subarachnoid haemorrhage has also been documented by a number of research groups. Patients possessing an ε4 allele were more likely to suffer from an unfavourable outcome after subarachnoid haemorrhage (Dunn et al., 2001, Niskakangas et al., 2001, Leung et al., 2002, Lanterna et al., 2005). There is evidence of an association between the ε4 allele and risk of subarachnoid hemorrhage (Tang et al., 2003, Sudlow et al., 2006). Subsequent studies have demonstrated that apoE levels in the CSF decrease after subarachnoid haemorrhage, and postulated that a poor outcome is linked to lower levels of apoE, although this effect is irrespective of genotype (Kay et al., 2003, Kay et al., 2003).

1.7.2.4 Global ischaemia

Post-mortem analysis of human brain from patients following an episode of global ischaemia revealed increased neuronal and glial apoE immunoreactivity in all sectors of the hippocampus as compared to controls (Horsburgh et al., 1999). The degree of

neuronal apoE immunoreactivity was strongly linked to the extent of neuronal damage observed in the global ischaemia patients. However, there was no association observed between apoE genotype and neuronal damage or apoE immunoreactivity. Two clinical studies have been published investigating the association of apoE with outcome after global ischaemia as caused by cardiac arrest, with conflicting results. Schiefermeier et al., (2000) demonstrated that patients homozygous for the ε3 allele were more likely to survive following cardiac arrest and were also predisposed towards a favourable neurological outcome. Possession of at least one ε4 or ε2 allele was therefore linked to an unfavourable outcome, although the number of patients homozygous for *APOE*-ε2 and ε4 was too small for in depth analysis of genotype effect. In contrast, a later study found no significant association between *APOE* genotype and outcome after cardiac arrest (Longstreth et al., 2003). The reason for the disparity between the two studies may have arisen due to the use of a larger, more heterogenous group of patients in the Longstreth study.

1.7.2.5 Traumatic brain injury

Traumatic brain injury (TBI) is defined as when a sudden trauma inflicts damage to the brain. TBI cases can be broadly defined into two groups; closed head injuries and penetrating head injuries. Closed head occurs when the head violently hits an object but there is no penetration of the skull, whereas penetrating head injuries occur when an object pierces the skull into brain tissue. Due to the variability in types and causes of TBI, there is a broad spectrum of focal and diffuse damage observed in the aftermath of TBI. ApoE polymorphism has been associated with a poorer outcome after traumatic brain injury (Teasdale et al., 1997, Friedman et al., 1999, Lichtman et al., 2000, Liberman et al., 2002, Crawford et al., 2002, Chiang et al., 2003). In the first study to demonstrate this association, it was found that the possession of one or more *APOE*-ε4 allele increased the likelihood of an unfavourable outcome after TBI to 57%, compared to 27% in the patients without an *APOE*-ε4 allele (Teasdale et al., 1997). In a group of veterans and active duty military personnel who had suffered from a mild episode of TBI, the presence of an *APOE*-ε4 allele was found to cause impairments in memory, specifically in learning and recall (Crawford et al., 2002). A recent study extended on these findings and demonstrated that following moderate to

severe TBI, subjects carrying the ε4 allele were impaired on tests of verbal memory, motor speed, fine motor coordination, visual scanning, attention and mental flexibility (Ariza et al., 2006). Analysis of autopsy material has revealed a number of pathological changes in ε4 carriers, particularly an increased presence of cerebral amyloid angiopathy and cerebrovascular contusions (Leclercq et al., 2005, Smith et al., 2006). A neurological and behavioural study on professional boxers, who regularly underwent chronic TBI during their sporting career, it was found that ε4 carriers were more likely to suffer from chronic neurological deficits (Jordan et al., 1997). Similarly, in a group of older American football players subjected to repeated head trauma throughout their careers, possession of the ε4 allele was linked to impaired cognitive performance (Kutner et al., 2000).

1.7.3 Animal models for investigating the role of apoE

1.7.3.1 Localisation and upregulation of apoE in animal models of brain injury

Further information on the distribution of apoE following brain injury was obtained from various animal models. In normal rodent brain, apoE was distributed in astrocytic cells of the CNS and within the non-myelinating cells of the PNS (Boyles et al., 1985). However, in a model of rat global ischaemia induced by cardiac arrest, apoE was observed localized to neurons 6 hours following the insult (Kida et al., 1995) rising to maximal expression 7 days post-ischaemia. Further investigation of the distribution of apoE following global ischaemia in the rat revealed increased astrocytic apoE at 24 hours reperfusion, followed by an increase in neuronal apoE at 72 hours reperfusion (Horsburgh and Nicoll, 1996). These data suggest that apoE is produced and secreted by astrocytes for neuronal uptake following injury. Interestingly, these changes in apoE upregulation and redistribution mirror the progression of damage after global ischaemia. Consistent with this hypothesis, other researchers have demonstrated upregulation of apoE protein in neurons, astrocytes and macrophages following focal cerebral ischaemia in the rat, while apoE mRNA was only found expressed in astrocytes and macrophages (Nishio et al., 2003, Kamada et al., 2003). Injury induced alterations in apoE have also been observed in other rodent species. Upregulation of apoE protein was observed in the selectively

vulnerable hippocampus of gerbils after transient global ischaemia (Hall et al., 1995, Ishimaru et al., 1996). A parallel study demonstrated upregulation of apoE and GFAP mRNA in ischaemic gerbil brain (Ali et al., 1996). Similarly, upregulation of apoE was observed in vulnerable regions associated with global ischaemic damage in mouse brain (Horsburgh et al., 1999). Other animal models of brain injury also induce spatiotemporal alterations of apoE. Following acute subdural haematoma in rat, apoE levels are elevated and rapidly redistributed to neurons (Horsburgh et al., 1997). Recently, it has been shown that traumatic brain injury induced through fluid percussion in rats causes both an acute and chronic upregulation of apoE protein and mRNA (Iwata et al., 2005).

1.7.3.2 Transgenic models of apoE-deficient mice

The development of apoE-deficient mice provided another avenue for investigation into the role of apoE in brain injury. ApoE-deficient mice have been developed by a number of groups (Piedrahita et al., 1992, Van Ree et al., 1994, Plump et al., 1992). These mice have a uniformly poorer outcome after brain injury, as shown through models of global ischaemia (Horsburgh et al., 1999, Sheng et al., 1999, Kitagawa et al., 2002), focal ischaemia (Laskowitz et al., 1997, Kitagawa et al., 2001), traumatic brain injury (Lomnitski et al., 1997, Chen et al., 1997, Lynch et al., 2002) and ageing (Masliah et al., 1995). These studies cumulatively demonstrate that apoE exerts a neuroprotective effect against brain injury. This neuroprotective role was confirmed by a number of studies showing amelioration of neurological and pathological deficits in apoE-deficient mice by infusion of recombinant apoE. Infusion of recombinant apoE3 and E4 reversed cognitive deficits and participated in restoration of neuronal structure (Masliah et al., 1997). Intraventricular infusion of apoE in apoE-deficient mice subjected to global ischaemia significantly reduced ischaemic neuronal damage by approximately 50%. The neuroprotective effects of apoE infusion were also observed in wild-type mice following global ischaemia (Horsburgh et al., 2000).

1.7.3.3 Differences between human and mouse apoE

Unlike human apoE, mouse apoE does not exist in multiple isoforms. Mouse apoE is 285 amino acids in length, 14 shorter than human apoE (Rajavashisth et al., 1982). Mouse apoE contains arginine at residue 112 and glutamate at 255, giving it a sequence similarity to human apoE4. However, the lack of an arginine at position 61 on mouse apoE means that mouse apoE cannot display the same domain interaction as human apoE4. Therefore, mouse apoE3 has a functional similarity to human apoE3, with a preferential binding for HDL rather than VLDL. Replacement of mouse threonine at position 61 with arginine via gene targeting introduces domain interaction and allows the altered mouse apoE to behave like human apoE4 (Raffai et al., 2001). Mouse apoE is predominantly astrocytic, with no neuronal apoE reported in normal mouse brains. Human apoE is also principally astrocytic, although expression of apoE mRNA has been demonstrated in cortical and hippocampal neurons in mice (Xu et al., 1999).

1.7.3.4 Transgenic models of human apoE-expressing mice

Mice only express one isoform of apoE compared to the three found in humans. Therefore, the development of human apoE isoform transgenic mice was an integral step in determining isoform specific differences for the role of apoE. Xu et al., (1996) introduced human *APOE* ε2, ε3 and ε4 genes into the apoE-deficient mice produced by Piedrahita et al., (1992). These mice were generated through the use of genomic fragments which contained the regulatory regions. Therefore, expression of apoE was under the control of the human promoter. The expression of human apoE normalises the high serum cholesterol observed in apoE-deficient mice. Western blot analysis revealed presence of human apoE protein in the expected tissues; serum, brain, liver, kidney, spleen, heart and skeletal muscle. Importantly, the pattern of apoE immunocytochemical localisation for these mice resembles human and primate brain rather than rodent brain. ApoE immunoreactivity was observed in glial cells, and to a lesser degree in neurons, as opposed to the rodent pattern, which is strictly glial. Therefore, information gleaned on the role of apoE isoform from these mice can be reasonably translated to the human situation. Accordingly, these transgenic

mice were utilised in this thesis in order to elucidate apoE isoform differences on MHP36 stem cell integration.

Other strains of human apoE transgenic mice have been generated in order to investigate cell specific localisations of apoE. In the CNS, apoE is synthesized by glia, primarily astrocytes (Boyles et al., 1985, Pitas et al., 1987), and also by microglia (Nakai et al., 1996, Stone et al., 1997). Therefore, Sun et al. (1998) created transgenic mice in which expression of human *APOE*-ε3 and ε4 is under control of the astrocyte-specific GFAP promoter. These GFAP-apoE mice expressed human apoE in astrocytes from development into the adult period, with a similar expression pattern to endogenous mouse GFAP and apoE. Human apoE levels from adult mouse brain forebrain were comparable to levels from human cortex. Another strain of transgenic mice was generated with expression of human *APOE*-ε3 and ε4 under control of the neuron-specific enolase (NSE) promoter (Raber et al., 1998, Buttini et al., 1999). The rationale for generating these mice was based on the findings that apoE physiologically localises to neurons in humans, along with the well documented propensity of apoE to redistribute from glia to neurons following neuronal damage. Human apoE expression was localised to the brain and testes, with no apoE found in plasma. Therefore, these mice had raised cholesterol levels, similar to that seen in apoE-deficient mice. A similar pattern of neuronal apoE expression was observed for both NSE-apoE3 and NSE-apoE4 lines, with a high intensity of staining in the neocortex and hippocampus.

Researchers have utilised these human apoE transgenic mice in order to elucidate the role of apoE isoform on brain injury. Human *APOE*-ε4 transgenic mice exhibited increased ischaemic neuronal damage compared to human *APOE*-ε3 mice from the Xu strain following transient global ischaemia (Horsburgh et al., 2000). Similarly, in the same strain of mice, *APOE*-ε4 mice were more susceptible than *APOE*-ε3 mice to various forms of brain damage; namely a larger infarct volume following focal ischaemia (Sheng et al., 1998); increased mortality and poorer neuropathology after closed head injury (Sabo et al., 2000); and impaired neuronal plasticity following entorhinal cortex lesion (White et al., 2001). Neuronal specific expression of human

apoE3, but not apoE4, protected against excitotoxin induced neuronal damage (Buttini et al., 1999). These results confirm clinical studies that the *APOE*-ε4 allele is associated with a poorer outcome after brain injury. Taken together, these studies provide a wealth of evidence that apoE has a role in regulating the response and outcome following injury to the CNS. Whilst the mode of action by which apoE exerts these beneficial effects remains to be elucidated, researchers have implicated apoE in a variety of possible mechanisms.

1.7.4 Mechanisms of apoE in moderating brain damage

1.7.4.1 Excitotoxicity

In the past few years, there has been increasing evidence that apoE influences excitotoxic damage and that this is isoform dependent. *In vivo* studies have shown that kainic acid injections induce upregulation in apoE mRNA (Montpied et al., 1999) and protein, coupled with subsequent localisation to neurons (Boschert et al., 1999). Following kainic acid challenge in human apoE3 and apoE4 transgenic mice in which apoE is under the control of the NSE promoter, it has been shown that apoE3 exerts neuroprotective effects against excitotoxic damage, whilst no protection was conferred through apoE4 expression (Buttini et al., 1999). Application of physiologically relevant concentrations of apoE partially protected against NMDA induced excitotoxicity in both primary mixed neuronal-glial cultures and in a neuronal cell line (Aono et al., 2002). Further investigation suggested that the receptor binding region of apoE was responsible for mediating the neuroprotective effect (Aono et al., 2003). In primary neuronal-glial cultures exposed to hydrogen peroxide, treatment with apoE confers partial protection (Lee et al., 2004). ApoE treatment does not affect the release of glutamate induced by hydrogen peroxide, but instead increases the rate of glutamate reuptake, suggesting that apoE protects against oxidative stress by reducing secondary glutamate excitotoxicity. Co-application of recombinant human apoE3 or apoE4 with NMDA on primary hippocampal neurons revealed an isoform specific effect on calcium response (Qiu et al., 2003). ApoE4 significantly increased both the resting calcium levels and the calcium response to NMDA, whilst apoE3 exerts an opposite effect. This was coupled with an increase in neurotoxicity with apoE4 treatment. However,

subsequent work demonstrated that alteration of calcium influx through NMDA receptors is due to ligand binding to apoE receptors, such as LRP or apoER2 (Bacskai et al., 2000, Ohkubo et al., 2001, Qiu et al., 2002).

1.7.4.2 Anti-oxidative capacity

A variety of studies have suggested that apoE may have anti-oxidative properties. Purified apoE, commercially purchased recombinant apoE and apoE conditioned media were all able to protect B12 cells from peroxide free radical induced cytotoxicity *in vitro* (Miyata and Smith, 1996). There was an isoform specific effect in the anti-oxidative potential of apoE, with apoE2 > apoE3 > apoE4. As well as protecting against chemically induced oxidative stress, apoE is also able to modulate beta-amyloid (Aβ) induced oxidation (Lauderback et al., 2002). *In vivo* studies on apoE-deficient mice demonstrated that plasma and lipoproteins obtained from these mice are more susceptible to lipid peroxidation, both in the presence or absence of a free radical generating substance (Hayek et al., 1994). Further studies have attributed this susceptibility to decreased levels of antioxidants in apoE-deficient mice, leading to a deleterious imbalance in oxidant/antioxidant levels (Ramassamy et al., 2001, Shea et al., 2002). Oxidative stress is a common feature of ischaemia and traumatic brain injury. The poorer outcome of apoE-deficient mice after closed head injury is therefore partially attributable to a diminished ability to counteract the deleterious effects of oxidative damage (Lomnitski et al., 1997, 1999). Pre-treatment of apoE-deficient mice with the anti-oxidant vitamin E markedly ameliorated ischaemic neuronal damage (Kitagawa et al., 2002). Infusion of apoE also reduces the extent of 4-hydroxynonenal (4-HNE) immunoreactivity in mouse brain following global ischaemia (Horsburgh et al., 2000). 4-HNE activity is a toxic marker for lipid peroxidation and has been associated with the pathology of Alzheimer's disease and global ischaemia (McKracken et al., 2001). Taken together, these studies strongly suggest that apoE exerts its neuroprotective effect through anti-oxidative action. The aforementioned effects of apoE on excitotoxicity have also been linked to the anti-oxidative properties of apoE (Buttini et al., 1999, Lee et al., 2004).

1.7.4.3 Cytoskeletal support

The neuronal cytoskeleton consists of three major components; actin filaments, microtubules and neurofilaments. Preservation of the neuronal cytoskeleton is an important factor for maintaining structural and functional stability. Ultrastructural examination of synapses from apoE-deficient mice revealed a disruption of dendritic structure, characterised by extensive dendritic vacuolation. This was coupled with a decrease in immunostaining for the cytoskeletal markers microtubule associated protein 2 (MAP2), alpha and beta-tubulin (Masliah et al., 1996), strongly suggesting that the presence of apoE is required for maintenance of the synapto-dendritic structure. ApoE demonstrates isoform specific interactions with several cytoskeletal proteins, including actin, MAP2, tau and neurofilament-M (Strittmatter et al., 1994, Huang et al., 1994, Fleming et al., 1996). Specifically, apoE3 undergoes high affinity binding to these proteins whilst apoE4 does not. It has been hypothesized that apoE3 binding to tau prevents self-aggregation of tau to form paired helical fragments and neurofibrillary tangles, whilst promoting the association of tau with beta-tubulin for increased microtubule stability (Roses et al., 1996). Conversely, the inability of apoE4 to modulate this results in accumulation of hyperphosporylated tau in humans and mice expressing the APOE-ε4 gene (Tesseur et al., 2000, Brecht et al., 2004, Thaker et al., 2003). ApoE3 stimulates β-tubulin polymerisation and stabilisation of microtubules, whilst apoE4 destabilises microtubule assembly (Nathan et al., J Biol Chem, 1995). Microtubule reorganization and assembly is strongly associated with the maintenance and modulation of neurite outgrowth. Cell culture studies have shown that apoE is able to modulate neurite outgrowth in Neuro-2A cells (Bellosta et al., 1995, DeMattos et al., 1998), rabbit dorsal root ganglion cells (Handelmann et al., 1992, Nathan et al., 1994), and adult mouse cortical neurons (Nathan et al., 2002). This modulation is dependent on apoE isoform, with apoE3 and apoE2 inducing neurite outgrowth, whilst apoE4 acts in an inhibitory manner. However, it has been shown that apoE does not escape from the endocytic pathway into the cytosol, and is therefore unable to interact directly with any of the cytoskeletal components (DeMattos et al., 1999). This raises the issue of how apoE is able to mediate cytoskeletal changes. It has been postulated that apoE may exert cytoskeletal

influence through binding to cell surface receptors and susbsequent signal transduction (Nathan et al., 2002, Ohkubo et al., 2001, Hoe et al., 2005)

1.7.4.4 Immune modulation

ApoE also has also been shown to exhibit immunomodulatory properties. ApoE suppresses proliferation of both $CD4^+$ and $CD8^+$ T cell lymphocytes and it exerts this inhibition by partially reducing the activity of interleukin-2 (Kelly et al., 1994). In mixed neuronal-glial cultures from apoE-deficient mice, preincubation with human recombinant apoE blocked glial secretion of tumour necrosis factor α (TNF-α). This effect was independent of cell viability (Laskowitz et al., 1997). Microglial activation and release of TNF-α was also suppressed by biologically relevant concentrations of apoE (Laskowitz et al., 2001). Other inflammatory molecules downregulated by apoE include interleukin 1β and interleukin 6 (Lynch et al., 2001). The immune modulation properties of apoE also manifest on a biologically relevant level, with apoE-deficient mice exhibiting increased susceptibility to endotoxaemia after lipopolysaccharide injection and impaired immunity after infection with *Klebsiella pneumonia* (de Bont et al., 1999) or *Listeria monocytogenes* (Roselaar and Daugherty, 1998). ApoE-deficient mice did not differ from control C57Bl/6 mice in thymic, splenic or bone marrow lymphocyte populations. However, apoE-deficient mice had significantly higher levels of antigen-specific IgM and impaired delayed type hypersensitivity after immunisation with tetanus toxin, suggesting that apoE modulates the humoral and cell-mediated immune response (Laskowitz et al., 2000). ApoE has also been hypothesized to exert an anti-inflammatory role in the CNS through attenuation of Aβ induced glial activation (Hu et al., 1998).

1.8 Role of ApoE Receptors in Cellular Communication

1.8.1 The LDL receptor family

ApoE binds to members of the LDL receptor family. The LDL receptor family is an evolutionary ancient gene family of structurally conserved cell-surface proteins. In mammals, there are seven core members of the LDL receptor family (Figure 1.5). These are the LDL receptor (LDLR), the LDL receptor-related protein (LRP1), the VLDL receptor (VLDLR), the apoER2 receptor, megalin (a.k.a. gp330, LRP2), the

LRP1b receptor and multiple epidermal growth factor repeat containing protein 7 (MEGF7). ApoE has been demonstrated to be a ligand for the majority, but not all of these receptors. Members of the LDL receptor gene family share five common motifs: 1) a ligand binding type cysteine-rich repeat domain, 2) epidermal growth factor type cysteine-rich repeats, 3) a YWTD (tyrosine, tryptophan, threonine, aspartate) domain that fold in β-sheets to form a propeller structure, 4) a single transmembrane segment, 5) a cytoplasmic tail containing one or more "NPxY" (Asp-Pro-x-Tyr) motifs which function as endocytosis signals and are involved in signal transduction. Some members of the LDL receptor family contain an O-linked sugar domain directly preceding the transmembrane segment, but otherwise there is an absence of other structural domains. Extended members of the LDL receptor family include LRP5, LRP6 and LR11 (a.k.a SORLA). These receptors are closely related but do not fulfil the stringent structural requirements to be classified as a core family member. The primary function of LDL receptor family members is to regulate cholesterol homeostasis by receptor-mediated endocytosis of lipoproteins particles. However, there is growing experimental evidence that the LDL receptor family may also have an additional role in signal transduction. The following members of the LDL R family are able to bind apoE.

1.8.1.1 LDLR

The LDL receptor (LDLR) was the first member of the LDL receptor family to be identified by Brown and Goldstein whilst investigating the genetic background of the disease familial hypercholesterolaemia (Brown and Goldstein, 1986). It is ubiquitously expressed in all tissues are varying levels, including the brain. The main physiological function of the LDLR is to regulate cholesterol homeostasis by transporting lipoprotein particles into cells. Unlike the following members of the LDL receptor family, the LDLR does not appear to have a critical role in the development of the nervous system. In a strain of rabbits (Kita et al., 1982) with a defective LDLR gene and transgenic LDLR knockout mice (Ishibashi et al., 1993), as well as in humans with familial hypercholesterolaemia, neural development is unaffected.

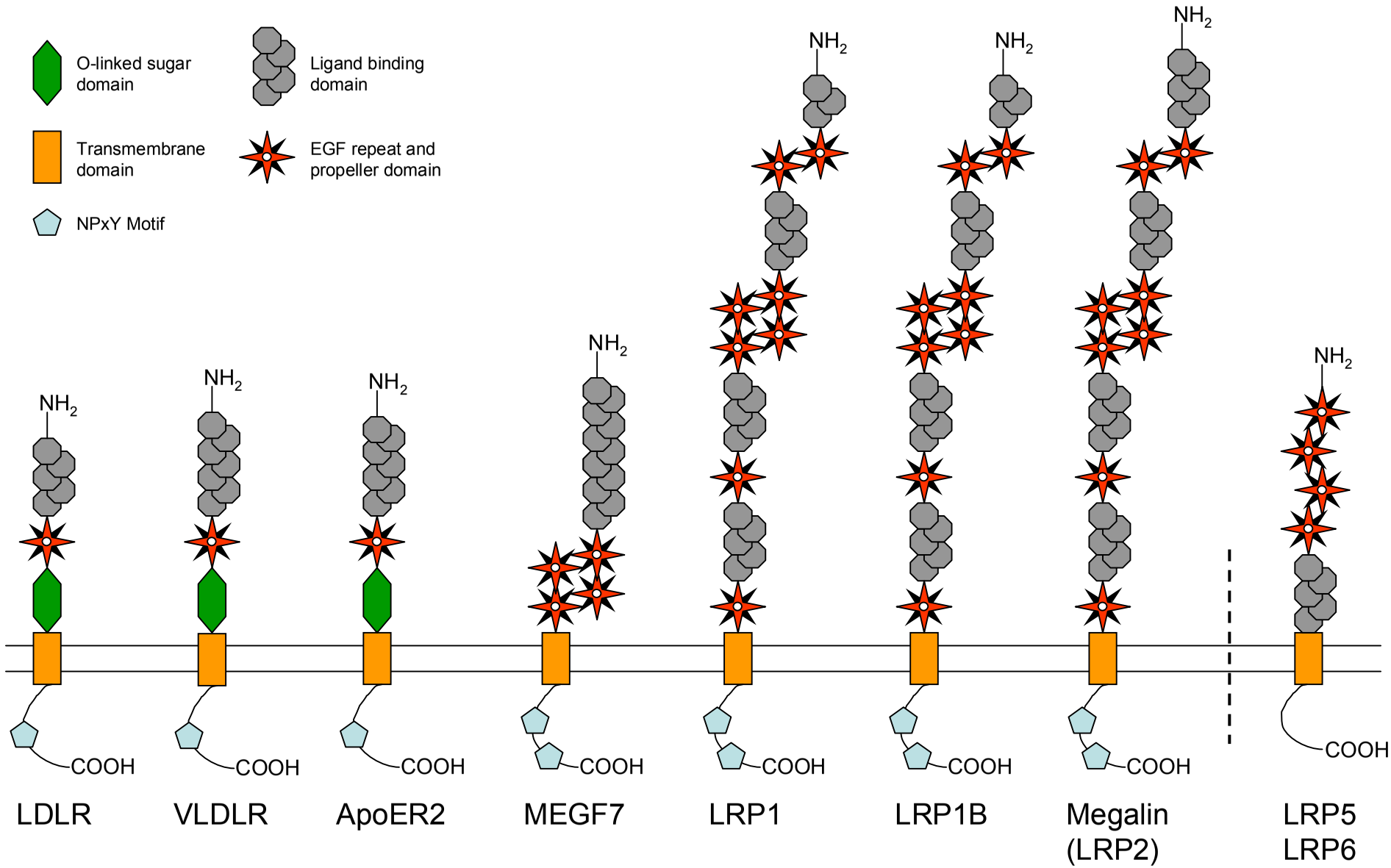

Figure 1.5 Schematic representation of the LDL receptor gene family in mammals
The seven core members of the mammalian LDL receptor family are shown on the left of the dotted line. An extended member of the gene family (LRP5/6) is shown on the right of the dotted line.

1.8.1.2 LRP1

LRP1 is an extremely large protein (~600 kDa) ubiquitously expressed throughout the body, although primarily abundant on hepatocytes and neurons. LRP1 can recognize over 30 different ligands. Physiologically, LRP1 acts as a receptor for endocytosis of chylomicron remnants and signal transduction (Herz and Strickland, 2001). *Lrp1*-deficient mice do not undergo normal neural development and are embryonic lethal (Herz et al., 1992), demonstrating that the LRP1 has an integral role in embryogenesis. Transgenic mice selectively lacking LRP1 in exhibit severe behavioural and motor abnormalities including tremor, ataxia, hyperactivity and eventually suffer from premature death. However, the CNS of these animals is histoanatomically normal, suggesting that this phenotype is a result of a functional defect in LRP1-deficient neurons (May et al., 2004). Interaction of α-2-macroglobulin with LRP1 regulates calcium response to NMDA in primary cultured neurons (Qiu et al., 2002), implicative of a role in synaptic transmission. Further evidence arises from the finding that LRP1 lies in close proximity to the NMDA receptor in dendritic synapses and co-precipitates with PSD-95 and subunits of the NMDA receptor from neuronal cell lysates (May et al., 2004). LRP1 is also involved in the proteolytic processing of amyloid precursor protein (APP) to generate Aβ, providing a possible link with Alzheimer's disease (Pietrzik et al., 2002).

1.8.1.3 Megalin / LRP2

Megalin (a.k.a. LRP2) is another large member of the LDL receptor family with a similar size to LRP1. It is commonly expressed on absorptive and secretory epithelia, with the highest level of expression on the epithelial cells that line the proximal tubules in the kidney. Megalin can bind a variety of ligands, including lipoproteins, vitamin-binding proteins, and hormones and signalling molecules. Physiologically, megalin functions as a scavenging receptor for reuptake of low molecular weight proteins. One well-characterised example is the reuptake of vitamin D binding protein from the glomerular filtrate in the proximal renal tubules, with megalin deficient mice suffering from proteinuria and vitamin D deficiency (Nykjaer et al., 1999). These knockout mice also suffer from a defect in forebrain development,

resulting in a fusion of the forebrain hemispheres termed holoprosencephaly (Willnow et al., 1996). Mutations in the sonic hedgehog (Shh) gene also cause a holoprosencephalic syndrome (Belloni et al., 1996, Roessler et al., 1996), implying that megalin may be involved in Shh signalling. Initial studies suggested that a conditional deletion of megalin in the neuroepithelium leads to a loss of Shh expression in the ventral forebrain, which occurs due to an increase in Bmp4 signalling, a negative regulator of Shh (Spoelgen et al., 2005). It appears that megalin is able to regulate signal transduction of the Shh signalling pathway, and it may do this by directly binding to Bmp4 (Spoelgen et al., 2005).

1.8.1.4 VLDLR

The VLDLR has a very similar primary structure to LDLR, differing only in an additional cysteine-rich repeat domain in the ligand binding motif. This similarity results in a similar binding affinity to apoE as LDLR. However, there is no expression of VLDLR in the liver. Instead, VLDL receptors are located in developing and adult brain, heart and skeletal muscle. The expression pattern of the VLDLR suggest a minimal role in lipoprotein metabolism, a fact borne out by VLDLR knockout mice, which do not suffer from any deficiency in VLDL metabolism and have a similar lipoprotein profile to normal mice (Frykman et al., 1995). The main physiological role of the VLDLR is regulation of migration and layering of neurons in the cortex and cerebellum during development, a role also performed by the apoE receptor 2 (apoER2) in association with the reelin ligand.

1.8.1.5 ApoER2

ApoER2 has a close structural similarity to the LDLR and therefore also to the VLDLR. Similar to VLDLR, it is not expressed in the liver, suggestive of a primary role other than lipoprotein metabolism. Instead, apoER2 expression is limited to the brain and testes (Novak et al., 1996, Stockinger et al., 1998), and is abundantly expressed on neurons (Stockinger et al., 1998, Wolf et al., 1992). Knockout mice deficient in apoER2 appear normal, but the males are virtually sterile, demonstrating that apoER2 is critical for sperm production or survival. These mice also suffer from a developmental defect in the neocortex and hippocampus, evidenced by a failure of

the neurons to migrate to their proper positions. This defect is also manifest in VLDLR knockout mice, and has a striking phenotype similar to *reeler* mutant mice (Trommsdorff et al., 1999).

1.8.1.6 ApoER2 and VLDLR interact with the Reelin signalling pathway

Reeler mutant mice were originally discovered in the early 1950s (Falconer, 1951). This genetic mutation manifests by incomplete development of the foliation pattern of the cerebellum. Reelin is a large secreted protein expressed primarily in nervous tissues. Functional mutations in reelin result in disrupted formation of the neocortex, cerebellum and spinal cord during development (D'Arcangelo et al., 1995). On a microscopic level, the loss of reelin expression interferes with radial migration and final positioning of the neurons in the regions affects, resulting in the classical laminated appearance of the cortex. Aside from VLDLR / apoER2 deficient mice; there are two other mutant strains which are phenotypically indistinguishable from reeler mice, but have a mutation located on a different gene. The genetic defect on these mice, termed *scrambler* and *yotari*, was mapped to the Disabled-1 (*dab1*) gene (Sheldon et al., 1997, Ware et al., 1997). As expected, Dab1 deficient mice also exhibit the same phenotype (Howell et al., 1997), but a strain of mice deficient in both Reelin and Dab1 did not suffer from a compounded phenotype, suggesting that Reelin and Dab1 are components in a linear pathway that determines cortical development. As Reelin is a secreted, extracellular protein, and Dab1 is a cytoplasmic adaptor protein, the discovery of the VLDLR / apoER2 knockout mouse phenotype strongly suggested that both these neuronal apoE receptors could function as receptors for Reelin (Tromsdorff et al., 1999). Reelin binding to apoER2 and VLDLR is inhibited by the presence of apoE (D'Arcangelo et al., 1999). Supporting evidence for the roles of VLDLR and apoER2 in the Reelin signalling pathway came from blockade of Reelin binding with recombinant receptor associated protein, a universal inhibitor of ligand binding for members of the LDL receptor family. In the absence of Reelin binding to the apoE receptors, no tyrosine phosphorylation of Dab1 occurred, which is an essential step in the Reelin signalling pathway (Howell et al., 2000). The Reelin signalling pathway can also affect microtubule stabilization,

with Reelin and VLDLR / apoER2 deficient mice exhibiting hyper-phosphorylation of the microtubule stabilizing protein, tau (Hiesberger et al., 1999). Two downstream signalling pathways have been implicated in this process. Reelin can activate the phosphatidylinositol-3-kinase (PI3K) / protein kinase B (PI3K/AKT) pathway, which then inhibits the tau kinase, glycogen synthase kinase 3β (GSK3β) (Beffert et al., 2002, Bock et al., 2003). Alternatively, Reelin can bind to the Ser/Thr kinase cyclin-dependent kinase 5 (cdk5) pathway. Cdk5 can bind to a number of substrates that regulate microtubule assembly, including tau and NUDEL (Ohshima et al., 2001, Beffert et al., 2004). Interestingly, Reelin has also been implicated in synaptic plasticity. The VLDLR / apoER2 knockout mouse displays long-term memory deficits for contextual fear conditioning, and slice electrophysiology on these animals reveals moderate to pronounced impairments in LTP. In a converse experiment using slices taken from wildtype mice, application of Reelin enhanced tetanus dependent LTP. This enhancement in LTP required the presence of apoER2 and VLDLR (Weeber et al., 2002). Further work has shown that apoER2 associates with NMDA receptors at the postsynaptic density, and that Reelin is able to increase NMDA receptor mediated whole cell current dependent on the splicing of apoER2 (Beffert et al., 2005).

1.8.1.7 LRP5 and LRP6

Other LDL receptor family members involved in cell signalling are LRP5 and LRP6. These receptors are intimately involved in the Wnt signalling pathway; although at the current time there is inconclusive evidence that apoE can act as a ligand (Kim et al., 1998). A recent paper has shown that apoE4 was able to inhibit the canonical Wnt signalling pathway *in vitro* through the LRP5 and LRP6 receptor (Caruso et al., 2006).

1.8.2 Role of apoE in cell signalling pathways

The fact that the majority of these LDL receptors can bind apoE raises the possibility that apoE is able to modulate various signal transduction pathways. ApoE has been shown to inhibit smooth muscle cell migration and proliferation (Ishigami et al., 1998, Ishigami et al., 2000, Hui and Basford, 2005). ApoE binds to heparan sulphate

proteoglycans through its primary role in lipoprotein transport. However, through this binding and subsequent activation of inducible nitric oxide synthase, apoE is also able to regulate inhibition of cell proliferation (Ishigami et al., 2000, Swertfeger and Hui, 2001). In contrast, inhibition of cell migration by apoE appears to be mediated by binding to LRP1 and subsequent activation of cyclic AMP-dependent protein kinase A (Swertfeger et al., 2002, Zhu and Hui, 2003). Binding of the LRP1 receptor by certain ligands such as apoE and α2-macroglobulin has been shown to increase neurite outgrowth through activation of the extracellular signal-regulated kinase 1 and 2 (ERK1/2) (Qiu et al., 2004). Phosphorylation of ERK1/2 leads to translocation of ERK1/2 to the nucleus of the cell, where it can then phosphorylate the cyclic AMP response binding element protein (CREB). CREB is a multipurpose transcription factor that has been implicated in a wide variety of mechanisms, such as synaptic plasticity, cell proliferation and protection of the brain from neurodegeneration (Deisseroth et al., 1996, Della Fazia et al., 1997, Mantamadiotis et al., 2002), suggesting that apoE binding can influence a large variety of events. However, Ohkubo et al., (2001) suggested that the activation of CREB by apoE was isoform dependent, with apoE4 but not apoE3 able to stimulate CREB transcription through the ERK1/2 cascade. Interestingly, CREB activation by apoE4 induced a number of genes including the anti-apoptotic gene *Bcl-2*, suggesting a possible route by which apoE could influence cell survival. ApoE has also been suggested to influence quiescence and survival of human neural progenitor cells through regulation of chemokines (Krathwohl and Kaiser, 2004). Activation of CCR3 and CXCR4 receptors by their respective chemokines eotaxin and SDF-1 inhibited cell proliferation and induced cellular quiescence. These quiescent progenitor cells maintained their multipotential ability to differentiate into neurons and astrocytes. However, apoE3 but not apoE4 was able to reverse the inhibitory effects of the chemokines. This suggests that apoE may be able to regulate cell proliferation and differentiation in an isoform-dependent manner.

As described previously, apoER2 and VLDLR interactions with Reelin have been implicated in synaptic plasticity. Reelin binding to apoER2 and VLDLR serves to enhance synaptic transmission in the hippocampus (Weeber et al., 2002) and this

enhancement can be modulated by splicing of apoER2 (Beffert et al., 2005). Another association between apoE and Reelin ligands has been demonstrated by Ohkubo et al. (2003). Upon mating of Reelin deficient mice to apoE deficient mice, that discovered that tau phosphorylation increased as the amount of apoE protein decreased. These alterations in tau phosphorylation were paralleled with an increase in the activity of the protein kinase glycogen synthase kinase-3β (GSK-3β). These data suggest that the ligand binding of apoE and Reelin to the receptors apoER2 and VLDLR mediates tau phosphorylation through a signal transduction cascade involving activation of GSK-3β.

These findings were substantiated by a recent comprehensive study that directly implicated apoE in three major signalling pathways; the ERK, c-jun N-terminal kinase (JNK) and Dab1 pathways (Hoe et al., 2005). Treatment of primary neurons with apoE or an apoE-derived peptide for the receptor binding domain significantly increased ERK1/2 and Dab1 phosphorylation whilst decreasing activation of JNK1/2. The activation of ERK1/2 and Dab1 are dependent on the calcium influx via the NMDA receptor. Co-immunoprecipitation experiments demonstrated that the apoER2 receptor interacts with the NMDA receptor in a multi-protein complex with PSD-95 (Hoe et al., 2006). These results were consistent with previous findings that apoE receptors and by implication their ligands, are able to influence calcium influx through NMDA receptors (Qiu et al., 2003, Beffert et al., 2005, Ohkubo et al., 2001, Bacskai et al., 2000). Taken together, these results suggest that apoE may influence molecular mechanisms of memory. ApoE mediated regulation of JNK1/2 required γ-secretase and G protein activity. Interestingly, apoER2 and LRP can be cleaved by the γ-secretase complex so that the intracellular component is released into the cytoplasm (May et al., 2003), suggesting that regulation of JNK signalling is through the production of soluble fragments of these LDL receptors.

1.9 Potential Role of ApoE in Survival, Migration and Differentiation of Grafted MHP36 Stem Cells

1.9.1 Key factors indicative of apoE-mediated support

The previous sections have demonstrated the integral role of apoE in providing support and promoting a favourable outcome after brain damage. ApoE may exert a neuroprotective influence, reducing the extent of damage in a variety of neurological disorders (Saunders et al., 1993, Strittmatter et al., 1993, Horsburgh et al., 1999, Sheng et al., 1999, Kitagawa et al., 2002, Laskowitz et al., 1997, Kitagawa et al., 2001, Lomnitski et al., 1997, Chen et al., 1997, Lynch et al., 2002, Masliah et al., 1995). The support role of apoE is also illustrated through synaptic remodelling of damaged circuitry (Poirier et al., 1991, 1993, Petit-Turcotte et al., 2005). Alternative mechanisms exist through which apoE could modulate protection and plasticity, such as excitotoxicity (Boschert et al., 1999, Buttini et al., 1999), anti-oxidation (Miyata and Smith, 1996, Pederson et al., 2000), cytoskeletal support (Masliah et al., 1996) and immune modulation (Laskowitz et al., 1997, Laskowitz et al., 2001). ApoE may also influence cell signalling pathways which are implicated in survival, migration and differentiation (Ishigami et al., 1998, Ishigami et al., 2000, Swertfeger et al., 2002, Zhu and Hui, 2003, Hoe et al., 2005). In particular, apoE promotes the survival of human neural progenitor cells (Krathwohl and Kaiser, 2004).

1.9.2 Initial evidence for the association of apoE with MHP36 stem cell grafts

The previously referenced study by Modo et al., (2003) was the first to postulate a link between apoE and MHP36 neural stem cell graft integration. MHP36 grafts induced an upregulation of apoE contralateral to the focal ischaemic lesion, suggesting that the stem cell grafts act in conjunction with apoE to promote reorganization and remodelling of the brain circuitry after damage. Another preliminary study has confirmed upregulation of apoE in association with MHP36 grafts (Dr Iris Reuter, Personal Communication). Intriguingly, these upregulated levels of apoE were maintained over a period of 6 weeks, during which time the animals exhibited functional recovery. These preliminary studies have demonstrated

that there is an association between apoE and MHP36 stem cell integration. This thesis will extend on previous findings and investigate the interaction between apoE and MHP36 neural stem cell graft survival, migration and differentiation in mammalian brain.

1.10 Aims of Thesis

This thesis tests the hypothesis that apoE is critical in stem cell integration and investigates whether this effect is *APOE* genotype dependent, in a mouse model of global cerebral ischaemia. The specific aims to test this hypothesis are as follows:

1. To characterise neural stem cell grafts in a mouse model of global ischaemia

2. To investigate the influence of apoE on MHP36 neural stem cell grafts in a mouse model of global ischaemia

3. To investigate the influence of *APOE* genotype on MHP36 neural stem cell grafts in a mouse model of global ischaemia

Chapter 2

Materials and Methods

2.1 Animals

Mice were communally housed in a conventional unit with a twelve-hour light/dark cycle and given unrestricted access to food and water. All procedures were carried out under licence from the Home Office with the approval of the University of Edinburgh Ethical Review Panel and subject to the Animals (Scientific Procedures) Act 1986.

2.1.1 C57Bl/6J mice

Adult male C57Bl/6J mice weighing between 25-30g were purchased from Charles River. C57Bl/6J is the most widely used inbred strain, due to the fact that they breed well and are long-lived. It is commonly used as the background strain for the production of transgenic mice.

2.1.2 *APOE* transgenic mice

Two strains of apoE transgenic mice were used in this thesis. The apoE-deficient mouse (also referred to as the *APOE*-KO mouse) generated by Dr Nobuyo Maeda (Piedrahita et al., 1992) and the human apoE3 and E4 isoform specific transgenic mice generated by Dr Allen Roses (Xu et al., 1996). Piedrahita et al., (1992) used a targeting plasmid to inactivate the endogenous mouse *APOE* gene in mouse embryonic stem (ES) cells. Chimeric mice heterozygous for the disrupted mouse *APOE* gene were generated by blastocyst injection. Mice homozygous for the disrupted *APOE* gene were bred from two sets of heterozygous mice. Both homozygous and heterozygous were born at the expected frequency and were in good health. Immunodiffusion tests confirmed that the homozygous animals were unable to synthesize mouse apoE. The *APOE*-KO mice used in this thesis were purchased from Charles River UK and bred at the University of Edinburgh.

Xu et al., (1996) isolated and purified human genomic DNA from the lymphoblasts of individuals verified to be homozygous carriers for the *APOε2, ε3* and *ε4* alleles. This DNA was used to form cosmid libraries, which were screened with *APOE* and *APOC1* cDNA in order to identify clones that contained all the regulatory elements required for *APOE* transcription. The selected clones were digested with restriction

enzymes to generate *APOE* genomic fragments, which were microinjected into single cell embryos fertilized by *APOE*-KO mice from the Maeda strain. The mothers were on a background strain of C57Bl/6J x DBA/2J. The offspring were checked for expression of the human *APOE* transgene through use of the polymerase chain reaction (PCR). Founder mice were bred to *APOE*-KO mice to produce animals homozygous for the human *APOE* transgene, and backbred further into *APOE*-KO strains in order to remove the genetic influence of the DBA/2J background strain. Three transgenic mouse lines were generated for *APOE*-ε2 (*ε2-205, ε2-222, ε2-267*), five lines for *APOE*-ε3 (*ε3-393, ε3-414, ε3-428, ε3-437, ε3-453*) and four lines for *APOE*-ε4 (*ε4-20, ε4-43, ε4-64, ε4-81*). Each of these lines carries multiple copies (1-8) of the respective gene, and expression of APOE mRNA was confirmed in serum, along with expected organs such as the brain, liver, kidney, spleen and heart. In this thesis, the transgenic lines used were *APOE ε3-437* and *APOE ε4-81* which both carry two copies of the respective gene.

2.2 *In vivo* Mouse Model of Transient Global Ischaemia

Induction of global ischaemia was carried out by Dr Karen Horsburgh. Mice were anaesthetised with halothane (4% induction, 1.5% maintenance) in a mixture of oxygen and nitrous oxide (30:70). Core body temperature was monitored using a rectal probe and strictly maintained at 37^{o}C using a heating lamp. Global ischaemia was induced via occlusion of the bilateral common carotid arteries (BCCAo) (Kelly et al., 2001, Horsburgh et al., 1999). A small incision was made along the neck, and both common carotid arteries were carefully exposed. Micro-aneurysm clips were used to occlude both arteries for a set period of time (15 or 17 minutes). The clips were removed, and restoration of blood flow was confirmed before the animal was sutured closed. After surgery, the animal recovered in a heated incubator (30^{o}C) for 2 hours before being returned to the housing unit. Animals were provided with soft food following surgery and monitored on a daily basis.

2.3 Stereotaxic Surgery

Mice were anaesthetised with halothane (4% induction, 1.5% maintenance) in a mixture of oxygen and nitrous oxide (30:70) and securely mounted on a stereotaxic

frame (Kopf Instruments). An incision was made along the midline and the skull exposed. All the coordinates are based on bregma as a reference point (Table 2.1). The coronal plates at the caudal and hippocampal levels are shown in Figure 2.1

Direction	Caudate coordinates	Hippocampus coordinates
Medial / Lateral	+2 mm	+1.5 mm
Anterior / Posterior	+0.26 mm	–2 mm
Ventral	–3 mm	–1.5 mm

Table 2.1 Stereotaxic coordinates for the location of caudate and hippocampal injections

A burr hole was drilled at each target coordinate, the dura carefully exposed and a blunt-tip Microliter 7002 syringe (25 gauge, 2µl capacity, Hamilton Company), descended to the required depth. The cell suspension or vehicle (0.5µl at 25,000 cells/µl) was injected over 5 minutes, and the syringe was left in place for another 5 min after injection to allow diffusion of the contents away from the tip. The syringe was removed, and the animal sutured closed. After surgery, the animal recovered in a heated incubator (30^{o}C) for 1 hour before being returned to the housing unit. Animals were provided with soft food following surgery and monitored on a daily basis. In order to achieve reproducible proficiency at stereotaxic injection at the correct co-ordinates, syringe placement was assessed using ink injections prior to definitive studies of cell transplantation. A representative ink injection is shown in Figure 2.2.

2.4 The Rotarod Behaviour Test

The rotarod test is a measure of motor balance and coordination (Jones and Roberts, 1968). The animal was placed on the drum and allowed to orient itself against the direction of rotation before rotation commenced. On the day prior to the first test session, animals received one training session in which they were acclimatised to the rotarod testing environment and taught to run on a rotarod at low speeds (2-6 rpm). Animals were tested on the rotarod at speeds of 8, 16, 24 or 32 rpm for 60 seconds.

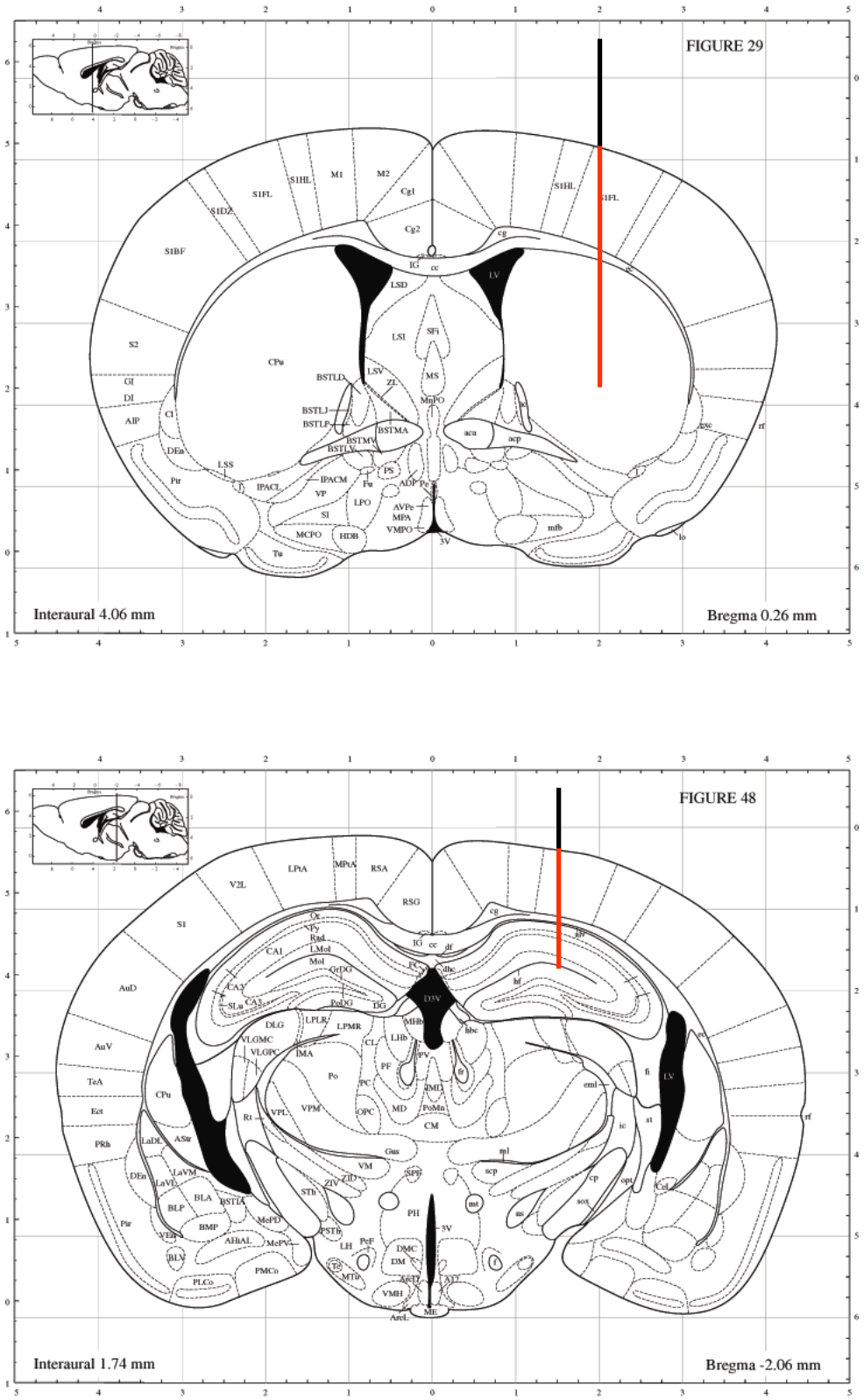

Figure 2.1 Coronal plates of the caudate nucleus (A) and hippocampus (B) illustrating the location of the stereotaxic injections

The depth to which the syringe is descended in outlined in red. (Plates taken from Paxinos and Franklin, The mouse brain in stereotaxic coordinates, 2001).

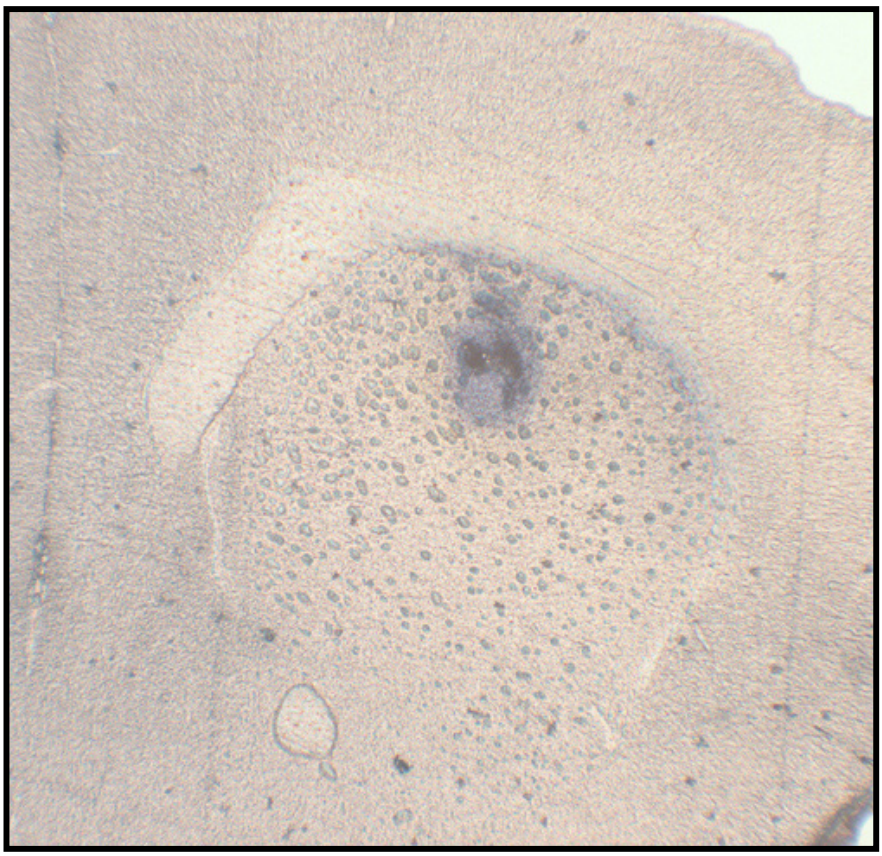

Figure 2.2 Representative micrograph of the ink injection
The ink injection demonstrates correct use of the stereotaxic frame for placement and descension of the Hamilton syringe.

The time taken for the animal to fall off the drum was recorded. Animals received two sessions per week on the rotarod, starting on the week after grafting. One session comprised of three trials at each rotation speed. The rotarod used in this thesis was a Series 8, manufactured by IITC Life Science. This model utilises 1¼ inch diameter textured drums for mice and has the capacity to run 5 lanes as a time.

2.5 Perfusion and Micro-dissection

Mice were anaesthetised with halothane (4% induction, 1.5% maintenance) in a mixture of oxygen and nitrous oxide (30:70) and a sternotomy performed. The diaphragm and ribcage were cut in order to expose the heart. A butterfly needle attached to a syringe pump (Harvard Apparatus) was inserted into the left ventricle. Approximately 25ml of heparinized, ice-cold saline (5000 units / 100ml) was perfused through the animal at a rate of 2.5ml/min^{-1}. The right atrium was cut following infusion in order to ensure complete flow through the animal. Loss of colour in the liver and paws were considered as the sign of a good perfusion. Following the saline perfusion, the animal was subsequently fixed by perfusion of approximately 25ml of 4% paraformaldehyde in phosphate buffer. Satisfactory fixation was observed by rigidity of the extremities. After fixation the animal was decapitated and the skull stored in 4% paraformaldehyde for 24 hours. The brain was then removed from the skull and post-fixed in 4% paraformaldehyde for a further 24 hours. In the event of an unsatisfactory perfusion fixation, the brain was immediately removed and post-fixed in paraformaldehyde for 48 hours.

If micro-dissection and freezing of tissue was required, the animal was rapidly perfused with heparinized ice-cold saline and decapitated. The brain was rapidly removed, transferred to a pre-chilled petri dish on ice and rinsed with ice-cold saline. It was then placed in a pre-chilled mouse brain matrix and 2mm coronal sections at the level of the caudate and hippocampus were cut. The coronal sections were transferred back to the petri dish for micro-dissection. The ipsilateral (hemisphere receiving the graft) and contralateral caudate nucleus and hippocampus were carefully removed using a pair of forceps and placed in individual, labelled 1.5ml

Eppendorf tubes before snap-freezing in liquid nitrogen. Frozen tissue was stored at –80°C.

2.6 Brain Processing and Sectioning

Following post-fixation, brains were cryoprotected by graded immersion in 10, 20 and 30% sucrose in phosphate buffer. The brains were then frozen by one of two methods. In the first method, the brain was rapidly immersed into liquid nitrogen for approximately five seconds until frozen. Although this method prevented slow freezing artefacts from water ice crystal formation, the lack of observation and fine control during the freezing process meant it was prone to poor morphology from overfreezing. The second method used is described by Callis (2004). Briefly, the cryoprotected brain was placed in a mouse brain matrix and 3mm coronal blocks were cut at the level of the caudate and hippocampus, taking into accounts the location of the injections. These coronal slices were embedded in OCT cryoembedding media (Sakura) in a plastic freezing mould. A plastic petri dish was floated on a pool of liquid nitrogen. The freezing mould containing the embedded brain was placed on top of the petri dish and allowed to freeze for five minutes. This method allows for fine control of the freezing process since the sample can be observed during freezing. Frozen brains were stored at –20°C. Coronal cryostat sections were cut at a thickness of 10μm.

2.7 MHP36 Cell Culture

MHP36 cells were obtained as a gift from ReNeuron Ltd. They were thawed from frozen stock and cultured in filtered DMEM:F12 (containing human serum albumin: 0.03%, Grifols, apo-transferrin: 94 μg/ml, Sigma, putrescine dihydrochloride: 16.2 μg/ml, Sigma, human recombinant insulin: 5 μg/ml, Sigma, L-thyroxine: 400 ng/ml, Sigma, Tri-iodo-thyronine: 337 ng/ml, Sigma, progesterone: 60ng/ml, Sigma, L-Glutamine: 2 mM, Sigma, sodium selenite: 40 ng/ml, Sigma, heparin: 10 units/ml, Sigma, gentamicin: 50 μg/ml, Invitrogen), supplemented by bovine fibroblast growth factor (bFGF: 1μg/ml media, Sigma) and interferon-γ (1μg/ml media, Peprotech). Cells were fed by changing half of the media every other day, and split by discarding the medium and washing with Hank's Balanced Salt Solution (HBSS, Invitrogen)

without Ca^{2+} and Mg^{2+} to remove debris and aid detachment. Cells were then incubated at 33°C with 5ml Versene (Invitrogen) containing 10µl 2% ethylene glycol-bis(2-aminoethylether)-N,N,N′,N′-tetraacetic acid (EGTA) per ml until dislodged. An equal amount of HBSS was added to inactivate the solution. Cells were spun down in a centrifuge at 1500 rpms for 5 mins. The pellet was aspirated and diluted in an appropriate volume of media for passaging. The cell suspension was plated into fibronectin coated tissue culture flasks and returned to the incubator at 33°C. Before grafting, cells were labelled with the red fluorescent marker PKH26 (Sigma). The PKH26 cell marker comprises a fluorescent dye with a long aliphatic tail allowing for stable incorporation into cell membrane. The labelling vehicle used (Diluent C) is an iso-osmotic aqueous solution which contains no physiological salts or buffers, detergents or organic solvents. A suspension of MHP36 cells was counted on a haemocytometer and then resuspended in diluent C at a density of 2.0×10^6 cells/ml. The PKH26 staining solution was prepared by diluting PKH dye in diluent C (working concentration of 10µm). The suspension of MHP36 cells was diluted with an equivalent volume of PKH26 staining solution (final concentration of 5µm) and immediately mixed in order to ensure homogenous staining. The cells were incubated in staining solution for 4 minutes. The staining reaction was stopped by addition of an equal volume of 1% bovine serum albumin in HBSS. The labelled cells were separated from the staining solution by centrifugation at 1500rpm for 10 minutes. The cell pellet was then washed by centrifugation at 1500rpm for 5 minutes in fresh HBSS. Labelled cells were suspended in 0.5mM N-acetyl-L-cysteine (NAC) in HBSS without Ca^{2+} or Mg^{2+} at a concentration of 25,000 cells/µl. Cells were aspirated to form a single cell suspension and checked for incorporation of the PKH26 label prior to grafting (Figure 2.3). Viability was assessed using trypan blue exclusion in a haemocytometer.

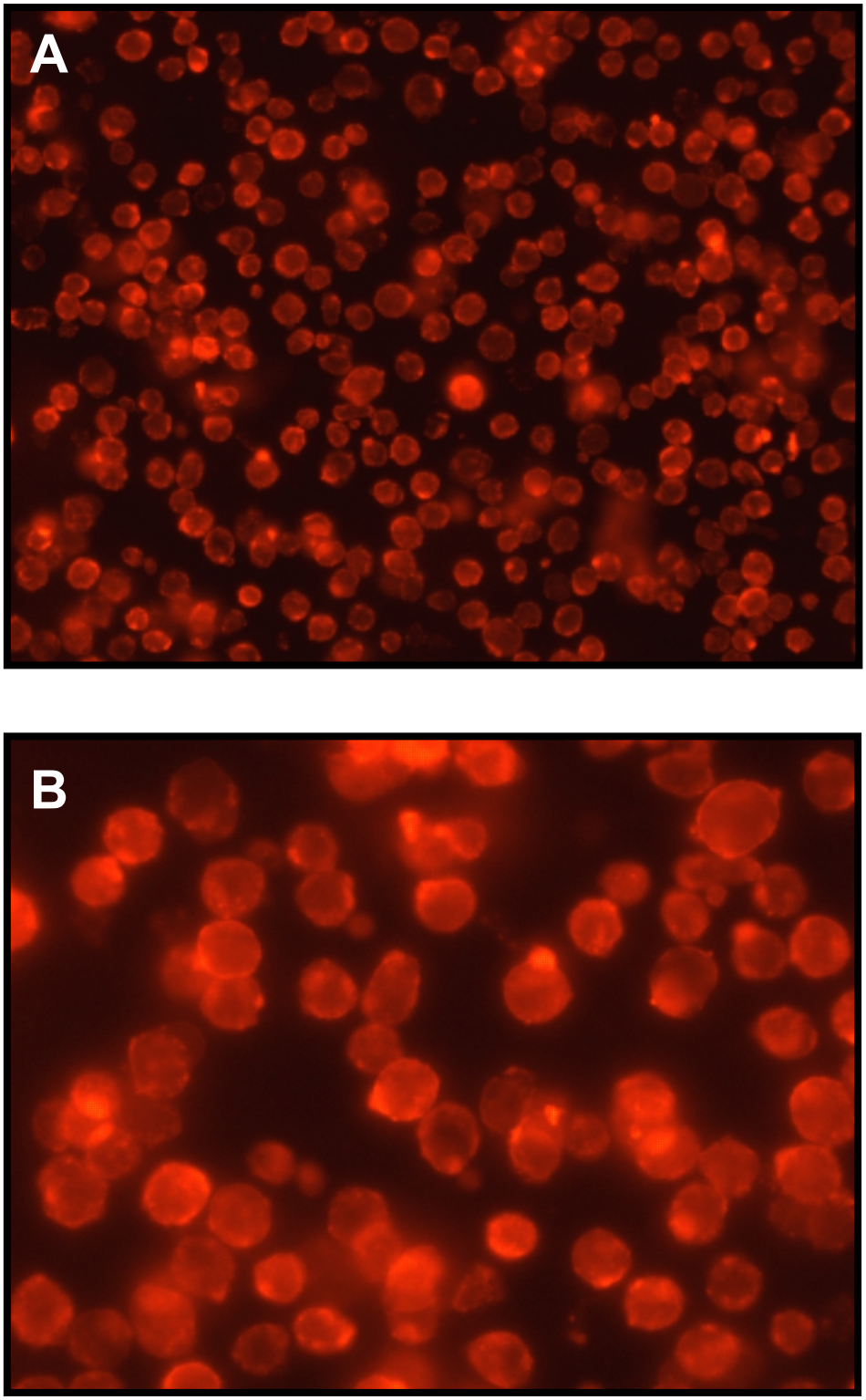

Figure 2.3 Representative images of PKH26 labelled MHP36 stem cells
Incorporation of the red fluorescent PKH26 marker into the membrane of MHP36 stem cells at 200x magnification (A) and 400x magnification (B).

2.8 Immunohistochemistry

2.8.1 Principles

Immunohistochemistry combines anatomical, immunological and biochemical techniques for the identification and localisation of specific tissue components by means of a specific antigen/antibody reaction tagged with a visible label. This thesis uses the avidin-biotin complex (ABC) method of immunohistochemistry (Figure 2.4). The ABC method (Hsu et al., 1981) utilises the high binding affinity (four binding sites per molecule) of avidin or strepavidin, a large glycoprotein from egg white, to biotin, a low molecular weight vitamin found in egg yolk. In brief, a biotinylated secondary antibody is bound to the primary antibody. While this takes place, a biotinylated enzyme (horseradish peroxidase or alkaline phosphatase) is incubated with avidin, forming the large avidin-biotin complex. This complex then binds to the biotinylated secondary antibody through one of the free binding sites on avidin, and a colourimetric substrate for the bound enzyme added in order to visualise the antigen. The tetravalent properties of avidin serve to amplify the reaction and increase signal intensity and sensitivity.

2.8.2 Protocol

Fixed sections were removed from the freezer and allowed to air dry for at least 1 hour. The slides were placed in a slide rack and rinsed in phosphate buffered saline (PBS) for 3 x 5 minutes. This served to equilibrate the sections and remove OCT, if present. Sections were dehydrated in graded alcohols (70%, 2 min, 90% 2 min, 100%, 2 x 5 min) and blocked for endogenous peroxidase activity in 0.5% hydrogen peroxidase in methanol for 30 minutes. Sections were rinsed in running tap water for 10min followed by a rinse in PBS. The dehydration and peroxidase steps were omitted for sections undergoing fluorescent immunostaining. If required, sections underwent antigen retrieval by boiling in a microwave in citric acid buffer, pH 6.0 for 2 x 5 minutes. Sections were left to cool for 30 minutes before proceeding. Sections were blocked in 2% bovine serum albumin, 10% normal serum in PBS for 1 hour. The normal serum was chosen to match the species of the secondary antibody. Primary antibodies were diluted in blocking solution and incubated overnight at 4^{o}C. The dilution of each primary antibody was optimised through a set of initial

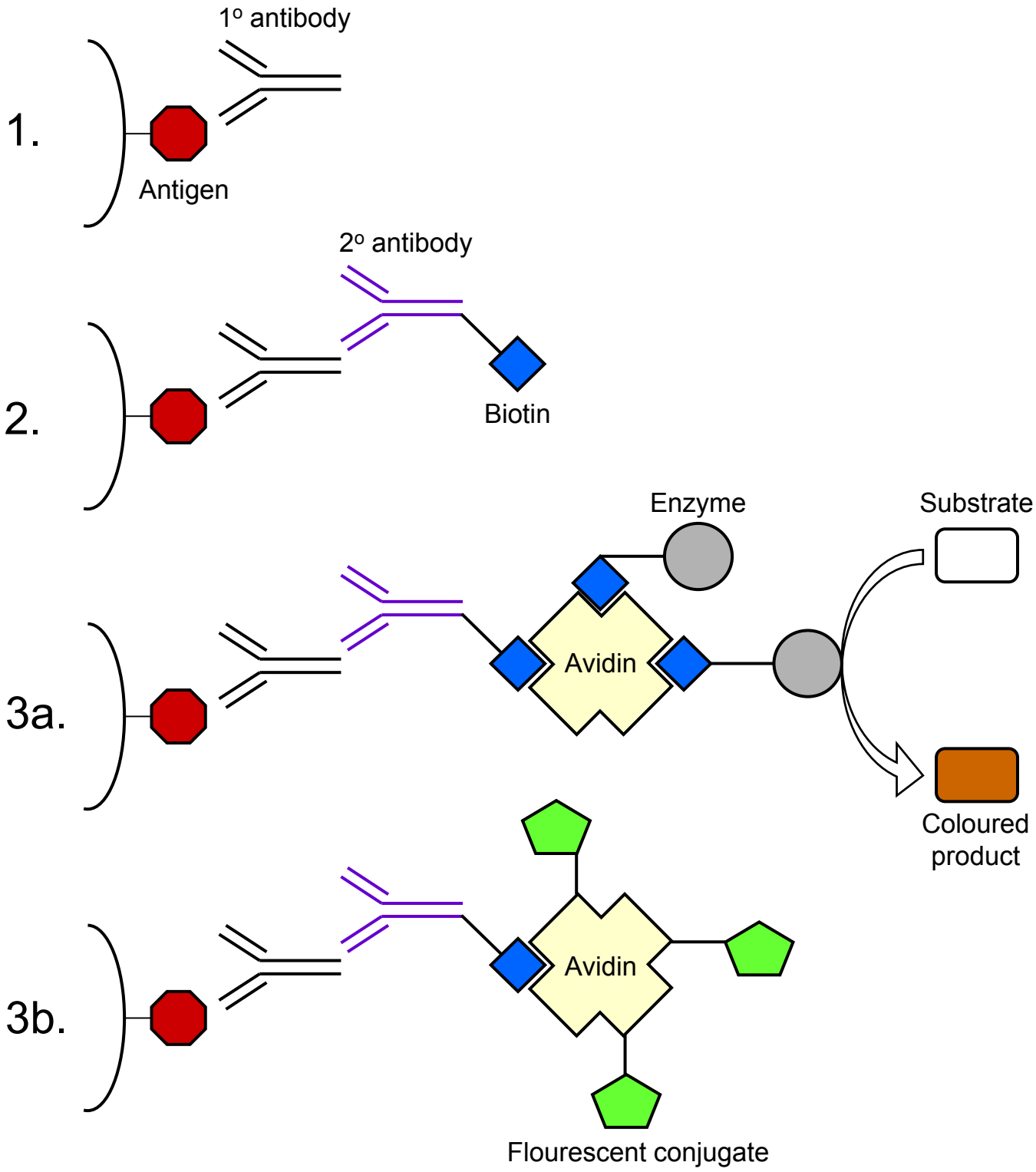

Figure 2.4 Sequence of steps in the ABC immunohistochemical reaction

1. Binding of the primary antibody to the antigen.
2. Binding of the biotinylated secondary antibody to the primary antibody.
3a. Binding of the ABC complex to the secondary antibody. Enzymatic reaction with the substrate produces a colourimetric product for detection
3b. Binding of the fluorescently-conjugated avidin to the secondary antibody.

immunohistochemistry experiments. For negative controls, primary antibody solution was omitted and sections incubated in blocking solution alone. Sections were rinsed in PBS for 2 x 10 minutes before incubation with the biotinylated secondary antibody for 1 hour at room temperature. Sections were rinsed in 2x10 min PBS prior to incubation with the avidin-biotin complex (Standard or Elite ABC kit, Vector, UK) or the fluorescent conjugate Strepavidin Alexa 488 (1:200, Molecular Probes) for 1 hour at room temperature. Fluorescent sections were rinsed in PBS, optionally counterstained with the nuclear DNA marker To-Pro-3 (Invitrogen) and cover slipped with Vectashield (Vector). Light microscope sections were rinsed in PBS for 3 x 5 minutes and visualised with diaminobenzidine (DAB, Vector). Sections were rinsed in water and counterstained with haematoxylin if required, then dehydrated through graded alcohols, cleared in xylene and cover slipped with DPX mountant.

2.9 Histology

2.9.1 Haematoxylin and Eosin staining

Haematoxylin and eosin staining was carried out in order to visualise ischaemic neurons. Fixed sections were removed from the freezer and allowed to air-dry for 1 hour. The slides were placed in a slide rack and rinsed in running tap water for 5 minutes. This served to equilibrate the sections and remove OCT, if present. Sections were dehydrated in graded alcohols (70%, 2 min, 90%, 2 min, 100%, 2 x 5 min, 90%, 2 min, 70%, 2 min) and rinsed in running tap water for 5 minutes. Sections were stained in haematoxylin (Gills, Surgipath) for up to 1 minute. After a quick rinse in running tap water, sections were differentiated in acid alcohol (1% HCL in 70% EtOH) and rinsed in running tap water for 2 minutes. The haematoxylin stained sections were then “blued” by immersion in Scots tap water for 2 minutes, followed by another rinse in running tap water for 2 minutes. Sections were stained in eosin (Surgipath) for up to 4 minutes. After a quick rinse in running tap water, sections were dehydrated in graded alcohols (70%, <2 min, 90%, 2 min, 100%, 2 x 5 min) and cleared in xylene for 15 minutes. Slides were coverslipped with DPX mountant.

2.9.2 Quantification of ischaemic damage

Haematoxylin and eosin stained sections were used to assess the extent of ischaemic damage using a 100mm^2 grid (attached to the microscope optics) at 400x magnification. Ischaemic neurons were defined by an intense, darkly stained pyknotic nucleus surrounded by eosinophilic cytoplasm (Figure 2.5). The number of morphologically normal neurons and neurons exhibiting ischaemic cell change were counted in a 25mm^2 region of the grid. Within the caudate nucleus, six regions surrounding the injection tract were assessed. These were selected in order to capture medial, lateral and ventral aspects of the caudate nucleus. Within the hippocampus, ischaemic damage was assessed in the CA2 pyramidal cell layer. Two sections were assessed for each animal and these sections were quantified twice in order to confirm reproducibility.

2.9.3 Quantification of MHP36 graft survival

MHP36 stem cell survival was assessed using either a semi-quantitative method based on fluorescence microscopy (Chapter 3) or a fully quantitative method based on confocal laser scanning microscopy (Chapters 4 and 5). The semi-quantitative method assessed MHP36 graft survival based on the extent of red fluorescence on the stem cells labelled with PKH26. Sections were assessed for MHP36 graft survival in selected regions in the caudate nucleus using a 100mm^2 grid (attached to the microscope optics) at 200x magnification. The degree of cellular red PKH26 fluorescence based on percentage coverage of the grid was assessed using a scoring system as follows; 0, no labelled cells, 1, <25% labelled cells, 2, 25-50% labelled cells, 3, 50-75% labelled cells, 4, >75% PKH26 labelled cells. Following the completion of the study described in Chapter 3, confocal assessment was preferred for quantification of MHP36 graft survival as it allowed for fully quantitative assessment. Confocal z-series images were captured in selected regions in either the caudate nucleus or hippocampus. These z-series images were analysed for the number of PKH26 labelled MHP36 cells.

Primary Antibody	Species, type	Supplier	Dilution	Blocking Solution	Secondary Antibody, Dilution
NeuN (Neuron Specific Nuclear Protein)	Mouse, Monoclonal	Chemicon	1:1000	10% Horse serum, 0.5% BSA in PBS	Biotinylated Anti-Mouse (Rat Adsorbed), 1:100
GFAP (Glial Fibrillary Acidic Protein)	Mouse, Monoclonal	Chemicon	1:1000	10% Horse serum, 0.5% BSA in PBS	Biotinylated Anti-Mouse (Rat Adsorbed), 1:100
F4/80	Rat, Monoclonal	Caltag Laboratories	1:100	10% Goat serum, 0.5% BSA in PBS	Biotinylated Anti-Rat, 1:100
ApoE	Goat, Polyclonal	Chemicon	1:1000	10% Rabbit serum, 0.5% BSA in PBS	Biotinylated Anti-Goat, 1:100

Table 2.2 Details of primary and secondary antibodies and the relevant solutions used for immunohistochemistry

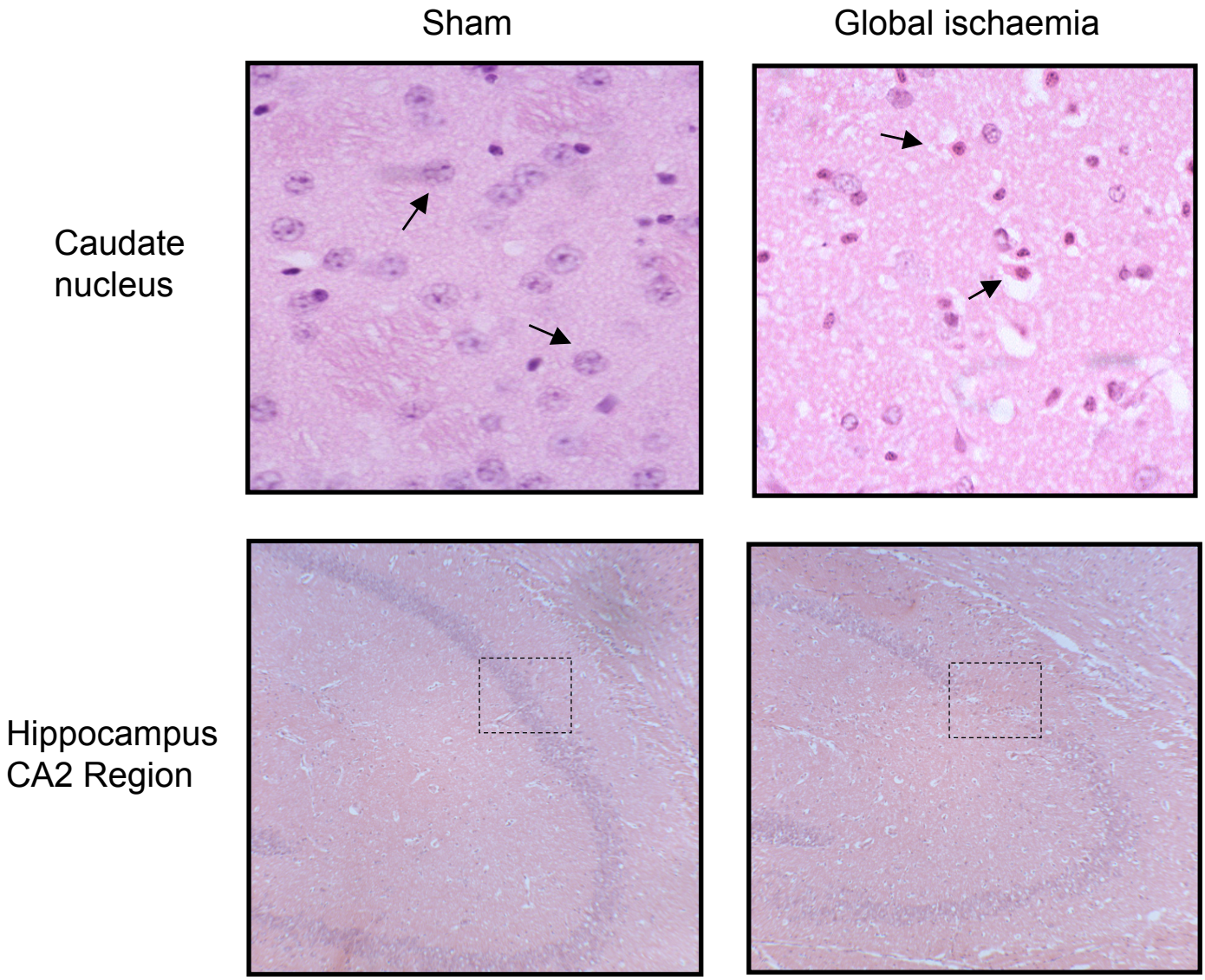

Figure 2.5 Representative images highlighting the morphological features of mouse global ischaemia in the caudate nucleus and hippocampus

Normal and ischaemic neurons (arrows) are shown in sections taken from the caudate nucleus in sham and ischaemic mice. Ischaemic neurons are identifiable by their triangular morphology and darkly stained pyknotic nuclei. Mouse global ischaemia is also characterised via a loss of neurons in the CA2 pyramidal field in the hippocampus (dashed box).

2.9.4 Quantification of MHP36 graft migration

Migration of PKH26 labelled MHP36 cells was assessed in a medial, lateral and ventral direction away from the injection tract. The distance of migration in each direction was measured using a 100mm^2 grid (attached to the microscope optics) at 200x magnification. At this magnification, the length of one side of the grid is equivalent to 0.5mm. Two sections were assessed for each animal and these sections were quantified twice in order to confirm reproducibility.

2.9.5 Quantification of GFAP immunoreactivity

Sections were assessed for GFAP immunoreactivity in selected fields in the caudate nucleus and hippocampus using a 100mm^2 grid (attached to the microscope optics) at 400x magnification. GFAP positive reactive astrocytes with defined cell bodies and processes were counted within each grid. Two sections were assessed for each animal and these sections were quantified twice in order to confirm reproducibility.

2.9.6 Quantification of F4/80 immunoreactivity

Sections were assessed for F4/80 immunoreactivity in selected fields in the caudate nucleus using a 100mm^2 grid (attached to the microscope optics) at 400x magnification. Individual microglia / macrophage were difficult to define with precision and thus a semi-quantitative assessment was used. The degree of F4/80 immunostaining based on percentage coverage of the 100mm^2 grid was assessed using a scoring system as follows; 0, no staining, 1, < 25% staining, 2, 25-50% staining, 3, 50-75% staining, 4, > 75% staining.

2.9.7 Immunofluorescent analysis

Sections were assessed for co-localization of phenotypic markers for neurons (NeuN), astrocytes (GFAP) and microglia / macrophage (F4/80) with PKH26 as a marker for transplanted MHP36 cells in selected fields in the caudate nucleus and hippocampus using a confocal laser scanning microscope (Zeiss). Confocal z-series images were captured at the selected fields. Neuronal and astrocytic differentiation was determined by counting the number of labelled cells co-localizing with PKH26 after counting the number of PKH26 positive cells within the same field. In addition,

confocal laser microscopy was used to assess the co-localisation of PKH 26 labelled cells with the DNA marker To-pro-3.

2.10 Protein Analysis

2.10.1 Tissue homogenisation

Tissue samples were removed from the –80^{o}C freezer, weighed immediately and placed on dry ice. One protease inhibitor tablet (Roche) was dissolved in 25ml ice-cold modified radioimmunoprecipitation (RIPA) buffer. The tissue was placed in a 1 ml glass-glass Dounce homogeniser and 5X volume of modified RIPA buffer was added (5 ml per 1 g). The tissue was homogenised with ten controlled strokes of the pestle and left for 15 minutes on ice. The homogenised tissue was transferred to a 1.5ml Eppendorf tube, centrifuged at 10,000 rpm and 4^{o}C for 10 minutes. The supernatant was removed, aliquoted into a separate 1.5ml tube and frozen at –80^{o}C.

2.10.2 BCA protein assay

Protein concentration of homogenised tissue was determined using the bicinchoninic acid (BCA) protein assay kit (Pierce). The kit utilises the capacity of protein to reduce Cu^{2+} ions to Cu^{+} ions in an alkaline medium. Subsequently, the levels of Cu^{+} are detected in a colourimetric reaction with BCA. The purple-coloured reaction product formed by the chelation of one Cu^{+} ion with two molecules of BCA exhibits a strong absorbance at 562nm. The absorbance of the reaction product has a near-linear relationship with increasing protein concentration, allowing for accurate detection of protein levels in the range of 20 to 2000 μg/ml.

A standard curve ranging from 20 to 1500 μg/ml was prepared in triplicate using bovine serum albumin (BSA, 2000μg/ml) diluted in homogenisation buffer. 50 parts of BCA reagent A (Sodium carbonate, sodium bicarbonate, bicinchoninic acid and sodium tartrate in 0.1M sodium hydroxide) was added to 1 part BCA reagent B (4% cupric sulphate) to form the BCA working reagent (WR). Homogenised tissue samples were removed from the freezer and thawed on ice. Triplicate dilutions of each sample (1:10 or 1:15) were prepared in homogenisation buffer. 50μl of each sample replicate or BSA standard was added to 1ml WR in a 1.5ml Eppendorf tube

and incubated for 30 minutes at 37^{o}C. The tubes were allowed to cool to room temperature. The reaction product was aliquoted into spectrophotometer cuvettes and the absorbance measured at 562nm. The protein concentration of each unknown sample was calculated from the standard curve.

2.10.3 SDS-PAGE electrophoresis

Sodium dodecyl sulphate polyacrylamide gel electrophoresis (SDS-PAGE) allows separation of polypeptides based on molecular weight rather than intrinsic electrical charge. SDS is an anionic detergent that denatures the polypeptide backbone, destabilises hydrogen bonds and unfolds tertiary and secondary structures. SDS binds to protein in a ratio of approximately 1.4g SDS to 1g protein, and therefore imparts a net negative charge in proportion to polypeptide length. Addition of a reducing agent such as 2-mercaptoethanol breaks disulphide bonds, which converts the protein into a linear structure with a uniform negative charge.

SDS-PAGE electrophoresis was carried out using a Mini-PROTEAN II electrophoresis cell (BioRad). The glass plates were thoroughly cleaned in 70% ethanol and distilled water before use. The longer rectangular plate was laid on a flat surface, and two spacers placed along the short edges of the plate. The shorter plate was laid on top of the spacers to form the glass plate sandwich. The sandwich was slid into the clamp assembly and aligned so that the sandwich and the assembly were flush against a flat surface. The screws on the clamp assembly were tightened to secure the sandwich. The assembly was transferred to the casting stand for gel casting. A comb was placed into the gel sandwich and a mark made 0.5 cm below the teeth of the comb. The comb was removed and the resolving gel pipetted in to the level of the mark. SDS-saturated water was overlaid on top of the resolving gel to prevent it drying out. The 10% polyacrylamide resolving gel was left to polymerise for 1 hour. Following polymerisation, the SDS-saturated water was rinsed off with distilled water. The 4% polyacrylamide stacking gel was pipetted on top of the resolving gel to the top of the sandwich and the comb inserted. The stacking gel was left to polymerise for 45 minutes, and the comb was carefully removed. The wells formed by the comb were rinsed with running buffer and the

gels were transferred from the casting stand to the inner cooling core. The inner cooling core was placed into the Mini-PROTEAN II electrophoresis cell and the upper and lower buffer chambers were filled with the required amount of 1X running buffer. 20µg of protein homogenate was prepared to a volume of 10µl in the appropriate homogenisation buffer. An equal volume of 2-mercaptoethanol in Laemmli sample buffer (1:9 ratio) was added to each protein sample and boiled at >95^{o}C for 5 minutes in order to denature the protein. The samples were spun down before loading. The protein samples were loaded into each well. A pre-determined molecular weight marker was loaded into one well. The lid was placed on top of the cell, attached to a power supply and run at 60mA for 45 minutes.

2.10.4 Protein transfer

After separation of the protein sample by SDS-PAGE electrophoresis, the proteins were transferred to a membrane in a pattern replicating the original separation. The transferred membrane has a number of advantages to the original gel. The proteins are concentrated on the surface of the membrane rather than spread throughout the thickness of the gel, allowing easier detection via antibodies. Membranes are easier to handle than gels, and permit stripping and reprobing with different antibodies. Finally, the membrane provides a permanent record of the original gel. Polyvinylidene difluoride (PVDF) membranes are commonly used for transfer, as they offer a high protein binding capacity and are physically and chemically stable.

Once the gel had finished running, the sandwich plate was disassembled and the stacking gel cut away. The resolving gel was floated into transfer buffer and left to equilibrate for at least 15 minutes. The PVDF membrane and filter paper were cut to the dimensions of the gel. The filter paper and fibre pads were soaked in transfer buffer and the PVDF membrane activated by soaking in methanol. The transfer sandwich was assembled as shown in Figure 2.6, so that the proteins would transfer towards the anode and bind to the PVDF membrane. Care was taken to ensure no air bubbles were present in the transfer sandwich. The cassette was closed and placed in the transfer tank containing transfer buffer. The Bio-Ice cooling unit and a magnetic stirrer were added to the tank. The transfer buffer was stirred at a high speed in order

keep the ion distribution even. The lid was placed on top of the cell, attached to a power supply and transferred at 30V overnight.

2.10.5 Coomassie Blue staining

After transfer, the acrylamide gel was stained in Coomassie blue (BioRad) in order to check for equivalent loading of protein samples. The gel was immersed in coomassie blue and agitated on a rotary shaker for 1 hour. The coomassie blue stain was removed, and the gel destained in 10% methanol / 10% acetic acid overnight. An image was captured of the stained gel the following day.

2.10.6 Western blotting

Following transfer, the membrane was removed and marked for reference. The membrane was washed in 0.1% Tween 20 in PBS (PBS-T) at room temperature, before blocking in 10% non-fat dried milk in PBS-T overnight at 4^{o}C. All washing and incubation steps took place on an orbital shaker. After blocking, the membrane was rinsed in PBS-T before application of the primary antibody (Table 2.3) diluted in 10% non-fat dried milk in PBS-T. The membrane was incubated in primary antibody for 1-2 hours at room temperature. Following primary antibody incubation, the membrane was rinsed, and then washed for 3 x 5 minutes in PBS-T. The membrane was incubated in the appropriate HRP-labelled secondary antibody (Table 2.3) was diluted in 5% non-fat dried milk in PBS-T for 1-2 hours at room temperature, after which the membrane was rinsed and then washed 3 x 5 minutes in PBS-T.

Enhanced chemiluminescent (ECL) detection is a non-radioactive, highly sensitive and high-resolution method for detecting immobilized specific antigens conjugated to a HRP antibody. An equal volume of ECL detection solution 1 was mixed with detection solution 2 to obtain sufficient volume to cover the membranes. The membrane was drained of PBS-T and placed on a flat surface, protein side up and incubated in ECL reagent for 1 minute. Excess ECL reagent was drained off, and the membrane placed protein side down on a clean piece of cling film, wrapped up and air bubbles smoothed out using a glass rod. The wrapped membranes were taped

down, protein side up in an X-ray film cassette and transferred to a dark-light room. A sheet of autoradiography film (Hyperfilm ECL, Amersham) was placed on top of the wrapped membrane and the cassette closed for 15 seconds. The film was then removed and exposed using an automatic developer. Depending on the appearance of the first film, subsequent films were exposed to the membrane for varying times and developed.

2.10.7 Membrane stripping

Following ECL detection, membranes were stripped to remove primary and secondary antibodies in order to re-probe with a different antibody. An acidic pH solution alters the structure of the antibody so that the binding site is no longer active. Membranes were submerged in stripping solution (25mM Glycine-HCL, 1% w/v SDS, 0.1% Tween 20, pH 2.2) on an orbital shaker at room temperature for 1 hour. Membranes were then thoroughly washed for 3 x 5 minutes using large volumes of PBS-T. The membrane was then blocked in 10% non-fat dried milk in PBS-T before reprobing.

2.10.8 Image analysis

Developed films were visualised on a stable intensity desktop illuminator and bands were semi-quantified by measuring their Relative Optical Density (R.O.D.) using an AIS Image Analyser system (Imaging Research, Canada). Readings were normalised to background levels.

2.11 Statistics

Differences between two groups were assessed using the non-parametric Mann-Whitney *U* test. Differences between three groups were assessed using the non-parametric Kruskal-Wallis test and followed with Dunn's post-test. Non-parametric tests were chosen due to the fact that data obtained following global ischaemia does not conform to a normal distribution of data.

Primary Antibody	Species, type	Supplier	Dilution	Blocking Solution	Secondary Antibody, Dilution
ERK 1/2 (Extracellular signal-regulated kinase)	Rabbit, Polyclonal	Upstate	1:1000	10% Marvel Milk in PBS-Tween	HRP-linked ECL donkey anti-rabbit, 1:1000
Phospho-ERK 1/2	Rabbit, Polyclonal	Upstate	1:1000	10% Marvel Milk in PBS-Tween	HRP-linked ECL donkey anti-rabbit, 1:1000
JNK 1/2 (c-Jun N-terminal kinase)	Rabbit, Polyclonal	Cell Signaling Technology	1:1000	10% Marvel Milk in PBS-Tween	HRP-linked ECL donkey anti-rabbit, 1:1000
Phospho-JNK 1/2	Rabbit, Polyclonal	Cell Signaling Technology	1:1000	10% Marvel Milk in PBS-Tween	HRP-linked ECL donkey anti-rabbit, 1:1000

Table 2.3 Details of primary and secondary antibodies and relevant solutions used for western blotting

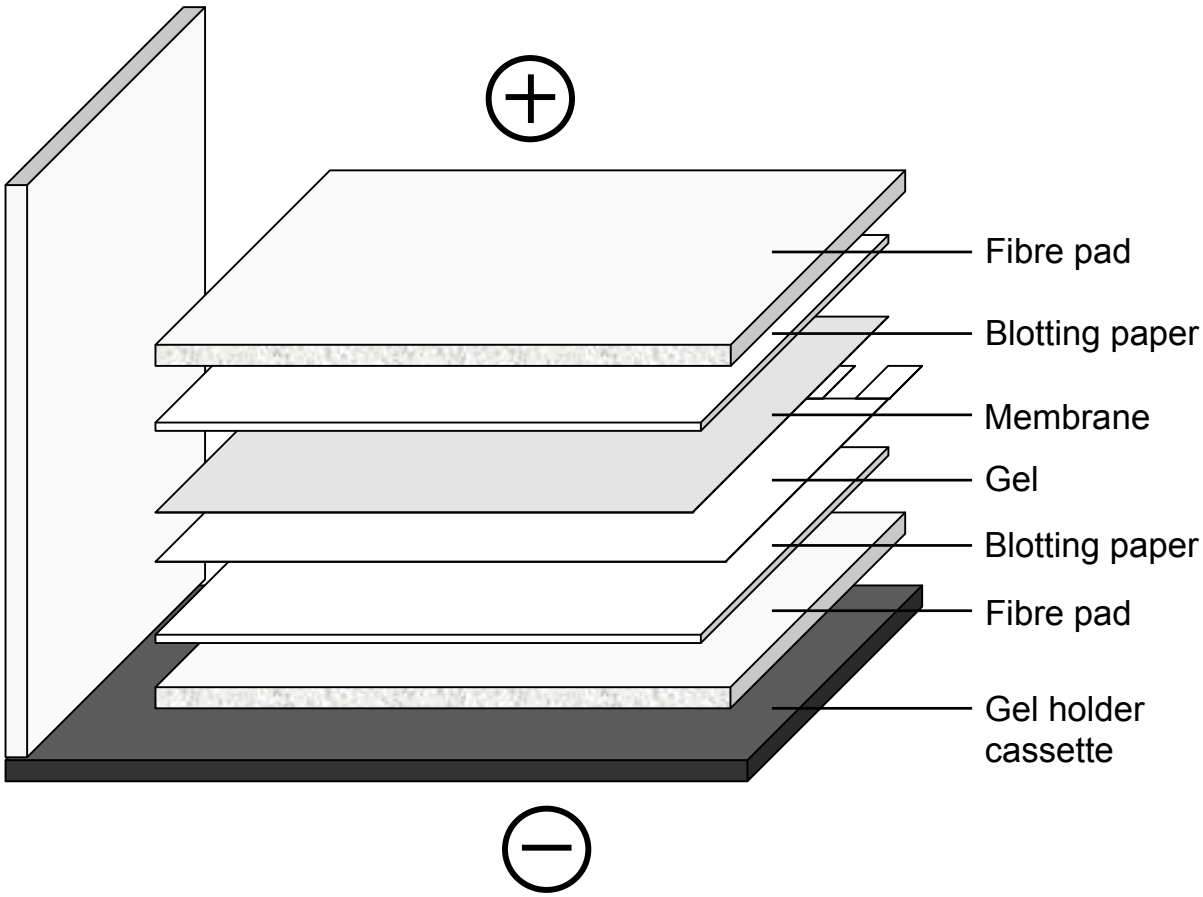

Figure 2.6 Assembly of the gel transfer sandwich
Negatively charged proteins transfer from the gel towards the positive anode and bind to the membrane.

Chapter 3
Characterisation of neural stem cell grafts in a mouse model of global ischaemia

3.1 Introduction

The "proof of principle" of neural stem cell transplantation as a therapy for brain damage has been shown by a number of different groups and with a variety of NSC lines. MHP36 grafts have been shown in rats to reverse age-associated deficits in spatial learning and memory as assessed by the water maze (Hodges et al., 2000), resolve motor associated deficits and reduce lesion volume following transient intraluminal middle cerebral artery occlusion (Veizovic et al., 2001, Modo et al., 2002, Modo et al., 2002). Following transplantation into lesioned primate brain, MHP36 grafts were shown to be as functionally effective as foetal grafts in promoting recovery (Virley et al., 1999). MHP36 cells have been shown to migrate across the corpus callosum towards an ischaemic lesion induced by tMCAo (Veizovic et al., 2001) and differentiate into site appropriate phenotypes (Modo et al., 2002).

The majority of studies to date have examined the survival and migration of stem cells in response to a focal injury (Veizovic et al., 2001, Kelly et al., 2004, Saporta et al., 1999, Riess et al., 2002). However, if the effectiveness of these stem cells is to be realised in human neurodegenerative diseases then it would be advantageous to characterise these cells in models of diffuse neuronal injury. Additionally, mechanisms of stem cell mediated recovery have yet to be elucidated. It is also possible that transplanted stem cells may also interact with various genetic factors. The investigation of stem cell transplants in genetically modified mice would provide an insight into selective genetic influences, and build on the information gained so far from studies utilising non-transgenic rat and primate models. In order to extend from the information obtained for neural stem cell studies in rat models, the first step would be to characterise neural stem cell grafts in a mouse model of diffuse neuronal injury. It is also important to verify whether the use of CsA immunosuppression has a significant effect on stem cell transplantation. Whilst CsA immunosuppression is commonly used clinically in order to prevent graft rejection during organ and bone marrow transplantation, chronic administration of CsA results in nephrotoxic side-effects. It has been demonstrated that CsA treatment did not influence the lymphocyte proliferation or expression of immune markers following MHP36

transplantation in a rat model of focal ischaemia (Modo et al., 2002). It will be interesting to discover whether the low immunogenicity of MHP36 cells is also evident in a mouse model of brain injury.

3.2 Aim

The aim of the study was to characterise neural stem cell grafts in a mouse model of diffuse neuronal injury induced by global ischaemia. We determined whether MHP36 grafts influenced the extent of ischaemic neuronal damage and the effects of the immunosuppressive agent cyclosporin A on graft survival, migration, differentiation and the host inflammatory response. Mice were assessed at a short-term (1 week) and long-term (4 week) time point post-transplantation.

3.3 Materials and Methods

3.3.1 Animals

Adult male C57Bl/6J mice weighing between 25-30g were purchased from Charles River. Animals were communally housed on a twelve-hour light/dark cycle with free access to food and water. All procedures were carried out under licence from the Home Office with the approval of the University of Edinburgh Ethical Review Panel and subject to the Animals (Scientific Procedures) Act 1986.

3.3.2 Bilateral common carotid artery occlusion

Dr Karen Horsburgh carried out the BCCAo procedure. Transient global ischaemia was induced by bilateral occlusion of the common carotid arteries for 17 minutes. This duration of ischaemia is associated with moderate and reproducible neuronal damage in the caudate nucleus. The procedure is described in detail in Chapter 2, Section 2.2.

3.3.3 Immunosuppression

Starting two days post-ischaemia, mice received daily injections of CsA (n = 21) (kindly donated by Novartis, 10mg/kg in saline, s.c.) or the equivalent volume of sterile saline (n = 25), for up to two weeks or until perfusion.

3.3.4 MHP36 stem cell transplantation

MHP36 cells were obtained as a gift from ReNeuron Ltd. They were cultured from frozen stock and maintained in an undifferentiated state at 33°C. (Passage number 52-70). Before grafting, cells were labelled with the membrane bound fluorescent marker PKH26 (Sigma). Labelled cells were suspended in 0.5 mM N-acetyl-L-cysteine (NAC) in Hank's balanced salt solution without Ca^{2+} or Mg^{2+} at a concentration of 25,000 cells/µl. Cells were aspirated to form a single cell suspension and checked for incorporation of the PKH26 label prior to grafting. Vehicle grafted mice received injections of NAC solution. Viability was assessed using trypan blue exclusion in a haemocytometer. Pre-graft viability averaged 90% and post-graft viability averaged 76%. Three days post-ischaemia, mice received a unilateral striatal graft of either MHP36 neural stem cells (n = 25) or vehicle (n = 21) as described in Chapter 2, Section, 2.3.

3.3.5 Histology

After 1 (n = 24) or 4 weeks (n = 22) post-transplantation, mice were transcardially perfused as described in Chapter 2, Section 2.5. The brains were post-fixed, cryoprotected in 30% sucrose and frozen by rapid immersion into liquid nitrogen. Coronal cryostat sections (10µm) were mounted onto poly-L-lysine coated slides. Sections at the level of the injection tract were stained with haematoxylin and eosin in order to visualise ischaemic neurons. Adjacent sections were mounted in Vectashield (Vector, UK) for fluorescent visualisation of MHP36 cells or processed for immunohistochemistry.

3.3.6 Quantification of ischaemic damage

Haematoxylin and eosin stained sections were used to assess the extent of ischaemic damage in the same fields used to quantify the immune response using a $25mm^2$ grid (attached to the microscope optics) at 400x magnification. The number of neurons exhibiting ischaemic cell change and morphologically normal neurons were counted in each grid. Ischaemic neurons were defined by an intense, darkly stained pyknotic nucleus surrounded by eosinophilic cytoplasm. The use of organic solvents in the

haematoxylin and eosin stain extracts the PKH26 fluorescent label from the membrane, preventing visualisation of ischaemic neurons and PKH26 labelled cells on the same section.

3.3.7 Quantification of MHP36 graft survival and migration

Sections were assessed for MHP36 graft survival at three areas, the injection tract, corpus callosum and caudate nucleus. Two fields were assessed per area using a 100mm^2 grid (attached to the microscope optics) at 200x magnification. Two sections were analysed per animal. MHP36 graft survival was semi-quantitatively assessed based on the extent of red fluorescence on the stem cells with PKH26 labelling. The degree of cellular red PKH26 fluorescence based on percentage coverage of the grid was assessed using a scoring system as follows; 0, no labelled cells, 1, <25% labelled cells, 2, 25-50% labelled cells, 3, 50-75% labelled cells, 4, >75% PKH26 labelled cells. Migration of PKH26 labelled MHP36 cells was assessed in a medial, lateral and ventral direction away from the injection tract. The distance of migration in each direction was measured using a 100mm^2 grid (attached to the microscope optics) at 200x magnification.

3.3.8 Immunohistochemistry

The inflammatory response was assessed using two antibody markers, that recognise reactive astrocytes (mouse monoclonal anti-human GFAP) or microglia / macrophage (rat anti-mouse F4/80). Neuronal differentiation of MHP36 cells was assessed using a marker for neuronal nuclei (mouse monoclonal anti-NeuN). The ApoE response was assessed using a marker for ApoE (Goat anti-human apoE). The immunohistochemistry protocol is described in Chapter 2, Section 2.8.

3.3.9 Quantification of immune response

Sections were assessed for GFAP, F4/80 and ApoE immunoreactivity in 6 different fields in the caudate nucleus using a 100mm^2 grid (attached to the microscope optics) at 400x magnification. Two sections were analysed per animal, and in each section the grid was positioned throughout the caudate nucleus such that medial, dorsal, ventral and lateral aspects of the nucleus were sampled. GFAP positive reactive

astrocytes with defined cell bodies and processes were counted within each grid. Individual microglia / macrophage were difficult to define with precision and thus a semi-quantitative assessment was used. The degree of F4/80 immunostaining based on percentage coverage of the 100mm^2 grid was assessed using a scoring system as follows; 0, no staining, 1, < 25% staining, 2, 25-50% staining, 3, 50-75% staining, 4, > 75% staining. ApoE-positive cells were counted within each grid.

3.3.10 Immunofluorescent analysis

Sections were assessed for co-localization of phenotypic markers for neurons (NeuN) and microglia / macrophage (F4/80) with PKH26 as a marker for transplanted MHP36 cells in 4 different fields in the caudate nucleus using a confocal laser scanning microscope (Zeiss). Neuronal differentiation was determined by counting the number of cells co-localizing with PKH26 after counting the number of PKH26 positive cells within the same field. In addition, confocal laser microscopy was used to assess the co-localisation of PKH26 labelled cells with the DNA marker To-pro-3.

3.3.11 Statistical analyses

Differences in the extent of ischaemic damage between vehicle and MHP36 grafted animals were assessed using the Mann-Whitney U-test. Differences in the percentage of PKH26 positive cells co-localizing with NeuN between saline and CsA treated mice were assessed using the Mann-Whitney U-test. For multiple comparisons, the Kruskal–Wallis test followed by Dunn's post test was used to test statistical differences in MHP36 graft survival, migration, GFAP, F4/80 and ApoE immunoreactivity between saline and CsA treated animals and between 1 week and 4 week mice. Correlations between MHP36 graft survival and migration to ischaemic damage, GFAP and F4/80 immunoreactivity were assessed using the Spearman correlation test.

3.4 Results

3.4.1 Ischaemic damage

At 1 week post-transplantation (Figure 3.1), there was a statistically significant reduction in the percentage of ischaemic neurons in MHP36 grafted mice as compared to vehicle grafted mice treated with saline (vehicle; 34 % ± 4.6 % vs. MHP36; 26 % ± 4.3 % ischaemic neurons, $p = 0.0013$). There was no difference in the percentage of ischaemic neurons in MHP36 grafted mice as compared to vehicle grafted mice treated with CsA at 1 week (vehicle; 30 % ± 4.2 % vs. MHP36; 38 % ± 5.9 % ischaemic neurons, $p > 0.05$). At 4 weeks post-transplantation (Figure 3.1) there was no significant difference in ischaemic neuronal damage between MHP36 and vehicle grafted mice treated with saline (vehicle; 34 % ± 6.1 % vs. MHP36; 26 % ± 24 %, $p > 0.05$). However, it was noted that one of the MHP36 grafted mice exhibited a marked increase in ischaemic neuronal damage as compared to the other 5 MHP36 grafted mice and 5 vehicle mice. MHP36 grafted mice treated with CsA exhibited a statistically significant reduction in ischaemic neuronal damage compared to vehicle mice (vehicle; 41 % ± 23 % vs. MHP36; 13 % ± 7.9 %, $p = 0.0173$). Representative images of normal and ischaemic neurons are shown in Figure 3.2.

3.4.2 MHP36 graft survival and migration

MHP36 cells were labelled with a red fluorescent marker, PKH26, which delineates the membrane with red punctate staining in order to facilitate visualisation post-transplantation. Transplanted PKH26 labelled MHP36 cells were clearly detected at both 1 and 4 weeks post-transplantation. There were no fluorescent cells observed in vehicle-grafted mice (Figure 3.3).

At 1 week post-transplantation, PKH26 labelled MHP36 cells were observed predominantly in the injection tract with fewer cells in the caudate nucleus and corpus callosum. CsA immunosuppression had no statistically significant effect on graft survival at this time point in any of the regions examined (Figure 3.4). At 4 weeks post-transplantation, MHP36 cells were detected to a similar extent in each of

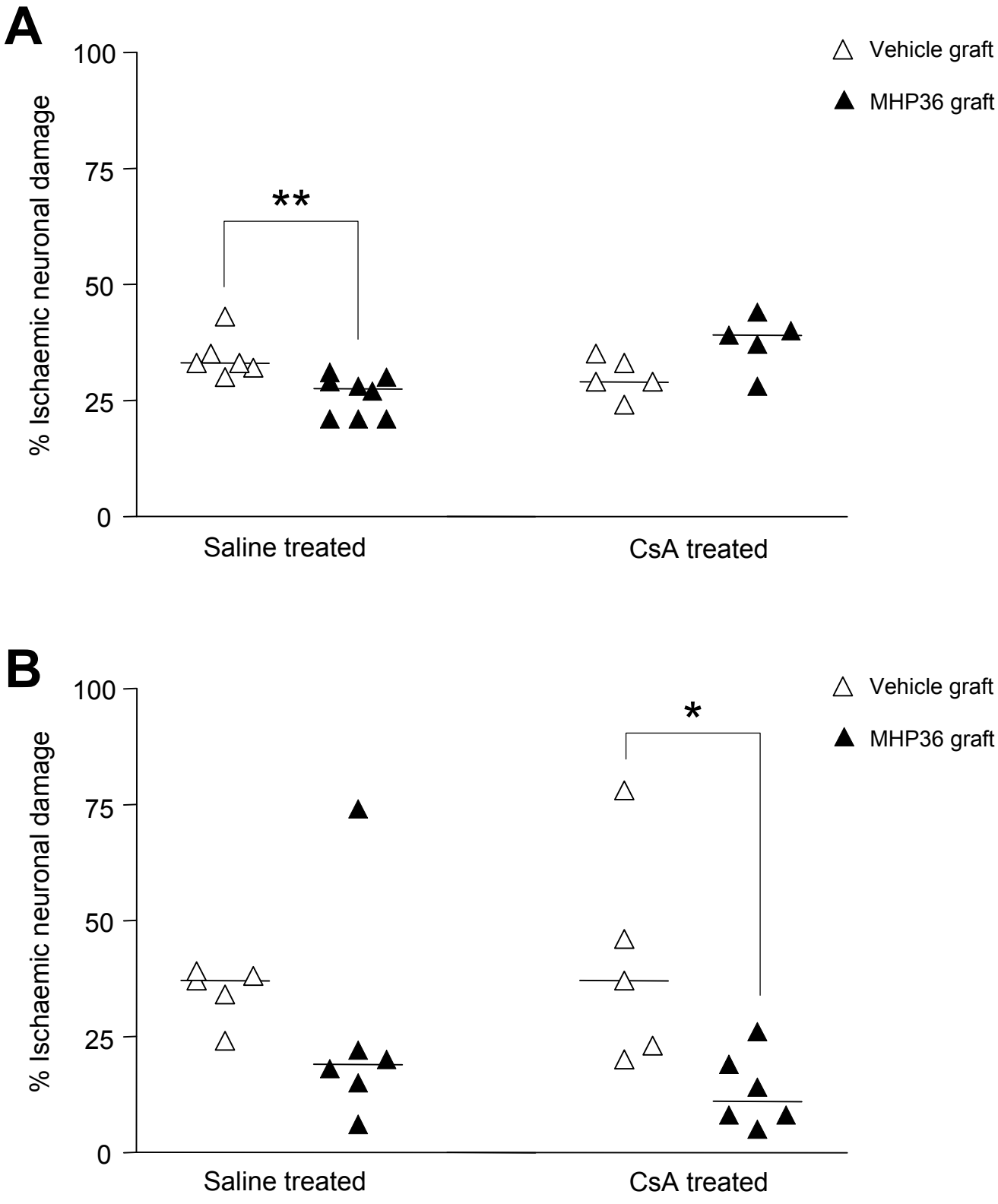

Figure 3.1 MHP36 grafts reduce the extent of ischaemic neuronal damage
Percentage of ischaemic neuronal damage in vehicle and MHP36 grafted mice at 1 week (A) and 4 weeks (B) post-transplantation in saline and CsA treated mice.
* $p < 0.05$, ** $p < 0.01$, Mann-Whitney U-test.

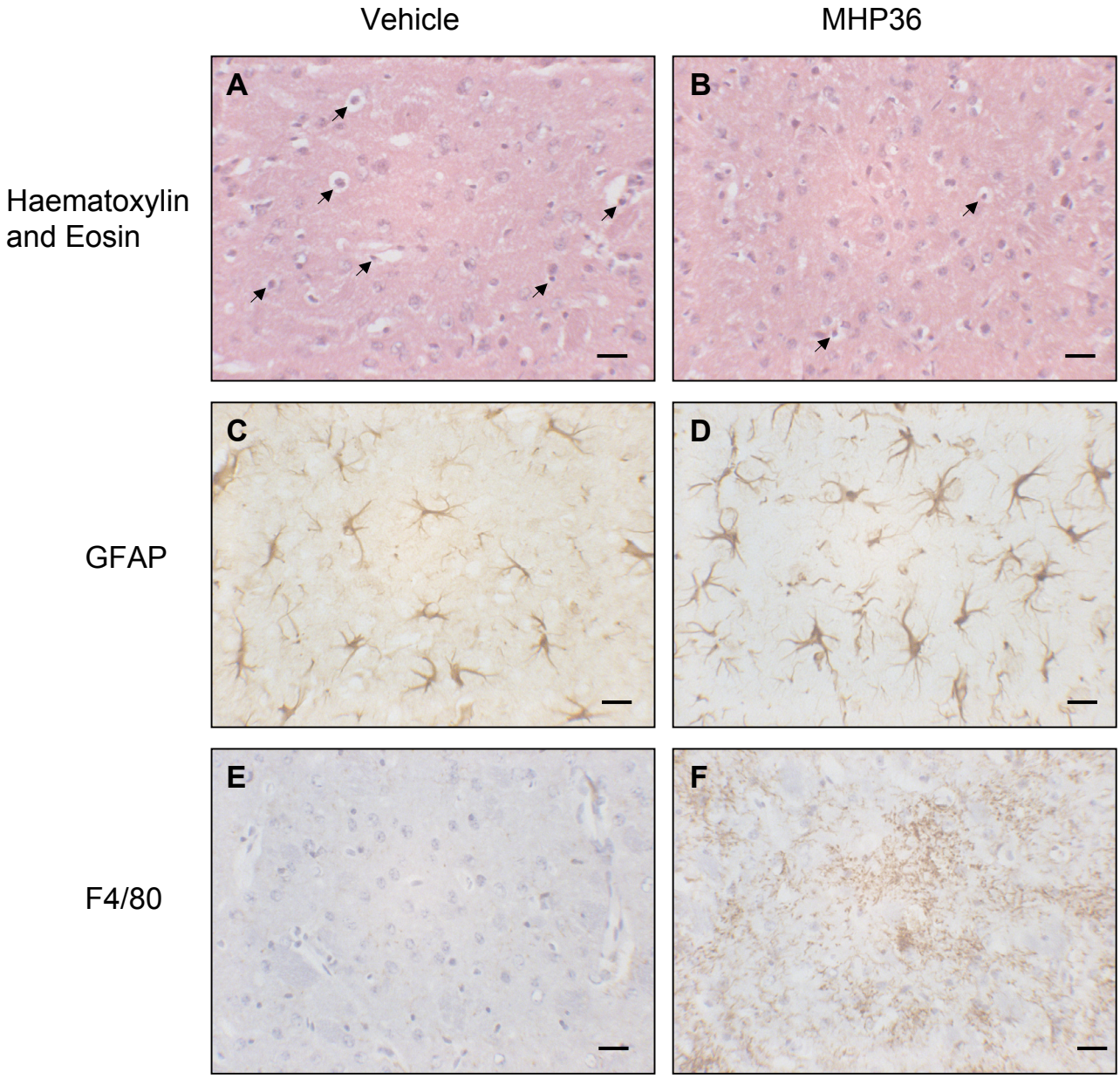

Figure 3.2 Representative images of normal and ischaemic neurons, reactive astrocytes and macrophage / microglia immunostaining

(A-B) Comparison of haematoxylin and eosin stained tissue from the caudate nucleus from vehicle (A) and MHP36 grafted (B) mice at 1 week post-transplantation. Ischaemic neurons are clearly identified by the intensely stained pyknotic nucleus surrounded by eosinophilic cytoplasm (arrows). Scale bar = 20μm.

(C-D) Comparison of GFAP stained tissue from the caudate nucleus from vehicle (C) and MHP36 grafted (D) mice at 1 week post-transplantation. The number of GFAP positive reactive astrocytes (brown) is similar in both vehicle and MHP36 grafted mice. The number of reactive astrocytes decreases in both vehicle and MHP36 grafted mice over time. Scale bar = 20μm.

(E-F) Comparison of F4/80 stained tissue from the caudate nucleus from vehicle (E) and MHP36 grafted (F) mice at 1 week post-transplantation. The extent of F4/80 positive microglia (brown) is upregulated in MHP36 grafted mice compared to vehicle grafted mice. Sections were counterstained with haematoxylin. Scale bar = 20μm. All images were taken from mice treated with saline.

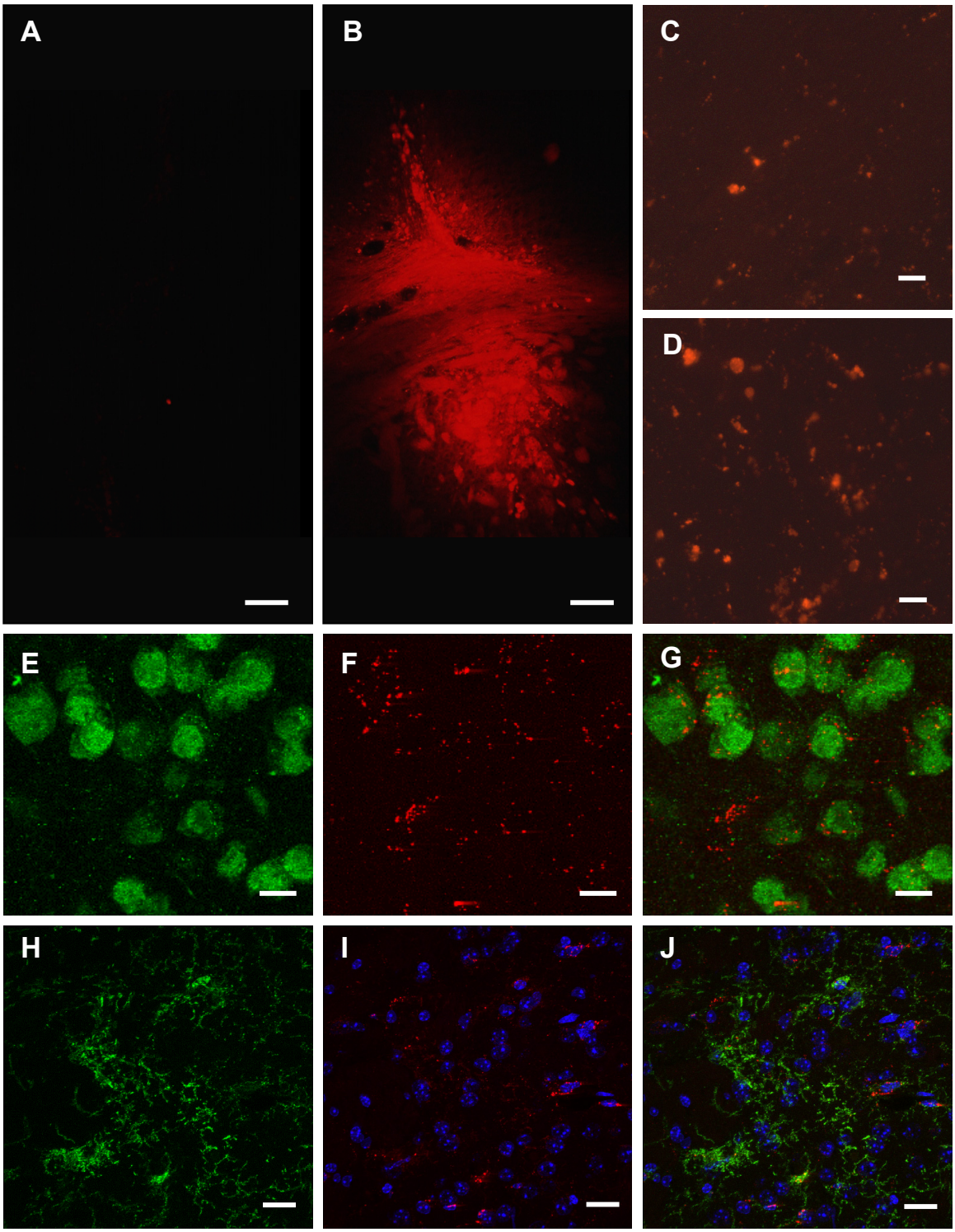

Figure 3.3 Visualisation of PKH26-labelled MHP36 cells

(A-B) Comparison of the injection tract after vehicle (A) and MHP36 cell (B) injection at 4 weeks post-transplantation. Scale Bar = 100μm. There is no fluorescence visible along the injection tract in the vehicle treated mouse, whilst in the MHP36 grafted mouse the injection tract is clearly labelled with red PKH26 fluorescence, indicating the presence of labelled MHP36 cells. Both mice received CsA immunosuppression. No difference was observed with saline-treated animals. At a higher magnification, MHP36 cells labelled with PKH26 are visible in the corpus callosum (C) and the caudate nucleus (D) at 4 weeks post-transplantation. Scale bar = 10μm.

Transplanted MHP36 cells (PKH26, red label) are shown in (F) and in the same section neurons are identified (E) with a neuronal nuclei marker (NeuN, green label) at 4 weeks post-transplantation. The merged image shows the distribution of membrane bound PKH26 around the neuronal nucleus (G). (E-G Scale bar = 10μm). Transplanted MHP36 cells (PKH26, red label) co-localise with a nuclear DNA stain (To-pro-3, blue label) at 1 week post-transplantation (I). In the same section microglia/macrophage (H) are identified (F4/80, green label). The merged image (J) indicates that the MHP36 cells do not co-localise with microglia/macrophage. (H-J, Scale bar = 20μm).

the regions. There was no statistically significant effect on MHP36 graft survival by CsA immunosuppression in any of the regions examined 4 weeks post-transplantation (Figure 3.4). There was no significant difference in the extent of cells surviving in any of the regions at 4 weeks as compared to 1 week post-transplantation. However, there was a visible trend towards a reduction in the extent of cells surviving within the injection tract at 4 weeks post-transplantation as compared to 1 week post-transplantation, in conjunction with an increase in the extent of cells surviving within the surrounding caudate nucleus and corpus callosum.

Migration of MHP36 cells occurred in a medial, lateral and ventral direction away from the injection tract. At 1 week post-transplantation, the distance migrated was variable between the individual mice and ranged from 0.1 to 0.8 mm. The cells migrated a similar distance in all directions (Figure 3.5). CsA immunosuppression did not significantly affect the migration of MHP36 cells in any direction ($p > 0.05$). Similarly at 4 weeks post-transplantation there was no statistically significant effect of CsA immunosuppression on cell migration in any direction ($p > 0.05$) (Figure 3.5). Although not statistically significant, the cells displayed a trend to migrate further at 4 weeks post-transplantation in comparison to 1 week post-transplantation. No MHP36 cells were detected in the hemisphere contralateral to the injection 1 week or 4 weeks post-transplantation. There was no significant correlation between the extent of ischaemic damage and the extent of graft survival or migration.

3.4.3 Neuronal differentiation of MHP36 cells

PKH26 labelled MHP36 stem cells were co-localised with the neuronal nuclei marker NeuN in the caudate nucleus at both 1 week and 4 weeks post-transplantation (Figure 3.3). Approximately 50% of PKH26 labelled MHP36 cells co-localized with NeuN, in both saline and CsA treatment groups at both 1 week and 4 weeks post-transplantation (Figure 3.6). There was no statistical difference between saline and CsA treated mice in the percentage of PKH26 labelled MHP36 stem cells co-localising with NeuN at 1 and 4 weeks post-transplantation (Figure 3.6).

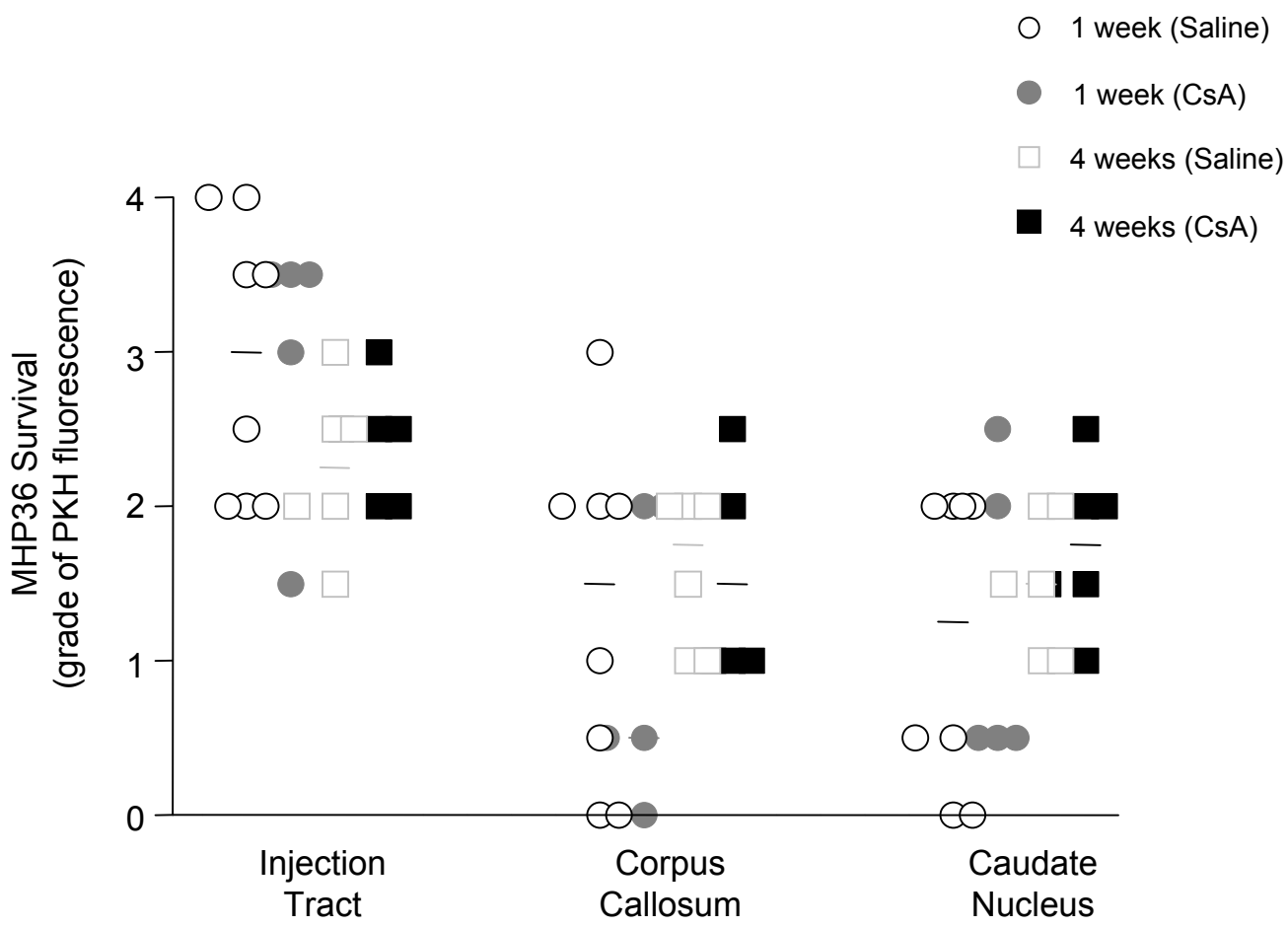

Figure 3.4 Robust survival of MHP36 cells
MHP36 cell survival as assessed by grading PKH26 fluorescently labelled cells at 1 week and 4 weeks post-transplantation with saline and CsA treatment. There was no significant difference in the extent of cell survival between 1 and 4 weeks post-transplantation. CsA immunosuppression did not statistically affect the survival of grafted cells.

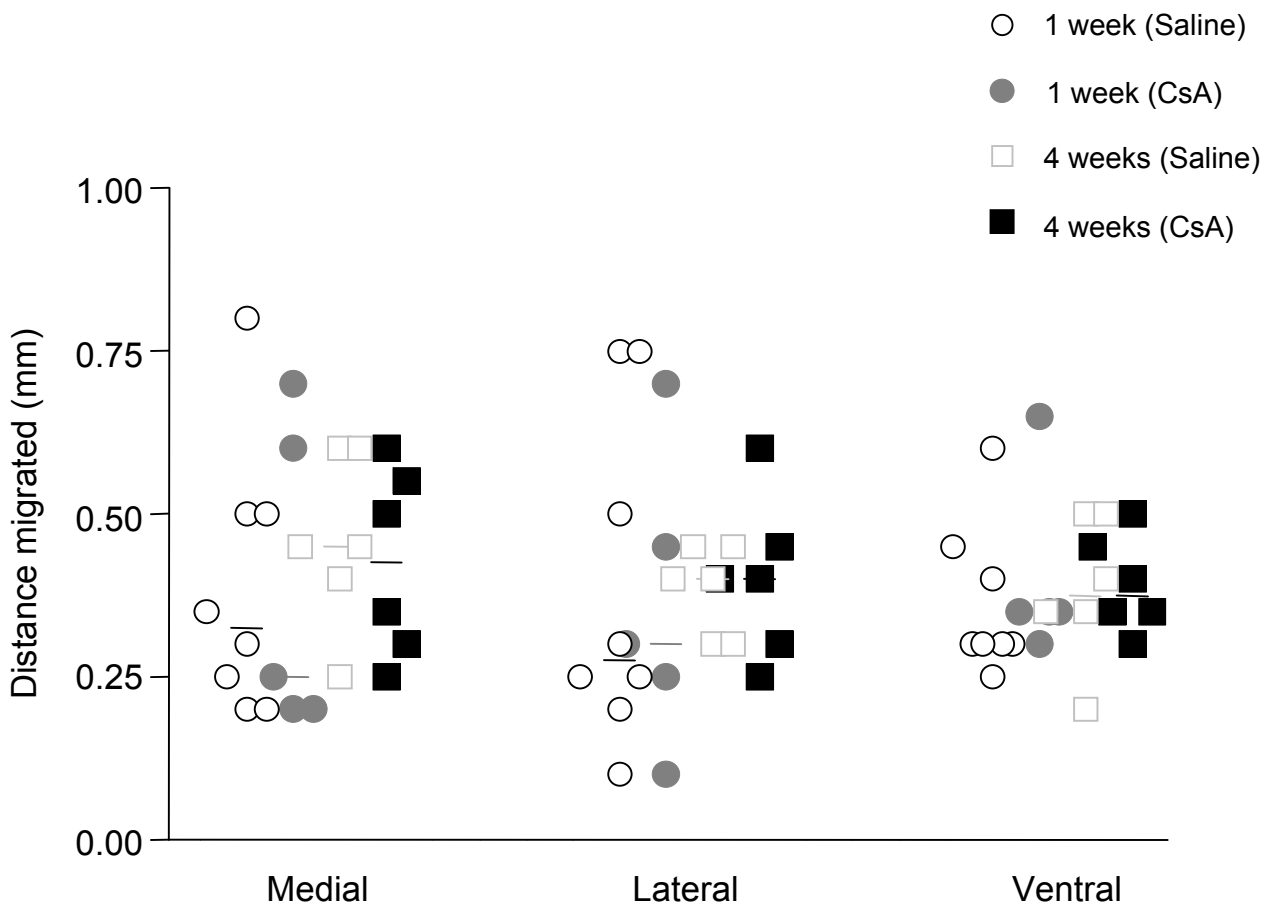

Figure 3.5 Migration of MHP36 cells
Distance migrated (mm) by MHP36 cells at 1 week and 4 weeks post-transplantation with saline and CsA treatment. Data are expressed as a scattergram (A) and as a bar graph (B). Migration was assessed in medial, lateral and ventral directions from the injection tract. There was a trend towards an increase in the distance migrated at 4 weeks compared to 1 week post-transplantation. CsA immunosuppression did not statistically affect the migration of grafted cells.

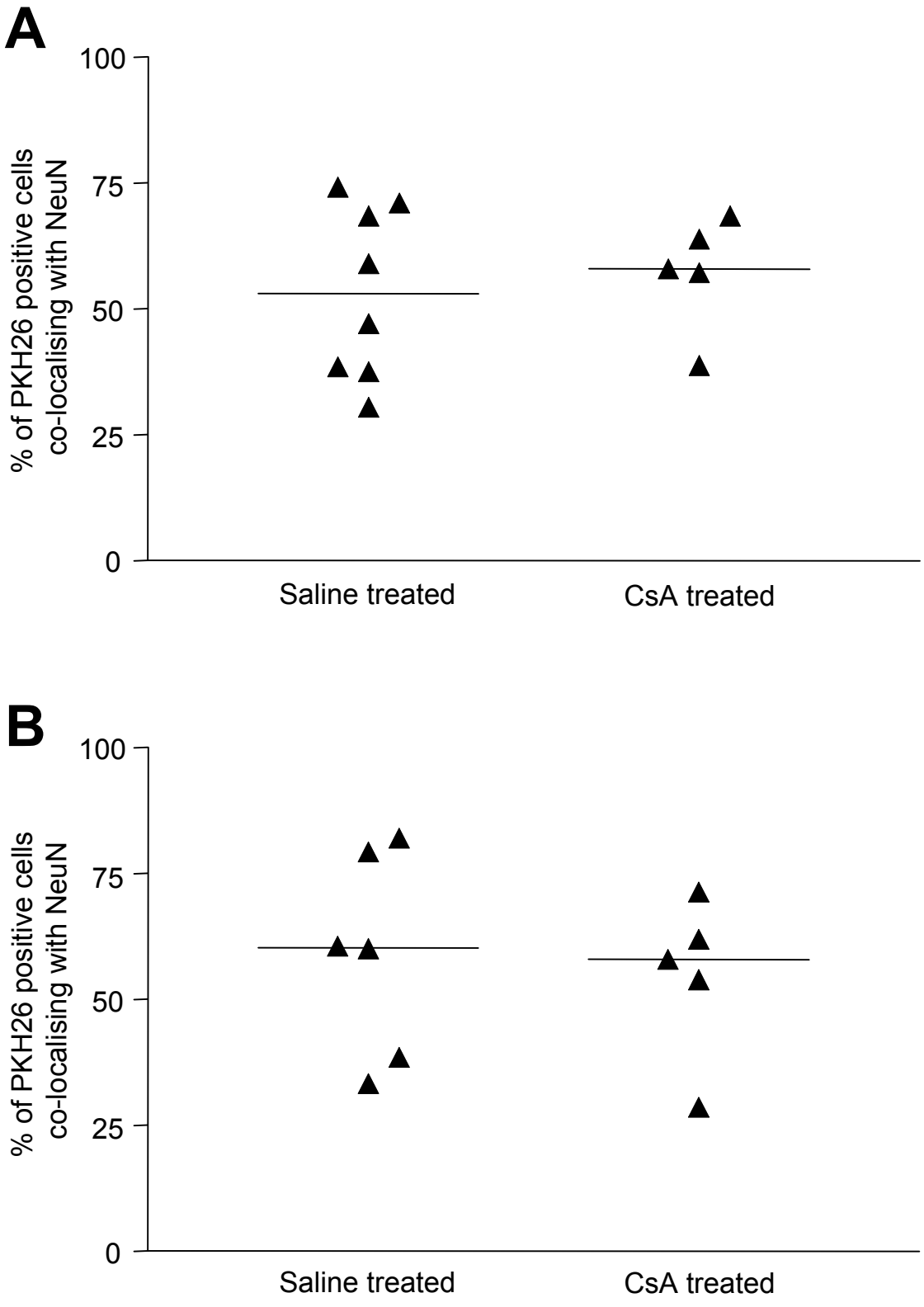

Figure 3.6 Neuronal differentiation of MHP36 cells
Percentage of PKH26 labelled MHP36 stem cells co-localising with NeuN at 1 week (A) and 4 weeks (B) post-transplantation in saline and CsA treated mice. There was no statistical difference between saline and CsA treated mice at both 1 week and 4 weeks.

3.4.4 Astrocytic response

At 1 week post-transplantation, in vehicle grafted mice that underwent global ischaemia there were reactive astrocytes predominantly at the site of needle injection and to a lesser extent in the caudate nucleus (Figure 3.7). Representative images of reactive astroctyes are shown in Figure 3.2. In MHP36 grafted mice, reactive astrocytes were evident in the injection site but also along the corpus callosum and in the caudate nucleus, mirroring the location of the MHP36 stem cells. There was a trend towards an increase in reactive astrocytes in MHP36 grafted mice as compared to vehicle, although this did not achieve statistical significance. There was no significant difference in the number of reactive astrocytes between CsA and saline treated mice that received MHP36 grafts ($p > 0.05$) or vehicle ($p > 0.05$). Similarly, at 4 weeks post-transplantation, there was no significant difference in the number of reactive astrocytes between CsA and saline treated mice that received MHP36 grafts ($p > 0.05$) or vehicle ($p > 0.05$). However, the number of reactive astrocytes significantly decreased at 4 weeks compared to 1 week in three groups (MHP36 grafted mice treated with CsA, $p < 0.05$, MHP36 grafted mice treated with saline, $p < 0.05$, vehicle grafted mice treated with CsA, $p < 0.05$) There was no statistically significant decrease in the number of reactive astrocytes between 1 and 4 weeks in vehicle grafted mice treated with saline ($p > 0.05$) (Figure 3.7). MHP36 cell survival and migration did not correlate with the number of astrocytes in any treatment group.

3.4.5 Microglial and macrophage response

At 1 week post-transplantation, MHP36 grafted mice expressed microglial aggregates and macrophage along the injection tract and in the caudate nucleus with a lesser degree of staining in the corpus callosum. Representative images of macrophage and microglia are shown in Figure 3.2. Vehicle grafted mice exhibited a diffuse stain along the injection tract, with few microglia in the caudate nucleus or corpus callosum. There was no statistically significant difference in the number of microglia / macrophage between CsA and saline treated mice that received MHP36 grafts ($p > 0.05$) (Figure 3.8). However, there was a significant increase in the number of microglia / macrophage in MHP36 grafted mice as compared to vehicle grafted mice treated with saline ($p < 0.01$) with a similar trend observed between

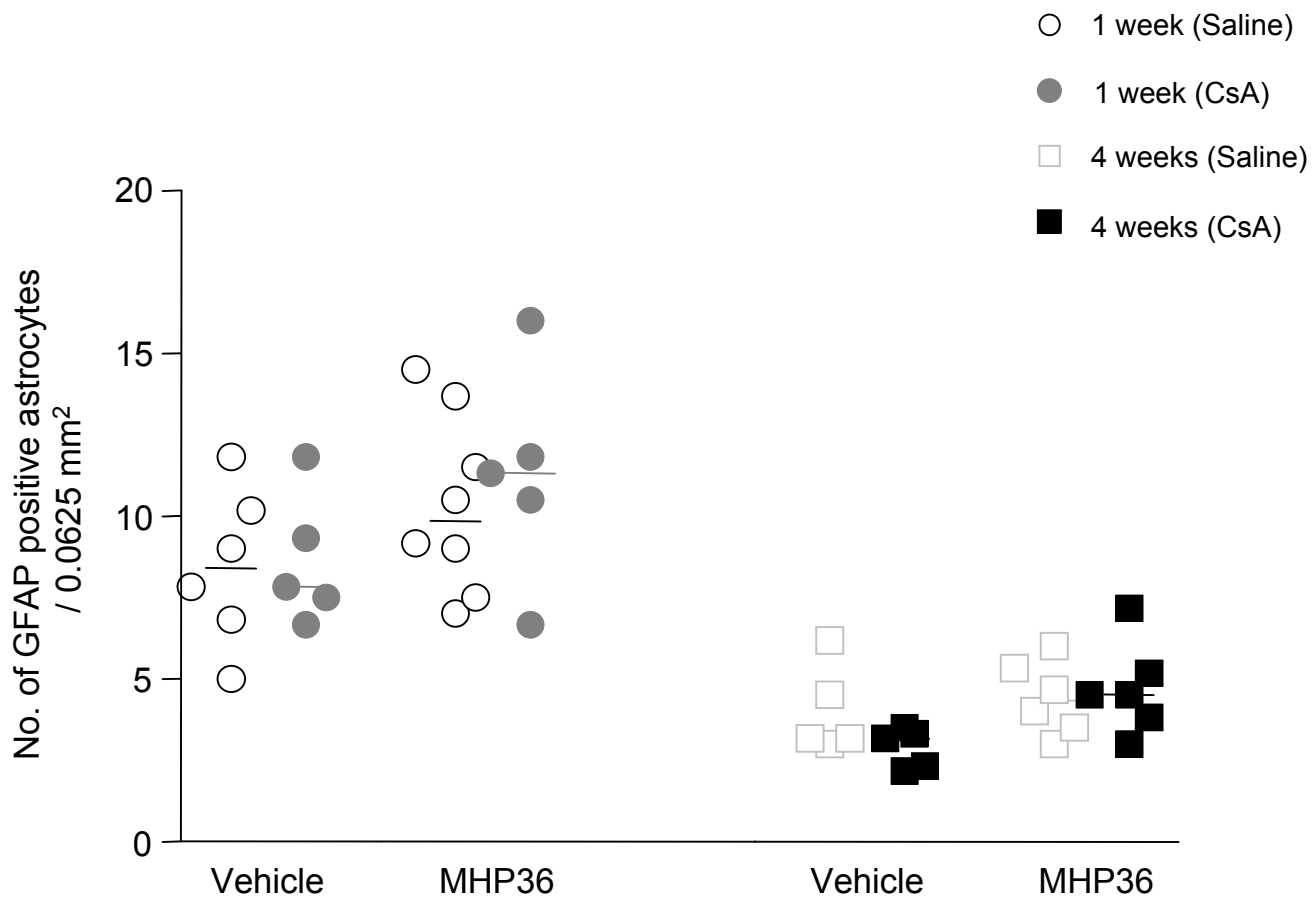

Figure 3.7 MHP36 grafts do not influence reactive astrocytosis
Number of GFAP positive reactive astrocytes after vehicle or MHP36 cell injection and receiving saline or CsA treatment at 1 week and 4 weeks post-transplantation. At both time points, there are no statistically significant differences between saline and CsA treated mice receiving either vehicle of MHP36 grafts. Mice examined at 1 week post-transplantation exhibit more reactive astrocytes compared to mice examined at 4 weeks in all treatment groups (Kruskal-Wallis test with Dunn's post test, MHP36 grafted mice treated with CsA * $p < 0.05$, MHP36 grafted mice treated with saline * $p < 0.05$, vehicle grafted mice treated with CsA * $p < 0.05$) except for vehicle grafted mice treated with saline.

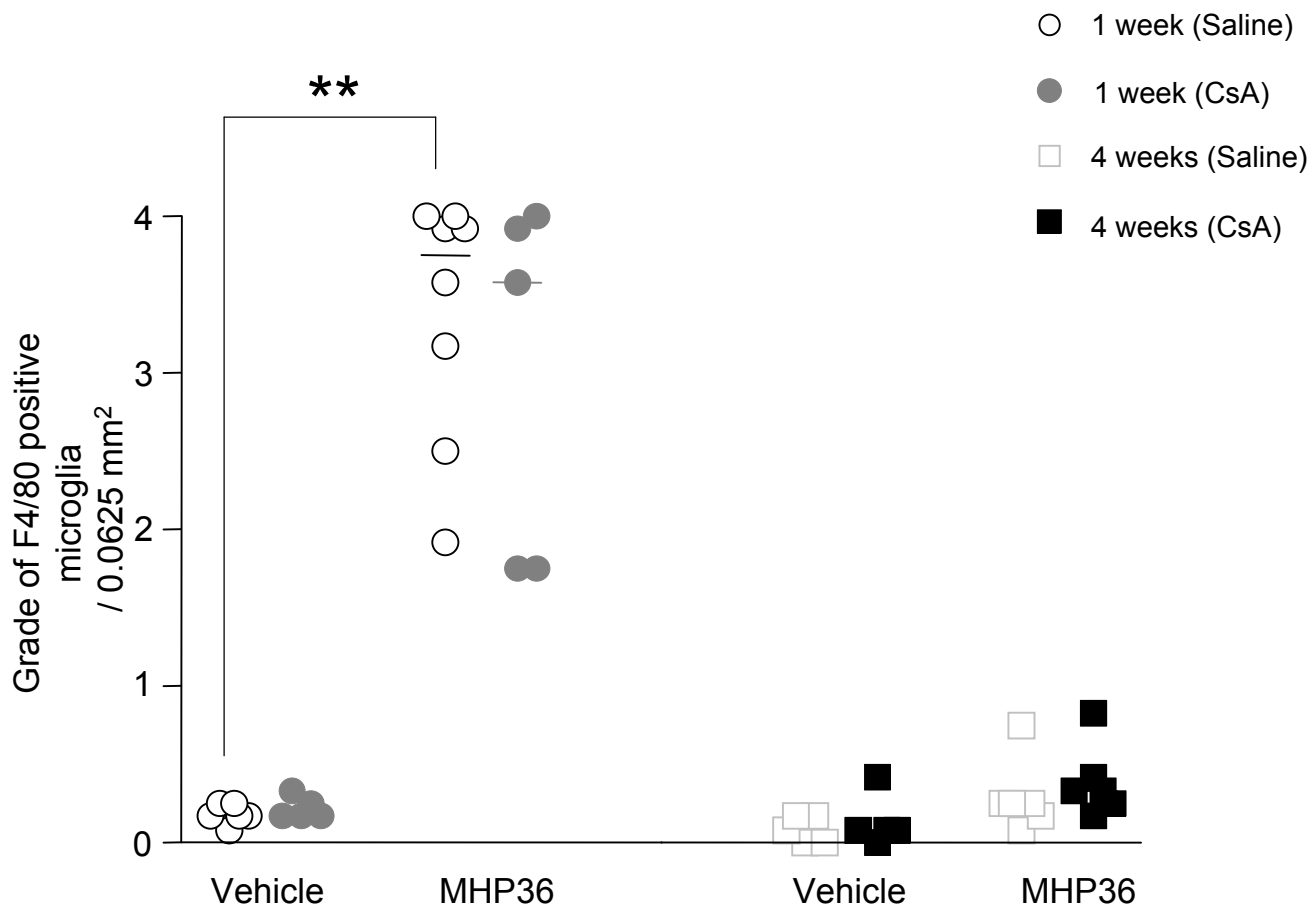

Figure 3.8 MHP36 grafts influence microglial immunoreactivity
Grade of F4/80 positive microglia after vehicle or MHP36 cell injection and receiving saline or CsA treatment at 1 week and 4 weeks post-transplantation. At both time points, there are no statistically significant differences between saline and CsA treated mice receiving either vehicle or MHP36 grafts. There is significantly increased expression of F4/80 staining at 1 week in MHP36 grafted as compared to vehicle grafted mice treated with saline (Kruskal-Wallis test with Dunn's post test, ** $p < 0.01$). A similar trend was observed between CsA treated mice although this was not statistically significant. This response was not present at 4 weeks transplantation when there was no significant difference in the extent of F4/80 immunoreactivity between vehicle and MHP36 grafted mice. MHP36 grafted mice treated with saline exhibit significantly reduced expression of F4/80 staining at 4 weeks compared to 1 week post-transplantation (Kruskal-Wallis test with Dunn's post test, ** $p < 0.01$) although this reduction is not statistically significant in CsA treated mice.

CsA treated mice, although this was not statistically significant ($p > 0.05$) (Figure 3.8). At 4 weeks post-transplantation, microglia / macrophage staining was distinctly localised to the injection tract, with only occasional microglia present in the caudate nucleus. There was no statistically significant difference in the number of microglia / macrophage between CsA and saline treated mice that received MHP36 grafts or vehicle ($p > 0.05$). There was a statistically significant reduction in the number of microglia / macrophage between 1 and 4 weeks in MHP36 grafted mice treated with saline ($p < 0.01$) although no significant reduction was observed in CsA treated mice (Figure 3.8). MHP36 cell survival and migration did not correlate with the number of macrophage or microglia in any treatment group (1 week: Saline treated; $p = 0.665$, $r = 0.18$, CsA treated; $p = 1.050$, $r = 0.00$. 4 weeks: Saline treated; $p = 0.297$, $r = -0.508$, CsA treated; $p = 0.419$, $r = 0.403$). In addition, co-localisation of PKH26 staining with the DNA marker, To-pro-3, demonstrated that the PKH26 label delineated the membrane of To-pro-3 labelled cells. This was observed at both 1 week and 4 weeks post-transplantation (Figure 3.3). The compressed image of triple co-localisation with To-pro-3, PKH26 and F4/80 (Figure 3.3J) suggests that some MHP36 cells may be phagocytosed by macrophage. However, examination of the individual confocal z-sections indicated that there was minimal co-localisation of PKH26 labelled MHP36 stem cells with F4/80 labelled microglia/macrophage in the caudate nucleus at either 1 week or 4 weeks transplantation, suggesting that the majority of MHP36 cells did not undergo phagocytosis.

3.4.6 ApoE immunoreactivity

At 1 week post-transplantation, apoE positive cells were evident along the injection tract and within the caudate nucleus. There was a trend towards a reduction in the number of apoE positive cells between CsA and saline treated mice that received vehicle grafts, although this was not statistically significant ($p > 0.05$) (Figure 3.9). ApoE expression was highly variable between animals. There was no significant difference in the number of apoE positive cells between CsA and saline treated mice that received MHP36 grafts ($p > 0.05$) (Figure 3.9). At 4 weeks post-transplantation, apoE positive cells were still visible within the caudate nucleus. At this time point, there was no significant difference in the number of apoE positive cells between CsA

and saline treated mice that received MHP36 grafts ($p > 0.05$) or vehicle ($p > 0.05$) (Figure 3.9). There was a trend towards a reduction in the number of apoE positive cells at 4 weeks compared to 1 week post-transplantation, although this was only statistically significant in the group of MHP36 grafted mice treated with CsA. MHP36 grafts did not induce increased apoE expression compared to vehicle grafts at either time point, suggesting that response of apoE is primarily directed against the ischaemic insult.

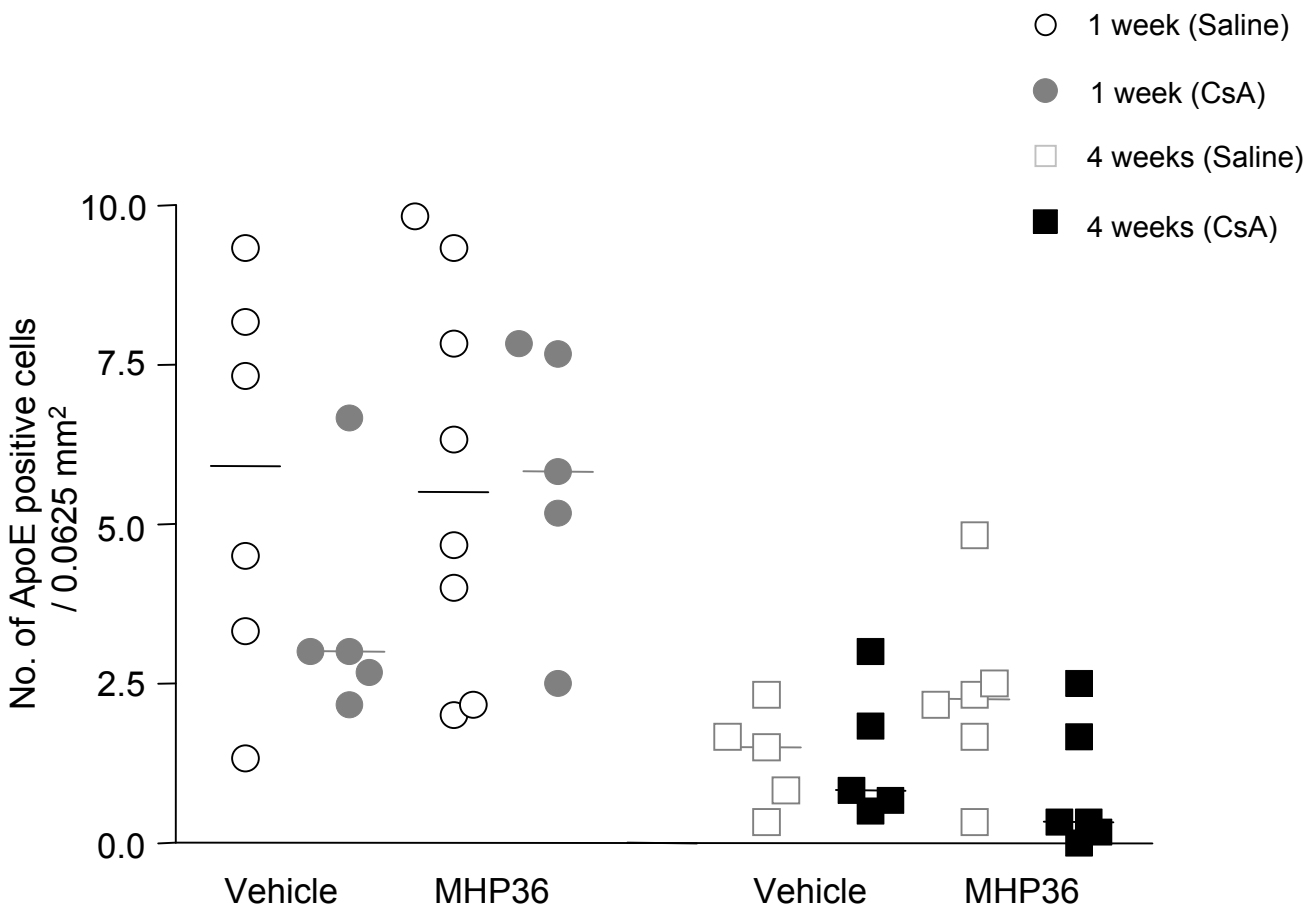

Figure 3.9 MHP36 grafts do not influence apoE immunoreactivity
Number of ApoE positive cells after vehicle or MHP36 cell injection and receiving saline or CsA treatment at 1 week and 4 weeks post-transplantation. At both time points, there are no statistically significant differences between saline and CsA treated mice receiving either vehicle of MHP36 grafts. There is an overall trend towards reduced ApoE immunoreactivity at 4 weeks post-transplantation as compared to 1 week post-transplantation, although this is only statistically significant in the MHP36 grafted mice treated with CsA.

3.5 Discussion

The present study aimed to characterise transplantation of the MHP36 neural stem cell line in a mouse model of diffuse neuronal damage induced by global ischaemia. MHP36 cells were demonstrated to survive and migrate in host ischaemic brain. Furthermore, MHP36 grafted mice exhibited a reduction in the extent of ischaemic damage as compared to vehicle grafted mice, associated with differentiation of MHP36 cells to a neuronal phenotype.

In the present study, global ischaemia performed in C57Bl/6J mice by bilateral occlusion of the common carotid arteries for 17 min induced selective and delayed neuronal damage in the caudate nucleus. The occlusion time of 17 min was chosen based on previous studies (Horsburgh et al., 1999, 2000) in order to produce moderate and reproducible levels of neuronal damage. Grafting of stem cells took place three days following induction of global ischaemia, in order to intervene when the ischaemic damage is maximal (Kelly et al., 2001). There are few prior studies investigating stem cell transplantation in global ischaemia. Previous studies have utilised the rat four-vessel occlusion model of global ischaemia, which causes a reproducible, focused loss of pyramidal neurons in the hippocampal CA1 region (Saporta et al., 1999, Sinden et al., 1997), in contrast to the highly diffuse neuronal damage observed in the mouse BCCAo model. Many other animal studies on neural stem cell transplantation have studied their effects in focal ischaemia models, associated with a unilateral infarct affecting all tissue elements (Kelly et al., 2004, Modo et al., 2002, 2002, Riess et al., 2002, Toda et al., 2001, Veizovic et al., 2001). Previous transplantation studies using MHP36 cells grafted into focal ischaemic rat brain have demonstrated the ability of these cells to migrate to the lesion site and reduce lesion volume (Veizovic et al., 2001). The present study builds and extends on this work to provide novel information on the ability of MHP36 cells to survive, migrate, differentiate and reduce the extent of ischaemic damage in a model of diffuse neuronal injury. This information is also relevant to the potential grafting of stem cells in human neurodegenerative diseases such as Alzheimer's disease in which cell death is diffuse and widespread.

3.5.1 MHP36 grafts reduce the extent of ischaemic neuronal damage

The results from this study indicated that the percentage of ischaemic neuronal damage was reduced in MHP36 grafted mice at both 1 week and 4 weeks post-transplantation. It is unlikely that this is a protective response and more likely that this is due to an increase in normal neurons within the area of damage. The data indicate that transplanted MHP36 cells are able to express a neuronal phenotype and that approximately 50% of grafted MHP36 cells differentiate into neurons. Interestingly, this percentage is not affected by either saline treatment or CsA immunosuppression or at the time point observed. MHP36 cells grafted following the 4VO rat model of global ischaemia primarily repopulated the lesioned CA1 field, with approximately 38% of grafted MHP36 cells expressing a neuronal phenotype (Hodges et al., 2000). Rapid expression of neuronal differentiation markers by MHP36 cells has been shown by Mellodew et al (2004), and is linked with downregulation of neural stem cell marker Nestin. In the same study, approximately 30-35% of grafted MHP36 cells differentiate into neurons in a quinolinic acid lesion model of damage (Mellodew et al., 2004) and a similar percentage was observed in a focal model of ischaemia (Modo et al., 2002). In both these studies, transplantation of the MHP36 cells took place 2-3 weeks after the lesion, which may account for the reduced percentage of differentiated MHP36 cells observed as compared to our study. The model of damage used may also affect the differentiation of transplanted MHP36 cells. Global ischaemia induces selective neuronal damage, in contrast to the indiscriminate damage to all cell types caused by focal ischaemia. Increased neuronal differentiation of MHP36 cells following global ischaemia suggests that the cells are able to selectively differentiate in response specific damaged environment. The extent of neuronal differentiation post-transplantation may also be cell-specific. For example, transplanted bone marrow stem cells undergo minimal neuronal differentiation (up to 2%) as demonstrated in a model of focal ischaemia, (Chen et al., 2001). The present study illustrates the potential of stem cell therapy in a mouse model of global ischaemia and supports other studies on the cell replacement properties of MHP36 stem cells (Modo et al., 2002, Sinden et al., 1997, Veizovic et al., 2001).

3.5.2 MHP36 stem cells survive and migrate in host ischaemic brain

The results show that MHP36 grafts survive for up to 4 weeks in host ischaemic brain, and that they migrate over time. These results support previous studies using the MHP36 neural stem cell line. MHP36 grafts have been shown to survive for up to 20 weeks post-transplantation and repopulate the lesioned CA1 layer in global ischaemic rat brain (Sinden et al., 1997). In other models of damage, MHP36 grafts migrate extensively to the infarcted hemisphere when transplanted into the intact hemisphere in a rat model of focal ischaemia (Veizovic et al., 2001). Interestingly, MHP36 grafts migrated differently depending on the extent of damage in the 4VO rat model of global ischaemia. 15 minutes of 4VO resulted in primarily CA1 cell loss, with some variable damage in the striatum and frontal cortex. MHP36 cells were observed in the CA1 field as soon as 1 week after the injury, but few MHP36 cells were observed elsewhere. However, after 30 minutes of 4VO, CA1 hippocampal cell loss was more extensive, with the CA3 field also afflicted. The extent of striatal and cortical damage was also increased. In these rats, MHP36 cells densely engrafted both the CA1 and CA3 fields, with some cells also observed in the striatum and cortex. These results suggest that to some degree, migration of MHP36 cells is dependent on the severity of damage (Hodges et al., 2000).

In our study, at 1 week post-transplantation, most MHP36 cells remained within the injection tract. At 4 weeks post-transplantation, surviving MHP36 grafts have a different pattern of expression compared to 1 week grafts. There were fewer MHP36 cells present in the injection tract, with increased numbers of cells in the surrounding areas at 4 weeks post-transplantation. Cells were observed in the caudate nucleus, a region that undergoes selective neuronal damage after global ischaemia, suggesting that the grafts were migrating in response to damage. MHP36 cells were also seen along the corpus callosum. Cells migrated away from the injection tract in medial, lateral and ventral directions to an average distance of 0.4mm. Analysis of overall migration between the groups indicated a trend towards an increase in distance migrated at 4 weeks compared to 1 week post-transplantation. Interestingly, the

furthest distance migrated by MHP36 cells in an individual mice was observed at 1 week rather than 4 weeks post-transplantation. This correlates with work showing that neural stem cells transplanted into intact rat striatum start migrating away from the injection tract at 3 days post-transplantation, reaching the maximal distance of 1.5mm away from the injection tract at 5 days post-transplantation (Lundberg et al., 1997). The NSCs used by Lundberg et al., exhibited a similar radial pattern of migration to the MHP36 cells in our study. Kelly et al., (2004) demonstrated similar findings with human neurospheres transplanted in and around the vicinity of the ischaemic core following distal MCAO. Neurospheres survived up to 4 weeks post-transplantation, and migrated up to 1.2 mm towards the lesion. Migration was lesion dependent in this study, with neurospheres migrating a distance of 0.2mm in non-lesioned rats. Chu et al., (2003), subjected rats to transient global cerebral ischaemia and then injected NSCs intravenously into the tail vein. These NSCs were observed in the damaged hippocampus at 56 days post-injection, suggesting that migratory cues from global ischaemic damage are able to target stem cell migration from the bloodstream towards the brain. It should be noted that all of these studies used the rat as the graft recipient and comparisons between migration distances should take into account the size differences between mouse and rat brain.

Although global ischaemia induces bilateral neuronal damage, no MHP36 cells were observed in the contralateral hemisphere. However, as the graft was placed in one damaged hemisphere, the grafted cells may predominantly remain in that region as previously shown (Modo et al., 2002). Migration of MHP36 cells along the corpus callosum was observed and this may be indicative of early migration to the contralateral hemisphere. Longer survival periods post-transplantation may determine whether cells can migrate to the contralateral hemisphere. MRI mapping of transplanted MHP36 cells after transient global ischaemia in the rat demonstrated migration from the injection tract along the corpus callosum towards the contralateral hemisphere by 7 days post-transplantation, suggesting that the MHP36 cells are capable of migrating in a bilateral lesion model (Modo et al., 2002). It should be noted that Modo et al., grafted stem cells above the hippocampus, which may have facilitated migration along the corpus callosum in contrast to the present study in

which MHP36 cells were transplanted in to the caudate nucleus, thereby potentially impeding the migration.

One caveat which should be considered is the limitation of PKH26 staining as a method of detecting transplanted cells. As not all of the MHP36 cells will survive the graft procedure, it is possible that the PKH26 label will leach out of these dead cells into the surrounding environment or be taken up into phagocytosing macrophage. Similarly, MHP36 cells that undergo cell division will have half the fluorescence intensity of the parent cell. This raises the issue of whether it is possible to accurately identify intact, viable MHP36 cells via the PKH26 label and use of fluorescent microscopy. In order to address these issues, we have used a To-pro-3 counterstain for labelling of nuclear DNA. MHP36 cells can therefore be identified via a To-pro-3 positive nuclei and a PKH26 delineated cell membrane. Staining with the microglia/macrophage marker F4/80 also suggests that the majority of PKH26 labelled MHP36 cells survive in the host brain and are not phagocytosed by macrophage. Unfortunately, current attempts to insert a green fluorescent protein (GFP) tag into the MHP36 cell line have not been successful due to gene silencing (Professor J. Price, Personal communication).

3.5.3 MHP36 stem cell grafts provoke a mild acute host inflammatory response

In this study, there were a number of mechanisms by which the inflammatory response (as visualised by reactive astrocytes, microglia and macrophage) could be modified including the effects of global cerebral ischaemia and needle injection. Additionally, the MHP36 cells are derived from the H-2K^{b}-tsA58 transgenic mouse, which was generated on a CBA/Ca x C57BL/10 background. The H-2K^{b} histocompatibility of the MHP36 cells may provoke a mild inflammatory response in the H-2B C57BL/6J host. Reactive astrocytes were present in all treatment groups associated with the effect of global ischaemia. However a localised glial scar in both MHP36 grafted and vehicle mice indicated that injury caused by physical insertion of the syringe had additionally induced an inflammatory response. Furthermore, there was an elevation in reactive astrocytosis and in particular a marked increase in

microglia / macrophage in MHP36 grafted mice as compared to vehicle mice indicating that the MHP36 cells evoked a further inflammatory response. Interestingly, this extensive inflammatory response decreased dramatically at 4 weeks post-transplantation to levels approaching that of vehicle mice. This suggests that the MHP36 cells are no longer recognised as foreign by host microglia and macrophage and are indicative of an acute, rather than a chronic inflammatory response. It may be that the heightened sensitivity of the host brain following the major inflammatory actions of global ischaemia and syringe injection are the cause for the increased response to the MHP36 stem cells. In addition, there was no fluorescent co-localisation of macrophage with MHP36 stem cells, indicating that these cells were not undergoing phagocytosis. Taken together, these results suggest that MHP36 grafts do not induce a marked and prolonged inflammatory response in host ischaemic mouse brain. A previous study on the immunological response induced by MHP36 grafts following a rodent model of focal ischaemia suggested that MHP36 stem cells have low immunogenic properties (Modo et al., 2002). The extent of immune response elicited by MHP36 grafts was investigated through a lymphocyte proliferation assay, grading of graft survival and expression of immune response markers. The trauma induced by focal ischaemia resulted in increased lymphocyte proliferation and upregulation of the immune markers MHC Class I, CD45 and CD11b around the injection tract. In particular, MHC Class I expression paralleled that of the glial scar produced from the syringe induced trauma, similar to the expression of microglial F4/80 observed in our study. Importantly, this pattern of immunoreactivity was not affected by MHP36 stem cell grafts, strongly suggesting that the host inflammatory response was directed against the focal ischaemic insult and the physical act of grafting. These results confirm the findings from our study that MHP36 stem cell grafts do not provoke a significant immune response from host brain.

Microglial inflammation has been shown to have a varying effect on NSC grafts. The pro-inflammatory effects of microglia have been well documented (Vilhardt et al., 2005) with graft rejection strongly associated with macrophage and microglial infiltration (Duan et al., 1995). Kelly et al., (2004) demonstrated a clear negative

correlation between graft survival and the number of IB4 positive inflammatory cells, with improved graft survival observed following transplantation into non-ischaemic tissue rather than into the ischaemic core. In the present study there was no correlation between graft survival or migration with the extent of the inflammatory response. Microglia can also have a beneficial effect on NSC grafts, aiding in migration, axonal growth and differentiation, possibly by secretion of growth factors or through cell-cell contact (Vilhardt et al., 2005). It has also been postulated that the common inflammatory response in all forms of brain damage may provide an intrinsic migratory signal for NSCs (Imitola et al., 2004). Grafting was timed to coincide with the peak ischaemic injury in an attempt to intervene as rapidly as possible. However, it is possible that the host ischaemic and inflammatory environment might impair graft survival. It may be advantageous to postpone transplantation until the ischaemic response has subsided. Further work is therefore necessary to determine the optimum time of transplantation in this global ischemic model.

3.5.4 Cyclosporin A immunosuppression does not affect MHP36 graft integration

The present study investigated whether immunosuppression influences MHP36 cell survival and migration. CsA is a cyclic undecapeptide that exhibits potent immunosuppressive activity by specifically blocking T-cell activation. In the T-cell cytoplasm, CsA binds to its immunophilin, cyclophilin to form a complex. This complex binds and inhibits the action of the enzyme calcineurin, preventing the dephosphorylation of the cytoplasmic component of the nuclear factor of activated T cells (NF-ATc). Therefore, NF-ATc is unable to translocate to the nucleus and bind to the nuclear component of nuclear factor of activated T cells (NF-ATn). Formation of the NF-ATc--NF-ATn complex is required for production of cytokines such as interleukin 2 (IL-2) and interferon-γ (IFN-γ). Both cytokines play an important role in the continuing immune response, with IL-2 essential for the proliferation and maturation of T-cells, and IFN-γ critical for the activation of macrophages. CsA immunosuppression has been commonly used in transplantation studies using NSCs (Chu et al., 2001, Kelly et al., 2004, Saporta et al., 1999) although few studies have

examined the effect of immunosuppression on graft survival and migration. During this study, mice were immunosuppressed with CsA prior to grafting and during the initial phase of graft survival. However, CsA did not have any statistically significant effect on the microglia / macrophage or reactive astrocyte response. There was also no statistically significant effect of CsA immunosuppression on MHP36 graft survival or migration. A possible explanation for the lack of an immunosuppressive effect is the inability of CsA to cross the blood-brain barrier (BBB) (Sakata et al., 1994). However, in this study, the blood-brain barrier has been physically broken following insertion of the needle. It has previously been shown that intravenous CsA is able to ameliorate ischaemic damage as long as the BBB has been opened (Uchino et al., 1995), although there was no clear evidence of this in our study. Another reason for the failure to observe any immunosuppressive effect may simply be down to the time points assessed. At 1 week post-transplantation, the immune response would be at a peak, making it difficult to assess any effect of immunosuppression. Conversely, at 4 weeks post-transplantation, CsA administration ended 2 weeks prior to assessment and the immune response has decreased naturally over time. This can be seen from comparing the reactive astrocyte and microglia / macrophage response at 1 week to the 4 week mice. Modo et al., (2002) have also demonstrated that there is no discernible effect of CsA immunosuppression on the expression of immune markers or the proliferation of lymphocytes in the cervical lymph nodes in MCAo lesioned brain within 2 weeks following grafting of MHP36 stem cells. Surprisingly, comparison of all experimental groups indicated better graft survival was achieved in the absence of CsA immunosuppression. The lack of an effect of CsA immunosuppression may simply be down to the mild inflammatory response provoked by the MHP36 cells. The low antigen presentation of the grafted MHP36 cells would not markedly stimulate activation of the immune system and upregulate lymphocyte proliferation, therefore negating the need for CsA immunosuppression. It would represent an enormous advantage if neural transplantation could be carried out in the absence of immunosuppression, given the side effects associated with immune suppression. However, other studies have shown that a triple combination of immunosuppressive drugs promote improved graft survival to CsA alone or no immunosuppression

(Pedersen et al., 1995, 1997). It is clear that the effectiveness of immunosuppression in neural grafts requires further investigation.

3.5.5 ApoE immunoreactivity

Upregulation of ApoE has been shown to take place following varying forms of brain damage; focal and global ischaemia, traumatic brain injury (Horsburgh and Nicoll, 1996, Iwata et al., 2005). In the present study, an immediate upregulation of apoE expression was observed at 1 week followed by a decrease at 4 weeks post-transplantation. The upregulation of apoE following brain damage is traditionally associated with breakdown and clearance of ischaemic cells, although it is also speculated to play an important role in repair and regeneration. There was no difference in the extent of apoE immunoreactivity between vehicle and MHP36 grafted mice. The upregulation of apoE may occur primarily as a result of global ischaemia, rather than as a response to the MHP36 cells. However, MHP36 cells grafted in a rodent model of focal ischaemia have been associated with upregulation and long-term maintenance of apoE levels (Dr. I. Reuter, Personal communication). Modo et al., (2003) investigated the pattern of apoE expression following MHP36 grafts in a rodent model of focal ischaemia. Sham operated animals exhibited minimal apoE expression. Intraparenchymal grafts of MHP36 cells were associated with increased apoE expression, in contrast to intraventricular grafts. Interestingly, intraparenchymal grafts also resulted in increased contralateral expression of apoE, suggestive of remodelling and reorganisation processes.

3.5.6 Summary

This study demonstrated that grafted MHP36 stem cells survive and migrate in a mouse model of global ischaemia. Grafted MHP36 cells differentiated into neurons and were able to reduce the extent of ischaemic neuronal damage. There was a minimal host immune response to the MHP36 grafts. The successful transplantation and characterisation of MHP36 grafts in mouse brain opens the door for future investigation into the genetic factors underlying stem cell graft integration via the use of *APOE*-transgenic mice.

Chapter 4

Influence of endogenous murine apoE on neural stem cell grafts in a mouse model of global ischaemia

4.1 Introduction

Apolipoprotein E (apoE) has many important roles in neurobiology, particularly in neurodegeneration, regeneration and repair (Herz and Beffert, 2000). In normal brain, apoE is synthesized and secreted by astrocytes. Following injury, apoE expression is induced in neurons. Thus, apoE can potentially regulate neuronal integrity. This has been observed in models of excitotoxicity (Boschert et al., 1999, White et al., 2001), focal ischaemia (Kitagawa et al., 2001) and global ischaemia (Hall et al., 1995, Kida et al., 1995, Horsburgh and Nicoll, 1996). Modo et al (2003) investigated the expression and distribution of apoE following grafting of MHP36 cells in a rat model of focal ischaemia. ApoE was upregulated in grafted animals and found to associate with differentiated neurons and astrocytes. These data suggested that apoE may be involved in the integration of neural stem cell grafts. Another preliminary study has shown upregulation and continued expression of apoE in association with MHP36 grafts, which was paralleled with functional recovery over a period of 6 weeks (Dr Iris Reuter, Personal Communication). ApoE has been implicated in mechanisms of anti-oxidation, excitotoxicity and cytoskeletal support (Miyata and Smith, 1996, Horsburgh et al., 2000, Boschert et al., 1999, Buttini et al., 1999, Strittmater et al., 1994, Masliah et al., 1996) which could all influence the survival and migration of transplanted stem cells. Interactions between apoE and the respective family of LDL receptors can affect a variety of downstream signalling pathways which may account for alterations to stem cell survival, migration and differentiation. In chapter 3, I demonstrated that MHP36 cells are able to survive, migrate and differentiate in a mouse model of global ischaemia, and also reduce the extent of ischaemic neuronal damage. With the availability of transgenic mice deficient in apoE (Piedrahita et al., 1992, Van Ree et al., 1994, Plump et al., 1992), it is now possible to address the question of whether endogenous apoE influences neural stem cell grafts in a mouse model of global ischaemia.

4.2 Aim

The aim of the study was to investigate whether apoE influences the survival, migration and differentiation of neural stem cell grafts in a mouse model of diffuse neuronal injury induced by global ischaemia, and also to examine cell signalling pathways which may be involved in these processes.

4.3 Materials and Methods

4.3.1 Study outline

Adult male wildtype C57Bl/6J (WT) mice and *APOE*-KO mice were used in this study (Chapter 2, Section 2.1) Transient global ischaemia was induced by bilateral occlusion of the common carotid arteries (BCCAo). Different durations of ischaemia were used, based on previous observations after studying different duration of global ischaemia in C57Bl/6J mice (Kelly et al., 2001) and studies demonstrating that *APOE*-KO mice are more susceptible to global ischaemia (Horsburgh et al., 1999). To ensure the extent of ischaemic neuronal damage was similar in WT and *APOE-KO* mice, an occlusion time of 17 minutes was chosen for WT mice, and occlusion times of 15 minutes and 17 minutes were chosen for *APOE*-KO mice.

Mice were immunosuppressed with CsA. Two weeks following global ischaemia, PKH26 labelled MHP36 cells (Passage number 59-67) were unilaterally grafted into the caudate nucleus and hippocampus (Chapter 2, Section 2.3). All mice received MHP36 grafts. Pre-graft viability averaged 91% and post-graft viability averaged 81%. 4 weeks post-transplantation, mice were transcardially perfused (Chapter 2, Section 2.5). The caudate nucleus and hippocampus was dissected from 14 animals (WT, 17m BCCAo, n = 5, *APOE*-KO, 15m BCCAo, n = 4, *APOE*-KO, 17m BCCAo, n = 5). 23 animals (WT, 17m BCCAo, n = 7, *APOE*-KO, 15m BCCAo, n = 9, *APOE*-KO, 17m BCCAo, n = 8) were processed for histology using the Callis method of freezing (Chapter 2, Section 2.6). Coronal cryostat sections (10μm) were mounted onto poly-L-lysine coated slides. Slides containing sections at the level of the injection tract were stained with haematoxylin and eosin in order to visualise the number of normal neurons. Slides adjacent to the ones taken for haematoxylin and

eosin staining were mounted in Vectashield for fluorescent visualisation of MHP36 cells or processed for immunohistochemistry using markers against NeuN and GFAP.

4.3.2 Quantification of ischaemic damage

The majority of studies investigating the extent of damage following global ischaemia terminate the animal within a week of the ischaemic insult (Horsburgh et al., 1999, Kelly et al., 2001). At this time point, damaged neurons undergoing ischaemic cell change are still clearly visible and morphologically distinct from normal neurons. In the present study, animals were examined six weeks following induction of ischaemia. The vast majority of ischaemic neurons have been degraded and cleared away by this time point, although a few neurons that are still undergoing homogenising cell change may be identified from their ghostlike appearance. As such, the classical method of identifying ischaemic damage (Auer & Sutherland, 2002, Lipton, 1999) becomes problematic. Therefore, another method of assessing neuronal damage was required. The number of morphologically normal neurons remaining was assessed as an index of ischaemic damage. H & E stained sections were used to assess the number of normal neurons using a 25mm^2 grid (attached to the microscope optics) at 400x magnification. Six fields were quantified in the ipsilateral and contralateral caudate nucleus, and one field for the ipsilateral and contralateral CA2 region of the hippocampus.

4.3.3 Quantification of MHP36 graft survival and migration

Sections were assessed for the number of surviving PKH26 labelled MHP36 cells using a confocal laser scanning microscope. Within the caudate nucleus, confocal z-series images were captured at six regions surrounding the injection tract and quantified for the number of MHP36 cells. Within the hippocampus, five confocal z-series images were captured along the granule cell layer of the CA region starting from the CA2 and progressing along the CA1 towards the septum. Migration of PKH26 labelled MHP36 cells was assessed in a medial, lateral and ventral direction away from the injection tract in both the caudate nucleus and hippocampus. The

distance of migration in each direction was measured using a 100mm^2 grid (attached to the microscope optics) at 200x magnification.

4.3.4 Immunofluorescent analysis

Sections were assessed for co-localization of phenotypic markers for neurons (NeuN) and astrocytes (GFAP) with PKH26 as a marker for transplanted MHP36 cells. Within the caudate nucleus, confocal z-series images were captured in five different fields medial, lateral and ventral to the injection tract in the caudate nucleus. Within the hippocampus, confocal z-series images were captured in four different fields along the granule cell layer of the CA region starting at the CA2 and progressing along the CA1. Neuronal and astrocytic differentiation was determined by counting the number of cells co-localizing with PKH26 after counting the number of PKH26 positive cells within the same field.

4.3.5 Western blotting

Frozen caudate and hippocampal samples were homogenized and assayed for protein concentration (Chapter 2, Section 2.10). 25μg of protein from ipsilateral and contralateral regions were loaded and separated on a SDS polyacrylamide gel along with a molecular weight marker. Separated protein samples were transferred onto a PVDF membrane overnight. Following transfer, the gel was stained with Coomassie blue to confirm equal loading of protein in each lane. The membrane was placed, protein side up, in a 50ml centrifuge tube and blocked in 10% non-fat dried milk in PBS-T before probing with antibodies (Table 2.3). Antibodies bound to the membrane were detected using enhanced chemiluminescence. Membranes were sequentially stripped and reprobed with a variety of antibodies. The relative optical density of protein bands were measured (Chapter 2, Section 2.10.8) and quantified.

4.3.6 Statistical analyses

A Kruskal-Wallis test followed by Dunn's post-test was used to assess statistical differences between the groups.

4.4 Results

4.4.1 Ischaemic damage

The number of morphologically normal neurons was assessed as an index of ischaemic neuronal damage. Within the contralateral caudate nucleus, there were significantly higher numbers of normal neurons in WT mice compared to *APOE*-KO mice subjected to 15 minutes BCCAo (18.14 ± 2.37 vs. 13.70 ± 1.92 normal neurons per 0.0625mm^2, $p < 0.05$). A similar trend was observed compared to *APOE*-KO mice subjected to 17 minutes BCCAo, although this difference was not statistically significant (18.14 ± 2.37 vs. 14.13 ± 2.93 normal neurons per 0.0625mm^2, $p > 0.05$). The number of morphologically normal neurons was assessed in the ipsilateral caudate nucleus which received the graft of MHP36 stem cells. In this hemisphere the number of normal neurons was similar between WT (16.38 ± 1.53 normal neurons per 0.0625mm^2) and *APOE*-KO mice subjected to 15 minutes BCCAo (16.63 ± 1.48 normal neurons per 0.0625mm^2), although neurons were reduced in number in *APOE*-KO mice subjected to 17 minutes BCCAo (13.56 ± 2.01 normal neurons per 0.0625mm^2) (Figure 4.1). Taken together, the data show that in the ungrafted contralateral caudate nucleus, *APOE*-KO mice have a reduced neuronal number than WT mice, consistent with increased susceptibility to ischaemic damage. However, in the grafted ipsilateral caudate nucleus, *APOE*-KO mice subjected to 17 minutes BCCAo maintain reduced neuronal number compared to WT mice. Interestingly, *APOE*-KO mice subjected to 15 minutes BCCAo also have comparable numbers of normal neurons to WT mice. This could be suggestive of neuronal replacement by the grafted stem cells or alternatively explained by the MHP36 cells exerting a neuroprotective effect.

The number of neurons remaining was also assessed in the CA2 region of the hippocampus (Figure 4.2). In the contralateral CA2 region, *APOE*-KO mice subjected to 17m BCCAo have fewer normal neurons compared to *APOE*-KO mice subjected to 15 minutes BCCAo (14.50 ± 6.37 vs. 23.00 ± 5.87 normal neurons per 0.0625mm^2, $p < 0.05$) and WT mice (14.50 ± 6.37 vs. 21.71 ± 3.73 normal neurons per 0.0625mm^2, $p > 0.05$), although the latter comparison is not statistically

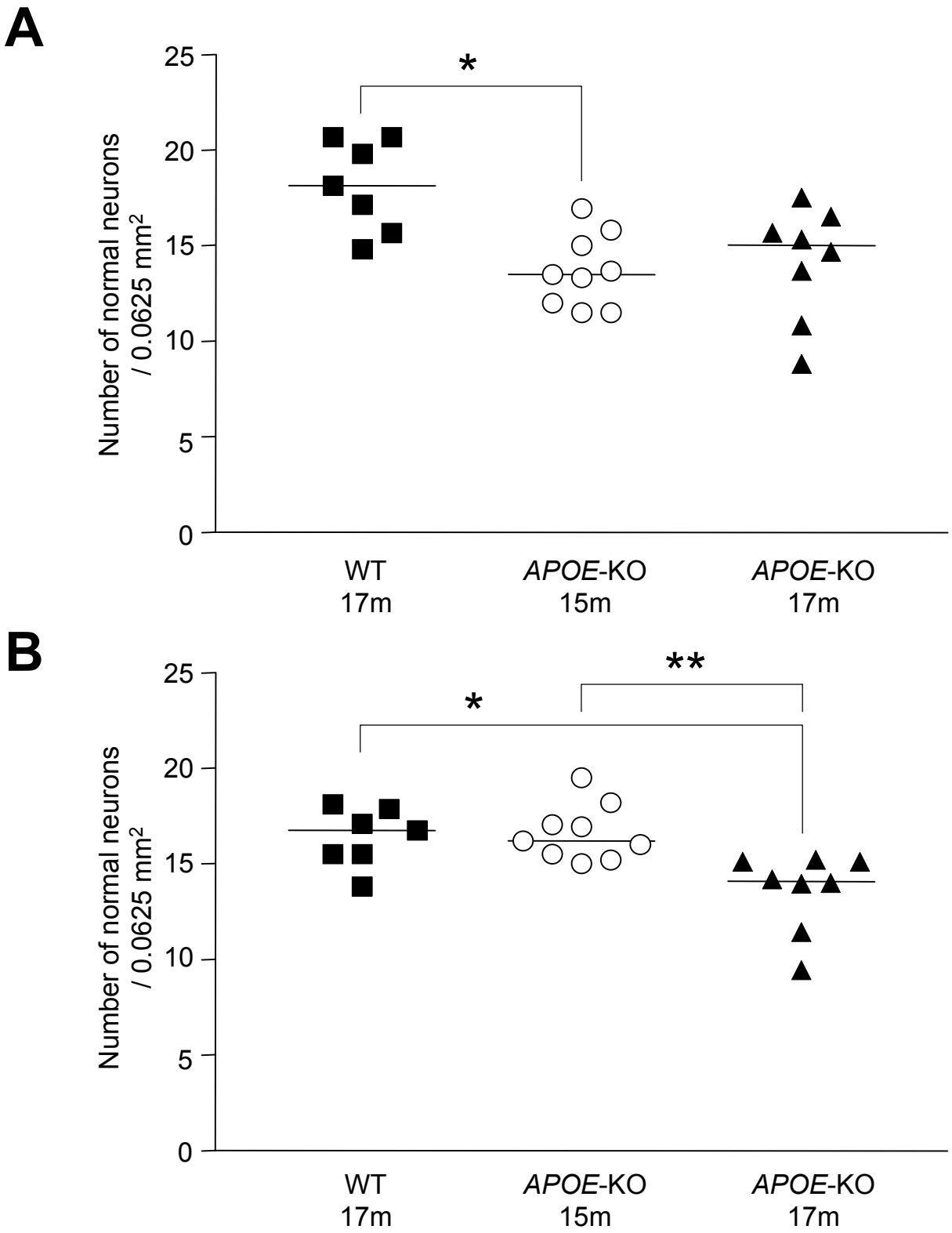

Figure 4.1 Number of morphologically normal neurons within the caudate nucleus

Number of normal neurons per 0.0625 mm^2 in WT mice subjected to 17m BCCAo and *APOE*-KO mice subjected to 15m and 17m BCCAo within the contralateral (A) and ipsilateral (B) caudate nucleus. Data are expressed as individual data points, with the bar indicating the median. In the contralateral hemisphere, WT mice have significantly more normal neurons compared to *APOE*-KO mice subjected to 15m BCCAo. However, in the ipsilateral hemisphere, *APOE*-KO mice subjected to 17m BCCAo have significantly fewer normal neurons compared to the other two groups. * $p < 0.05$, ** $p < 0.01$ using Kruskal-Wallis test with Dunn's post-test.

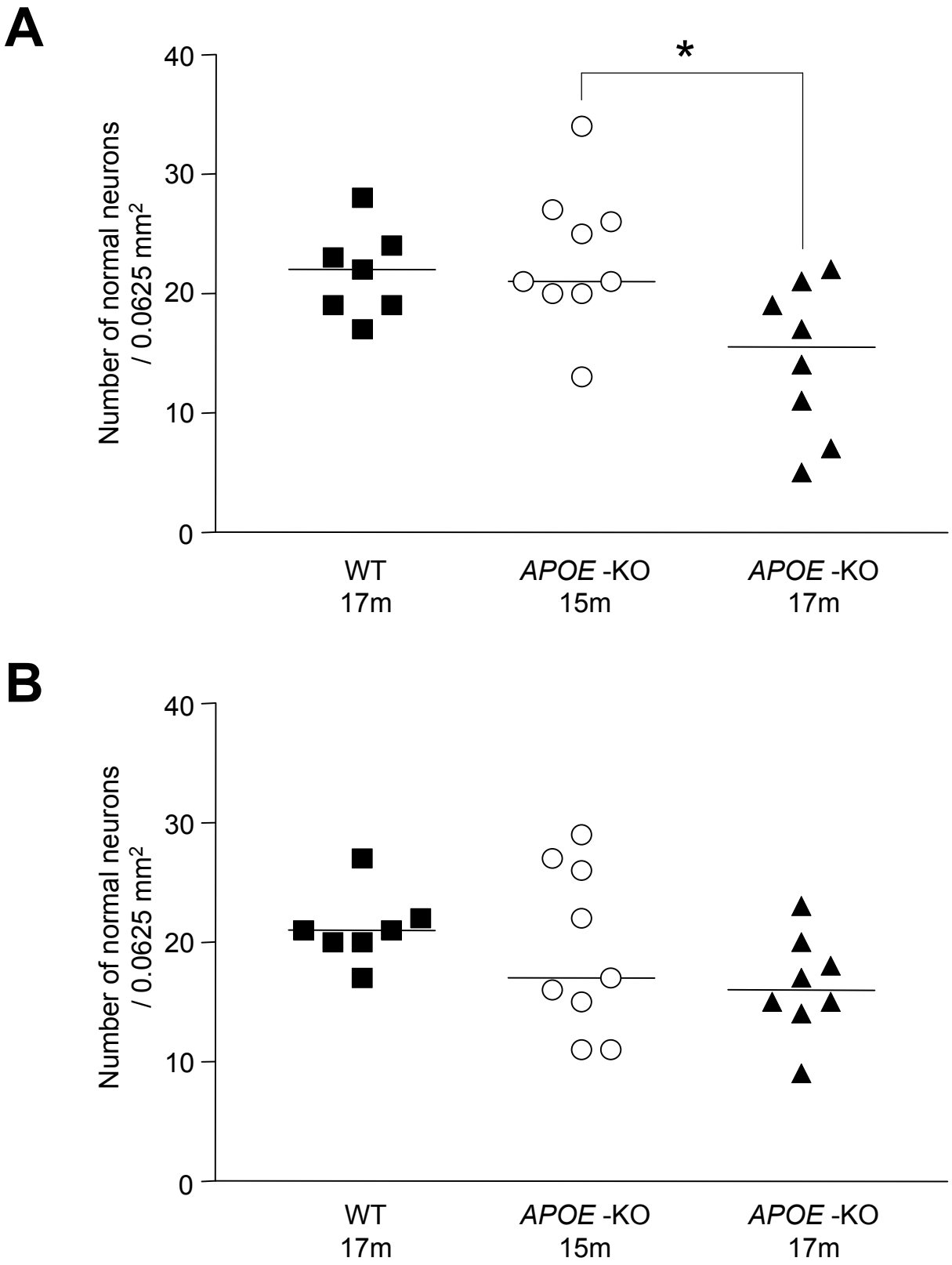

Figure 4.2 Number of morphologically normal neurons within the hippocampus
Number of normal neurons per 0.0625 mm^2 in WT mice subjected to 17m BCCAo and *APOE* -KO mice subjected to 15m and 17m BCCAo within the contralateral (A) and ipsilateral (B) hippocampus. Data are expressed as individual data points, with the bar indicating the median. *APOE* -KO mice subjected to 15m BCCAo have significantly more normal neurons than *APOE* -KO mice subjected to 17m BCCAo in the contralateral hemisphere. * $p < 0.05$ using Kruskal-Wallis test with Dunn's post-test.

significant. A similar trend was observed in the grafted ipsilateral CA2 region. WT mice exhibited a similar neuronal density to *APOE*-KO mice subjected to 15 minutes BCCAo (21.14 ± 30.2 vs. 19.33 ± 6.87 normal neurons per 0.0625mm^2, $p > 0.05$). *APOE*-KO mice subjected to 17 minutes BCCAo exhibited the fewest number of normal neurons (16.38 ± 4.21 normal neurons per 0.0625mm^2), although there are no statistically significant differences between the groups (Kruskal-Wallis test, $p > 0.05$).

4.4.2 MHP36 graft survival and migration

Survival of MHP36 stem cells in the caudate nucleus was significantly improved in WT mice compared to *APOE*-KO mice subjected to 15 minutes BCCAo (8.06 ± 2.25 vs. 1.77 ± 0.56 PKH26 positive MHP36 cells per 0.0350mm^2, $p < 0.01$) and 17 minutes BCCAo (8.06 ± 2.25 vs. 1.68 ± 0.81 PKH26 positive MHP36 cells per 0.0350mm^2, $p < 0.01$) (Figure 4.3). Similarly, survival of MHP36 stem cells in the hippocampus is significantly improved in WT mice compared to *APOE*-KO mice subjected to 15 minutes BCCAo (5.17 ± 1.57 vs. 2.42 ± 1.14 PKH26 positive MHP36 cells per 0.0350mm^2, $p < 0.05$) and 17 minutes BCCAo (5.17 ± 1.57 vs. 2.31 ± 0.94 PKH26 positive MHP36 cells per 0.0350mm^2, $p < 0.05$) (Figure 4.4). These data strongly suggest that apoE is an important factor in promoting MHP36 stem cell survival.

Migration of MHP36 stem cells was assessed in a medial, lateral and ventral direction away from the injection tract. Within the caudate nucleus, there was an overall trend towards increased migration in all three directions in WT mice as compared to *APOE*-KO mice (Figure 4.5). The migration of stem cells was significantly greater in WT mice compared to *APOE*-KO mice subjected to 15 minutes BCCAo in both a lateral axis (0.75 ± 0.28 vs. 0.35 ± 0.17 mm, $p < 0.05$) and a ventral axis (0.67 ± 0.18 vs. 0.26 ± 0.16 mm, $p < 0.01$). There was no significant difference in MHP36 migration between WT and *APOE*-KO mice within the hippocampus (Figure 4.6).

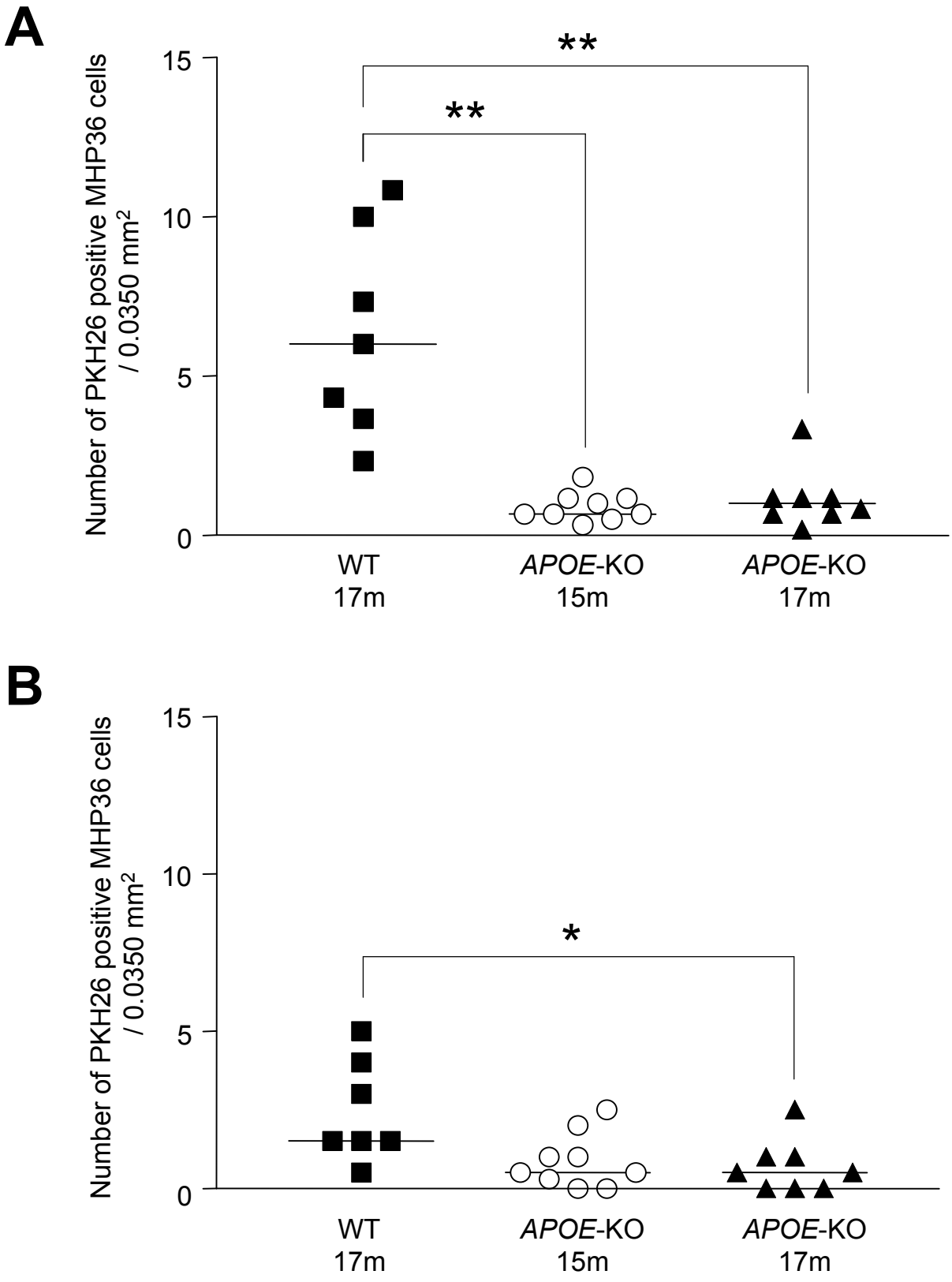

Figure 4.3 Survival of MHP36 cells within the caudate nucleus
Number of PKH26 positive MHP36 cells per 0.0350 mm^2 in WT mice subjected to 17m BCCAo and *APOE*-KO mice subjected to 15m and 17m BCCAo within the caudate nucleus (A) and the corpus callosum (B). Data are expressed as individual data points, with the bar indicating the median. In both regions, the survival of MHP36 cells is significantly higher in WT mice compared to both groups of *APOE*-KO mice.
* $p < 0.05$, ** $p < 0.01$ using Kruskal-Wallis test with Dunn's post-test.

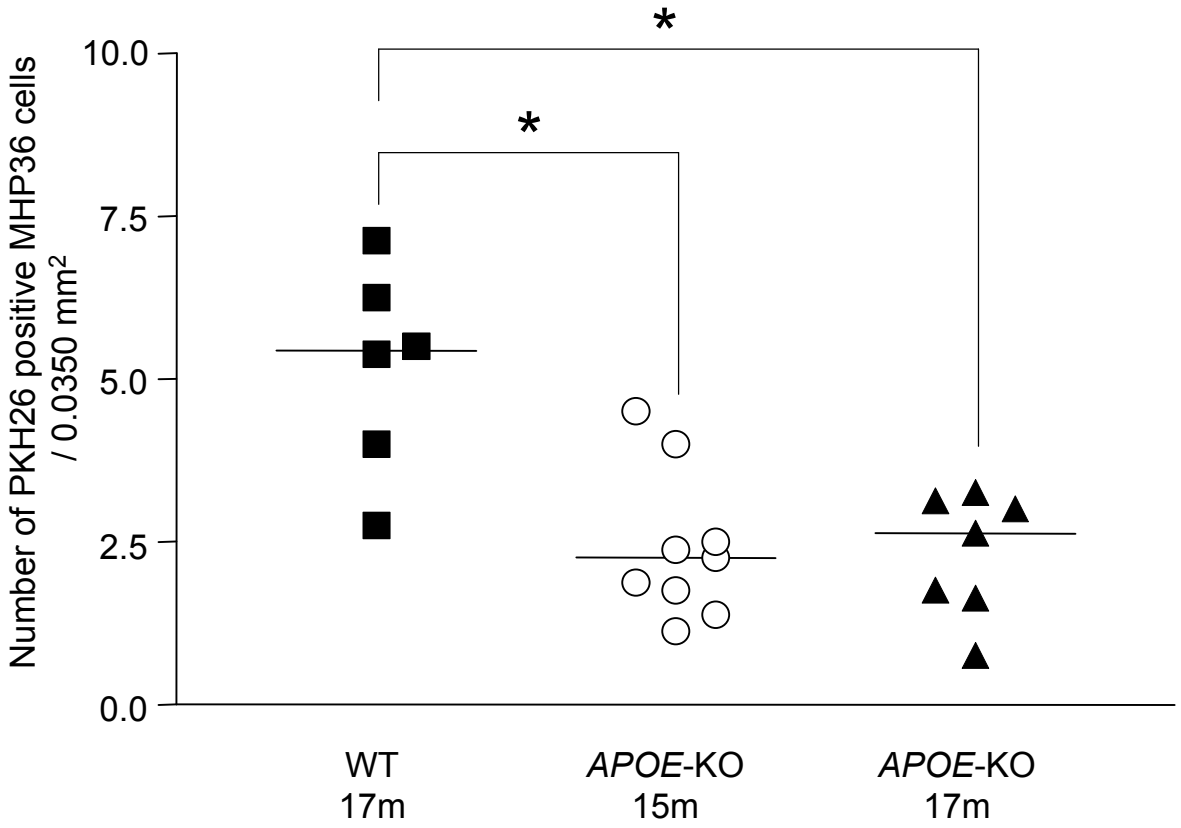

Figure 4.4 Survival of MHP36 cells in the hippocampus
Number of PKH26 positive MHP36 cells per 0.0350 mm^2 in WT mice subjected to 17m BCCAo and *APOE*-KO mice subjected to 15m and 17m BCCAo within the hippocampus. Data are expressed as individual data points, with the bar indicating the median. Significantly more MHP36 cells survive in WT mice compared to both groups of *APOE*-KO mice. * $p < 0.05$ using Kruskal-Wallis test with Dunn's post-test.

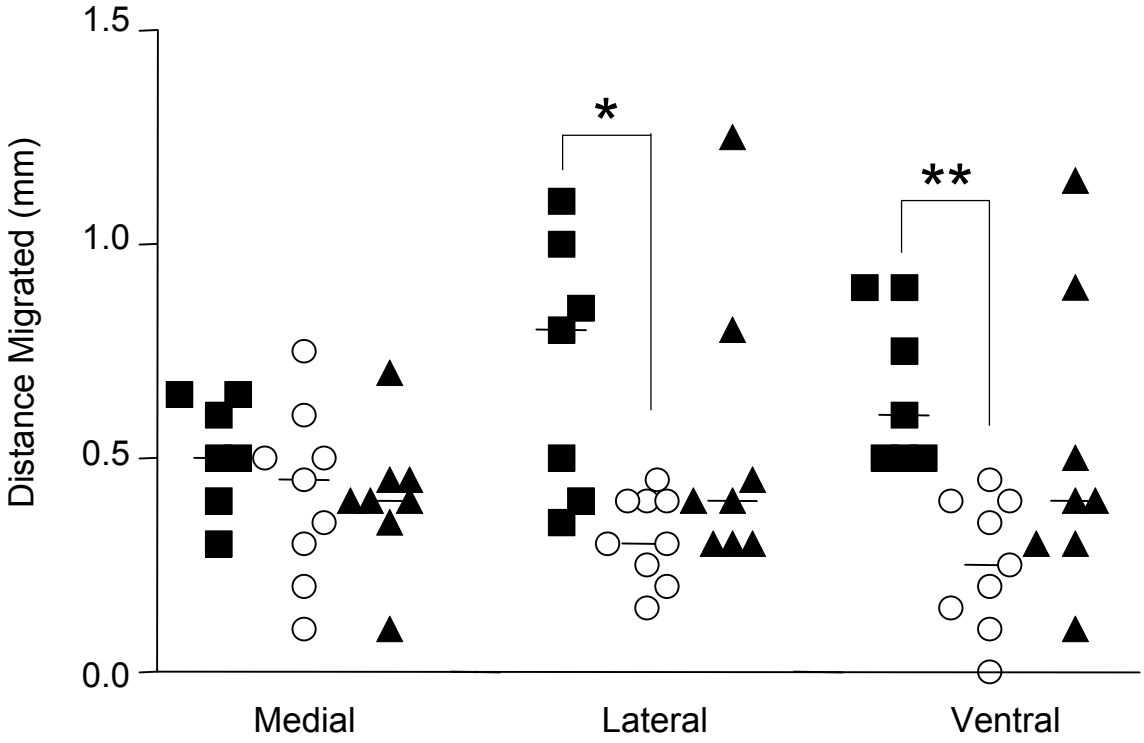

Figure 4.5 Migration of MHP36 cells within the caudate nucleus
Distance migrated (mm) by MHP36 cells in WT mice subjected to 17m BCCAo and *APOE*-KO mice subjected to 15m and 17m BCCAo within the caudate nucleus. Migration was assessed in medial, lateral and ventral directions away from the injection tract. Data are expressed as individual data points, with the bar indicating the median. Migration was significantly further in WT mice subjected to 17m BCCAo compared to *APOE*-KO mice subjected to 15m BCCAo in lateral and ventral directions.
* $p < 0.05$, ** $p < 0.01$ using Kruskal-Wallis test with Dunn's post-test.

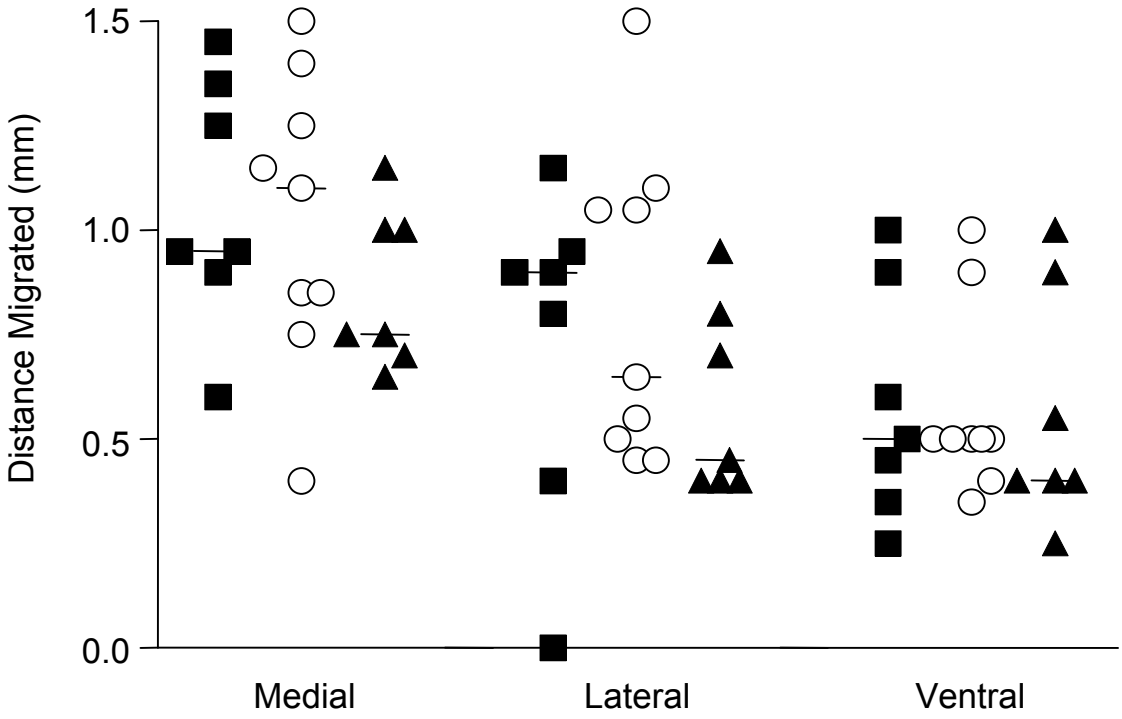

Figure 4.6 Migration of MHP36 cells in the hippocampus
Distance migrated (mm) by MHP36 cells in WT mice subjected to 17m BCCAo and APOE-KO mice subjected to 15m and 17m BCCAo within the hippocampus. Migration was assessed in medial, lateral and ventral directions away from the injection tract. Data are expressed as individual data points, with the bar indicating the median. There was no statistical difference in distance migrated in the hippocampus between the three groups of mice.

4.4.3 Neuronal differentiation of MHP36 cells

Within the caudate nucleus, a significantly higher proportion of grafted MHP36 cells differentiated into a neuronal phenotype in WT mice compared to *APOE*-KO mice subjected to 15 minutes BCCAo (79.79 ± 6.90 % vs. 25.02 ± 17.14 % MHP36 cells colocalised with NeuN, $p < 0.01$) and 17 minutes BCCAo (79.79 ± 6.90 % vs. 17.84 ± 13.76 % MHP36 cells colocalised with NeuN, $p < 0.01$) (Figures 4.7 and 4.8). A similar distinction between the genotypes was observed in the hippocampus, although the percentage of neuronally differentiated cells was reduced compared to the caudate nucleus. Significantly more grafted MHP36 cells differentiated into a neuronal phenotype in WT mice compared to *APOE*-KO mice subjected to 15 minutes BCCAo (30.58 ± 4.25 % vs. 14.55 ± 14.52 % MHP36 cells colocalised with NeuN, $p < 0.05$) and 17 minutes BCCAo (30.58 ± 4.25 % vs. 9.36 ± 10.39 % MHP36 cells colocalised with NeuN, $p < 0.05$) (Figures 4.9 and 4.10). These data are summarised as pie charts in Figure 4.15.

4.4.4 Astrocytic differentiation of MHP36 cells

Within the caudate nucleus, WT mice exhibited a trend towards reduced astrocytic differentiation of grafted MHP36 cells compared to *APOE*-KO mice, although this was not statistically significant (Figures 4.11 and 4.12). Approximately 8.31 ± 6.95 % of MHP36 cells expressed an astrocytic phenotype in WT mice compared to 19.10 ± 10.65 % of MHP36 cells in *APOE*-KO mice subjected to 15 minutes BCCAo and 24.21 ± 27.77 % of MHP36 cells in *APOE*-KO mice subjected to 17 minutes BCCAo. However, the converse situation was observed within the hippocampus. A significantly higher proportion of grafted MHP36 cells differentiated into an astrocytic phenotype in WT mice compared to *APOE*-KO mice subjected to 15 minutes BCCAo (48.62 ± 11.23 % vs. 20.61 ± 10.74 % MHP36 cells colocalised with GFAP, $p < 0.05$) and 17 minutes BCCAo (48.62 ± 11.23 % vs. 14.30 ± 10.05 % MHP36 cells colocalised with GFAP, $p < 0.01$) (Figures 4.13 and 4.14). These data are summarised as pie charts in Figure 4.15.

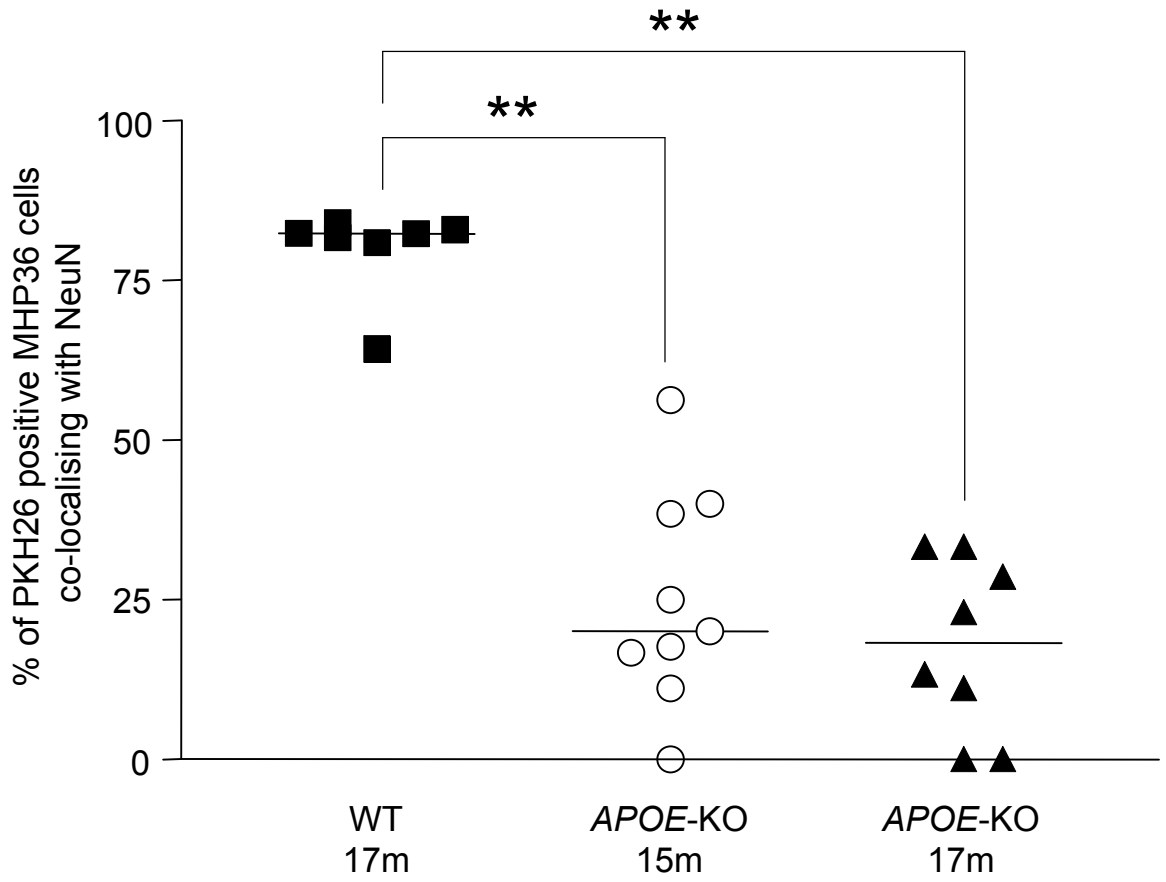

Figure 4.7 Neuronal differentiation of MHP36 cells within the caudate nucleus
Percentage of PKH26 positive MHP36 cells co-localising with NeuN in WT mice subjected to 17m BCCAo and *APOE*-KO mice subjected to 15m and 17m BCCAo within the caudate nucleus. Significantly more MHP36 cells differentiate into a neuronal phenotype in WT mice compared to both groups of *APOE*-KO mice. Data are expressed as individual data points, with the bar indicating the median.
** $p < 0.01$ using Kruskal-Wallis test with Dunn's post-test.

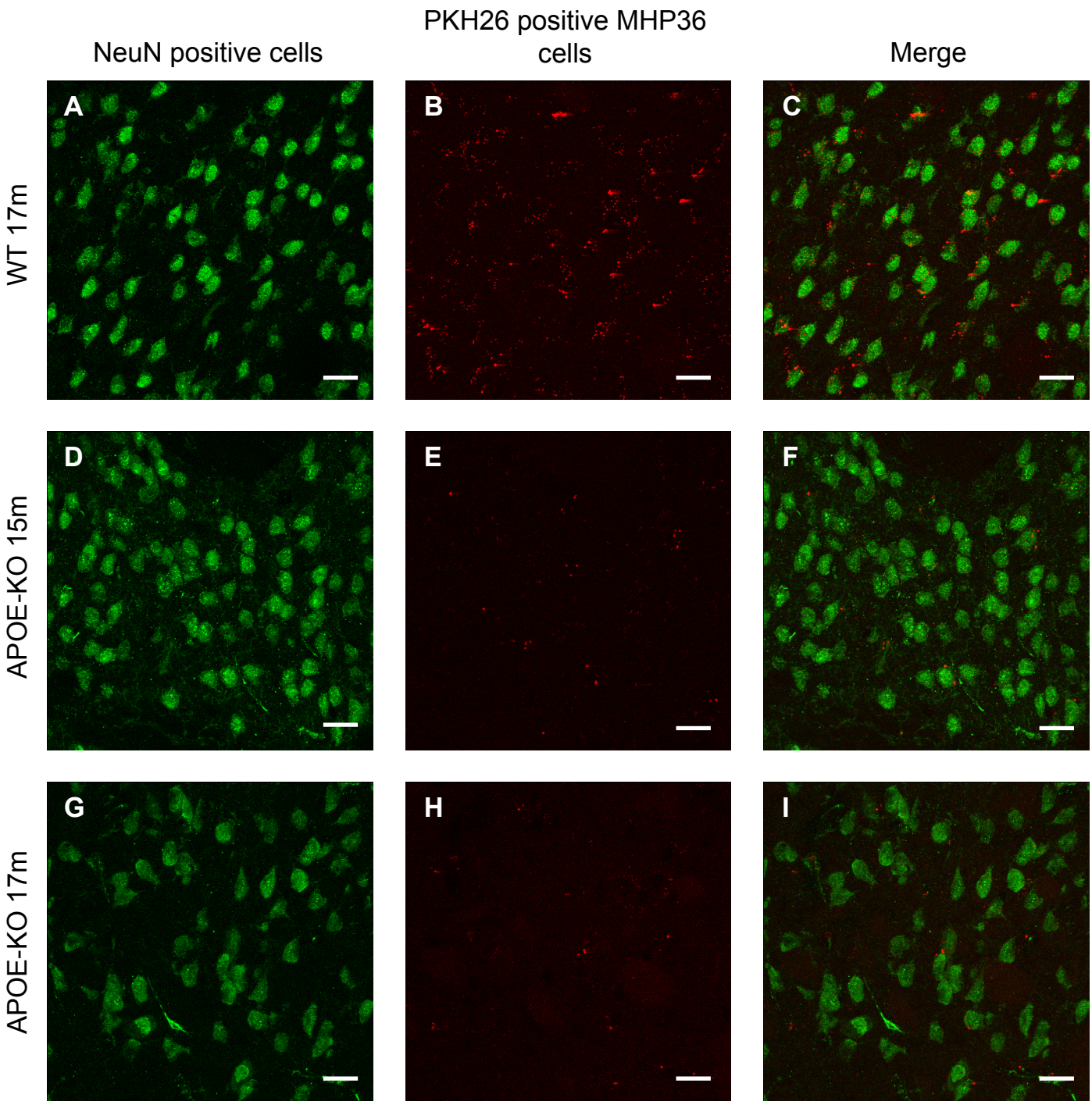

Figure 4.8 Representative confocal images illustrating neuronal differentiation of MHP36 cells in the caudate nucleus

Confocal images of PKH26 positive MHP36 cells (red) co-localised with the neuronal marker NeuN (green) in WT mice subjected to 17m BCCAo (Panels A-C) and APOE-KO mice subjected to 15m (Panels D-F) and 17m BCCAo (Panels G-I) within the caudate nucleus. Increased neuronal differentiation was observed in WT mice. The survival of MHP36 cells was also improved in the WT mice compared to both groups of APOE-KO mice (Panels B, E and H). Scale bar = 20 μm.

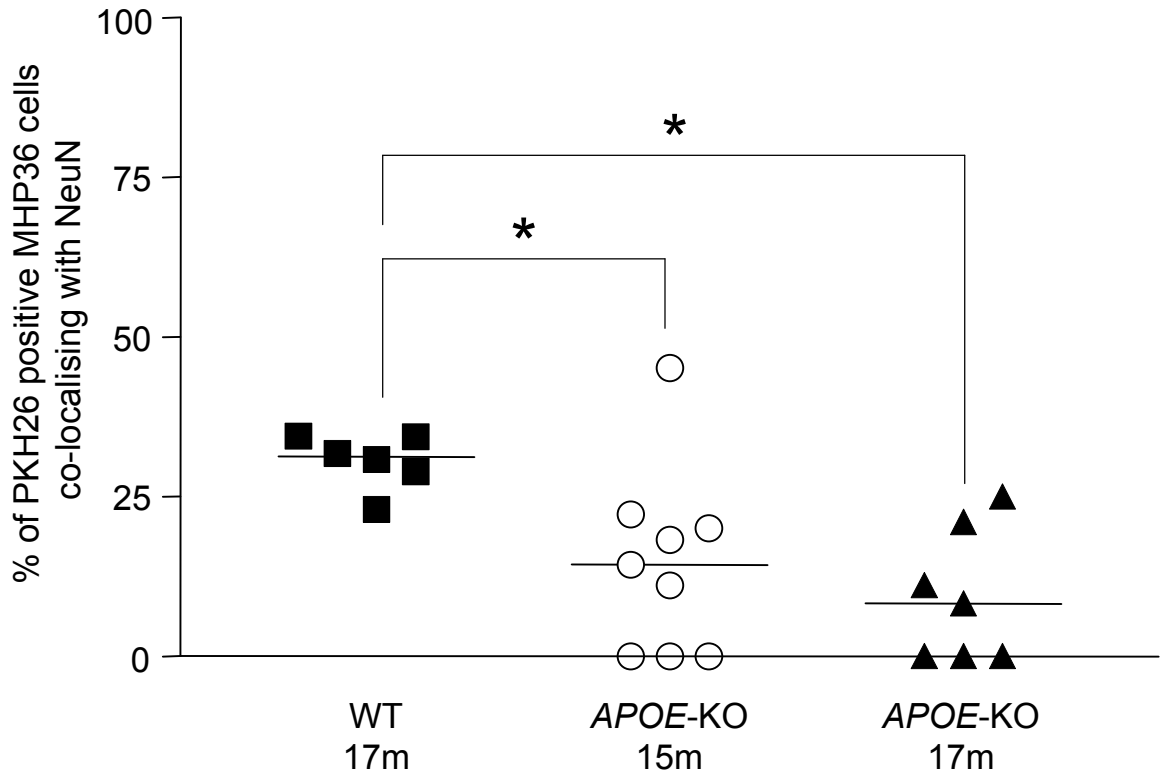

Figure 4.9 Neuronal differentiation of MHP36 cells within the hippocampus
Percentage of PKH26 positive MHP36 cells co-localising with NeuN in WT mice subjected to 17m BCCAo and *APOE*-KO mice subjected to 15m and 17m BCCAo within the hippocampus. Data are expressed as individual data points, with the bar indicating the median. Significantly more MHP36 cells differentiate into a neuronal phenotype in WT mice compared to both groups of *APOE*-KO mice.
* $p < 0.05$ using Kruskal-Wallis test with Dunn's post-test.

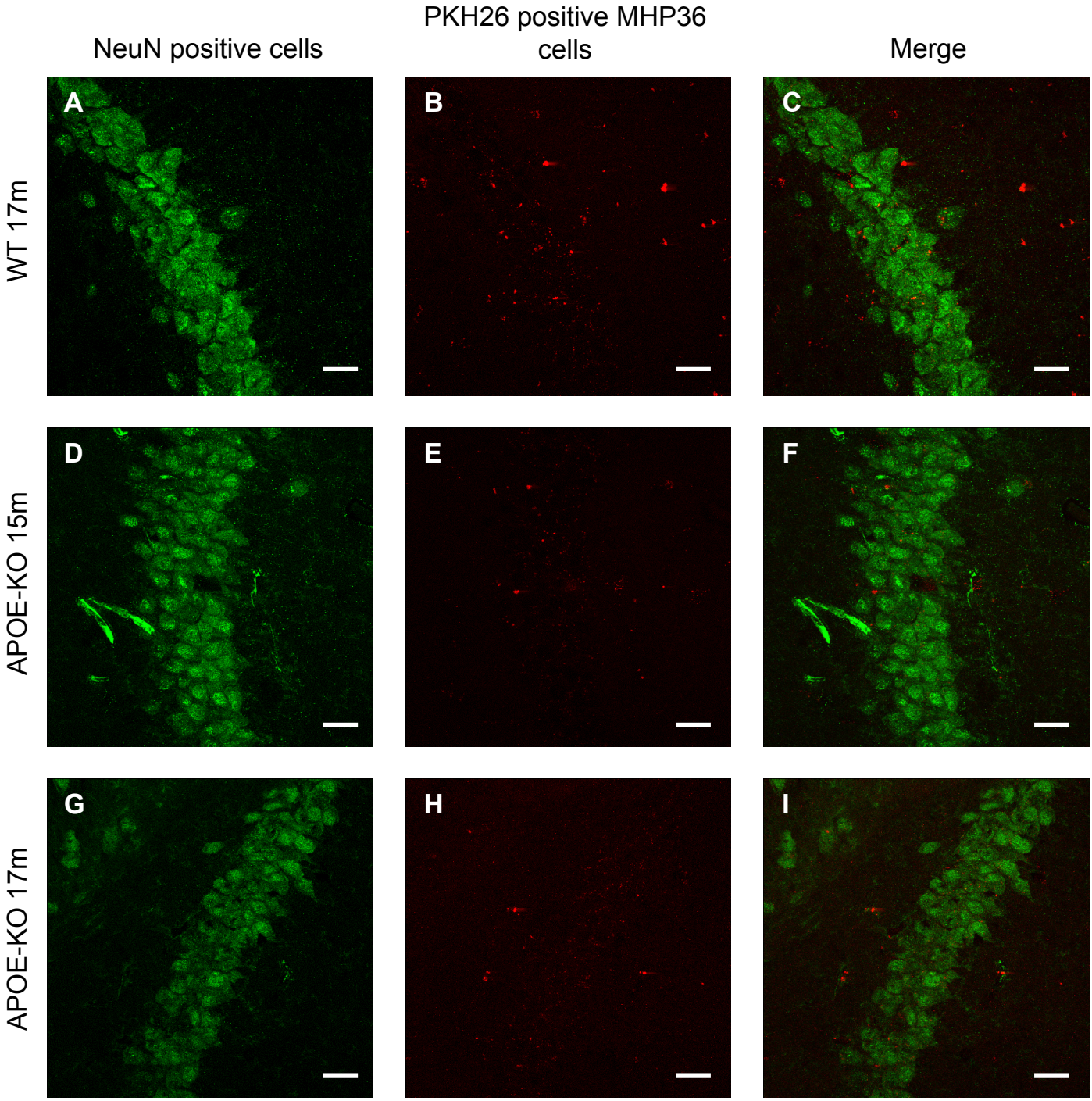

Figure 4.10 Representative confocal images illustrating neuronal differentiation of MHP36 cells in the hippocampus

Confocal images of PKH26 positive MHP36 cells (red) co-localised with the neuronal marker NeuN (green) in WT mice subjected to 17m BCCAo (Panels A-C) and APOE-KO mice subjected to 15m (Panels D-F) and 17m BCCAo (Panels G-I) within the hippocampus. Increased neuronal differentiation was observed in WT mice. The survival of MHP36 cells was also improved in the WT mice compared to both groups of APOE-KO mice (Panels B, E and H). Scale bar = 20 μm.

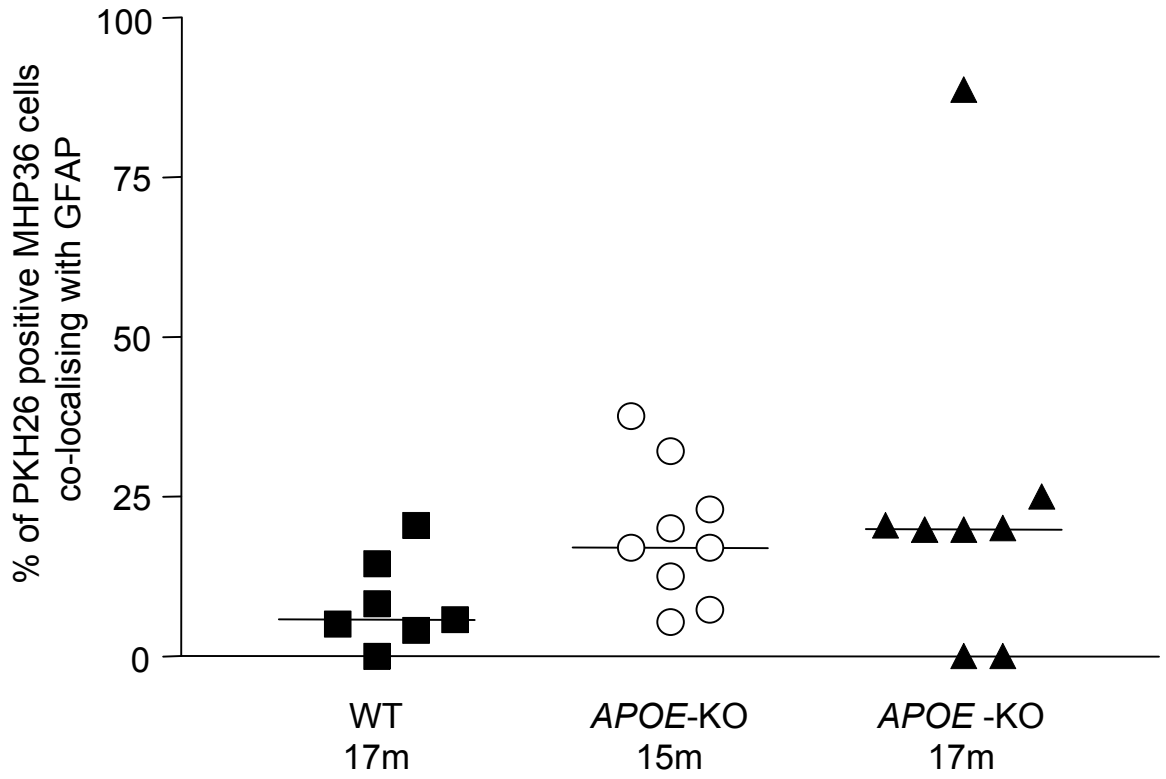

Figure 4.11 Astrocytic differentiation of MHP36 cells in the caudate nucleus
Percentage of PKH26 positive MHP36 cells co-localising with GFAP in WT mice subjected to 17m BCCAo and *APOE* -KO mice subjected to 15m and 17m BCCAo within the caudate nucleus. There is a trend towards reduced astrocytic differentiation in WT mice as compared to *APOE* -KO mice. Data are expressed as individual data points, with the bar indicating the median.

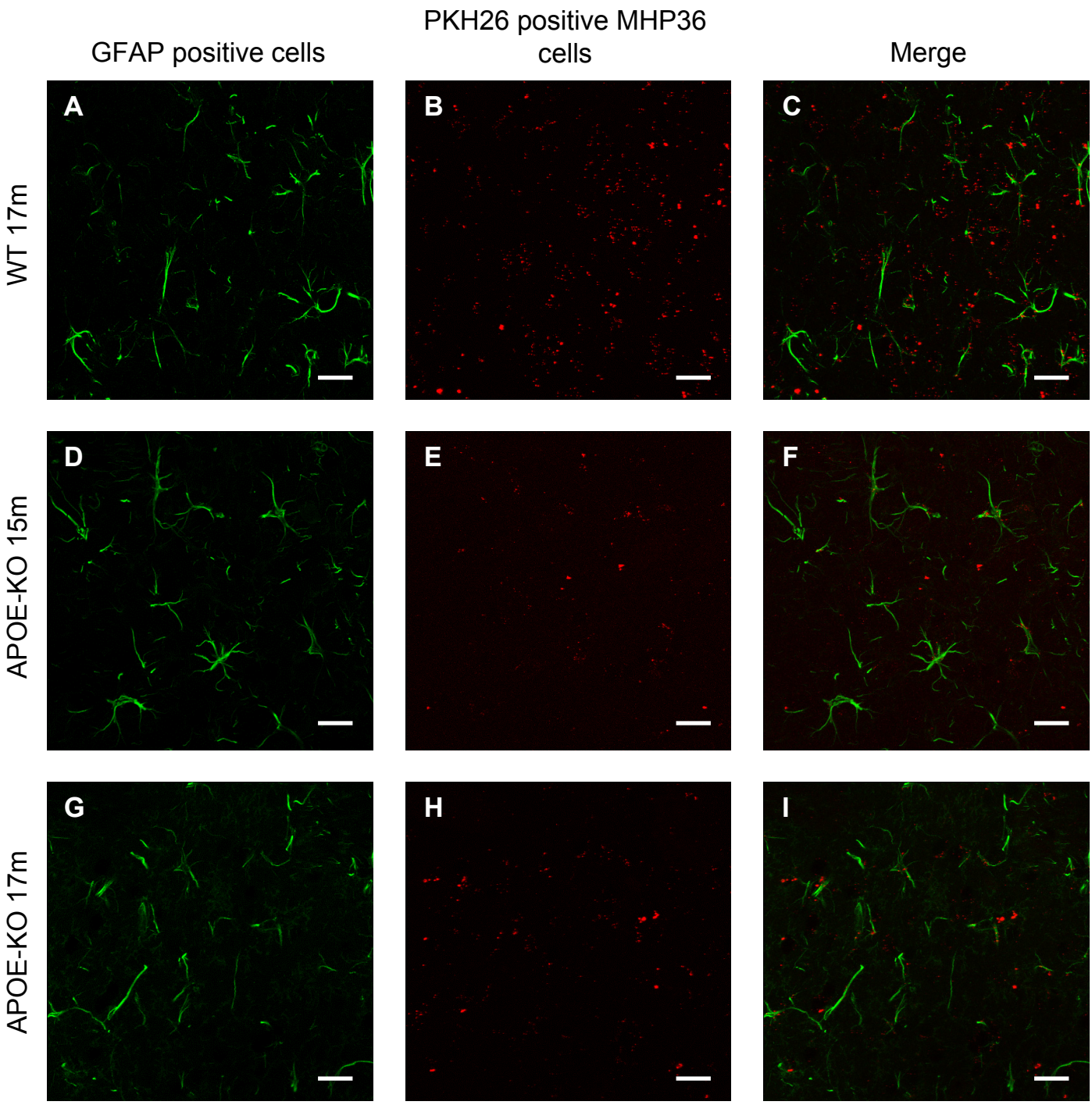

Figure 4.12 Representative confocal images illustrating astrocytic differentiation of MHP36 cells in the caudate nucleus

Confocal images of PKH26 positive MHP36 cells (red) co-localised with the neuronal marker NeuN (green) in WT mice subjected to 17m BCCAo (Panels A-C) and APOE-KO mice subjected to 15m (Panels D-F) and 17m BCCAo (Panels G-I) within the caudate nucleus. The survival of MHP36 cells was also improved in the WT mice compared to both groups of APOE-KO mice (Panels B, E and H). Scale bar = 20 μm.

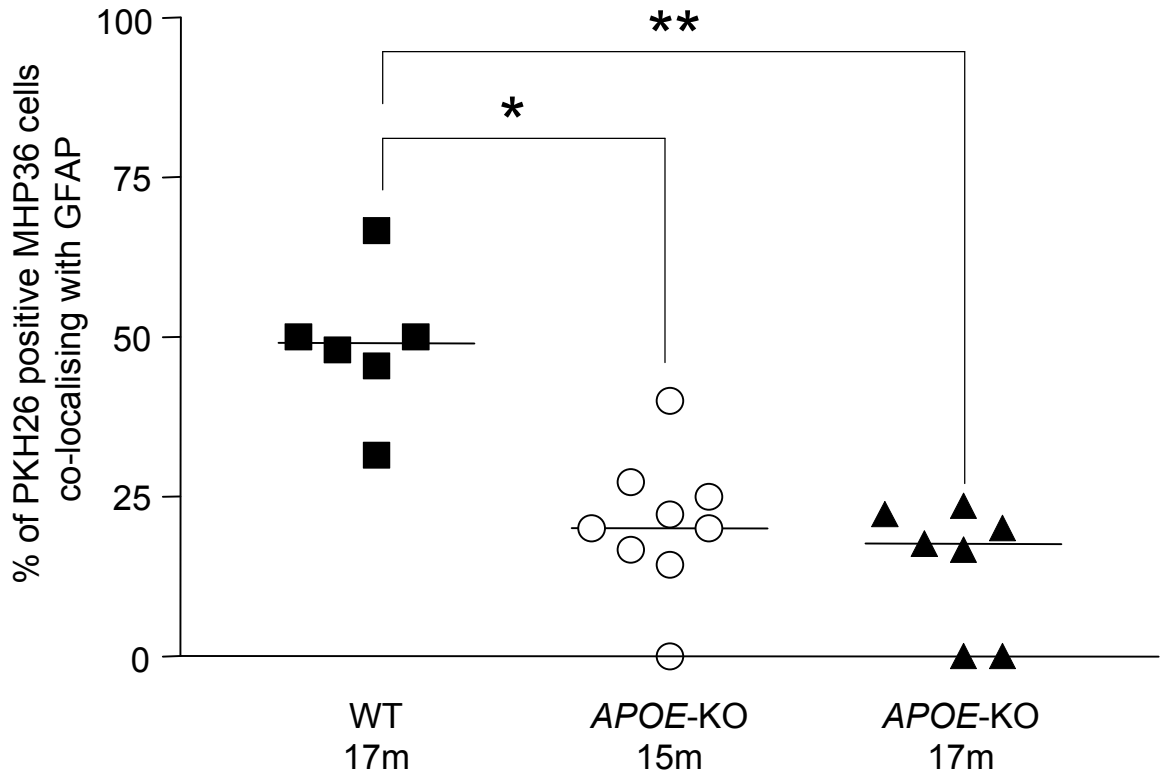

Figure 4.13 Astrocytic differentiation of MHP36 cells within the hippocampus
Percentage of PKH26 positive MHP36 cells co-localising with GFAP in WT mice subjected to 17m BCCAo and *APOE*-KO mice subjected to 15m and 17m BCCAo within the hippocampus. Data are expressed as individual data points, with the bar indicating the median. Significantly more MHP36 cells differentiate into a astrocytic phenotype in WT mice compared to *APOE*-KO mice.
* $p< 0.05$, ** $p < 0.01$ using Kruskal-Wallis test with Dunn's post-test.

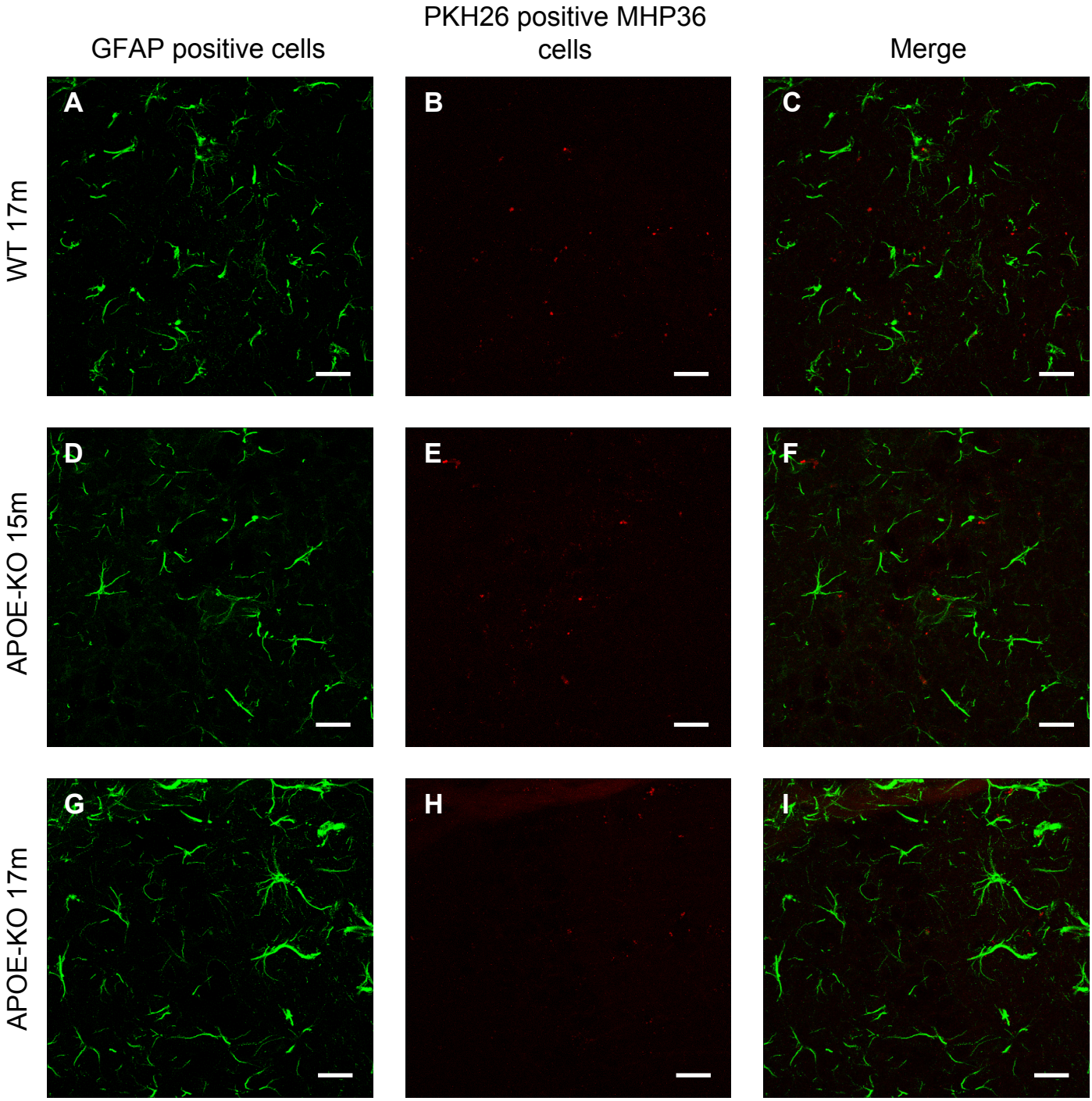

Figure 4.14 Representative confocal images illustrating astrocytic differentiation of MHP36 cells in the hippocampus

Confocal images of PKH26 positive MHP36 cells (red) co-localised with the astrocytic marker GFAP (green) in WT mice subjected to 17m BCCAo (Panels A-C) and APOE-KO mice subjected to 15m (Panels D-F) and 17m BCCAo (Panels G-I) within the hippocampus. Increased astrocytic differentiation was observed in WT mice. The survival of MHP36 cells was also improved in the WT mice compared to both groups of APOE-KO mice (Panels B, E and H). Scale bar = 20 μm.

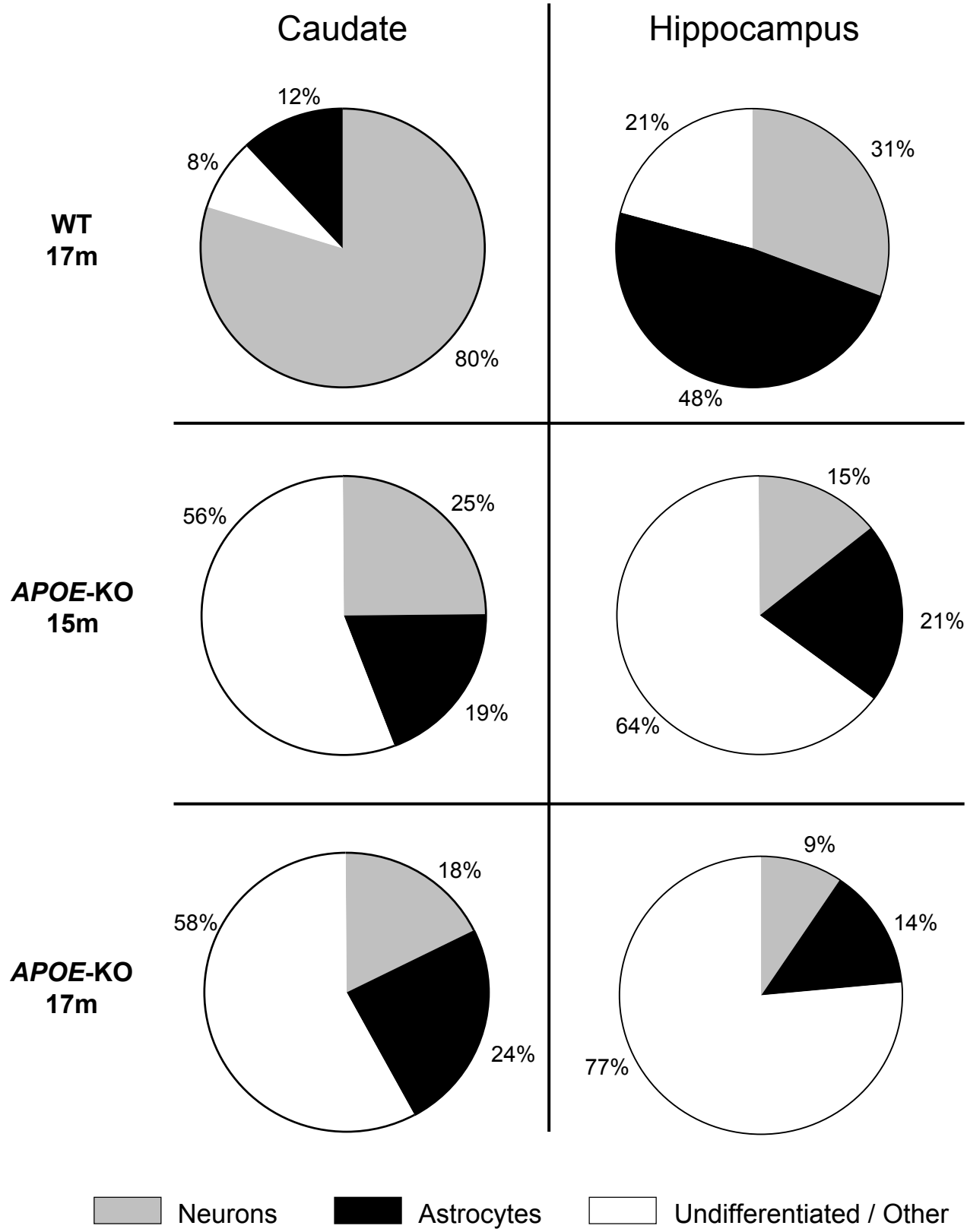

Figure 4.15 MHP36 cells grafted into WT mice exhibit an increased likelihood of differentiation

Pie charts showing the percentage of MHP36 cells differentiating into a neuronal, astrocytic or undetermined phenotype in WT mice subjected to 17m BCCAo and *APOE*-KO mice subjected to 15m and 17m BCCAo within the caudate nucleus and hippocampus.

4.4.5 Protein levels

In a separate study, the protein levels of ERK 1/2, JNK 1/2 and their respective phosphorylated forms were measured in homogenates derived from the caudate nucleus and hippocampus of the three groups of mice. A single protein band was detected at 44kDa for ERK 1, 42 kDa for ERK2, 46kDa for JNK1 and 54kDa for JNK2. The phosphorylated forms of these proteins were detected at the same molecular weights. Within the caudate nucleus, there was no significant change in levels of ERK 1 or 2 (both unphosphorylated and phosphorylated) in either the ipsilateral or contralateral hemisphere within the three groups (Figures 4.16 and 4.17). However, there was a trend towards an increase in phosphorylated ERK 1 and 2 in *APOE*-KO mice subjected to 15 minutes BCCAo (Phosphorylated ERK1; Contralateral hemisphere, WT, 0.219 ± 0.06 vs. 15m BCCAo, 0.301 ± 0.14 vs. 17m BCCAo, 0.244 ± 0.04 R.O.D., $p > 0.05$; ipsilateral hemisphere, WT, 0.188 ± 0.07 vs. 15m BCCAo, 0.336 ± 0.10 vs. 17m BCCAo, 0.234 ± 0.03 R.O.D., $p > 0.05$. Phosphorylated ERK2; contralateral hemisphere, WT, 0.078 ± 0.02 vs. 15m BCCAo, 0.147 ± 0.05 vs. 17m BCCAo, 0.115 ± 0.05 R.O.D., $p > 0.05$; ipsilateral hemisphere, WT, 0.061 ± 0.02 vs. 15m BCCAo, 0.160 ± 0.07 vs. 17m BCCAo, 0.103 ± 0.06 R.O.D., $p > 0.05$). There was no significant difference in levels of JNK 1 or 2 in either the ipsilateral or contralateral caudate nucleus within the three groups (Figure 4.18), although a difference in the levels of phosphorylated JNK 1 and 2 was observed (Figure 4.19). Significantly higher levels of phosphorylated JNK 2 were observed in the ipsilateral hemisphere of *APOE*-KO mice subjected to 15 minutes BCCAo compared to WT mice subjected to 17 minutes BCCAo. This group of *APOE*-KO mice also exhibited a trend towards increased levels of phosphorylated JNK 1 in the same hemisphere.

Within the hippocampus, there was no significant change in the levels of ERK 1 and 2 or JNK 1 and 2 (unphosphorylated or phosphorylated) in the ipsilateral or contralateral hemisphere within the three groups (Figures 4.20 to 4.23). However, similar to that observed in the caudate nucleus, there was a trend towards an increase in levels of phosphorylated JNK 1 and 2 in the ipsilateral hemisphere of *APOE*-KO mice subjected to 15 minutes BCCAo (Figure 4.23).

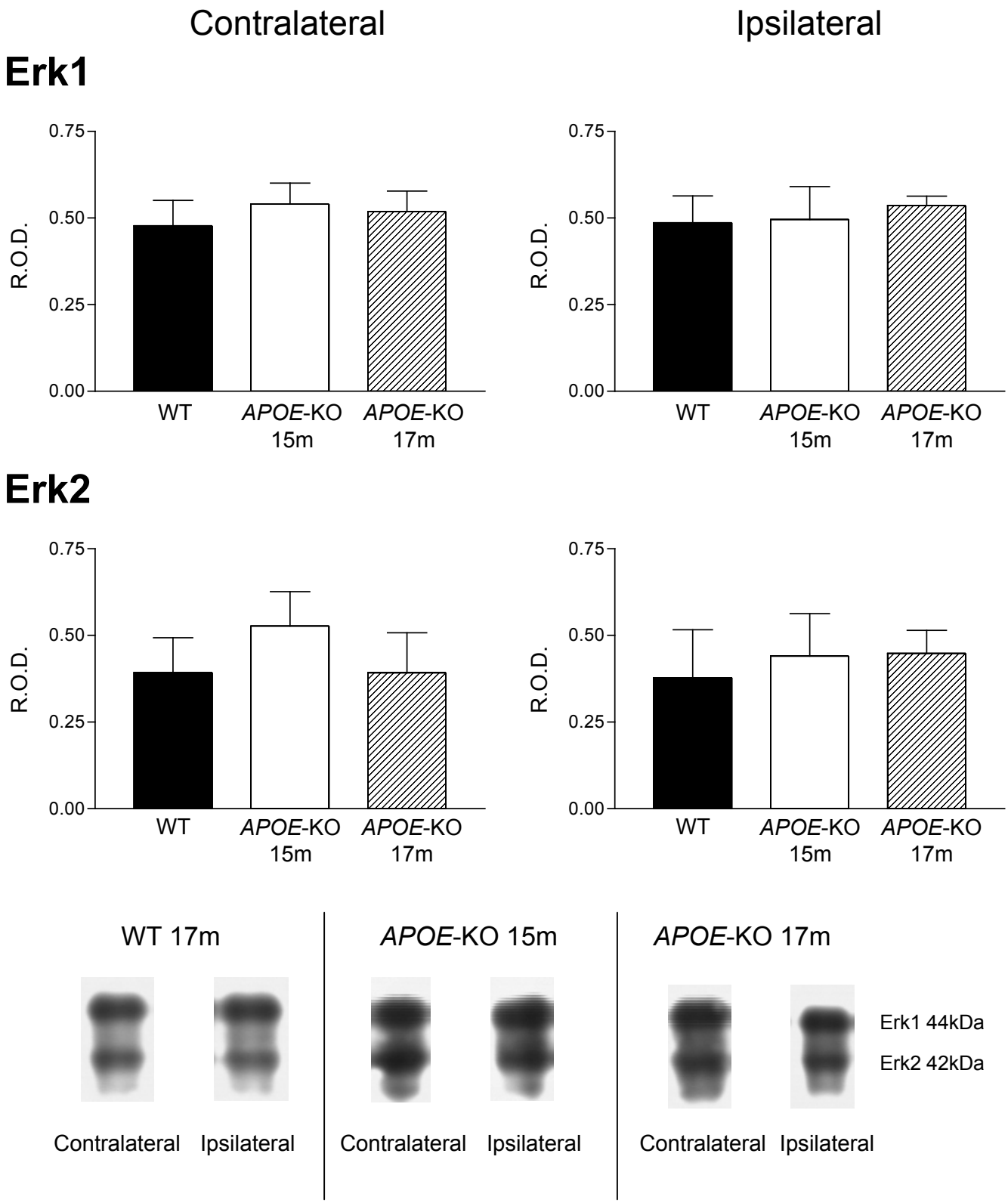

Figure 4.16 Western blot analysis of ERK1 and 2 in the caudate nucleus
Erk 1 and 2 immunoreactivity in the contralateral and ipsilateral caudate nucleus from WT mice subjected to 17m BCCAo and *APOE*-KO mice subjected to 15m and 17m BCCAo. Relative optical density measurements were taken for both Erk 1 (44kDa) and 2 (42kDa). Data are mean ± S.D. $p > 0.05$ using one way ANOVA.

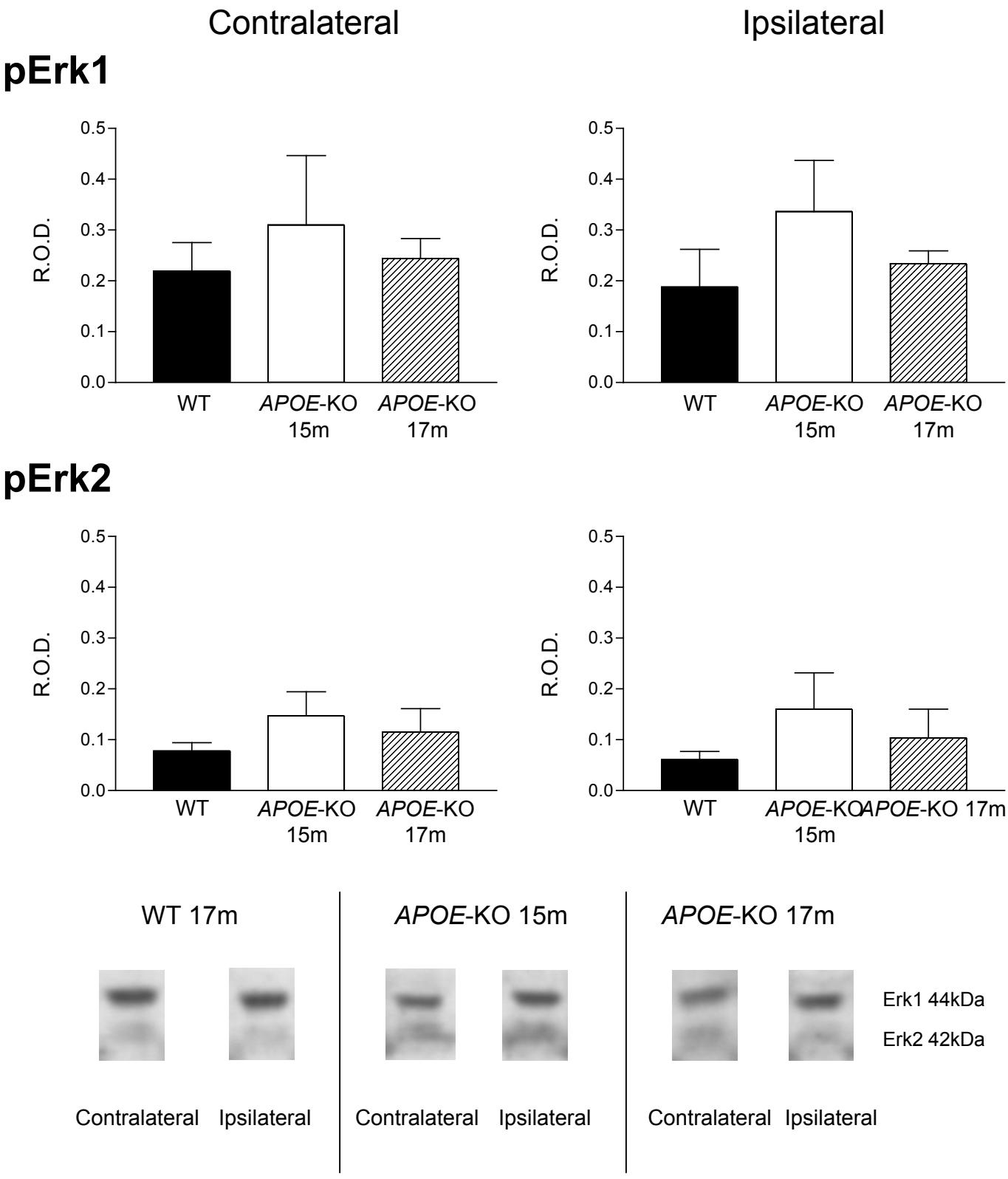

Figure 4.17 Western blot analysis of phosphorylated Erk1 and 2 in the caudate nucleus

Phosphorylated Erk 1 and 2 immunoreactivity in the contralateral and ipsilateral caudate nucleus from WT mice subjected to 17m BCCAo and *APOE*-KO mice subjected to 15m and 17m BCCAo. Relative optical density measurements were taken for both pErk 1 (44kDa) and 2 (42kDa). Data are mean ± S.D. $p > 0.05$ using one way ANOVA.

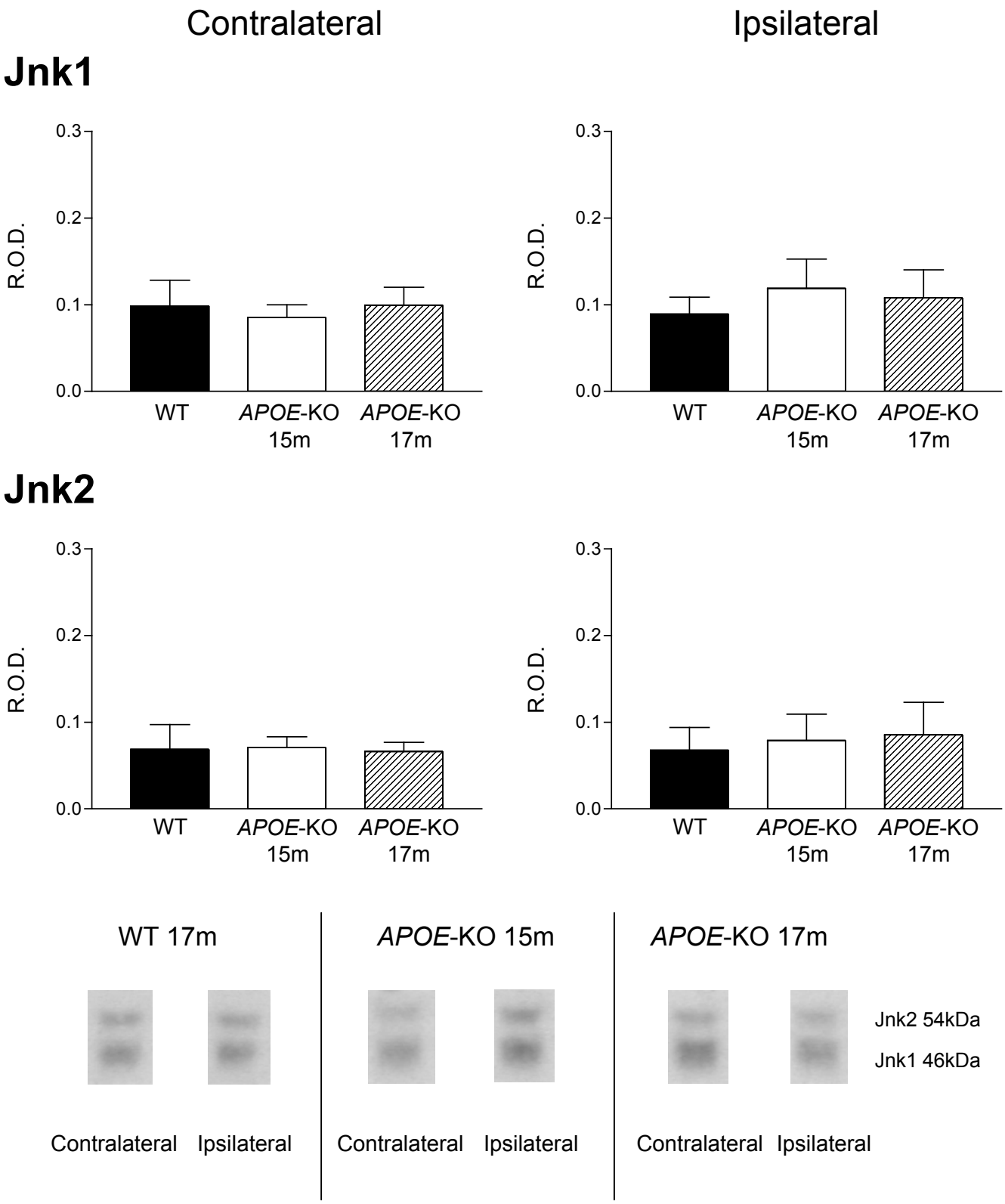

Figure 4.18 Western blot analysis of Jnk1 and 2 in the caudate nucleus
Jnk 1 and 2 immunoreactivity in the contralateral and ipsilateral caudate nucleus from WT mice subjected to 17m BCCAo and *APOE*-KO mice subjected to 15m and 17m BCCAo. Relative optical density measurements were taken for both Jnk 1 (46kDa) and 2 (54kDa). Data are mean ± S.D. $p > 0.05$ using one way ANOVA.

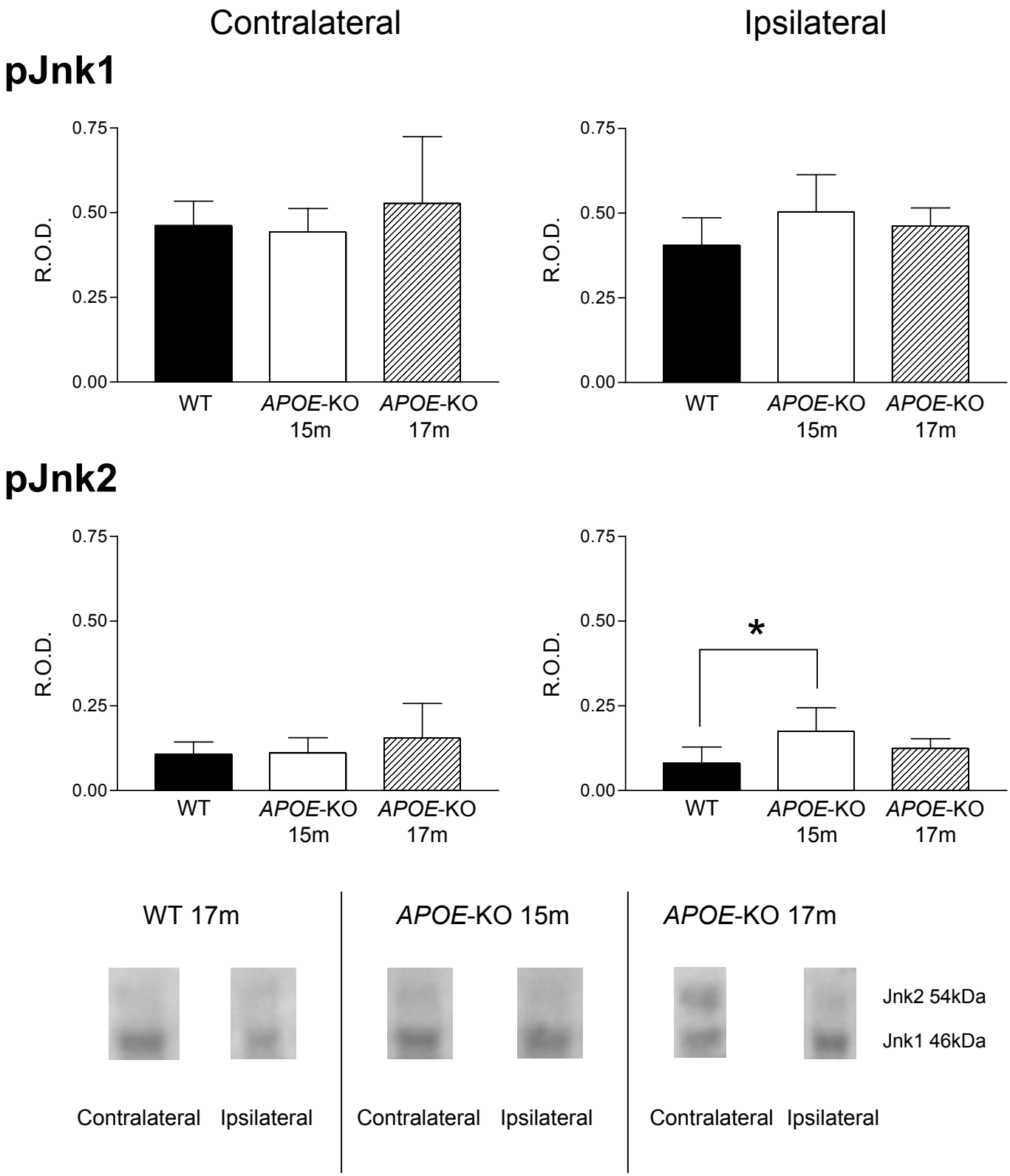

Figure 4.19 Western blot analysis of phosphorylated Jnk1 and 2 in the caudate nucleus

Phosphorylated Jnk 1 and 2 immunoreactivity in the contralateral and ipsilateral caudate nucleus from WT mice subjected to 17m BCCAo and *APOE*-KO mice subjected to 15m and 17m BCCAo. Relative optical density measurements were taken for both pJnk 1 (46kDa) and 2 (54kDa). Data are mean ± S.D. * $p < 0.05$ using one way ANOVA.

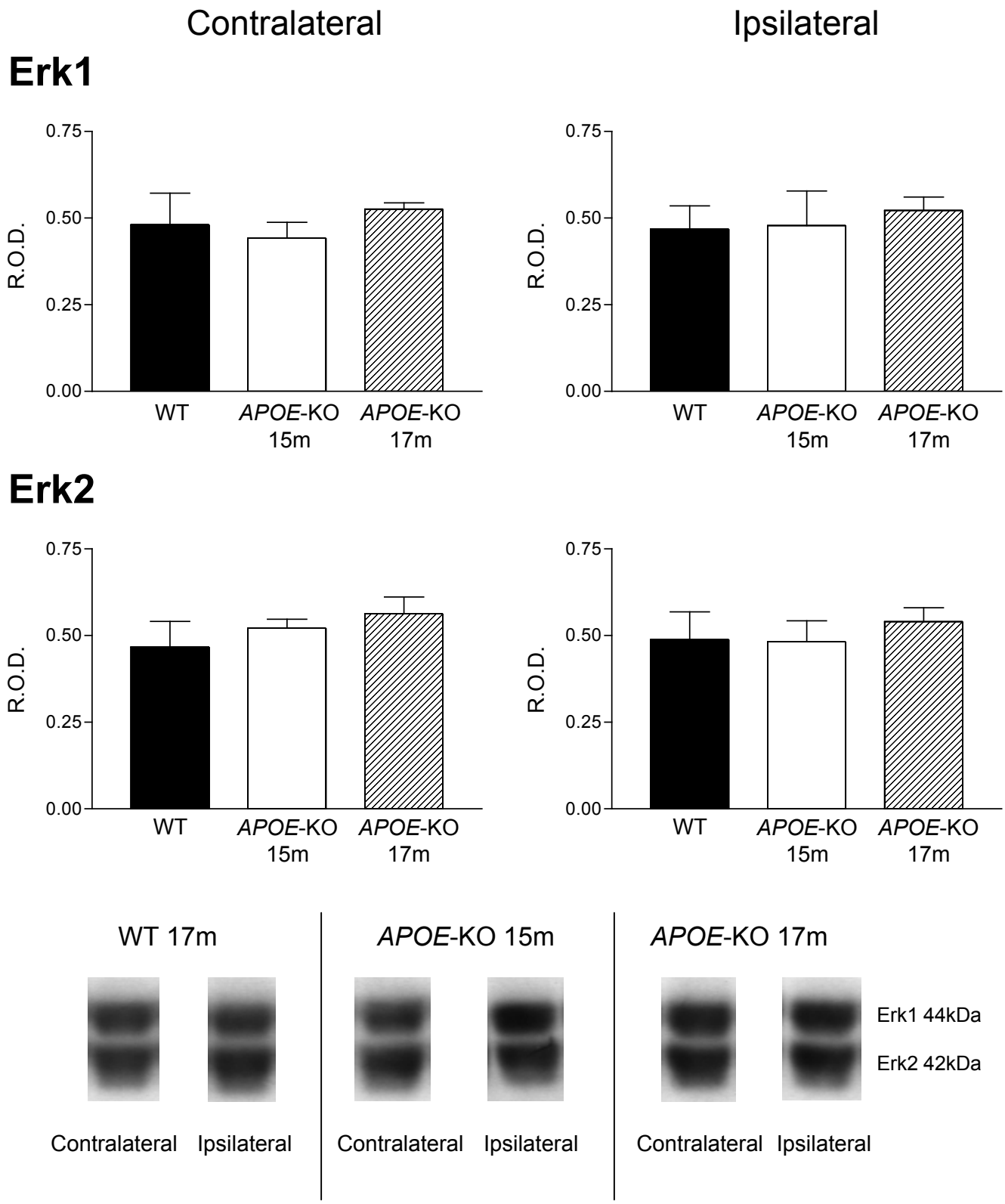

Figure 4.20 Western blot analysis of Erk1 and 2 in the hippocampus
Erk 1 and 2 immunoreactivity in the contralateral and ipsilateral hippocampus from WT mice subjected to 17m BCCAo and *APOE*-KO mice subjected to 15m and 17m BCCAo. Relative optical density measurements were taken for both Erk 1 (44kDa) and 2 (42kDa). Data are mean ± S.D. $p > 0.05$ using one way ANOVA.

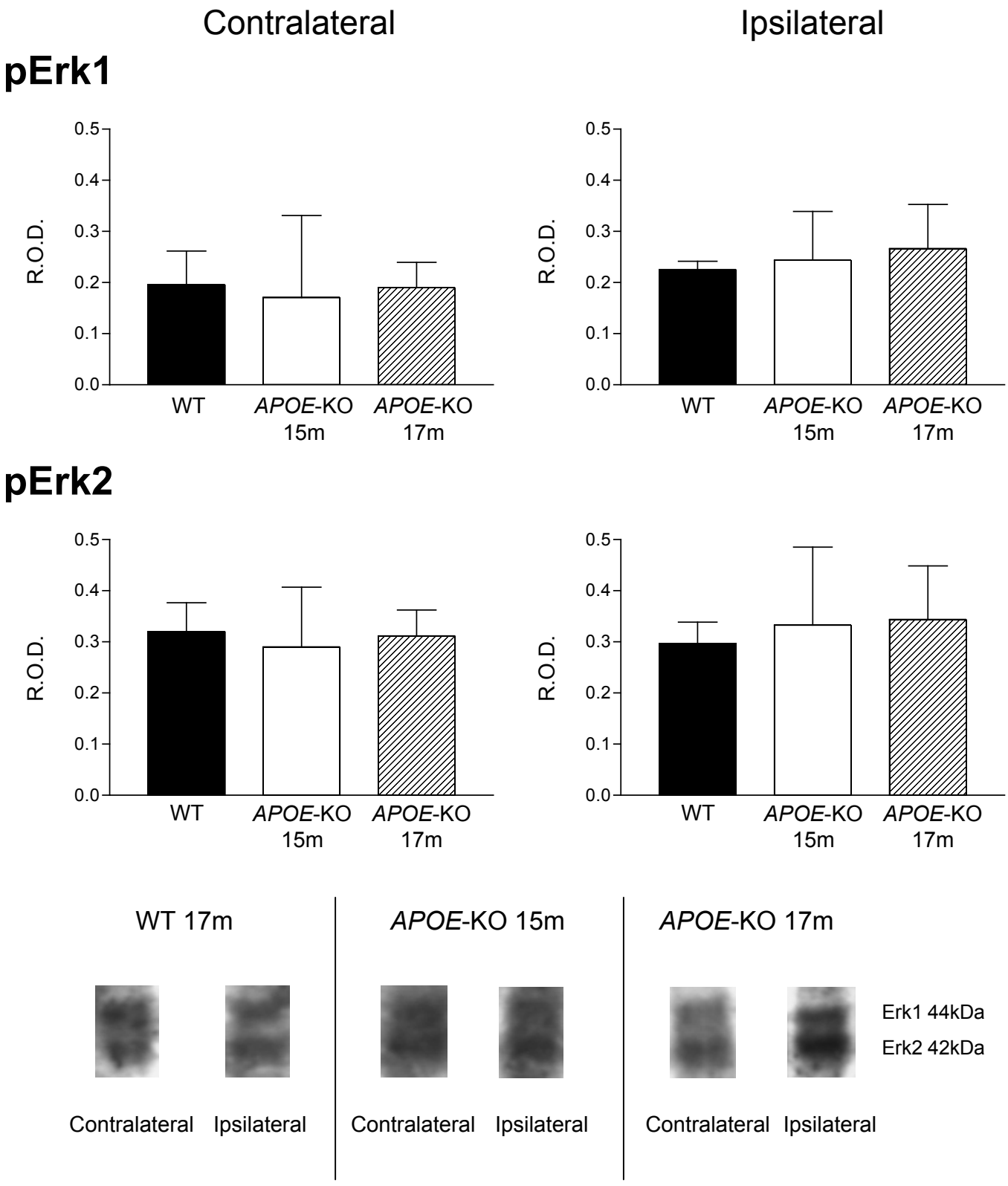

Figure 4.21 Western blot analysis of phosphorylated Erk1 and 2 in the hippocampus

Phosphorylated Erk 1 and 2 immunoreactivity in the contralateral and ipsilateral hippocampus from WT mice subjected to 17m BCCAo and *APOE*-KO mice subjected to 15m and 17m BCCAo. Relative optical density measurements were taken for both pErk 1 (44kDa) and 2 (42kDa). Data are mean ± S.D. $p > 0.05$ using one way ANOVA.

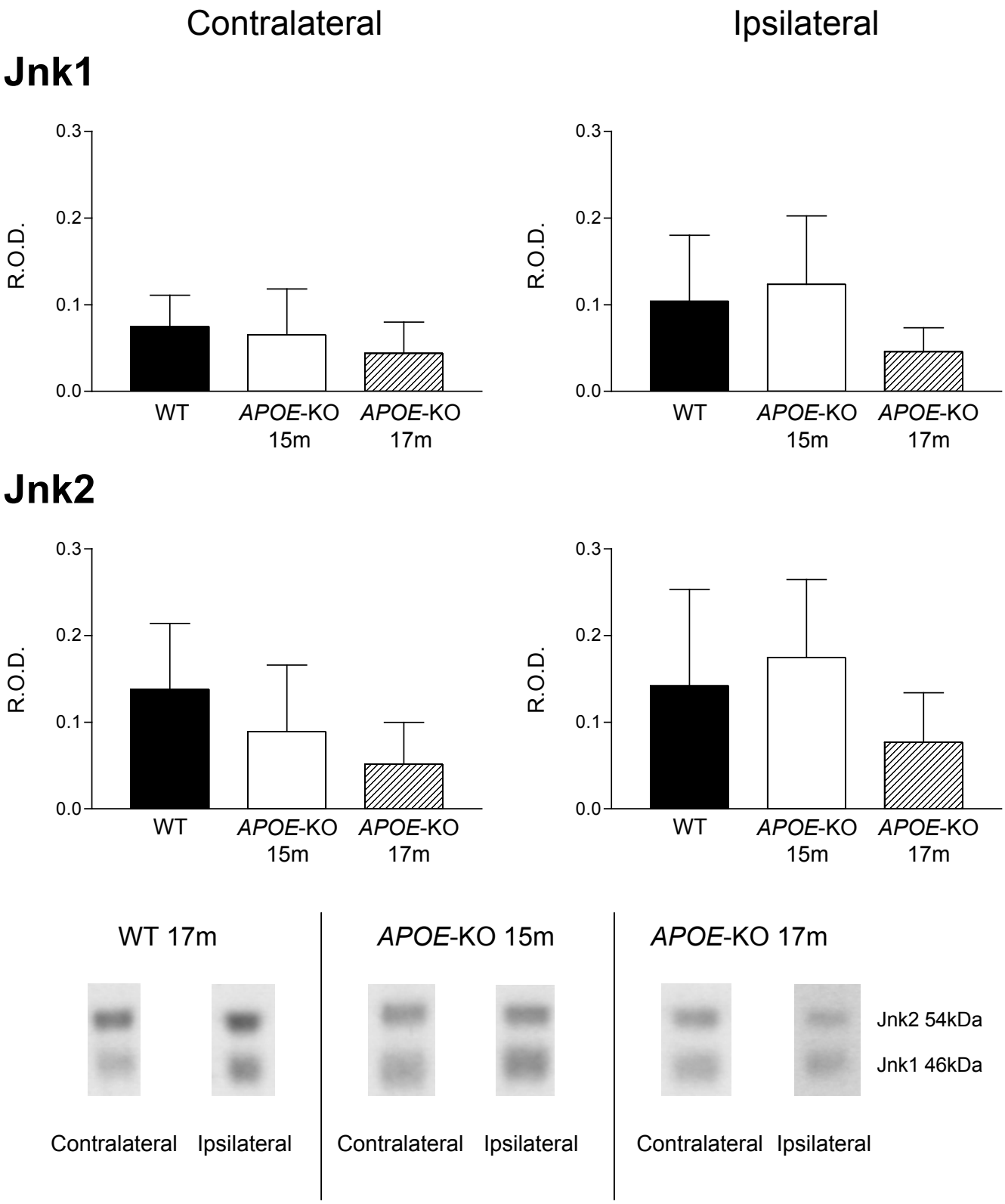

Figure 4.22 Western blot analysis of Jnk1 and 2 in the hippocampus
Jnk 1 and 2 immunoreactivity in the contralateral and ipsilateral hippocampus from WT mice subjected to 17m BCCAo and *APOE*-KO mice subjected to 15m and 17m BCCAo. Relative optical density measurements were taken for both Jnk 1 (46kDa) and 2 (54kDa). Data are mean ± S.D. $p > 0.05$ using one way ANOVA.

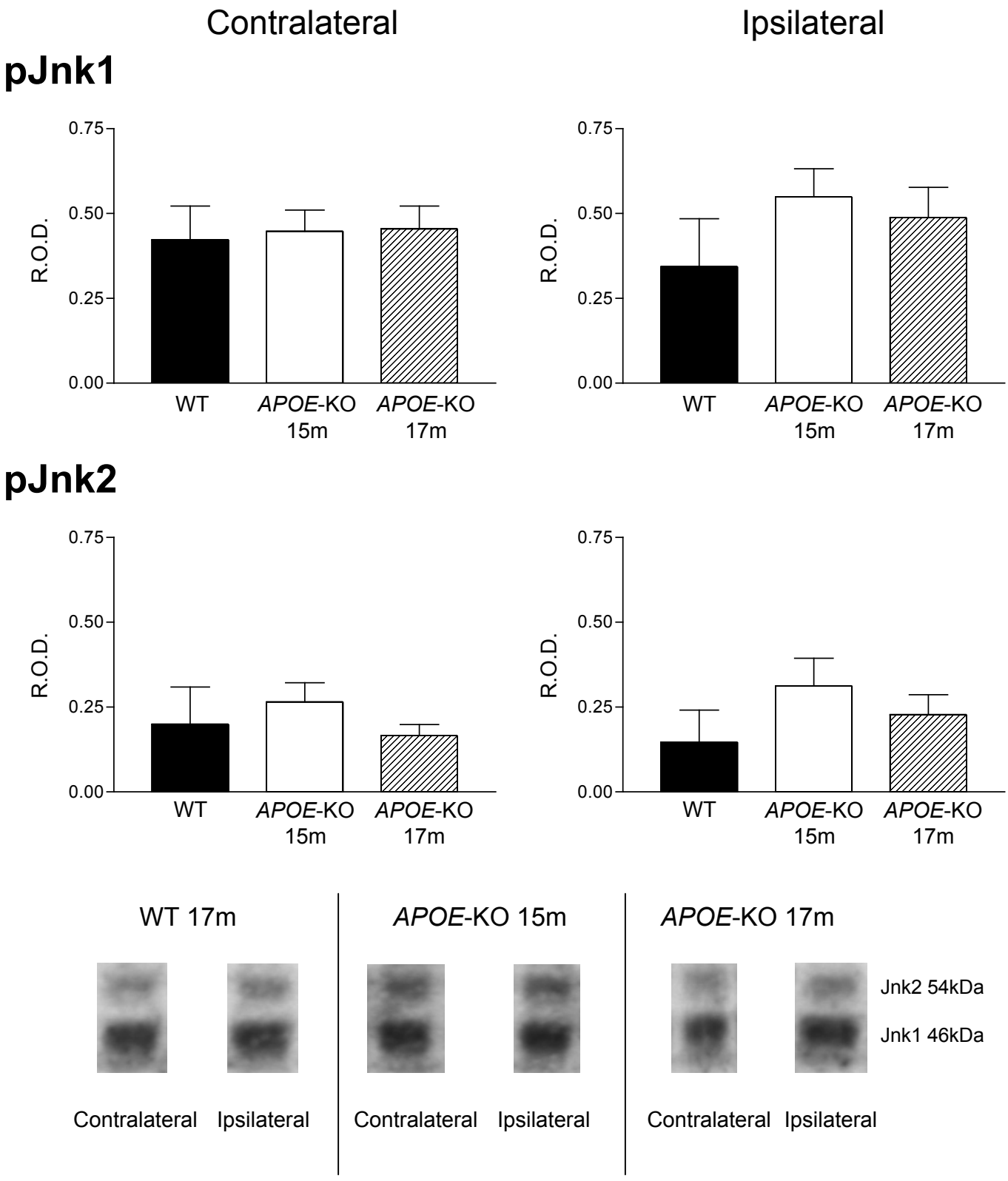

Figure 4.23 Western blot analysis of phosphorylated Jnk1 and 2 in the hippocampus

Phosphorylated Jnk 1 and 2 immunoreactivity in the contralateral and ipsilateral hippocampus from WT mice subjected to 17m BCCAo and *APOE*-KO mice subjected to 15m and 17m BCCAo. Relative optical density measurements were taken for both pJnk 1 (46kDa) and 2 (54kDa). Data are mean ± S.D. $p > 0.05$ using one way ANOVA.

4.5 Discussion

This study demonstrated that endogenous apoE has a major role in MHP36 neural stem cell survival, migration and differentiation in a mouse model of global ischaemia. The presence of apoE was linked to improved MHP36 survival and migration and enhanced neuronal differentiation. This enhancement was associated with changes in JNK signal transduction, a protein associated with cell survival.

4.5.1 Endogenous apoE influences the ability of stem cells to reduce ischaemic neuronal damage

At the outset of this study it was recognised that *APOE*-KO mice are more susceptible than WT mice to ischaemia (Laskowitz et al., 1997, Horsburgh et al., 1999). Thus, in *APOE*-KO mice, two durations of ischaemia were employed (one of a shorter duration, and one of an exact duration to WT mice) to produce ischaemic neuronal damage comparable and more extensive than WT mice. This was so that any differences observed could not be attributed to the variation in the extent of ischaemic damage. However, despite lowering the duration of ischaemia, in the ungrafted contralateral caudate nucleus, WT mice had greater numbers of normal neurons than both *APOE*-KO groups. Interestingly, in the grafted ipsilateral hemisphere, grafts of MHP36 cells result in an increased number of normal neurons in WT and *APOE*-KO mice subjected to a comparable degree of damage. However, MHP36 grafts were not able increase the number of normal neurons in *APOE*-KO mice subjected to a greater degree of ischaemic neuronal damage. A similar trend is observed in the grafted ipsilateral hippocampus. Overall, the data suggest that following grafting with MHP36 cells, an increase in the number of normal neurons is observed in *APOE*-KO mice with comparable damage to that of WT mice, but not to the same degree in *APOE*-KO mice with more extensive neuronal damage. All three groups of mice received equal numbers of MHP36 stem cells, suggesting that the regenerative properties are similar. The *APOE*-KO mice subjected to 17 minutes BCCAo might require a larger infusion of MHP36 cells in order to repair or replace the more extensive ischaemic damage. However, a major point that needs to be addressed is whether the increase in number of normal neurons following MHP36 grafts occurs as a result of neuronal replacement (i.e. regeneration), or as a result of

protection against ischaemic cell loss (i.e. neuroprotection). The haematoxylin and eosin stain used for identifying normal and ischaemic neurons does not distinguish between host and grafted cells. Therefore, it is not possible in this thesis to equivocally identify which mechanism is utilised by the grafted MHP36 stem cells. Clearly, it would be advantageous to use a fluorescent method to identify normal and ischaemic neurons as this would allow for co-localisation with PKH26 to be performed. There are a number of fluorescent DNA-binding stains which can be used to label neurons, such as DAPI and propidium iodide. However, whilst these stains provide neuronal morphology which can be used as an indicator for ischaemic neurons, the clarity of identification fails to reach that observed in haematoxylin and eosin staining. An eosin dye containing a fluorescein derivative, termed EA 50, has been demonstrated to provide fluorescent identification of ischaemic neurons, in correlation with Fos and Jun AP-1 immunoreactivity (Chen and Liu, 1996). However, technical aspects precluded the use of this dye in our study, as the activity of the dye was dependent on freshly fixed tissue and paraffin sections of less that 4μm thickness. There is also the possibility that the transplanted stem cells influence the extent of ischaemic damage through both the mechanisms described. This is illustrated through the multipotent differentiation of MHP36 cells into neurons, suggestive of replacement, and also astrocytes, suggestive of support and protection. Importantly, in this study, grafted MHP36 cells underwent neuronal and astrocytic differentiation in both WT and APOE-KO mice, although the proportions of differentiated cells varied significantly depending on genotype.

Alternatively, it may be that the extent of damage and the resultant environment influences the response of the transplanted stem cells. Neural transplantation studies in focal ischaemic models have demonstrated that transplantation into the ischaemic core usually results in failure of the grafted cells to survive, whereas the likelihood of survival is increased by transplantation away from the core, i.e. into the ischaemic penumbra or the undamaged hemisphere (Kelly et al., PNAS, 2004, Lundberg et al., 1997, Modo et al., 2002). The deleterious survival may be due to the total lack of trophic and structural support in the ischaemic core. Similarly, in our study, the extensively damaged environment in *APOE*-KO mice subjected to 17 minute

BCCAo may negatively influence the ability of MHP36 cells to repair and replace lost neurons.

4.5.2 MHP36 graft survival and migration is impaired in *APOE*-KO mice

This study demonstrates that MHP36 neural stem cells exhibit a significant impairment in survival when grafted into *APOE*-KO mice as compared to *APOE*-expressing WT mice. MHP36 cell survival is approximately five-fold greater in the caudate nucleus, and approximately two-fold greater in WT mice as compared to *APOE*-KO mice in the hippocampus. These results strongly suggest that endogenous apoE aids the survival of grafted MHP36 cells. The ability of apoE to mediate lipid transport and redistribution has been linked with regeneration in damaged PNS and CNS. ApoE scavenges free cholesterol from the damaged environment and subsequently redistributes this cholesterol for biosynthesis during axonal regeneration following sciatic nerve injury (Boyles et al., 1989). A similar regenerative role in the CNS has been demonstrated for apoE in after deafferation of the entorhinal cortex *in vitro* (Teter et al., 1999) and *in vivo* (Poirier et al., 1993, White et al., 2001). In the latter studies, upregulation and expression of apoE paralleled clearance of cholesterol and other lipid debris in the acute phase post-injury. This was followed by increased neuronal uptake of lipoproteins, concomitant with cholinergic reinnervation. Interestingly, apoE expression was also observed at a longer term, in association with markers of synaptic regeneration and remodelling. Recently, it has been suggested that apoE may affect regeneration through modulation of the astroglial inflammatory response (Champagne et al., 2005). This regenerative role of apoE may assist the survival of transplanted MHP36 cells. ApoE performs a number of other functions which may also be implicated in stem cell survival. It has been demonstrated that in the absence of apoE, the extent of damage is amplified following brain injury (Horsburgh et al., 1999, Sheng et al., 1999, Laskowitz et al., 1997, Lomnitski et al., 1997). ApoE has been shown to modulate excitotoxicity, anti-oxidation and inflammation (Miyata and Smith, 1996, Horsburgh et al., 2000, Boschert et al., 1999, Buttini et al., 1999, Laskowitz et al., 2000). These three processes are all components of the pathophysiological cascade that occurs

after ischaemic events and traumatic injury (Chapter 1, Figure 1.1). As discussed previously, the extent of ischaemic damage and subsequent pathological environment may negatively impact on MHP36 survival. Therefore, the beneficial effects of apoE in this study may be due to the neuroprotective effects of apoE following brain injury, rather than through a direct interaction between apoE and the MHP36 stem cells.

A number of studies have shown that addition of neurotrophins and other pro-survival molecules can aid the survival of grafted stem cells. Martinez-Serrano et al (1995) transduced nerve growth factor (NGF) cDNA into a line of Hib5 neural progenitor cells. These NGF-expressing Hib5 cells were transplanted into rat striatum one week prior to induction of MCAo (Andsberg et al., 1998). It was found that these cells were able to ameliorate ischaemic damage 48 hours after the ischaemic insult. However, non-NGF producing cells did not exert a protective effect, leading the authors to conclude that NGF secretion alone was responsible for the reduction in ischaemic damage.

Given that the majority of cells transplanted into the CNS fail to survive, Wei et al., (2005) investigated whether transplantation of ES cells overexpressing the anti-apopototic gene *bcl-2* would affect cell survival and functional outcome. Seven days after an episode of MCAo, rats were grafted with either unmodified ES cells or Bcl-2 overexpressing ES cells. Western analysis confirmed that there was still a high level of Bcl-2 in the grafted brain up to 35 days following transplantation. Analysis of cell death using a TUNEL assay showed that significantly fewer Bcl-2 ES cells were TUNEL positive compared to WT ES cells. Interestingly, overexpression of Bcl-2 also appeared to affect differentiation. Approximately 58% of Bcl-2 ES cells were NeuN positive, compared to approximately 34% of WT ES cells. Functional recovery was also improved with Bcl-2 ES cells compared to WT ES cells, although this was only evident 21 days after transplantation. Similarly, mouse ES cells transfected with the cell adhesion molecule L1 survive better than non-transfected ES cells following transplantation after spinal cord injury (Chen et al., 2005). However, all these studies have genetically modified stem cells in order to overexpress the

protein of interest. This is the first study to demonstrate that intrinsic genetic factors expressed at physiological levels may affect graft survival.

Migration of grafted MHP36 stem cells is also affected by the presence of apoE. Within the caudate nucleus, MHP36 stem cells migrated further away from the injection tract in WT mice compared to *APOE*-KO mice. Medial migration was around 0.5 mm throughout all three groups, probably due to the fact that the injection site was located approximately 1 mm from the ventricles (Chapter 2, Figure 2.1). Therefore, the distance of medial migration from the injected cell bolus would be restricted. It would be interesting to investigate whether transplanted MHP36 cells enter the ventricles and migrate along the rostral/caudal axis. However, migration of MHP36 cells was not restricted in lateral and ventral directions in the caudate nucleus. In these directions, there was a definite trend towards improved migration in WT mice. Migration was significantly further compared to *APOE*-KO mice subjected to 15 minutes BCCAo. A smaller, non-significant difference in migration was observed compared to *APOE*-KO mice subjected to 17 minutes BCCAo, as migration in this group was more variable. It should be noted that this group was also subjected to more extensive ischaemic neuronal damage. Interestingly, these results differ from a previous study demonstrating more extensive MHP36 migration in conjunction with increased cell loss in the 4-VO model of rat global ischaemia (Hodges et al., 2000). Migration and engraftment of the lesioned hippocampus was more prevalent after the damage caused by 30 minutes occlusion compared to 15 minutes occlusion. This discrepancy could result from the difference between the species and models of global ischaemia. The 4-VO model selectively damages CA1 pyramidal neurons in the rat, compared to the CA2 damage induced by BCCAo in the mouse.

However, no *APOE*-dependent effects on migration were observed in the hippocampus. Whilst migration distances were further in the hippocampus as opposed to the caudate nucleus, migration between the three groups was similar. This may be due to the location of the hippocampal graft. Cells were injected above the CA1 pyramidal cell layer, in close proximity to the corpus callosum. MHP36 cells

were able to migrate easily in medial and lateral directions along the white matter tract of the corpus callosum, irrespective of other factors (Figure 4.6). On average, MHP36 cells migrated around 1 mm in a medial direction and around 0.7 mm in a lateral direction. The average migration distance in a ventral direction was a shorter 0.55 mm.

A previous study within the thesis investigated the survival and migration of grafted MHP36 cells 4 weeks post-transplantation in WT mice (Chapter 3, Wong et al., 2005). MHP36 survival was semi-quantitatively assessed in that study, whereas a fully quantitative approach was used in the present study, making it difficult to accurately compare survival between the two studies. In the previous study, grafted MHP36 cells in WT mice examined at 4 weeks post-transplantation were found to migrate approximately 0.4 mm in all directions from the injection tract. In this study, MHP36 cells in WT mice migrated further in all directions, to distances of approximately 0.51 mm in a medial direction, 0.71 mm in a lateral direction and 0.66 mm in a ventral direction. The major difference between the studies was the time of graft. In the previous study, MHP36 cells were grafted 3 days post-ischaemia, at the time of maximal ischaemic damage. Whilst this time point is ideal for a therapeutic intervention, survival and subsequent migration of stem cells depends on the host environment. The ischaemic caudate nucleus is a multifaceted environment of pathophysiological mechanisms including glutamate induced excitotoxicity, oedema, free radical activation and inflammation (Chapter 1, Figure 1.1). These conditions will dramatically impair the likelihood of stem cell survival (Kelly et al., 2004). In contrast, grafting took place in this study 2 weeks post-ischaemia. At this time point, the pathophysiological response has decreased. Therefore, the enhanced survival observed in this study may be a result of transplantation into a less hostile environment, which may also account for the subsequent increase in migration distance. This suggests that neural stem cell replacement therapies for stroke may be more suited to long-term repair and replacement, rather than amelioration of the initial insult.

ApoE may influence stem cell migration through interactions with cytoskeletal proteins. ApoE-deficient mice exhibit impaired dendritic structure and a reduction in levels of MAP2, α and β-tubulin (Masliah et al., 1996). ApoE has also been linked to polymerisation and stabilisation of microtubule assemblies (Nathan et al., 1995), the regulation of which is a postulated mechanism by which apoE can modulate neurite outgrowth (Bellosta et al., 1995, Handelmann et al., 1992). Taken together, these data suggest that the presence of apoE is integral for optimal migration of transplanted stem cells. The presence of apoE may provide structurally stable synaptic and dendritic architecture in host brain for the integration of transplanted stem cells. Once the stem cells are stably integrated, apoE may then assist in the reorganisation of microtubule formations in order to provide a framework for the migration of stem cells away from the graft site.

4.5.3 Differentiation of stem cells is impaired in *APOE*-KO mice

There was a marked difference in the differentiation profiles of surviving MHP36 stem cells in WT mice and *APOE*-KO mice. Interestingly, the differentiation profile also varied depending on whether the graft was placed in the caudate nucleus or the hippocampus (Figure 4.15). Within the caudate nucleus, the presence of apoE is associated with significantly increased differentiation of grafted MHP36 cells to a neuronal phenotype. In WT mice, approximately 80% of MHP36 cells were positive for NeuN. Out of the remainder, 12% were positive for GFAP, leaving 8% of cells non-neuronal or astrocytic. These cells may have remained in an undifferentiated state following transplantation or express a different phenotype. In *APOE*-KO mice, approximately 20% of MHP36 cells were positive for neuN and GFAP, whilst the majority (approximately 60%) were non-neuronal or astrocytic. Taken together with the previous data, it appears that in WT mice, MHP36 stem cells are being driven towards neuronal differentiation in order to replace dead and damaged neurons following a global ischaemic insult. This supports the previous data showing the increase in the number of normal neurons in the ipsilateral caudate nucleus, and lends further credence to the suggestion that MHP36 grafts ameliorate ischaemic neuronal damage through a mechanism of neuronal replacement. However, in

APOE-KO mice, a critical factor or factors may be missing in order to drive neuronal differentiation. As described previously, *APOE*-KO mice subjected to 15 minutes BCCAo exhibit a similar neuronal number to WT mice subjected to 17 minutes BCCAo, yet these *APOE*-KO mice have impaired MHP36 survival and neuronal differentiation. It is obvious that any observed increase in neuronal number cannot be down to neuronal replacement by MHP36 grafts in these *APOE*-KO mice. This suggests that either intrinsic repair mechanisms ameliorated damage in these mice, or that the MHP36 grafts are providing support and repair without neuronal replacement. The increased astrocytic differentiation observed in *APOE*-KO mice may reflect this provision of trophic support. These differentiation results support the hypothesis that MHP36 stem cells are able to replace lost cells through neuronal differentiation, whilst still maintaining the ability to exert a neuroprotective influence. We have provided strong evidence that the presence of apoE is a critical factor in determining the proportion of MHP36 cells that undergo neuronal differentiation. It is likely that other factors also influence stem cell differentiation. These factors may be spatial/physical, such as the location of insult, severity of damage, and specific cell types affected. Other biological markers other than apoE may also be involved, such as inflammatory cytokines and chemokines.

Within the hippocampus, MHP36 cells grafted into *APOE*-KO mice have a similar differentiation profile to that observed in the caudate nucleus. The majority of cells (64% in *APOE*-KO mice subjected to 15m BCCAo, 77% in *APOE*-KO mice subjected to 17m BCCAo) do not express a neuronal or astrocytic phenotype. In WT mice the differentiation profile is altered so that the largest proportion (48%) of MHP36 cells were determined to be GFAP positive. 31% of the MHP36 cells are positive for NeuN, leaving 21% of cells non-neuronal or astrocytic. This WT differentiation profile is also distinct from that observed in the caudate nucleus. This may be related to the finding that the number of normal neurons remaining in the hippocampus was unaltered, which corresponds with the fact that the majority of MHP36 cells did not differentiate into neurons in the hippocampus, unlike in the caudate nucleus. The increased astrocytic differentiation observed in WT mice may be due to the difference in environment. It should be noted that the marked reduction

in survival in *APOE*-KO mice may affect the likelihood of differentiation into either neurons or astrocytes. Overall the data clearly demonstrate that apoE strongly influences the survival and differentiation of MHP36 cells.

The influence of apoE on neuronal differentiation has not been investigated previously *in vivo* but has been investigated *in vitro* cell culture. It has been shown that human neuronal-like cells (SH-SY 5Y and Kelly cell lines) derived from neuroblastoma are able to synthesise apoE (Dupont-Wallois et al., 1997). Soulié et al., (1999) measured apoE mRNA in human neuroblastoma SH-SY 5Y cells in relation to neuronal differentiation. Addition of nerve growth factor (NGF) induced differentiation of SH-SY 5Y cells into neuronal cells. During the first 4 days of NGF treatment, apoE mRNA decreases and then increases over the subsequent 3 days. The observed increase in apoE mRNA synthesis from NGF 4 days to 7 days was downregulated by administration of exogenous apoE. Interestingly, this downregulation was apoE isoform specific. ApoE4 was most efficient, followed by apoE3 and then apoE2. The same group extended these findings by investigating apoE protein and mRNA levels in human teratocarcinoma NT2 cells (Ferreira et al., 2000). Undifferentiated NT2 cells expressed apoE mRNA and protein. Treatment of these cells with retinoic acid induced differentiation into hNT neurons, which was associated with a downregulation of apoE mRNA and protein levels to the degree that fully mature hNT neurons barely expressed apoE. Taken together, these data suggest that synthesis and expression of apoE may regulate neuronal differentiation. However, it remains to be seen whether apoE expression functions as an effector or marker in this system. Harris et al., (2004) carried out further work on neuronal expression of apoE and discovered that treatment of mature hNT neurons or mouse primary neurons with astrocyte conditioned media rapidly upregulated apoE expression. This effect was observed with media obtained from the C6 astrocytic cell line and also with media from primary astrocytes derived from *APOE*-KO mice. Interestingly, this astrocyte mediated upregulation of apoE expression could be abolished by treatment with U0126, an inhibitor of the ERK signalling pathway, whilst inhibition of the JNK pathway had no effect on apoE expression. These results

suggest that neuronal expression of apoE is regulated by an astrocyte secreted factor or factors and that this expression is dependent on the ERK signalling pathway.

There are number of possible reasons for the disparity in differentiation profile between the caudate nucleus and the hippocampus in WT mice. Transient global ischaemia is associated with a defined hierarchy of neuronal damage. The caudate nucleus is particularly vulnerable, followed by the pyramidal regions of the hippocampus. Rosen and Williams (2001) estimated the number of neurons in the WT mouse striatum to be 1.72 ± 0.15 million. Approximately 12,500 MHP36 cells were grafted into the caudate nucleus and hippocampus. Given the widespread neuronal loss observed in the caudate, if grafted cells differentiate in order to replace the damaged neurons, this would require the majority of grafted cells. However, the CA1 and CA2 hippocampus region is a much smaller, more focused area that also undergoes selective neuronal damage. Abusaad et al., (1999) estimated that there are 437,500 ± 37,500 neurons in the CA1, CA2 and CA3 regions in the pyramidal cell layer of C57Bl/6J mice. Based on the proportion of the CA2 region to the rest of the pyramidal cell layer (Paxinos and Franklin, 2001), it can be calculated that there should be approximately 35,000 ± 3000 neurons in the CA2 region. Therefore, unlike the situation in the caudate nucleus, a much smaller proportion of grafted MHP36 cells would be required to differentiate into neurons in order to repopulate this region. It remains to be determined whether transplanted stem cells undergo division following grafting, although anecdotal evidence suggests that the cells may undergo up to two cycles of division (Dr Tonya Bliss, Personal communication). This may leave a sizeable proportion of MHP36 cells for providing trophic support, resulting in the increased proportion of MHP36 cells differentiating into astrocytes in the hippocampus. The higher proportion of undifferentiated MHP36 cells in the hippocampus may either be waiting for a suitable cue, or have differentiated into another cell type such as an oligodendrocyte.

In the previous study (Chapter 3, Wong et al., 2005), approximately 56% of MHP36 cells grafted into the caudate nucleus differentiated into neurons in WT mice at both 1 week and 4 weeks post-transplantation. This is in comparison to the 80% neuronal

differentiation observed in WT mice in this study. As mentioned previously, the delay in grafting from 3 days post-ischaemia to 2 weeks post-ischaemia may influence the increased differentiation due to the less hostile environment. There is also the possibility that enhanced neuronal differentiation was simply due to the increased survival time of 6 weeks post-ischaemia for the animals. These factors illustrate the variability endemic to *in vivo* studies when comparing data on survival, migration and differentiation. *In vitro* experiments allow for greater control over these variables, allowing for consistent assessment of stem cell properties. Co-culture of MHP36 cells seeded onto primary cultures of mouse embryonic cortex revealed the temporal progression in differentiation (Mellodew et al., 2004). After four days in co-culture, MHP36 cells began to differentiate into astrocytes. The proportion of astrocytes stabilised after 8 days *in vitro* to about 60%. Neurons emerged after 7 days *in vitro* and stabilised at around 17% of the total population. Finally, oligodendrocytes appeared after 8 days *in vitro* to represent about 9% of MHP36 cells. This differentiation profile varies from what was observed in WT and *APOE*-KO mice in this study, demonstrating the extent to which *in vivo* factors can affect stem cell differentiation.

4.5.4 Endogenous apoE may influence cell signalling pathways

Activation of LDL receptors by apoE or another ligand has been implicated in a variety of signal transduction mediated processes, including neuronal migration (Dulabon et al., 2000), neurite outgrowth (Qiu et al., 2004) and calcium influx (Bacskai et al., 2000, Qiu et al., 2002). These signal transduction pathways may directly influence the survival, migration and differentiation of grafted stem cells. ApoE mediated induction of signal transduction pathways has been linked with the inhibition of cell migration and proliferation, although this was related to smooth muscle cells, as opposed to stem cells or neural progenitor cells (Ishigami et al., 1998, Hui and Basford, 2005). ApoE exerts these inhibitory effects through binding to different receptors; inhibition of smooth muscle migration occurs via LRP1 binding and activation of protein kinase A (Swertfeger et al., 2002, Zhu and Hui, 2003); inhibition of smooth muscle proliferation takes place via heparan sulphate

proteoglycan binding and activation of inducible nitric oxide synthase (Ishigami et al., 2000, Swertfeger and Hui, 2001).

We investigated protein levels of ERK 1 and 2, JNK 1 and 2 and their activated, phosphorylated forms in the caudate nucleus and hippocampus of WT and *APOE*-KO mice in the presence of stem cell grafts post-ischaemia. These proteins were selected based on a study by Hoe et al., (2005) who investigated the signalling pathways stimulated by apoE in primary neuronal cultures. In this report, apoE activation of lipoprotein receptors led to increased levels of phosphorylated ERK1/2 and decreased levels of phosphorylated JNK1/2. Treatment of the cells with alpha-2-macroglobulin also increased phosphorylation of ERK1/2, but did not affect JNK1/2 levels, suggesting that activation of ERK1/2 is governed by the LRP receptor. ERK and JNK, along with p38 are members of the mitogen-activated protein kinase family (MAPK). The MAPK family act as a convergence point for a number of extracellular signal pathways and have been linked to cell proliferation, apoptosis, differentiation and inflammation (Johnson and Lapadat, 2002).

The data described in this thesis chapter indicated that levels of unphosphorylated ERK1/2 did not vary significantly between the groups, although there was a trend towards an increase in phosphorylated ERK1/2 levels in *APOE*-KO mice subjected to 15m BCCAo within the caudate nucleus. This appears to contrast with the results from Hoe et al., (2005), who demonstrated apoE-induced activation of ERK1/2 via the LRP receptor. However, the LRP receptor has a variety of ligands other than apoE. It has been previously shown that neuronal expression of apoE depends on the activity of the ERK pathway (Harris et al., 2004). Interestingly, a study by Ohkubo et al (2001) showed that apoE4 stimulated transcription of the cAMP-response element binding protein (CREB) through activation of the ERK cascade in rat primary hippocampal neurons. This activation of CREB led to downstream induction of the anti-apoptotic gene *Bcl-2*, which has been associated with improved neuronal survival after brain injury (Honkaniemi et al., 1996, Chen et al., 1997, Asahi et al., 1997, Clark et al., 1997). In contrast, treatment with apoE3 was unable to activate the ERK pathway and therefore did not stimulate CREB transcription. However, all

these experiments took place in a carefully regulated *in vitro* cell culture environment, and therefore may not translate similarly to the *in vivo* situation observed in our study.

It should be noted that the western blot analysis carried out in this chapter has a technical limitation. The R.O.D. of each protein band were normalised against the background intensity of the respective film for semi-quantitative analysis. Ideally, an internal control should have been run on each gel for a housekeeping protein such as actin or beta-tubulin, in order to control and correct of any loading errors and to act as a reference for quantitation. Unfortunately, both these proteins have a similar molecular weight to ERK1/2 and JNK1/2, which would have made interpretation of the blots difficult. It has also been suggested that the levels of these proteins may vary following brain injury, which would also limit their suitability as an internal control (Liu and Xu, 2006). In the absence of an internal control, the gel was stained with Coomassie blue after transfer to check for equal loading in each lane. However, it would have been advantageous to use a non-interfering internal control such as Glyceraldehyde-3-phosphate dehydrogenase (GAPDH) in order to bypass this limitation.

Stimulation of the ERK1/2 pathway via SDF-1 has also been implicated in proliferation of neural progenitor cells *in vitro* (Gong et al., 2006). Recently, a novel rodent gene encoding for a neural regeneration protein (NRP) has been discovered (Gorba et al., 2006). This protein appears to act in a similar manner to SDF-1, with initial findings suggesting that neural regeneration protein is able to induce neural migration, proliferation, enhanced survival and increased neuronal differentiation. Of these biological activities, neural regeneration protein was shown to promote neural migration through activation of the ERK1/2 pathway.

Activation of JNK1/2 is a well-established marker for neuronal death, although there is also some evidence that JNK1/2 plays a role in regeneration and repair (Xia et al., 1995, Herdegren et al., 1997). The data indicated a trend towards was an increase in phosphorylated JNK 1 and 2 associated with the ipsilateral hemisphere in *APOE*-KO

mice compared to WT mice with equivalent levels of ischaemic damage. *In vitro* studies have demonstrated that JNK1/2 activation occurs prior to neuronal apoptosis (Xia et al., 1995). This has been supported by *in vivo* studies, showing upregulation of phosphorylated JNK1/2 following transient global ischaemia in the gerbil (Kiessling, 1993), and prolonged phosphorylation of JNK1/2 after MCAo in the rat (Herdegen, 1998). In the latter study, a large proportion of neurons expressing phosphorylated JNK1/2 were also positive for the apoptotic TUNEL marker. As described earlier, apoE binding to lipoprotein receptors results in decreased phosphorylation of JNK1/2 (Hoe et al., 2005). In concordance with these findings, we observed higher levels of phosphorylated JNK1/2 in the ipsilateral hippocampus and caudate nucleus of *APOE*-KO mice subjected to 15 minutes BCCAo compared to WT mice. It is reasonable to speculate that this may be linked to the decreased survival of grafted MHP36 stem cells in the *APOE*-KO animals. There is also accumulating evidence linking JNK with the regulation of cell migration. Activation of JNK is closely associated with an increase in cell migration (Shin et al., 2001, Hauck et al., 2001). Inhibition of JNK markedly impedes the rate of migration of a variety of different cell types, including smooth muscle cells, embryonic stem cells and cortical neurons (Huang et al., 2003, Yamauchi et al., 2003, Kavurma and Khachigian, 2003, Kawauchi et al., 2003). The finding that JNK modulates the actin cytoskeleton during development of the *Drosophila* embryo suggests a possible mechanism for JNK to regulate cell migration (Martin-Blanco et al., 2000). However, the increased activation of JNK1/2 observed in *APOE*-KO mice did not correlate to increased migration of MHP36 stem cells, which was markedly further in WT mice. *In vitro* studies would provide further insight into alterations in signalling proteins during stem cell integration.

Although the present study investigated the ERK and JNK pathways, apoE may interact with other signalling pathways and other lipoprotein receptors to influence neural stem cell integration. Two other members of the lipoprotein receptor family, apoER2 and the VLDL receptor are expressed predominantly in the brain and have been shown to play an important role in migration and localisation of neurons during development. Aside from apoE, the major ligand for these two receptors is Reelin.

Binding of Reelin induces phosphorylation of Dab1, which has been implicated in neuronal migration and synaptic plasticity. ApoE may also interact with the LRP5/6 receptors (Kim et al., 1998), which are involved in canonical Wnt signalling. The Wnt / β-catenin signalling pathway has been implicated in regulation of neuronal differentiation in a variety of stem and precursor cells (Haegele et al., 2003, Otero et al., 2004, Hirabayashi et al., 2004). Clearly, mechanistic insight into apoE regulation of stem cell integration requires further investigation.

4.5.5 Summary

This study has demonstrated that the presence of apoE strongly influences the survival, migration and differentiation of grafted MHP36 stem cells. While the exact signalling mechanisms involved in these *APOE*-mediated processes have yet to be determined, this study provides evidence for the involvement of JNK1/2 signalling. Further work will investigate whether the effect of apoE is isoform specific.

Chapter 5

Influence of *APOE* genotype on neural stem cell grafts in a mouse model of global ischaemia

5.1 Introduction

The previous study demonstrated that the presence of endogenous murine *APOE* plays a significant role in the integration and differentiation of MHP36 neural stem cell grafts following global ischaemia. However, humans express three different isoforms of *APOE*, namely *APOE*-ε2, ε3 and ε4 (Zannis et al., 1981). Although these isoforms only differ from each other by single amino acid substitutions at amino acid residues 112 and 158, these changes have profound effects on *APOE* structure and function. *APOE*-ε3 is the most common allele found in man, and is regarded as the benchmark "normal" *APOE*. In contrast, the *APOE*-ε4 allele is regarded as a deleterious allele, as it has been shown to be associated with increased risk of heart disease (Menzel et al., 1983), atherosclerosis (Davignon et al., 1988, Mahley and Huang, 1999), as well as poorer outcome after brain damage (Nicoll et al., 1995, 1996, Teasdale et al., 1997, and Alzheimer's disease (Corder et al., 1993, Saunders et al., 1993). Given that we have previously shown the importance of *APOE* on neural stem cell graft integration, the next step was to investigate whether different human *APOE* genotypes also influence stem cell grafts. Transgenic mice expressing the three human *APOE* isoforms were generated by introduction of the relevant gene into *APOE*-KO mice (Xu et al., 1996). These results will be pertinent for any future translation of stem cell therapies from the laboratory to the clinic.

5.2 Aim

The aim of the study was to investigate whether *APOE* genotype (*APOE*-ε3 or *APOE*-ε4) influences the survival, migration, differentiation of neural stem cell grafts and subsequent performance on a motor balance and coordination task following diffuse neuronal injury induced by global ischaemia.

5.3 Materials and Methods

5.3.1 Study outline

Adult male *APOE*-deficient mice (*APOE*-KO) and mice expressing human *APOE*-ε3 and *APOE*-ε4 were used in this study (Chapter 2, Section 2.1). The *APOE*-deficient mice used in this study were littermate controls, derived from breeding heterozygous

human *APOE*-ε3 or ε4 to homozygous *APOE*-KO mice. It was decided not to include a WT C57Bl/6J control group as the previous chapter had already illustrated the influence of endogenous apoE on MHP36 survival, migration and differentiation. In the case of the rotarod task, a study of the literature revealed that *APOE*-KO did not differ from WT mice in motor function, negating the need for a control group. Transient global ischaemia was induced by bilateral occlusion of the common carotid arteries (BCCAo). An occlusion time of 17 minutes was chosen based on the preceding chapter and a previous study in which *APOE*-ε3 and *APOE*-ε4 mice were subjected to BCCAo (Horsburgh et al., 2000). Mice were immunosuppressed with CsA as described in Chapter 2. Two weeks after global ischaemia, mice received unilateral grafts of PKH26-labelled MHP36 stem cells (Passage number 52-55) into the caudate nucleus and hippocampus. Pre-graft viability averaged 95% and post-graft viability averaged 89%). Mice were tested for functional recovery in motor balance and coordination using the rotarod test. The outline of the test is described in Chapter 2, Section 2.4. Animals received two sessions per week, starting on the week after grafting, giving a total of seven tests. 4 weeks post-transplantation, mice were transcardially perfused. 27 animals (*APOE*-KO; n = 9, *APOE*-ε3; n = 8, *APOE*-ε4, n = 10) were processed for histology using the Callis method of freezing (Chapter 2, Section 2.6). Coronal cryostat sections were cut (10μm) and mounted onto poly-L-lysine coated slides. Sections at the level of the injection tract were stained with haematoxylin and eosin to visualise the number of normal neurons. Adjacent sections were mounted and coverslipped in Vectashield for visualisation of PKH26-labelled MHP36 cells or stained with immunohistochemical markers against NeuN and GFAP as described in Chapter 2, Section 2.8.

5.3.2 Quantification of ischaemic damage

Haematoxylin and eosin stained sections were used to assess the extent of ischaemic damage in the same fields used to quantify the immune response using a 25mm^2 grid (attached to the microscope optics) at 400x magnification. The number of neurons exhibiting ischaemic cell change and morphologically normal neurons were counted in each grid. Ischaemic neurons were defined by an intense, darkly stained pyknotic nucleus surrounded by eosinophilic cytoplasm. Ischaemic damage was quantified in

the ipsi and contralateral caudate nucleus, and the ipsi and contralateral CA2 region of the hippocampus. Ischaemic neurons were identified following a haematoxylin and eosin stain. As described in Chapter 4, Section 4.3.2, the level of neuronal density as an index of surviving neurons was also assessed in the same regions used to assess ischaemic damage.

5.3.3 Quantification of MHP36 graft survival and migration

Sections were assessed for the number of surviving PKH26 labelled MHP36 cells using a confocal laser scanning microscope. Within the caudate nucleus, confocal z-series images were captured at six regions surrounding the injection tract and quantified for the number of MHP36 cells. Within the hippocampus, five confocal z-series images were captured along the granule cell layer of the CA region starting from the CA2 and progressing along the CA1 towards the septum. Migration of PKH26 labelled MHP36 cells was assessed in a medial, lateral and ventral direction away from the injection tract in both the caudate nucleus and hippocampus. The distance of migration in each direction was measured using a $100mm^2$ grid (attached to the microscope optics) at 200x magnification.

5.3.4 Immunohistochemistry

Neuronal differentiation of MHP36 cells was assessed using a marker for neuronal nuclei (mouse monoclonal anti-NeuN). Astrocytic differentiation of MHP36 cells was assessed using a marker for glial fibrillary acidic protein (GFAP). Primary antibodies were detected with a biotinylated secondary antibody followed by fluorescent strepavidin Alexa 488 (Invitrogen). The immunohistochemistry protocol is described in Chapter 2, Section 2.8.

5.3.5 Immunofluorescent analysis

Sections were assessed for co-localization of phenotypic markers for neurons (NeuN) and astrocytes (GFAP) with PKH26 as a marker for transplanted MHP36 cells. Within the caudate nucleus, confocal z-series images were captured in five different fields medial, lateral and ventral to the injection tract in the caudate nucleus. Within the hippocampus, confocal z-series images were captured in four different fields

along the granule cell layer of the CA region starting at the CA2 and progressing along the CA1. Neuronal and astrocytic differentiation was determined by counting the number of cells co-localizing with PKH26 after counting the number of PKH26 positive cells within the same field.

5.4 Results

5.4.1 Ischaemic Damage

The number of neurons remaining was assessed as an index of ischaemic neuronal damage. This was previously utilised and described in Chapter 4. Within the caudate nucleus, there was no difference in the number of normal neurons in the contralateral hemisphere between the three groups. In the ipsilateral hemisphere, there was a significant increase in the number of normal neurons in *APOE*-ε4 mice compared to *APOE*-KO mice (19.28 ± 4.63 vs. 16.32 ± 2.80 normal neurons per 0.0625mm^2, $p < 0.05$) (Figure 5.1). A similar trend was also observed with *APOE*-ε3 mice compared to *APOE*-KO mice (18.83 ± 2.73 vs. 16.32 ± 2.80 normal neurons per 0.0625mm^2, $p > 0.05$) although this comparison is not statistically significant.

The number of normal neurons was also examined in the CA2 region of the hippocampus. In the contralateral hemisphere, there was a trend towards increased neuronal number on *APOE*-ε3 mice as compared to both *APOE*-KO (24.00 ± 6.99 vs. 16.56 ± 8.90 normal neurons per 0.0625mm^2, $p > 0.05$) and *APOE*-ε4 mice (24.00 ± 6.99 vs. 15.90 ± 8.70 normal neurons per 0.0625mm^2, $p > 0.05$) (Figure 5.2). The same trend was observed in the ipsilateral hemisphere (*APOE*-ε3; 21.75 ± 6.76 vs. *APOE*-KO; 16.67 ± 7.00 normal neurons per 0.0625mm^2, $p > 0.05$ and vs. *APOE*-ε4; 17.90 ± 9.80 normal neurons per 0.0625mm^2, $p > 0.05$). None of these differences reached statistical significance.

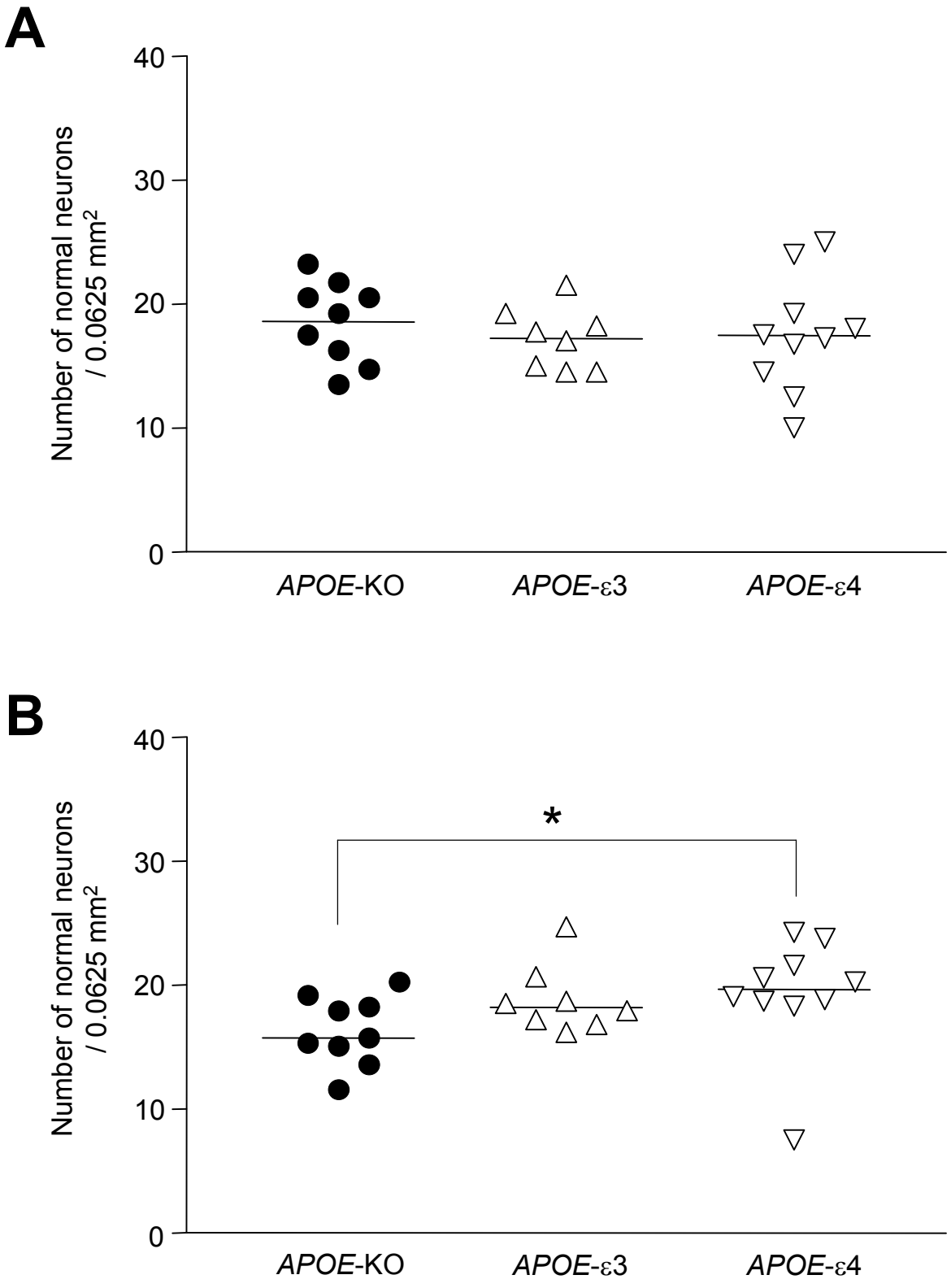

Figure 5.1 Number of morphologically normal neurons within the caudate nucleus

Number of normal neurons per 0.0625 mm^2 in *APOE*-KO, *APOE*-ε3 and *APOE*-ε4 mice subjected to 17m BCCAo within the contralateral (A) and ipsilateral (B) caudate nucleus. There were significantly higher numbers of normal neurons in the ipsilateral caudate nucleus of *APOE*-ε4 mice compared to *APOE*-KO mice. Data are expressed as individual data points, with the bar indicating the median. * $p < 0.05$, using Kruskal-Wallis test with Dunn's post-test.

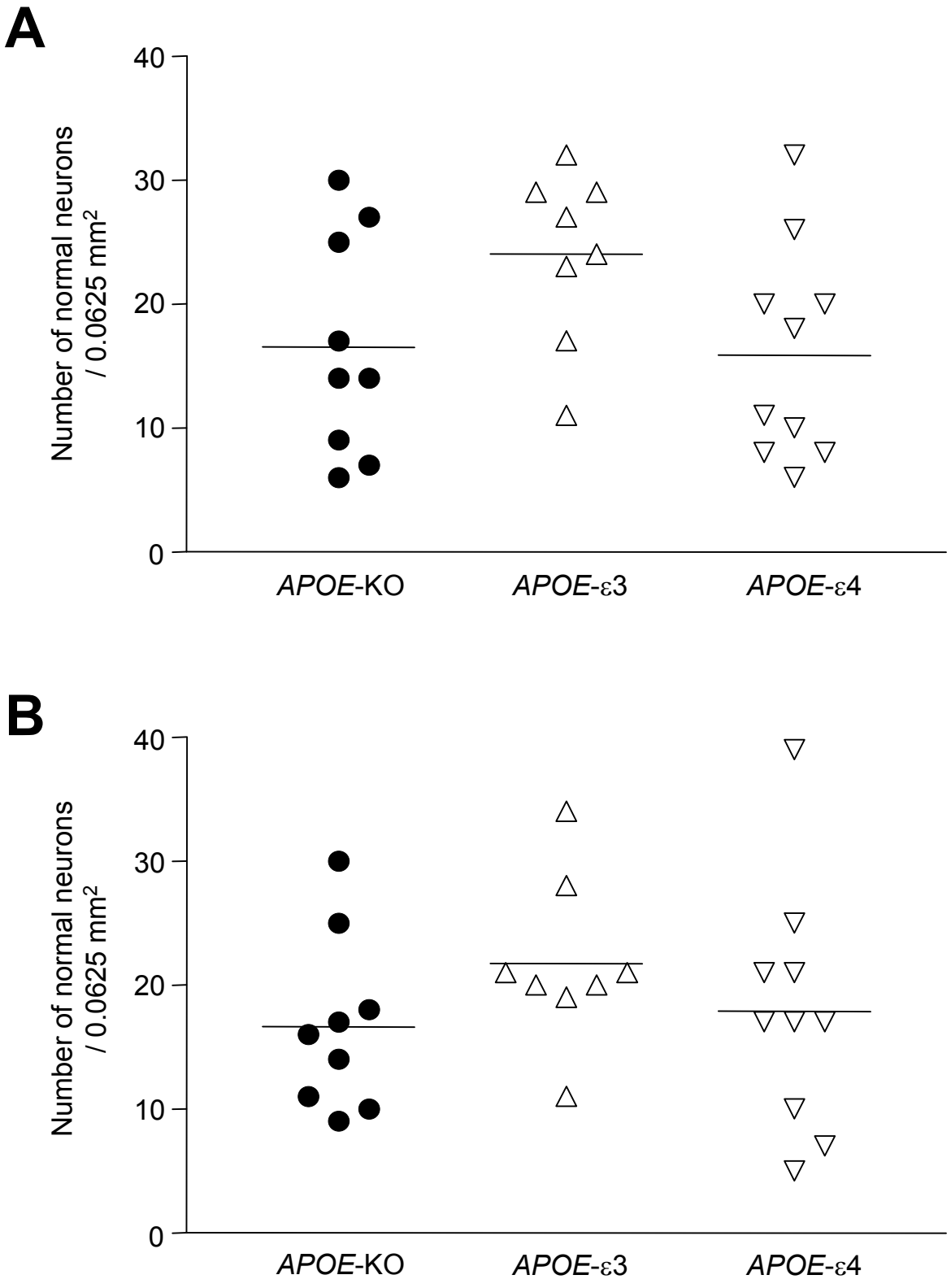

Figure 5.2 Number of morphologically normal neurons within the hippocampus
Number of normal neurons per 0.0625 mm^2 in *APOE*-KO, *APOE*-ε3 and *APOE*-ε4 mice subjected to 17m BCCAo within the contralateral (A) and ipsilateral (B) CA2 region of the hippocampus. There was a trend towards increased numbers of normal neurons in *APOE*-ε3 mice compared to the other genotypes, although this was not statistically significant. Data are expressed as individual data points, with the bar indicating the median. $p > 0.05$, using Kruskal-Wallis test with Dunn's post-test.

5.4.2 MHP36 survival and migration

In the caudate nucleus, survival of MHP36 stem cells was significantly improved in *APOE*-ε3 compared to *APOE*-ε4 mice (8.10 ± 2.89 versus 4.75 ± 3.04 PKH26 positive MHP36 cells per 0.0350mm^2, $p < 0.05$) or *APOE*-deficient mice (8.10 ± 2.89 versus 4.15 ± 1.49 PKH26 positive MHP36 cells per 0.0350mm^2, $p < 0.05$) (Figure 5.3 and 5.4). However, no significant difference in MHP36 survival was observed between the three groups in the hippocampus (Figure 5.5). It should be noted that markedly fewer MHP36 stem cells survived in the hippocampus as compared to the caudate nucleus.

As before, migration was assessed in a medial, lateral and ventral direction away from the injection tract. In the caudate nucleus, there was a marginal trend towards improved migration in *APOE*-ε3 and *APOE*-ε4 mice compared to *APOE*-deficient mice, although this was not statistically significant (Figure 5.6). In the hippocampus, *APOE*-KO and *APOE*-ε4 mice exhibited a trend towards increased migration compared to *APOE*-ε3 mice in a medial direction, although there were no significant differences in any of the three directions (Figure 5.7).

5.4.3 Neuronal differentiation of MHP36 stem cells

There was no significant difference in the proportion of MHP36 cells differentiating into a neuronal phenotype between the three groups in the caudate nucleus (Figures 5.8 and 5.9). In *APOE*-ε3 mice, approximately 35.79% ± 18.78% of grafted MHP36 cells expressed a neuronal phenotype compared to 26.11% ± 16.33% in *APOE*-ε4 mice and 27.96% ± 13.54% in *APOE*-KO mice. There were also no significant differences observed in neuronal differentiation of MHP36 cells between the three groups in the hippocampus. The largest proportion of MHP36 cells that differentiated into neurons was found in *APOE*-ε4 mice (26.52% ± 15.24%), followed by *APOE*-KO mice (19.33% ± 16.27%) and then *APOE*-ε3 mice (12.27% ± 17.78%) (Figures 5.10 and 5.11). These data are summarised as pie charts in Figure 5.14.

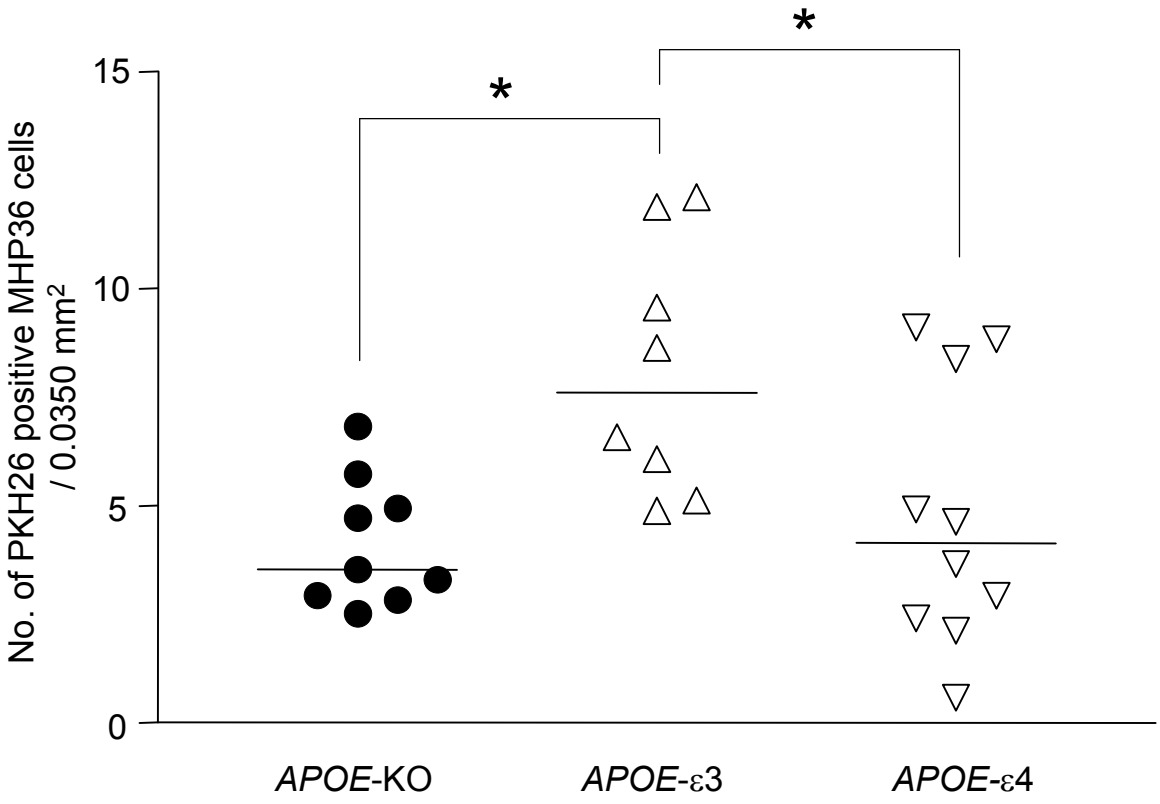

Figure 5.3 Number of PKH26 positive MHP36 cells in the caudate nucleus
The survival of MHP36 cells was significantly higher in *APOE*-ε3 mice as compared to *APOE*-KO and *APOE*-ε4. Data are expressed as individual data points, with the bar indicating the median. * $p < 0.05$, using Kruskal-Wallis test with Dunn's post-test.

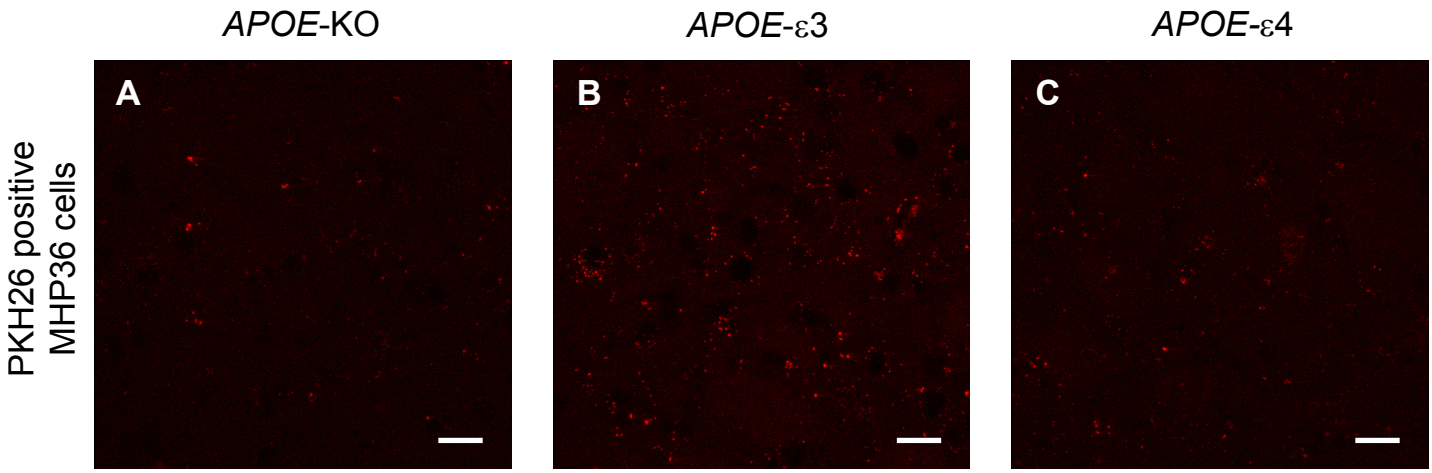

Figure 5.4 Representative confocal images illustrating survival of MHP36 cells in the caudate nucleus

Confocal images of PKH26 positive MHP36 cells (red) in *APOE*-KO(A), APOE-e3 (B) and *APOE*-ε4 (C) mice within the caudate nucleus. There was increased survival of MHP36 cells in *APOE*-ε3 mice compared to the other two groups. Scale bar = 20 μm.

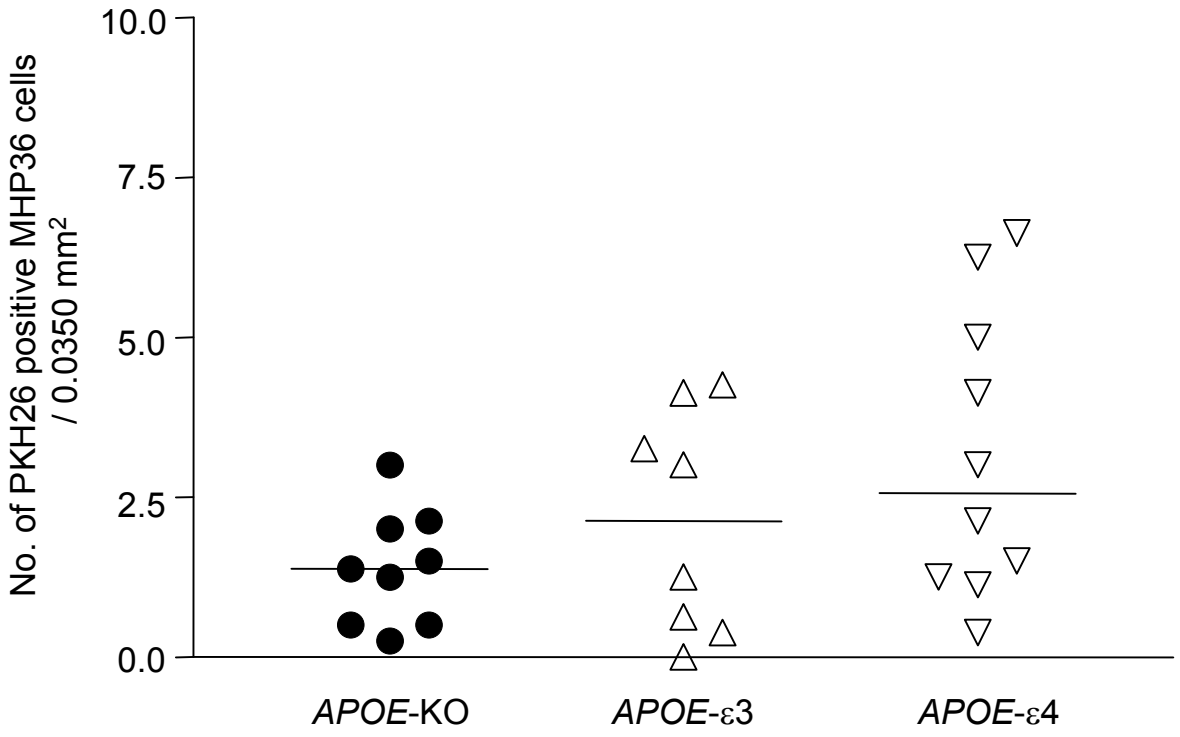

Figure 5.5 Number of PKH26 positive MHP36 cells in the hippocampus
There was a trend towards improved survival in *APOE*-ε3 and *APOE*-ε4 mice compared to *APOE*-KO mice,although this was not statistically significant. Data are expressed as individual data points, with the bar indicating the median. $p > 0.05$, using Kruskal-Wallis test with Dunn's post-test.

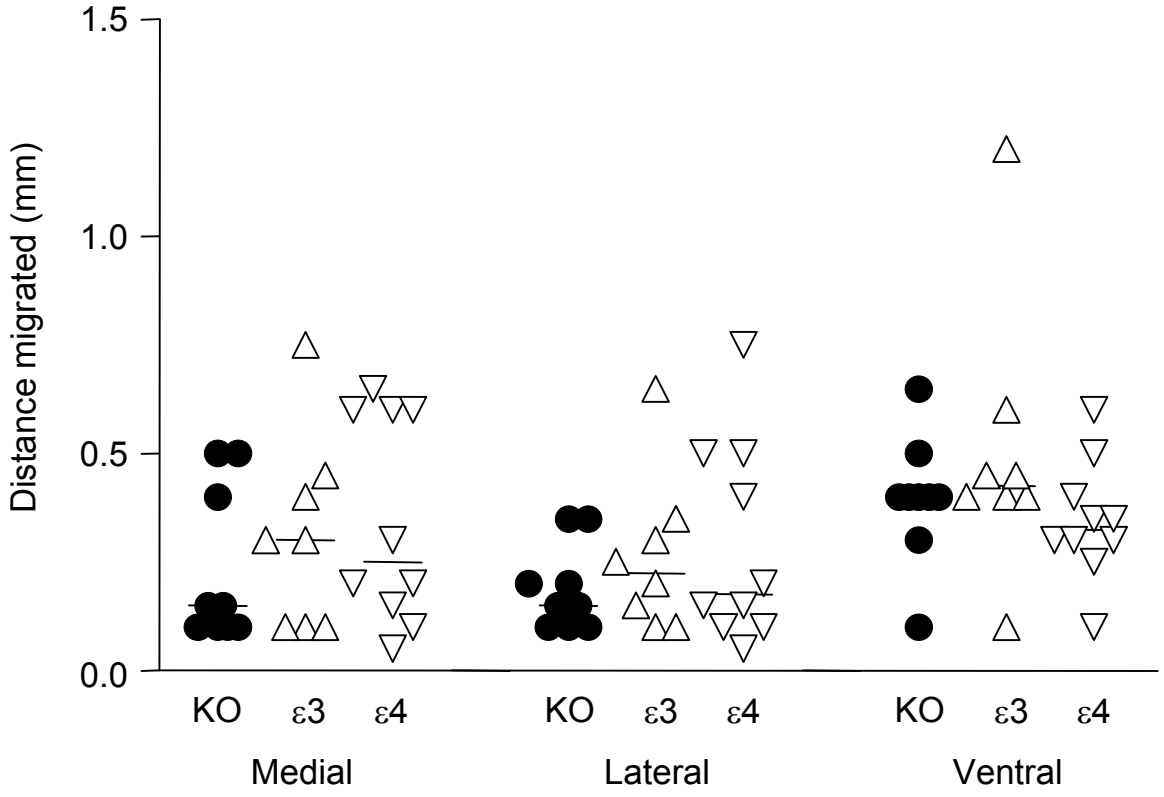

Figure 5.6 Migration of MHP36 cells in the caudate nucleus
Distance migrated (mm) by MHP36 cells in *APOE*-KO, *APOE*-ε3 and *APOE*-ε4 mice subjected to 17m BCCAo within the caudate nucleus. Migration was assessed in medial, lateral and ventral directions away from the injection tract. There was no significant difference between the three genotypes. Data are expressed as individual data points, with the bar indicating the median. $p > 0.05$, using Kruskal-Wallis test with Dunn's post-test.

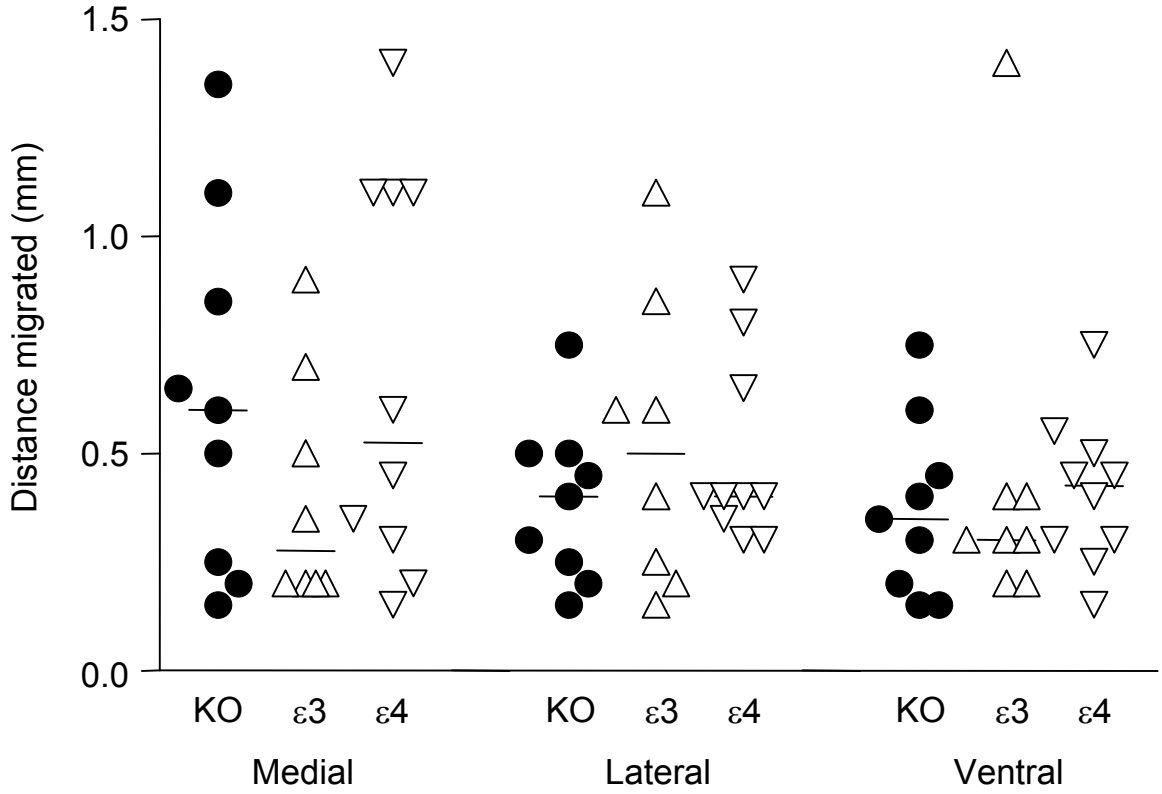

Figure 5.7 Migration of MHP36 cells in the hippocampus
Distance migrated (mm) by MHP36 cells in *APOE*-KO, *APOE*-ε3 and *APOE*-ε4 mice subjected to 17m BCCAo within the hippocampus. Migration was assessed in medial, lateral and ventral directions away from the injection tract. There was no significant difference between the three genotypes. Data are expressed as individual data points, with the bar indicating the median. $p > 0.05$, using Kruskal-Wallis test with Dunn's post-test.

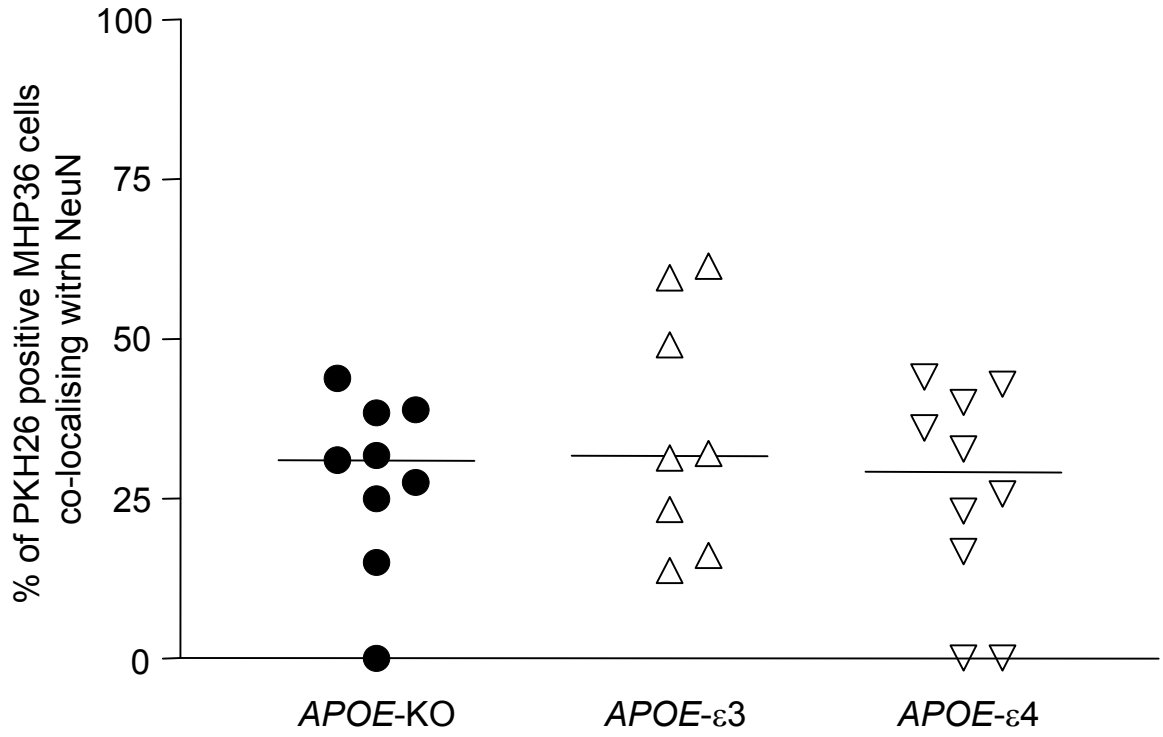

Figure 5.8 Percentage of PKH26 positive MHP36 cells co-localising with NeuN in the caudate nucleus

There was significant difference in neuronal differentiation between the three genotypes. Data are expressed as individual data points, with the bar indicating the median. $p > 0.05$, using Kruskal-Wallis test with Dunn's post-test.

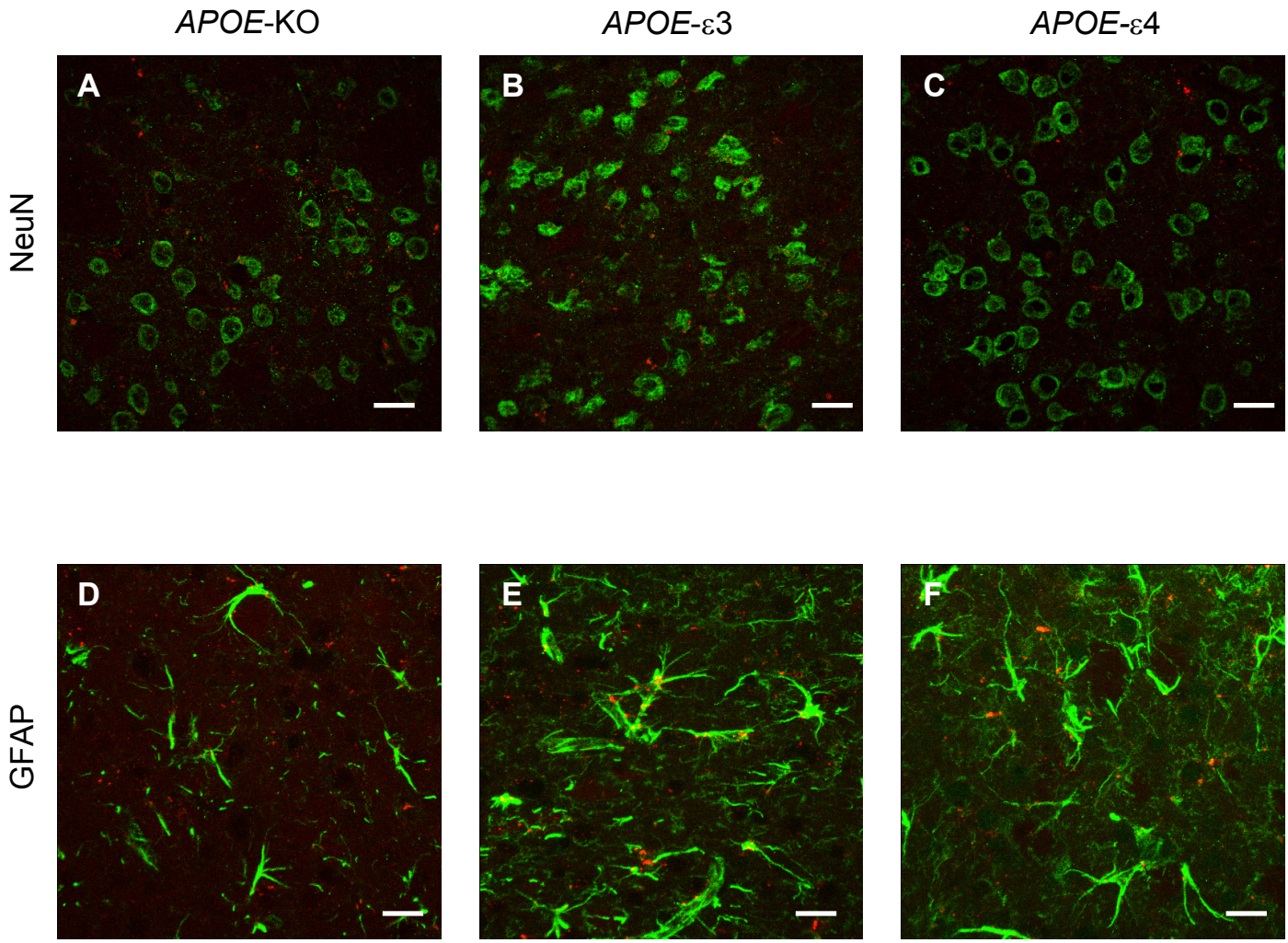

Figure 5.9 Representative confocal images illustrating differentiation of MHP36 cells in the caudate nucleus

Confocal images of PKH26 positive MHP36 cells (red) co-localising with the neuronal marker NeuN (green, Panels A-C) and the astrocytic marker GFAP (green, Panels D-F) in *APOE*-KO, *APOE*-ε3 and *APOE*-ε4 mice within the caudate nucleus. There was no difference in neuronal and astrocytic differentiation between the three groups of mice. Scale bar = 20 μm.

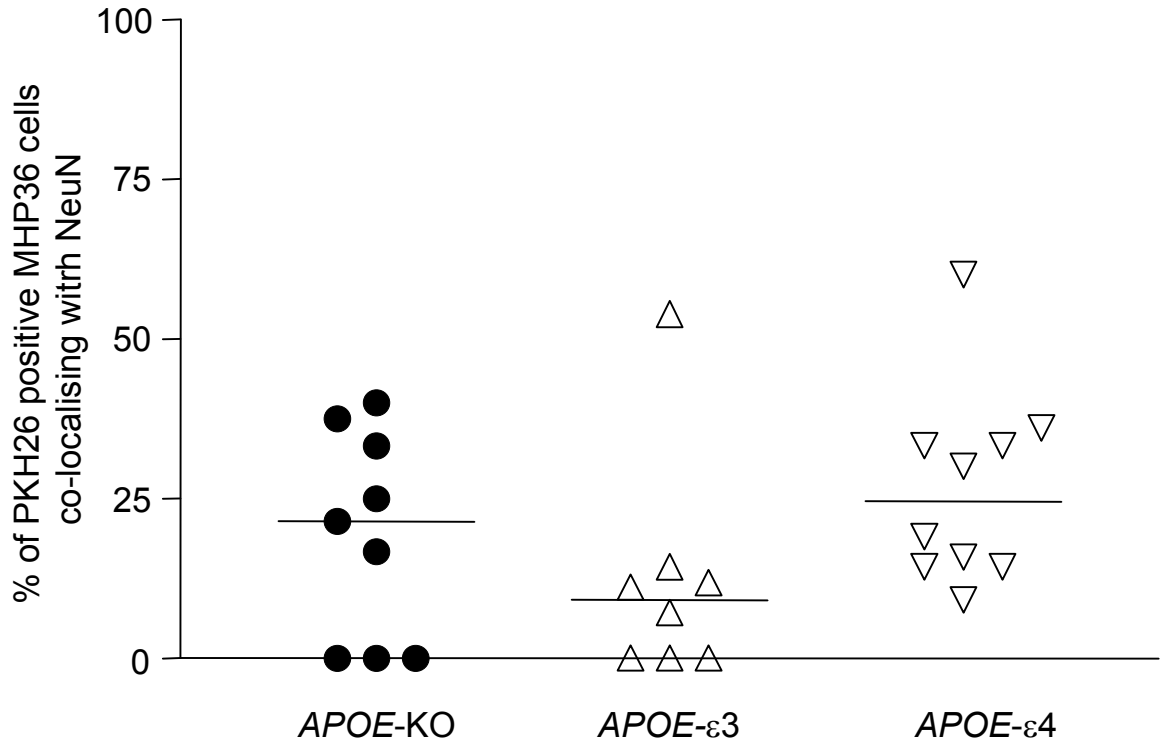

Figure 5.10 Percentage of PKH26 positive MHP36 cells co-localising with NeuN in the hippocampus

There was no significant difference in neuronal differentiation between the three genotypes. Data are expressed as individual data points, with the bar indicating the median. $p > 0.05$, using Kruskal-Wallis test with Dunn's post-test.

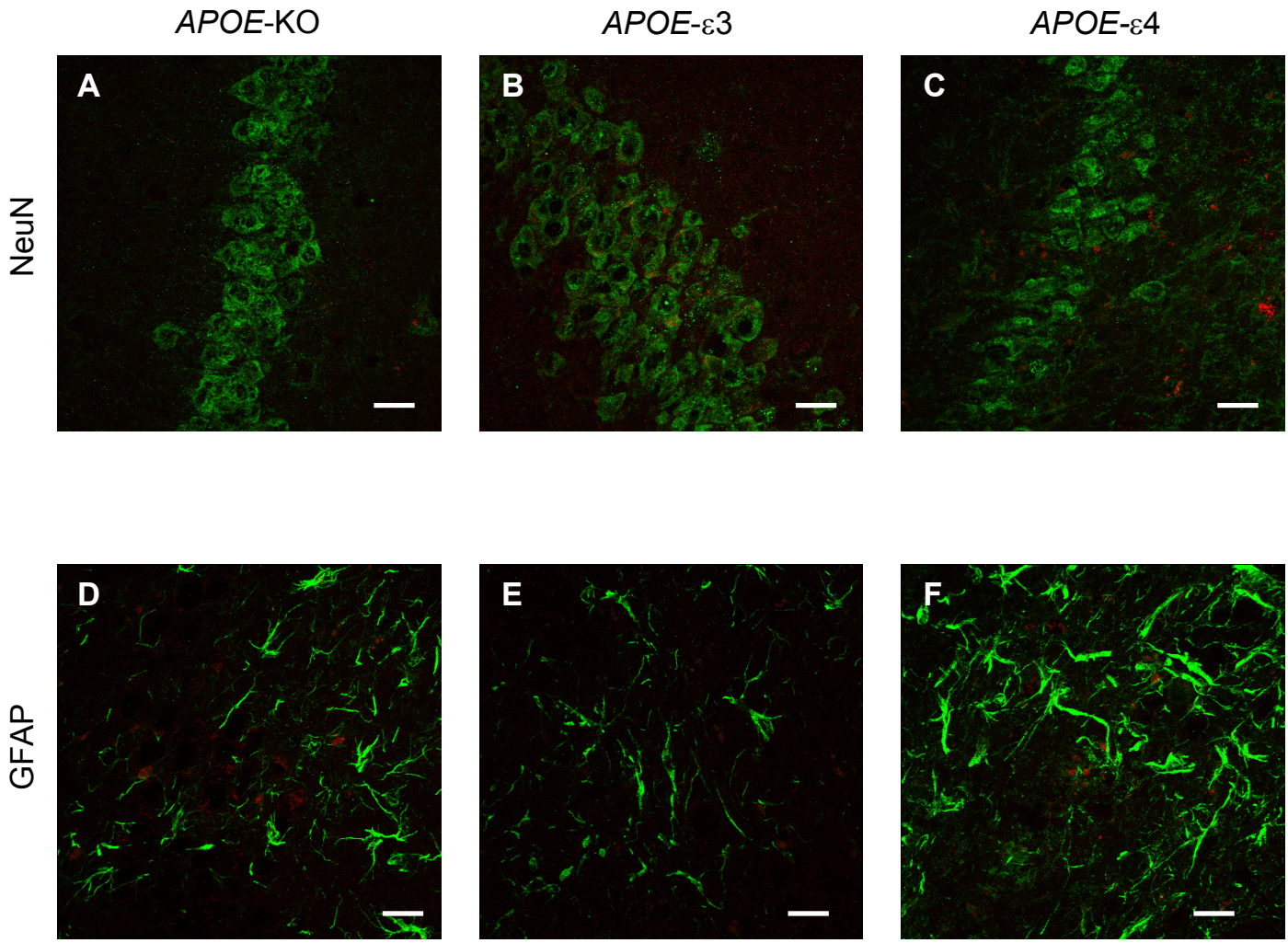

Figure 5.11 Representative confocal images illustrating differentiation of MHP36 cells in the hippocampus

Confocal images of PKH26 positive MHP36 cells (red) co-localising with the neuronal marker NeuN (green, Panels A-C) and the astrocytic marker GFAP (green, Panels D-F) in *APOE*-KO, *APOE*-ε3 and *APOE*-ε4 mice within the hippocampus. There was no difference in neuronal and astrocytic differentiation between the three groups of mice. Scale bar = 20 μm.

5.4.4 Astrocytic differentiation of MHP36 stem cells

Within the caudate nucleus, a similar proportion of MHP36 cells differentiated into an astrocytic phenotype in all three groups (Figures 5.9 and 5.12). Approximately 30.47% ± 15.94% of grafted MHP36 cells co-localised with an astrocytic marker in *APOE*-ε3 mice, compared to 25.14% ± 17.02% in *APOE*-ε4 mice and 25.51% ± 19.83% in *APOE*-KO mice. There was no significant difference between the groups. A similar distribution was noted in the hippocampus, where around 19.29% ± 14.79% of grafted MHP36 cells expressed an astrocytic phenotype in *APOE*-ε3 mice, compared to 13.37% ± 15.00% in *APOE*-ε4 mice, and 11.09% ± 14.69% in *APOE*-KO mice (Figures 5.11 and 5.13). These data are summarised as pie charts in Figure 5.14.

5.4.5 Rotarod analysis

All mice learnt how to balance and perform the rotarod task during the training session. The graphs showing the performance of each group of mice at the varying test speeds are shown in Figures 5.15 to 5.18. At all the rotation speeds, there were no genotype specific significant differences between the mice at any week post-transplantation. However, the latency to fall increased for all groups over time at all rotation speeds, suggesting that the mice were improving in motor balance and coordination. As expected, increasing the rotation speed resulted in decreased latency to fall for all groups of mice.

Due to the similar performance between the genotypes, I chose to calculate the area under the curve as an index of performance. At 8 rpm, the areas were as follows: *APOE*-KO: 172.6 ± 10.51 sq units, *APOE*-ε3: 173.8 ± 5.30 sq. units, *APOE*-ε4: 171.1 ± 9.10 sq. units. There was no difference between the three groups at this speed. At 16 rpm (*APOE*-KO: 155.8 ± 17.37 sq units, *APOE*-ε3: 155.6 ± 21.33 sq. units, *APOE*-ε4: 141.4 ± 25.30 sq. units), *APOE*-ε4 mice are marginally impaired in performance compared to *APOE*-KO and *APOE*-ε3 mice. However, this trend has altered at the increased speed of 24 rpm (*APOE*-KO: 97.08 ± 26.48 sq units, *APOE*-ε3: 87.10 ± 27.48 sq. units, *APOE*-ε4: 86.08 ± 37.74 sq. units). The human *APOE* transgenic mice exhibit similar levels of performance, and both are marginally

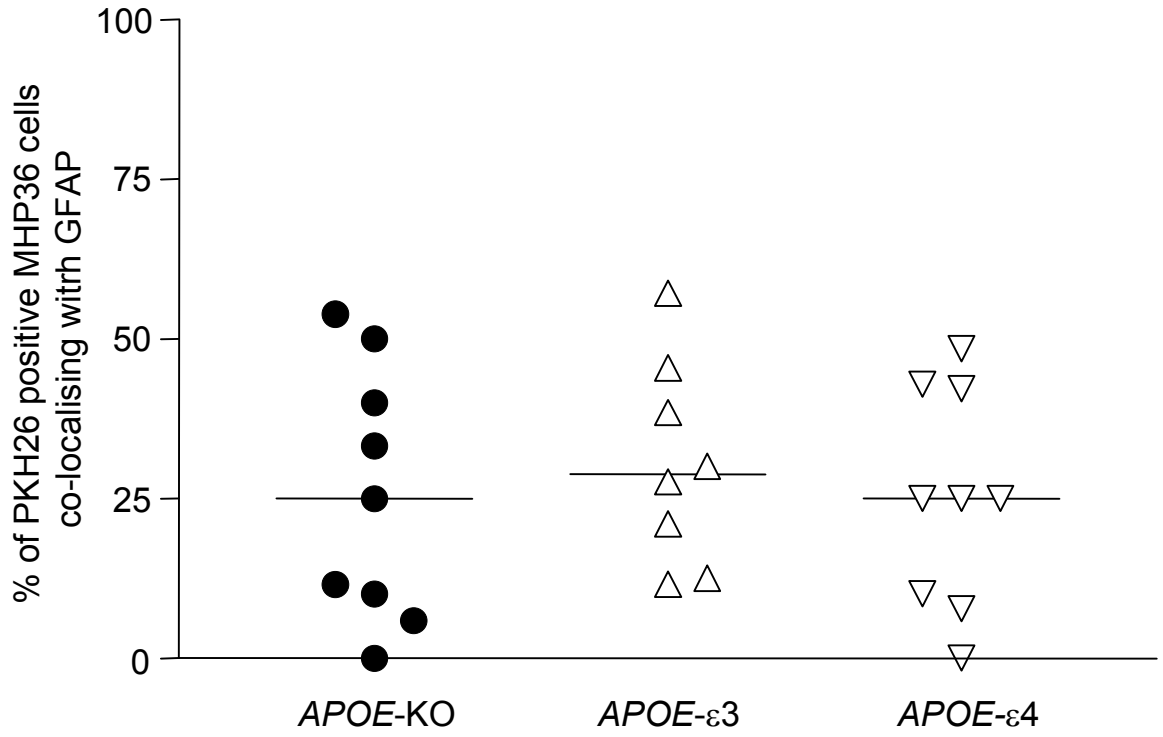

Figure 5.12 Percentage of PKH26 positive MHP36 cells co-localising with GFAP in the caudate nucleus

There was no significant difference in astrocytic differentiation between the three genotypes. Data are expressed as individual data points, with the bar indicating the median. $p > 0.05$, using Kruskal-Wallis test with Dunn's post-test.

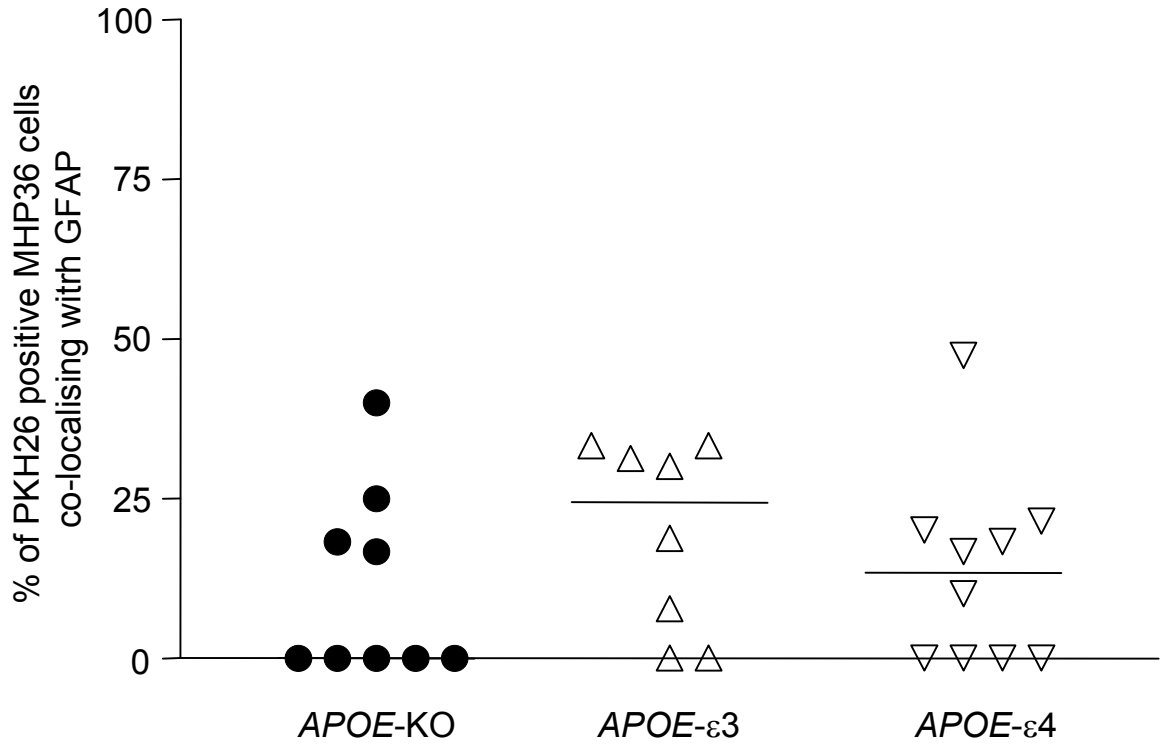

Figure 5.13 Percentage of PKH26 positive MHP36 cells co-localising with GFAP in the hippocampus

There was no significant difference in astrocytic differentiation between the three genotypes. Data are expressed as individual data points, with the bar indicating the median. The median value for *APOE*-KO mice is 0%. $p > 0.05$, using Kruskal-Wallis test with Dunn's post-test.

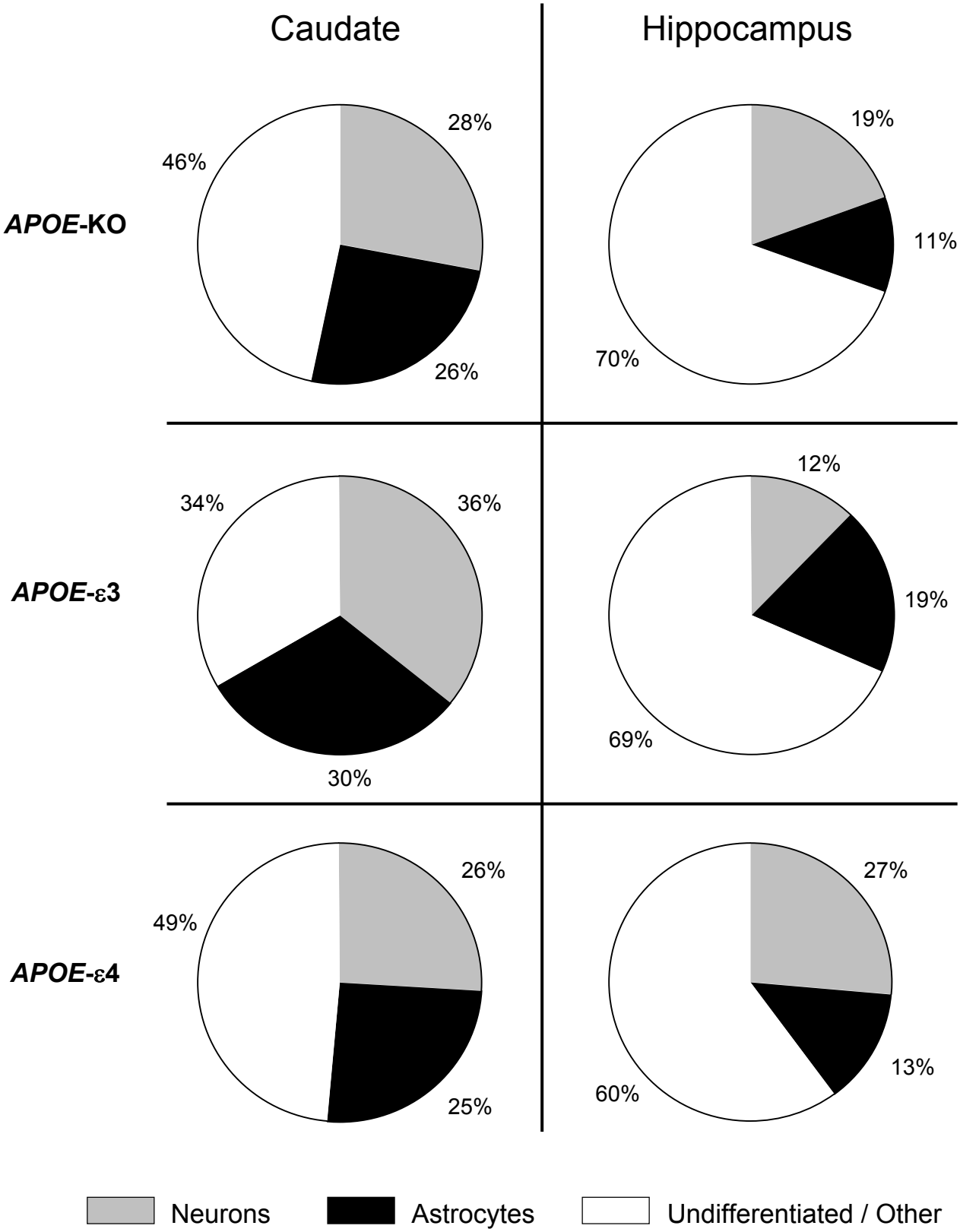

Figure 5.14 *APOE* genotype does not influence MHP36 stem cell differentiation
Pie charts showing the percentage of MHP36 cells differentiating into a neuronal, astrocytic or undetermined phenotype in *APOE*-KO, *APOE*-ε3 and *APOE*-ε4 mice in the caudate nucleus and hippocampus.

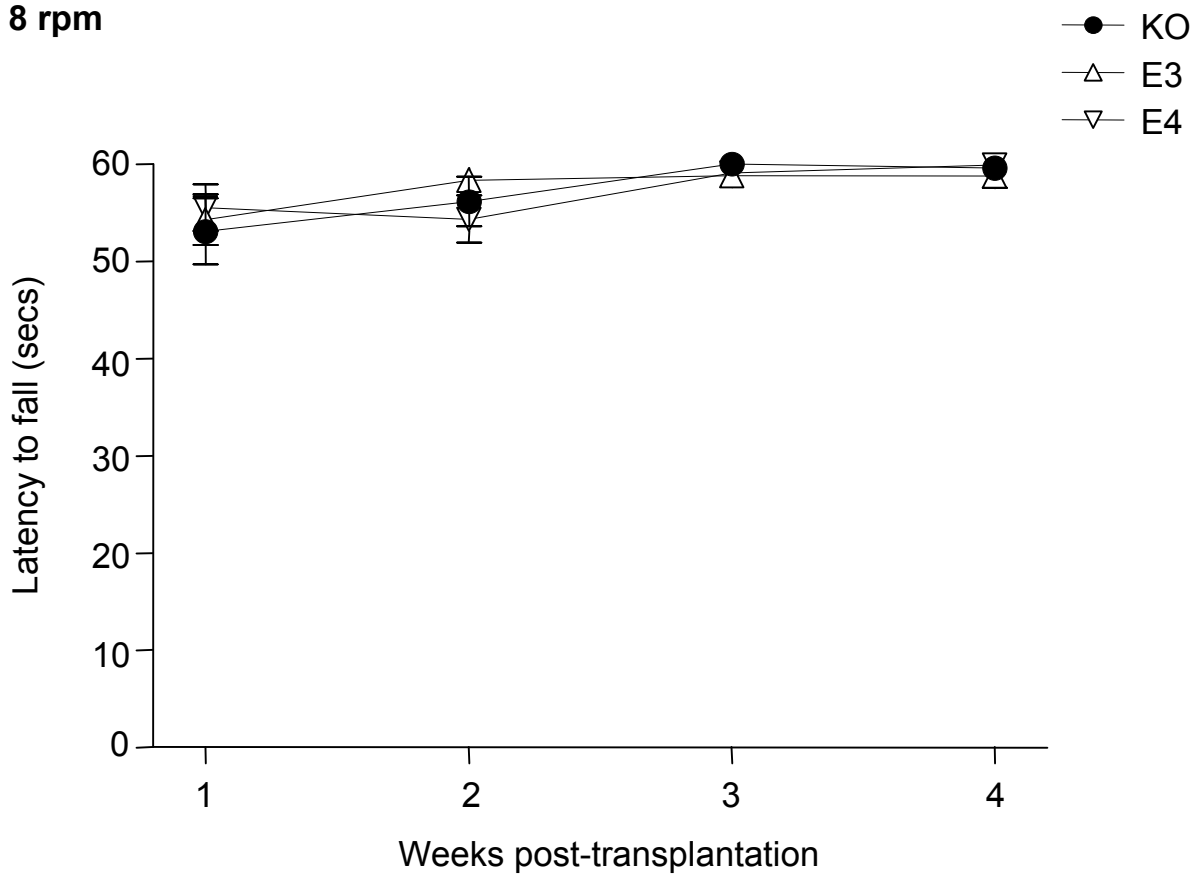

Figure 5.15 Motor performance on the rotarod test at 8 rpm
The latency to fall for each genotype was measured at each week post-transplantation. There was no significant difference between the three genotypes at each week. All three groups reached a plateau of near-optimal performance by the third week post-transplantation and maintained this through to the final week.. Data are presented as mean ± S.E.M. $p > 0.05$, using repeated measures ANOVA.

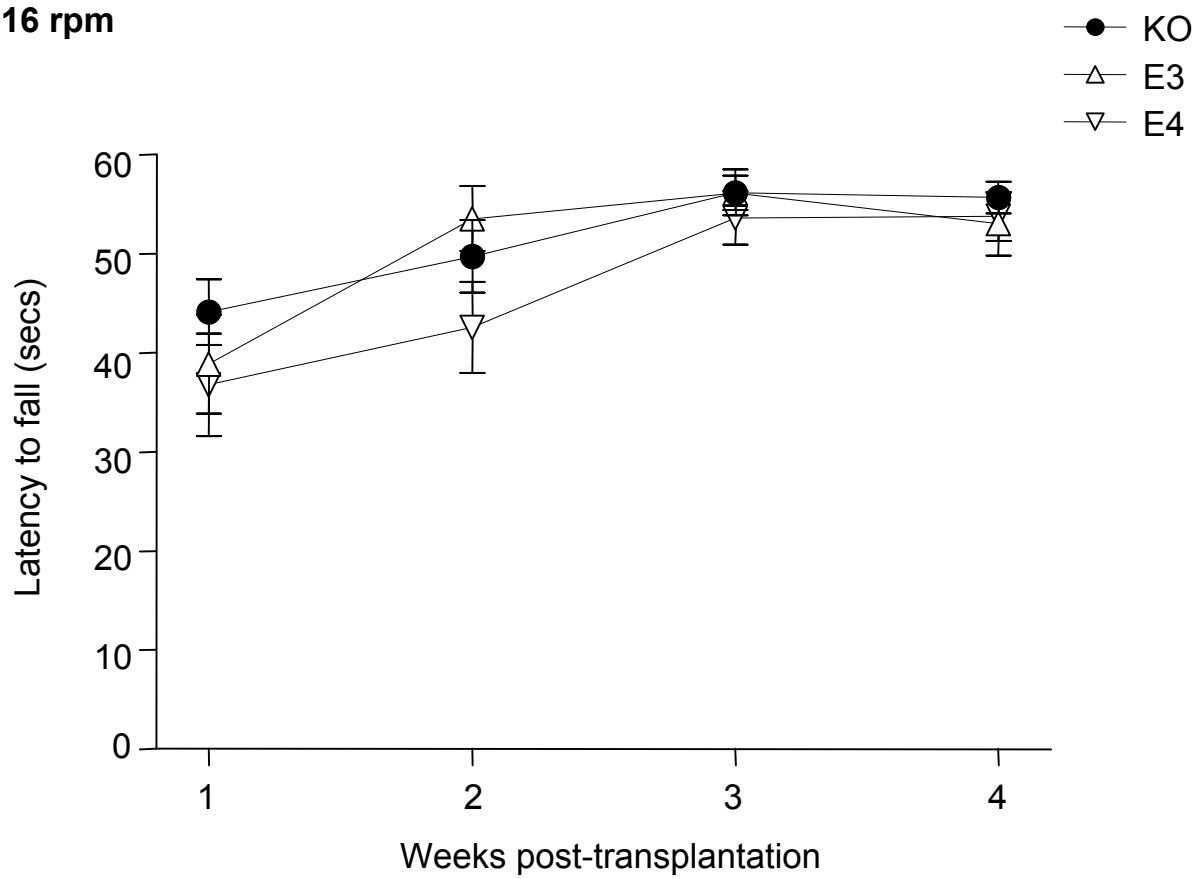

Figure 5.16 Motor performance on the rotarod test at 16 rpm
The latency to fall for each genotype was measured at each week post-transplantation. There was no significant difference between the three genotypes at each week. *APOE*-ε3 mice reached a plateau in performance by the second week post-transplantation, whilst *APOE*-KO and *APOE*-ε4 mice reached a plateau by the third week. Data are presented as mean ± S.E.M. $p > 0.05$, using repeated measures ANOVA.

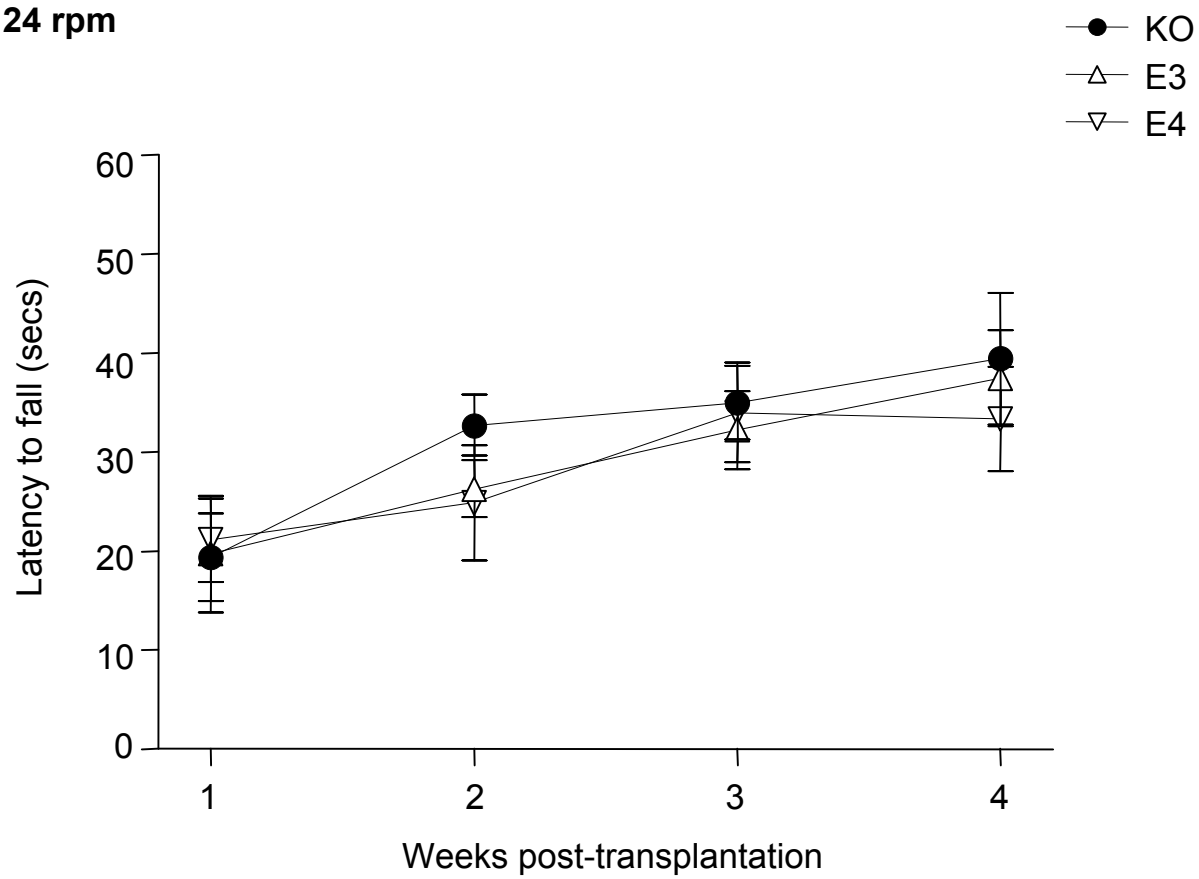

Figure 5.17 Motor performance on the rotarod test at 24 rpm
The latency to fall for each genotype was measured at each week post-transplantation. There was no significant difference between the three genotypes at each week. *APOE*-KO and *APOE*-ε3 mice improved in performance over the four weeks, whilst *APOE*-ε4 mice appeared to reach a plateau in performance by the third week. Data are presented as mean ± S.E.M. $p > 0.05$, using repeated measures ANOVA.

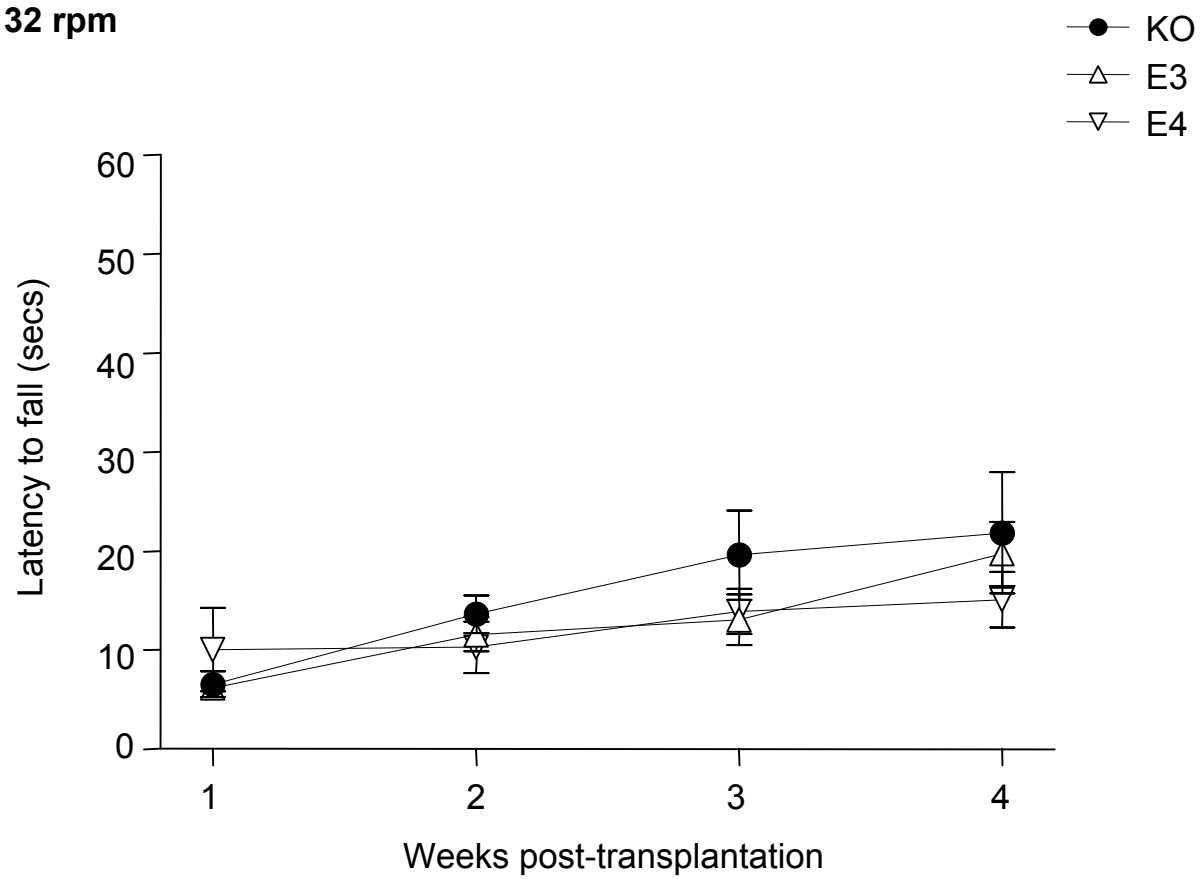

Figure 5.18 Motor performance on the rotarod test at 32 rpm
The latency to fall for each genotype was measured at each week post-transplantation. There was no significant difference between the three genotypes at each week. All three groups improved in performance over the four weeks. Data are presented as mean ± S.E.M. $p > 0.05$, using repeated measures ANOVA.

impaired compared to *APOE*-KO mice. This trend continues at the maximal speed of 32 rpm. (*APOE*-KO: 47.43 ± 26.10 sq units, *APOE*-ε3: 37.64 ± 16.66 sq. units, *APOE*-ε4: 36.81 ± 20.96 sq. units). None of these differences were statistically significant (Kruskal-Wallis with Dunn's post-test, $p > 0.05$). However, the trends provided by these data suggest that *APOE*-ε4 mice are marginally impaired on the rotarod task of motor balance and coordination compared to *APOE*-KO mice at moderate and high speeds. *APOE*-ε3 mice are able to perform at the same level as *APOE*-KO mice at moderate speeds, but their performance deteriorates to levels approaching that of *APOE*-ε4 mice at higher speeds.

5.5 Discussion

This study demonstrated that MHP36 graft survival was improved in *APOE*-ε3 transgenic mice compared to *APOE*-ε4 and *APOE*-KO mice. However, there was no *APOE* genotype specific influence on the migration and differentiation of grafted MHP36 stem cells. There was minimal evidence that motor recovery following ischaemia and stem cell grafts was affected by *APOE* genotype.

5.5.1 *APOE* genotype influences susceptibility to ischaemic damage

The results indicate that within the caudate nucleus, there was no difference in the number of normal neurons between *APOE*-ε3 and *APOE*-ε4 mice. Both the human *APOE*-expressing mice exhibited an increased number of normal neurons compared to *APOE*-KO mice. However, in the hippocampal CA2 region, *APOE*-ε3 mice exhibited a trend towards increased neuronal number compared to both *APOE*-ε4 and *APOE*-KO mice in both hemispheres. These results confirm previous work by our group on the differences in susceptibility of human *APOE*-expressing transgenic mice to the effects of global ischaemia (Horsburgh et al., 2000). Histopathological analysis of *APOE*-ε3 and *APOE*-ε4 mice three days after induction of global ischaemia showed similar levels of ischaemic damage in the caudate nucleus in the two transgenic lines. However, examination of the CA1 pyramidal cell layer indicated a clear genotype specific difference. *APOE*-ε4 mice had markedly more ischaemic damage in this region compared to the *APOE*-ε3 mice (Horsburgh et al.,

2000). Although this study investigated ischaemic damage at an acute time point, compiling the data from these two studies demonstrates that *APOE*-ε4 mice have a definite regional susceptibility to global ischaemia in the hippocampus. *APOE*-ε4 mice have also been shown to be more susceptible that *APOE*-ε3 mice to other forms of brain damage, such as focal ischaemia (Sheng et al., 1998) and traumatic brain injury (Sabo et al., 2000). Thus, stem cell integration may be affected differently in the caudate nucleus and the hippocampus.

5.5.2 *APOE* genotype influences MHP36 graft survival but has no effect on migration

The results from this study demonstrate that there was increased survival of MHP36 stem cells in *APOE*-ε3 mice as compared to both *APOE*-ε4 and *APOE*-KO mice within the caudate nucleus. The increased MHP36 cell survival in APOE-ε3 mice may reflect the beneficial effects of apoE3 compared to apoE4 described in the literature. ApoE3 has been shown to exert a neuroprotective effect through reduction of excitotoxicity, whilst apoE4 does not confer protection (Buttini et al., 1999). The anti-oxidative potential of apoE3 is also superior to apoE4 (Miyata and Smith, 1996). These two properties of apoE3 could serve to reduce the extent of ischaemic damage, therefore providing a less hostile environment for the grafted MHP36 cells, and increasing the chances of survival. Alternatively, apoE3 may be involved in structural remodelling and support for the grafted stem cells. ApoE3 stimulates polymerisation of β-tubulin and microtubule stabilisation, whereas apoE4 destabilises the assembly or microtubules (Nathan et al., 1995). The ability of apoE3 to preserve the neuronal cytoskeleton could provide structural support for the survival and integration of grafted stem cells into host brain. Linked to this, apoE3 has been shown to induce neurite outgrowth compared to inhibition of outgrowth by apoE4 (Nathan et al., 1994, Bellosta et al., 1995, Nathan et al., 2002), suggesting another mechanism by which apoE could aid the survival of transplanted MHP36 stem cells. Interestingly, apoE3 has been associated with inhibition of cell proliferation, particularly endothelial and tumor cells (Ishigami et al., 1998, Vogel et al., 1994, Zeleny et al., 2002). In contrast, apoE4 is the least effective of all apoE isoforms regarding the inhibition of smooth muscle cell proliferation (Zeleny et al.,

2002). These findings appear somewhat contradictory with the findings that apoE3, not E4 markedly promotes MHP36 neural stem cell survival, and lend further credence to the hypothesis that apoE3 assists graft survival through support mechanisms. However, it should be noted that the apoE4-mediated inability to inhibit cell proliferation is linked with cancerous disease conditions, suggesting that the inhibitory role of apoE3 is an essential regulatory function (Liestol et al., 2000, Moysich et al., 2000).

Whilst MHP36 stem cells do not survive in the hippocampus to the same degree as in the caudate nucleus, there was a slight trend towards improved survival in *APOE*-ε3 and ε4 mice as compared to *APOE*-KO mice in this region. An interesting comparison can be made with the previous study. Similar numbers of PKH26 positive MHP36 cells were observed in the caudate nucleus of C57Bl/6J and *APOE*-ε3 mice (approximately 8 cells per 0.0350 mm^2). However, more MHP36 cells survived in *APOE*-KO mice from the current study (approximately 4 cells per 0.0350mm^2) compared to the equivalent mice from the previous study (*APOE*-KO, 17m BCCAo, approximately 1.7 cells per 0.0350 mm^2). Both studies followed the same experimental procedure, with the only major difference being the administration of behavioural testing on the rotarod in the current study. The mandatory exercise on the rotarod may account for the increase in stem cell survival in *APOE*-KO mice in this study as compared to the previous study. It has been well documented that exercise can increase endogenous neurogenesis (Van Praag et al., 1999), and the mechanisms that underlie this may also promote graft survival. However, a possible caveat is that exercise-mediated neurogenesis classically takes place in the dentate gyrus of the hippocampus (van Praag et al., 1999, van Praag et al., 2005) rather than the SVZ, the region where changes relating to striatal grafts would be expected. Combined with this, there was no increase in the survival of MHP36 cells in the hippocampus of *APOE*-KO mice from this study compared to *APOE*-KO mice from the previous study.

No significant differences were observed in distance migrated between the three groups. However, there was a trend towards improved migration in *APOE*-ε3 and ε4

mice as compared to *APOE*-KO mice within the caudate nucleus. As expected from the previous chapter, MHP36 cells migrated further when grafted into the hippocampus rather than into the caudate nucleus. Migration in the hippocampus was also more variable. Comparison of migration distance between this study and the previous study does not reveal any major difference. *In vitro* data from the literature suggests that human apoE inhibits smooth muscle cell migration (Ishigami et al., 1998, Swertfeger et al., 2002, Zhu and Hui, 2003) via binding to LRP1 and activation of cAMP protein kinase A. All three human apoE isoforms inhibit smooth muscle cell migration to an equal degree, which could explain why no apoE isoform difference was observed for MHP36 stem cell migration.

5.5.3 *APOE* genotype does not significantly influence MHP36 stem cell differentiation

There was no *APOE* genotype specific significant difference in the percentage of MHP36 cells expressing either a neuronal or astrocytic phenotype either in the caudate nucleus or hippocampus. Examination of the differentiation profiles (Figure 5.14) suggests that within the caudate nucleus, there is an overall trend towards increased astrocytic and neuronal differentiation in *APOE*-ε3 mice compared to *APOE*-KO and *APOE*-ε4 mice. However, this is probably linked to the increased survival of MHP36 cells observed in this region in the *APOE*-ε3 mice (Figure 5.3), rather than through any genotype specific effect on differentiation. This is supported by the other differentiation profiles which show that the majority of MHP36 cells in all three groups of mice do not differentiate into neurons or astrocytes and either remain undifferentiated or are expressing a non-neuronal, non-astrocytic phenotype (Figure 5.14). The same charts show the similarity in differentiation profile between the mice. This consistent similarity suggests that there may be a baseline level of differentiation depending on the host region, which may be induced by a factor or factors that are either present in the host environment, or secreted by the transplanted stem cells.

5.5.4 *APOE* genotype does not influence motor recovery

No differences in motor performance on the rotarod were observed between *APOE*-KO, *APOE*-ε3 or *APOE*-ε3 transgenic mice in this study. All groups improved in performance over time, at all four test speeds. Interestingly, *APOE*-KO mice consistently exhibited a trend towards improved motor balance and coordination compared to both human *APOE*-transgenic groups as assessed by comparison of the area under the curve, although none of these differences were statistically significant.

The lack of an observable genotype difference may be attributed to the selective neuronal damage associated with transient global ischaemia. The striatum is intimately involved in motor function and coordination, hence the choice of the behavioural rotarod test. However, all three groups exhibited similar numbers of normal neurons, and by extension, a similar degree of ischaemic damage in the striatum (Figure 5.1). There was a variation in number of normal neurons remaining in the hippocampus, with a trend towards increased number in *APOE*-ε3 mice compared to *APOE*-KO and *APOE*-ε4 mice, but this is unlikely to affect motor performance on the rotarod. It may be possible that motor performance tests are simply not sensitive enough to detect any changes in APOE transgenic mice, even in the aftermath of brain damage. In particular, it is also important to take into account whether the damage induced is unilateral (such as in models of focal ischaemia) or bilateral (such as the model of global ischaemia used in this thesis). Unilateral models offer greater sensitivity for detection as deficits in one hemisphere manifest on a variety of behavioural tasks such as the staircase pellet reaching test (Montoya et al., 1991), the rotameter and the rotarod. However, it could be argued the design of this thesis has resulted in a unilateral model, as a unilateral injection of neural stem cells was delivered into a bilateral model of damage.

Hippocampal deficits are more suited to investigation through spatial learning and memory tasks such as the Morris water maze or 8-arm radial maze. Previous studies have demonstrated in rats that underwent 4VO induced global ischaemia, MHP36 grafts were able to repopulate the lesioned CA1 layer and restore ischaemia related spatial deficits in acquisition of a hidden platform in the water maze (Sinden et al.,

1997, Hodges et al., 2000). MHP36 grafted rats showed faster escape latencies and shorter swim distances than ischaemic, sham grafted rats. The performance of MHP36 grafted rats was similar to that of a group of sham ischaemia control rats.

The Maeda strain of *APOE*-KO mice used in this study has been thoroughly investigated for their behavioural phenotype compared to wildtype C57Bl/6J littermate controls in a variety of tasks (Anderson et al., 1998). These investigators discovered no difference between *APOE*-KO and wildtype mice aged between eight to ten months in a series of neurological tests, cumulative locomotor activity or rotarod performance. These mice were not subject to any lesion which could have affected their performance. In the water maze trial, there was no genotype effect on the path length required to locate the platform in either the cued or the place task. As predicted from the locomotor activity tests, there was no difference in swim speed between the *APOE*-KO and wildtype mice. The probe trial demonstrated that both groups also exhibited spatial learning, as evidenced by the fact that they spent an equal preference time for the quadrant that previously contained the platform. Further evidence suggesting that apoE is not essential for motor recovery after injury came from a study by Goldstein et al (2000). There was no difference in the ability of *APOE*-KO mice from the Maeda strain to traverse along a narrow beam compared to wildtype C57Bl/6J mice following a unilateral sensorimotor cortex ablation. Both groups were virtually identical in their initial motor deficit, subsequent recovery rate and final levels of functional performance.

Conflicting results were obtained from different strains of *APOE*-KO mice. Oitzl et al., (1997) also used the water maze to assess spatial learning and memory in the Van Ree strain (Van Ree et al., 1994) of *APOE*-KO mice. In this study, almost all *APOE*-KO mice failed to find the underwater platform, whereas heterozygous mice acquired the task over time. The *APOE*-KO mice also did not develop any strategy to locate the platform, but instead repetitively swam and bumped against the sidewall of the pool for the duration of the trial. No differences in locomotor activity or swim speed were found between the *APOE*-KO mice and the heterozygous group, ruling out the possibility that motor disturbances are responsible for the abnormal “wall-bumping”

behaviour. The authors conclude that this Van Ree strain of *APOE*-KO mice suffer from a spatial learning deficit. Later studies demonstrated that exposure of these *APOE*-KO mice to a stressful environmental experience (rat stress) resulted in a decrease in corticosterone concentration, concomitant with improved spatial learning on the water maze (Grootendorst et al., 2001). Interestingly, the APOE-KO mice adopted a persistent goal-directed search strategy rather than the concentric "wall-bumping" strategy observed previously. Another strain of *APOE*-KO mice created by Breslow (Plump et al., 1992) has also been assessed for working and reference memory in a water maze task. Over a four-day period, mice were given twice-daily trials to locate a submerged platform. Both *APOE*-KO and control mice displayed decreasing latencies to reach the platform over subsequent days, showing an improvement over time. However, an *APOE* genotype dependent effect was observed during the two daily trials. Control mice improved their performance in the second daily trial as compared to the first trial, but there was no difference in latencies between the two daily trials in *APOE*-KO mice. The data suggest that whilst the Breslow strain of *APOE*-KO mice is not impaired in reference memory, they have a deficit in working memory. This deficit has been linked to cholinergic impairments in the hippocampus and frontal cortex (Gordon et al., 1995). Common to the other two strains of *APOE*-KO mice, the Breslow strain did not differ from control mice in swimming speed. Although *APOE*-KO mice from the Maeda strain exhibited widespread neuronal degeneration throughout the hippocampus after mild induction of concussive-like brain injury, this is not paralleled with any deficits in motor function (Han and Chung, 2000). However, induction of similar closed head injury in *APOE*-KO mice from the Breslow strain resulted in prolonged motor and cognitive deficits as compared to control mice. These behavioural deficits were observed in conjunction with overt bilateral neuronal death in the hippocampus of the *APOE*-KO mice. Taken together, these studies demonstrate a clear background difference between the three *APOE*-KO strains in behavioural measures of learning and memory.

Exposure to an enriched environment can also influence motor function in *APOE* transgenic mice (Levi et al., 2003). Three week old *APOE*-ε3, *APOE*-ε4, *APOE*-KO

(all derived from the Maeda strain) and C57Bl/6J mice were placed either in regular cages without additional items or cages containing exploratory items such as tunnels, toys, and running wheels. Motor performance was assessed by measuring the latency to fall from a rotarod rotating at 10 rpm over a 60s trial. Initially, *APOE*-ε4 and *APOE*-KO mice housed in a regular environment exhibited a quicker latency to fall compared to regularly housed *APOE*-ε3 and C57Bl/6J mice. However, subsequent training improved the performance of *APOE*-ε4 and *APOE*-KO mice to the same level as control mice. In contrast, all of the mice housed in an enriched environment performed equally and optimally in the rotarod trials. Whilst these mice did not receive any form of neurological insult, the results suggest that the *APOE* genotype has minimal effects on motor performance and coordination, and that these effects can be countered with exposure to an enriched environment. Similarly, all the mice in our study were housed with a cardboard tunnel for exercise and exploration, which may explain the lack of an observable genotype difference in motor performance between the three groups. The same study by Levi et al., (2003) also investigated learning and memory using the T-maze paradigm. Environmental enrichment increased the speed of learning and also prolonged the duration of working memory in wild type mice. *APOE*-ε3 mice but not *APOE*-ε4 mice improved in learning and memory in response to an enriched environment. An interesting observation was the fact that C57Bl/6J mice expressing endogenous mouse apoE performed better on these learning and memory tasks compared to the corresponding human *APOE*-ε3 expressing mice. One possible explanation for this discrepancy arises from differences in the background strain of these mice. Lominska et al., (2001) have demonstrated that six month old apoE-deficient mice bred onto the C57BL/6J background exhibited impairment in learning on an olfactory based radial arm maze. Notably, this impairment was not observed in wildtype C57BL/6J mice, or in apoE-deficient or wildtype mice on the FVB/N background. It is possible that the *APOE*-ε3 and ε4 mice used in our study have inherited the behavioural deficits of the *APOE*-KO mice used for derivation as they are heterozygous for the *APOE*-KO genotype, even though the *APOE*-KO strain was generated on a C57Bl/6J background.

A recent study from our group investigated learning and memory in young and aged *APOE*-KO, *APOE*-ε3 and *APOE*-ε4 mice with wildtype C57Bl/6J controls (Kennedy et al., in press). On a normal serial spatial learning task, *APOE*-KO, human *APOE* transgenics and WT mice all learn to the same ability. However, on the more demanding Atlantis platform spatial learning task, where the animal has swim to and remain within in the region of the platform for a set amount of time before the platform rises, *APOE*-KO mice are impaired compared to WT controls in both young and aged mice. Intriguingly, this cognitive impairment was 'rescued' in young mice expressing human *APOE*-ε3 or *APOE*-ε4. However, no rescue effect was observed in aged human *APOE* transgenics. There was no genotype specific difference between the *APOE*-ε3 and ε4 strains. Therefore, it appears that the human *APOE* transgenic mice have a similar cognitive facility to wildtype C57BL/6J mice at a young age, but following age-related cognitive decline, their behavioural phenotype shifts to that similar to *APOE*-KO mice, although this can only be detected on a complex learning task. Results from this study reiterate the behavioural similarity between WT, *APOE*-KO and human *APOE* transgenic mice and further support previous data suggesting a phenotypic difference between endogenous mouse and human apoE.

5.5.5 Murine and human apoE display differences in structure, function and synthesis

A possible reason for results observed in this study may be due to the differences between murine *APOE* and the human form. The mouse and human *APOE* gene sequences share 78% homology and 70% amino acid homology (Rajavashisth et al., 1985). Like all animal *APOE*, mouse *APOE* only exists in one isoform. The gene sequence for mouse *APOE* encodes for the arginine residue at position 112 and glutamate at position 255, providing sequence similarity to human *APOE*-ε4. However, at residue 61, the mouse *APOE* gene sequence encodes threonine, in contrast to the arginine in human *APOE*. The absence of a charged residue at this position causes a conformational change, meaning that mouse *APOE* does not have the N-C terminal interaction of human *APOE*-ε4. Therefore, although mouse *APOE* has sequence similarity to human *APOE*-ε4, it has structural and functional similarity with human *APOE*-ε3. Still, if mouse *APOE* had complete functional similarity with

human *APOE*-ε3, we would have expected similar results between the C57BL/6J mice grafted with MHP36 cells in the previous study and the *APOE*-ε3 mice used in this study. Astrocytes derived from wildtype C57Bl/6J, *APOE*-KO and human *APOE*-ε3 and *APOE*-ε4 expressing mice secrete HDL particles composed of phospholipids, free cholesterol, along with apoE and apolipoprotein J (apoJ). However, HDL particles secreted from human E3 and E4 astrocytes contained less lipid than mouse wildtype particles, even though they contain twice as much apoE (Fagan et al., 1999). Endogenous mouse apoE appears to support the production of an HDL particle with a greater lipid:apoE ratio than human apoE, suggesting that mouse apoE may be more efficient at binding lipid than the human form.

There are other differences between the *APOE* transgenic mice and C57BL/6J wildtype mice, which may account for the difference observed. The pattern of apoE expression is altered in the *APOE* transgenic mice. During the creation of the human *APOE* transgenics, Xu et al. carried out immunocytochemical analysis for the location of *APOE* (Xu et al., 1996). In both wildtype and *APOE* transgenic mice, apoE-immunoreactive glia was present in all brain regions, and especially prevalent in the grey matter. Other apoE positive cells include the ependymal cells and Bergmann glia in the cerebellum. In the wildtype mice, no neurons were immunoreactive for apoE. In contrast, nearly all of the transgenic lines generated exhibited some degree of apoE-immunoreactivity in selected neurons. This was especially apparent in the cerebral cortex. ApoE positive neurons were always found in regions already containing immunoreactive glia. The presence of apoE in neuronal cells was validated by electron microscopy. The pattern of apoE expression in these transgenic mice mirrored that observed in human and non-human primate brain. This localisation of apoE expression was confirmed by in situ hybridisation (Xu et al., 1998). It should be noted that this constitutive neuronal expression of apoE is different from the upregulation of neuronal apoE observed in both human and mouse brain after damage.

Another difference between mouse and human apoE relates to its synthesis and secretion. Macrophages have long been identified as a source of apoE (Basu et al.,

1981). Following incubation with acetyl-LDL, macrophages internalise the lipoprotein and deliver it to lysosomes, where the cholesterol esters are hydrolysed. The free cholesterol re-esterifies in the cytoplasm and accumulates as cholesteryl ester droplets. In the presence of a cholesterol binding substance such as HDL in the surrounding medium, these cholesterol-loaded macrophages secrete large quantities of free cholesterol, along with apoE. This process of reverse cholesterol transport serves to regulate the cellular levels of cholesterol. ApoE acts as a ligand for delivery of the HDL-bound cholesterol to the liver, where it is excreted. Treatment of mouse peritoneal macrophages with acetyl-LDL stimulates in a 24-fold increase in the production of apoE, whereas the same treatment only results in a 2-fold increase in apoE production in human monocytes (Basu et al., 1982). Along with this reduction in apoE synthesis, human monocytes also secrete less apoE than mouse macrophages. ApoE constitutes approximately 1-2% of secreted protein in human monocytes, compared to approximately 4-5% in the mouse peritoneal macrophage (Basu et al., 1982). The marked reduction in the synthesis and secretion of apoE in human cells compared to mouse cells could explain the difference in MHP36 integration. Chapter 4 demonstrated the critical role of apoE on promoting MHP36 survival and migration, and directing the stem cells towards a neuronal phenotype. The *in vitro* studies suggest that apoE synthesis in mouse cells can be as much as 1100 % that of synthesis in human cells. This also manifests in the actual secretion of apoE, which is increased by at least 100 % in mouse cells as compared to human. Taken together, these data suggest that the lack of human apoE mediated effect on MHP36 integration may simply be due to insufficient levels of apoE in the human transgenic mice. This hypothesis could be investigated through exogenous delivery of human apoE to *APOE*-KO mice after an episode of global ischaemia and transplantation of stem cells. Infusion of apoE has been shown to ameliorate neurological deficits and exert a neuroprotective influence (Masliah et al., 1997, Horsburgh et al., 2000).

In retrospect, it is unfortunate that a wildtype C57Bl/6J control group was not included in this study. This would have allowed for replication and verification of the results from the previous study regarding WT and *APOE*-KO mice. Also, it would

have been interesting to observe any differences between the human *APOE* transgenic and WT mice. However, the general consensus from the literature outlined above strongly suggests that *APOE*-KO mice are minimally impaired in motor function, so any further insight from incorporating a WT group may have been limited. With the addition of the rotarod test for investigation of the functional integration of MHP36 grafts, it would also have been advantageous if a control group for ischaemia had been included, in order to determine the extent of ischaemia induced motor impairment. Future work could incorporate these experimental groups in order to ascertain the differences between mouse and human apoE.

5.5.6 Summary

In summary, there was no isoform specific effect (*APOE*-ε3 or ε4) on MHP36 neural stem cell migration, differentiation and motor recovery. The only exception was improved and robust MHP36 survival in the caudate nucleus of *APOE*-ε3 mice. However, for all the other endpoints, there was no discernable difference between *APOE*-KO mice and human *APOE* expressing transgenic mice. The previous study demonstrated a clear improvement in MHP36 survival, migration and differentiation in *APOE*-expressing wildtype C57Bl/6J mice compared to *APOE*-KO mice. Therefore, it was hypothesized that the *APOE*-ε3 and ε4 mice would exhibit a similar improvement in this study. The differences between mouse and human apoE and their interaction with the murine MHP36 cells may explain these somewhat contradictory findings. Further studies should investigate how species specific differences affect the influence of apoE on stem cells.

Chapter 6
General Discussion

There has been considerable investigation into the benefits of neural replacement therapy for neurological disorders. This thesis has extended on previous work by illustrating the therapeutic effects of neural stem cell grafts in a diffuse model of brain injury in the mouse, and provided initial evidence that the lipid transport protein, apoE, significantly influences the survival, migration and differentiation of grafted neural stem cells in host brain.

6.1 Summary of Thesis

Previous work illustrating the therapeutic potential of the MHP36 stem cell line utilised a variety of animal models of brain injury. In the rat, these include the 4-VO model of global ischaemia (Sinden et al., 1997), the MCAo model of focal ischaemia (Veizovic et al., 2001, Modo et al., 2002), lesion of the cholinergic system similar to that observed in Alzheimer's disease (Grigoryan et al., 2000) and age associated deficits (Hodges et al., 2000). In a promising step for future clinical applications, MHP36 grafts demonstrated functional reconstruction of the lesioned CA1 hippocampus in primates (Virley et al., 1999). However, there have been no studies into mouse models of brain injury with the MHP36 stem cell line. Overall, a search of the literature reveals comparatively few studies investigating neural stem cell transplantation as a therapy in mouse models of brain damage. Translating neural transplantation research to mouse models opens up the possibility of utilising transgenic mice in order to investigate genetic factors which may influence stem cell grafts. In this thesis I utilised various strains of *APOE* transgenic mice, specifically a knockout strain (*APOE*-KO) and strains expressing the human isoforms of apoE (*APOE*-ε3 and *APOE*-ε4).

However, due to the lack of neural transplantation research conducted with mouse models of brain damage, it was initially necessary to characterise MHP36 stem cell graft integration prior to conducting studies in transgenic mice. The model of brain damage used for all experimental studies in this thesis was the BCCAo model of global ischaemia. This model induces diffuse neuronal damage in the regions of the striatum and the hippocampus. MHP36 stem cells unilaterally transplanted into the striatum of C57Bl/6J mice subjected to 17 minutes global ischaemia survived up to 4

weeks post-transplantation. Further investigation into the characteristics of the transplanted MHP36 cells revealed that they migrated away from the injected area towards the regions of damage. The extent of ischaemic neuronal damage was reduced in MHP36 grafted mice compared to vehicle grafted mice, suggesting that the therapeutic properties of MHP36 stem cells can be translated to mouse models of brain damage. This reduction in neuronal damage was associated with neuronal differentiation of approximately half of all MHP36 cells. Importantly, the MHP36 grafts did not elicit a major, chronic inflammatory response as assessed by astrocytic and microglial reactivity. Immunosuppression with CsA did not affect the survival and migration of MHP36 stem cells or the degree of the inflammatory response. This study demonstrated successful transplantation and integration of MHP36 grafts into ischaemic mouse brain, and validated the therapeutic potential of MHP36 grafts.

The subsequent study extended on the initial characterisation results by incorporating *APOE*-KO mice in order to investigate the role of apoE on MHP36 stem cell survival migration and differentiation. C57Bl/6J mice with endogenous mouse apoE were compared to *APOE*-KO mice. Endogenous mouse apoE significantly improved MHP36 stem cell survival and migration in both the striatum and hippocampus. The percentage of MHP36 cells differentiating into a neuronal phenotype was also markedly increased in mice containing apoE. ApoE also promoted astrocytic differentiation of MHP36 cells in the striatum, but not in the hippocampus. Endogenous apoE influenced the ability of MHP36 cells to reduce the extent of ischaemic neuronal damage. Protein analysis on these mice revealed selective alterations in JNK cell signalling but not ERK signalling in *APOE*-KO mice but not C57Bl/6J mice, suggesting that the JNK pathway may be responsible for apoE mediated effects on MHP36 stem cell integration.

With the evidence that endogenous mouse apoE plays a critical role in MHP36 stem cell integration, the final study sought to identify whether human *APOE* genotype influenced MHP36 stem cell grafts. It has been well established that human *APOE* genotype can markedly influence outcome after brain injury, with possession of the *APOE*-ε4 allele linked to an unfavourable outcome. As the goal for neural

transplantation research is translation to the clinic, it is imperative to investigate human genetic factors which could affect patient outcome. *APOE* genotype is also a factor that can be controlled prior to clinical trials. Therefore, this study used transgenic mice expressing the human ε3 or ε4 isoforms on an *APOE*-KO background. The presence of human *APOE*-ε3 significantly improved MHP36 graft survival compared to human *APOE*-ε4. However, no human *APOE* genotype effect was observed on MHP36 graft migration. There was a trend towards increased neuronal and astrocytic differentiation in mice expressing human *APOE*-ε3. Functional assessment of motor balance and coordination of these mice did not reveal any human *APOE* genotype influence. These results suggest that human apoE has a minimal effect on MHP36 stem cell integration.

The data presented in this thesis support the initial hypothesis that apoE plays important roles in MHP36 stem cell integration as measured by survival, migration and differentiation. However, there was minimal evidence that this effect of apoE was dependent on human *APOE* genotype.

6.2 Host Mechanisms for Directing Neural Stem Cells

The finding that apoE significantly influences neural stem cell survival, migration and differentiation is a key step in elucidating the various mechanisms by which transplanted stem cells are able to exert a therapeutic influence. Few studies of neural transplantation therapy have investigated the actual mechanisms which affect stem cell integration. The data in this thesis demonstrates that transplanted stem cells interact with factors in host brain, and this interaction may be responsible for mediating the subsequent action of the grafted cell.

Further work on the role of apoE will revolve around how apoE exerts the ability to modulate stem cell integration. The myriad functions of apoE (lipid transport, modulation of excitotoxicity, anti-oxidation, and cytoskeletal support, described in section 1.7.4) have all been implicated as potential pathways for aiding stem cell survival, migration and differentiation. Whilst *in vivo* studies provide invaluable information on whole system interactions and physiologically relevant data, it may

be more useful to move to *in vitro* studies to focus on possible mechanism by which apoE interacts with stem cells. For example, Soulié et al., (1999) provided the initial evidence that apoE influences neuronal differentiation in SH-SY 5Y cells. It will also be relevant to discover why endogenous mouse apoE markedly influences MHP36 neural stem cells integration, but human apoE failed to do the same. Again, *in vitro* studies may be more useful, as data from the literature suggests that synthesis and secretion of apoE in mouse cells is markedly higher than in human cells (Basu et al., 1982, 1982), raising the possibility that a certain level of apoE is required in order to influence grafted stem cells. Clearly, the species aspect raises the possibility that we may require the use human stem cells in order to observe any beneficial effect of human apoE.

As described in Section 4.5.6, apoE may also interact with the Wnt signalling pathway through the LRP5/6 receptors (Kim et al., 1998). This is of interest as the canonical Wnt / β-catenin pathway has recently been investigated for its role in regulating neuronal differentiation. Wnt has been shown to promote neuronal differentiation of neurospheres (Muroyama et al., 2004), embryonic stem cells (Haegele et al., 2003, Otero et al., 2004), cortical neural precursor cells (Hirabayashi et al., 2004) and in dopaminergic precursors (Castelo-Branco et al., 2003, Castelo-Branco and Arenas, 2006).

Recently, a number of studies have identified another endogenous protein which may influence neural stem cell migration and proliferation, namely stromal cell derived factor-1 (SDF-1), one of the members of the chemotactic cytokine family. SDF-1 is an inflammatory cytokine which is upregulated by astrocytes and the local endothelium following injury (Zhou et al., 2002, Rubin et al., 2003). SDF-1 has only one cognate receptor, chemokine (C-X-C motif) receptor 4 (CXCR4). Interestingly, NSCs have been demonstrated to express CXCR4 (Tran et al., 2004), suggesting that the SDF-1 – CXCR4 pathway may be involved in targeting of stem cell movement. The importance of the interaction between SDF-1 and CXCR4 to homing and development has been demonstrated in haemotopoietic stem cells (Peled et al., 1999, Ponomaryov et al., 2000, Tavor et al., 2004). Recently, the SDF-1 – CXCR4

pathway has been implicated in directed migration of transplanted NSCs to the site of damage after cerebral hypoxic-ischaemic injury and focal ischaemia (Imitola et al., 2004, Robin et al., 2006). This pathway also regulates the migration of neural progenitors during development in the mouse embryo (Belmadani et al., 2005). As well as influencing migration, the SDF1-CXCR4 pathway has also lately been postulated to promote neural stem cell proliferation (Guo et al., 2005, Gong et al., 2006).

Another endogenous protein strongly implicated in regulation of stem cell survival is Notch, a cell membrane protein involved in determining cell fate during development (Lewis, 1998). Recently, the Notch signalling pathway has been linked with the maintenance of stem cell survival (Hitoshi et al., 2002, Oishi et al., 2004, Alexson et al., 2006). In the absence of Notch, apoptosis of neural progenitor cells and differentiating neurons is increased during development of the nervous system (Mason et al., 2006). Conversely, administration of Notch ligands and activation of the Notch signalling pathway promotes neural stem cell survival and increases the rate of neurogenesis after an ischaemic injury (Androutsellis-Theotokis et al., 2006).

These studies have provided initial information on the various host mechanisms which can influence stem cell survival (Notch), migration (SDF-1) and differentiation (Wnt). Additionally, data in this thesis has implicated apoE in assisting these functions. Further investigation is required into the interactions between apoE and these respective signalling proteins. Despite the fact that the mechanisms of neural stem cell transplant therapy remain to be completely elucidated, the eventual aim for neural transplantation therapy is translation to the clinic. Encouraging reports from proof-of-principle animal studies have led to a number of Phase I and II clinical trials. These have focused on three diseases, Parkinson's disease, Huntington's disease and ischaemic stroke.

6.3 Clinical Trials of Neural Transplantation

6.3.1 Parkinson's disease

Parkinson's disease was one of the initial neurological disorders targeted for neural replacement therapy. This is due to the unique pathology associated with the disorder, namely the selective loss of melanin-pigmented neurons in the substantia nigra, leading to a deficiency of dopamine in the striatum. Dopamine replacement through administration of the amino acid precursor L-DOPA provides symptomatic relief for Parkinson's disease patients, but the effective duration of this therapy is limited. However, this demonstration strongly suggested that replacement of the damaged dopaminergic neurons is a viable therapy for long-term treatment. Since 1987, approximately 350 patients with Parkinson's disease have received transplants of foetal dopaminergic neurons (Bjorklund, 2005). These studies were all open-label trials designed for safety and efficacy. Overall data from these trials demonstrate that these foetal neurons are able to survive and functionally integrate into Parkinson's disease brain. These grafts typically reduce motor scores on the Unified Parkinson Disease Rating Scale (UPDRS) by 30-50%, and this is linked with increased dopamine synthesis and retention as visualised by fluorodopa PET scanning in the grafted regions. Promisingly, the grafts appear to provide long-lasting symptomatic improvement in the majority of grafted patients, with graft-induced recovery of function maintained for up to 10 years in a number of patients. Based on these encouraging results, in 1993 the NIH supported the setup of two placebo-controlled double blind trials of foetal dopaminergic tissue for patients afflicted with advanced Parkinson's disease. The first of these studies to be published was the Denver/Columbia study (Freed et al., 2001). A total of 20 patients received grafts and no immunosuppression was provided. Overall, the grafted patients did not show a significant improvement in scores on the UPDRS compared to sham grafted patients, although this appeared to be related to age, as grafts did elicit a marked improvement in patients younger than 60 years of age. Five of the grafted patients displayed recurrence of dystonias and dyskinesias. However, patients in this study received less foetal tissue than in the open-label trials. Two grafted patients died of unrelated issues during the follow-up period. Autopsy analysis revealed that the numbers of dopaminergic neurons in the putamen ranged from 7000 to 40,000 (Freed

et al., 2001). This is in stark contrast to overall numbers from the open-label trials, which ranged from 80,000 to 135,000 (Kordower et al., 1995), clearly demonstrating that functional efficacy is related to the number of functioning dopaminergic neurons.

The second double-blind clinical trial was conducted in Tampa/Mount Sinai (Olanow et al., 2003). 23 patients received foetal tissue grafts from one or four donors and were monitored for 2 years. Patients received CsA immunosuppression for a period of 6 months. However, there was no difference between grafted and sham patients in UPDRS scores after the 24 months. The patients who did receive tissue from four donors did show marked improvement in their UPDRS scores up to six months after surgery but this deteriorated over the following months back to pre-operative readings. Whilst PET scanning revealed an increase in fluorodopa uptake in the grafted patients, approximately half of all grafted patients developed dyskinesias.

The overall results from these double-blind trials were not as promising as hoped. Interestingly, both trials showed a short-term improvement in UPDRS score (up to 6 months post surgery), although improvement plateaued at this time point in Denver/Columbia trial and began to deteriorate in the Tampa/Mount Sinai trial. In contrast, patients in the open-label trials continued to show improvement between 6 to 12 months after surgery and in some exceptional cases this extended into the subsequent year. As described previously, this difference may be attributable to the volume of tissue transplanted. However, another major difference between the trials was the use of immunosuppression. In the promising open-label trials, a high-dose triple immunosuppression regimen was used for at least 12 months (Wenning et al., 1997), compared to a 6 month low-dose CsA regimen in Tampa/Mount Sinai and an absence of immunosuppression in Denver/Columbia. It is eminently possible that the lack of significant functional improvement in the double-blind trials was due to a delayed immunogenic response to graft tissue and failure to properly integrate. Although this thesis has argued that CsA immunosuppression does not significantly influence the effects of grafted MHP36 stem cells, it is important to note the difference between a well-established and characterised stem cell line as compared to

allogeneic primary human tissue. The acute inflammatory response that may be induced from allogeneic grafts may be controlled with immunosuppression but in some cases, the response is merely delayed rather than diminished. In this delayed state, transplanted dopamine neurons are unable to survive and function optimally (Hudson et al., 1994, Shinoda et al., 1995), and there is every risk of the inflammatory response flaring up once immunosuppression is halted. The choice of patient selection also influences graft efficacy, as observed in the Denver/Columbia trial in the case of patient age. Despite the less than encouraging results from the two completed double-blind trials, it is promising to note that there were minimal complications associated with the procedure and no adverse effects of the graft were reported. Most of the problems associated with the trials have been linked to technical aspects of study design.

6.3.2 Huntington's disease

Five patients with Huntington's disease received bilateral transplantation of foetal striatal tissue. During the initial follow-up, conducted two years after surgery, three out of the five patients displayed improvements in motor and cognitive function compared to a reference group of untreated patients (Bachoud-Levi et al., 2000). These three patients also showed increased metabolic activity in the striatum and cortex during MRI and PET scanning, suggesting that the clinical improvement was due to functional graft effects (Gaura et al., 2004). Recently, a long term follow-up study 6 years after surgery was reported (Bachoud-Levi et al., 2006). The two patients who did not show any clinical improvement during the initial assessment 2 years after surgery continued to decline over the 6 year period. For the other three patients, the striking recovery in striatal and cortical regions observed at 2 years post surgery persisted over time. Their performance on cognitive tasks remained stable on non-timed tests, but progression of motor disability was demonstrated by deterioration on timed tasks. However, at this time point, the underlying progression of the disease is beginning to countermand the therapeutic effect of the grafts. Metabolic function deteriorated in non-grafted regions of the brain, suggesting that the foetal grafts have not been able to halt the disease, but merely impede the rate of progression. Nevertheless, the clinical improvement observed by the three patients

was also reflected in an improvement in their quality of life, with the patients regaining the ability to perform activities that they had lost before, such as cycling, work and playing a musical instrument. This is a clear demonstration of the potential offered through regenerative therapies, as this is the first treatment to induce prolonged benefit over the range of symptoms associated with Huntington's disease. Currently, a larger, multicentre Phase II trial in France is recruiting patients.

6.3.2 Stroke

Cell replacement trials for ischaemic stroke have used LBS neurons (Layton Bioscience Inc.) derived from the NT2 teratocarcinoma cell line (Chapter 1). The initial Phase I trial was an open study designed to test safety. Twelve patients with basal ganglia strokes of 6 months duration and static neurological deficits received stereotactic injections of either 2 million or 6 million LBS cells (Kondziolka et al., 2000). The patients received comprehensive follow-up monitoring with MRI and PET scans, and assessment on the National Institutes of Health Stroke Scale (NIHSS), European Stroke Scale (ESS) and Barthel Index (BI). No patient suffered from adverse effects attributed to the transplantation procedure, although there were side effects associated with immunosuppression. There was an overall improvement in the ESS, particularly in motor function, which correlated with increased metabolic activity on PET (Meltzer et al., 2001). A post-mortem examination of a patient who had not shown any clinical improvement upon assessment and died of an unrelated cause 2 years after surgery revealed neuronal phenotypes within the region of implantation without evidence of plasticity or integration. Importantly, there was no indication of safety issues associated with the stem cells (Nelson et al., 2002).

Based on the promising results from the Phase I trial, a Phase II trial was initiated. The format for this study was a randomized, open-label trial with blinded neurological evaluation (Kondziolka et al., 2005). However, this trial was open to patients with intracerebral hemorrhage as well as basal ganglia stroke. The first group of patients were randomized to transplantation of 5 million LBS cells in conjunction with rehabilitation versus rehabilitation alone. The second group of patients followed the same protocol, except transplant patients received 10 million

cells. From a safety standpoint, there were minimal complications associated with the surgical procedure, and no adverse neurological events were observed after surgery during the period of ongoing assessment. However, there was less evidence of efficacy in the Phase II trial. The transplant group did improve in ESS compared to the control group, but this was not statistically significant. The memory scores of transplanted patients were statistically improved compared to controls and pre-transplant baseline scores. Overall, the encouraging results and absence of severe side effects have merited a Phase IIb trial, designed to study efficacy (Kondziolka et al., 2005).

6.4 Future Directions

While a number of clinical trials have been conducted, with promising results in safety and efficacy, there is still plenty of basic science required prior to widespread clinical use of neural stem cell transplantation. As described previously, it will be essential to obtain further knowledge of the mechanisms by which grafted stem cells integrate with host tissue. However, there are a number of other issues which require investigation prior to widespread clinical adoption of neural transplantation.

It remains to be seen whether there is a universal stem cell which can be used for the majority of neural disorders, or whether specialised stem cells would be required for particular disorders. As described previously, Parkinson's disease is characterised by a specific loss of dopaminergic neurons, therefore transplantation therapies have centred on the use of partially differentiated dopaminergic stem cell progenitors or embryonic dopamine neurons (Bjorklund et al., 2003). In contrast, the cell types afflicted and the pattern of damage in stroke, Alzheimer's disease, ageing and traumatic brain injury is markedly more diffuse and widespread. In these cases, it would be more suitable to use a more naïve cell with multi- or pluripotent capability which can differentiate into all the cell types which may be lost in these disorders.

The type of neurological disorder also influences other factors which require further research. In disorders such as stroke and traumatic brain injury, the acute onset of damage creates a hostile brain environment which can be detrimental to stem cell

survival and subsequent migration and differentiation. It may be more advantageous in these cases to wait until the full extent of damage has been reached and utilise the regenerative capability offered by stem cell transplantation. However, the hostile environment causes an upregulation in inflammatory events. This inflammation can be detrimental for endogenous neurogenesis in the dentate gyrus (Ekdahl et al., 2003), but can also be beneficial for directing stem cell migration, such as in the example of SDF-1 directed migration (Imitola et al., 2004, Robin et al., 2006). It is therefore necessary to find the correct time window for transplantation in order to achieve optimal recovery. However, in the case of more chronic neurological disorders such as Huntington's, Parkinson's and Alzheimer's disease, neurological function decreases over a period of years. In some of these cases, it may take a few years before the disease can be clinically diagnosed. While this provides a large therapeutic window for transplantation, the progressive nature of these diseases means that therapeutic intervention has to take place prior to extensive cell loss.

The region of damage also affects the site of grafting. Some disorders display a highly specific region of damage. The particular deinnervation of the striatum in Parkinson's and Huntington's disease provides a specific target for transplantation. A study using focal ischaemia as a model of damage has demonstrated that transplanting stem cells into the extensively lesioned infarct markedly hinders stem cell survival, due to the pathological environment and the lack of trophic support (Kelly et al., 2004). It is generally accepted that transplanting into the intact hemisphere raises the likelihood of stem cell survival and allows for migration to the region of damage. However, the more diffuse lesions present in Alzheimer's disease and global ischaemia raise the issue of picking a suitable site for grafting.

Some of these technical issues may be overcome by advances in brain imaging. Whilst immunohistochemistry and microscopic visualisation allow for high-resolution imaging of stem cell grafts, this is only feasible in animal studies. It also represents a permanent endpoint. This could be carried out to a degree in human patients through the use of neural biopsy tissue, but is impractical for widespread use. Non-invasive imaging techniques are therefore preferential for long-term

monitoring of transplanted stem cells. Current molecular imaging techniques in use include PET scanning and MRI (Kirik et al., 2005). While the main use for these imaging techniques to date has been in observing the progression of neurological damage (e.g. dopaminergic system activity in Parkinson's disease, Kordower et al., 1995), recent approaches have used PET and MRI to visualise neural cell grafts *in vivo* (Franklin et al., 1999, Kondziolka et al., 2000, Roberts et al., 2006), allowing for longitudinal monitoring of grafts in patients.

Further work is also needed on the role of immunosuppression in stem cell transplantation therapy. Evidence from the literature is currently contradictory, with some studies suggesting that stem cell have a low immunogenic potential and therefore do not require immunosuppression (Modo et al., 2002, Weiss et al., 2003, Wennersten et al., 2006), which was also the finding from this thesis. However, other studies suggest that a comprehensive immune suppression regimen is required for optimal stem cell graft transplantation (Pedersen et al., 1995, 1997, Yan et al., 2006, Al Nimer et al., 2004). This discrepancy could be accounted for by differences in the transplant tissue. The extent of efficacy observed during the clinical trials of neural transplantation for Parkinson's disease have been linked to the immunosuppressive regime used (Bjorklund, 2005).

This thesis also successfully demonstrated the use of transgenic mice in the application of neural transplantation therapy. Whilst the *APOE* transgenic strains used in this thesis illustrated the influence of an endogenous genetic factor on stem cell integration, transgenic mice can be used for other investigations. Transgenic mouse models of disease can be used to investigate the potential of neural replacement therapy for a variety of conditions. For example, the Jackson Laboratory has transgenic mouse models of Alzheimer's disease, amyotrophic lateral sclerosis, epilepsy, Huntington's disease and Parkinson's disease. Transgenic mice can also be used to investigate the signalling pathways which might influence stem cell integration. In Chapter 4, the JNK signalling pathway was implicated in survival of MHP36 stem cells. The use of JNK-deficient mice would provide further information on the role of this signalling protein. Transgenic mice have also been refined for

inducible control of gene expression and region specific gene expression, both of which provide an extra regulatory step for investigating gene function.

6.5 Conclusion

The data presented in this thesis demonstrate that endogenous apoE strongly influences MHP36 graft survival, migration and differentiation. Although there was minimal evidence that human *APOE* genotype influences cell migration and differentiation, stem cell survival was markedly improved in a human *APOE*-ε3 allelic environment, which may affect the effectiveness of stem cells in *APOE*-ε4 individuals.

References

Abdulla, F.A., Abu-Bakra, M.A., Calaminici, M.R., Stephenson, J.D., Sinden, J.D. (1995). Importance of forebrain cholinergic and GABAergic systems to the age-related deficits in water maze performance of rats. *Neurobiol Aging.* **16(1)**, 41-52.

Abe, K., Aoki, M., Kawagoe, J., Yoshida, T., Hattori, A., Kogure, K., Itoyama, Y. (1995). Ischemic delayed neuronal death. A mitochondrial hypothesis. *Stroke*. **26(8)**, 1478-89.

Abusaad, I., MacKay, D., Zhao, J., Stanford, P., Collier, D.A., Everall, I.P. (1999). Stereological estimation of the total number of neurons in the murine hippocampus using the optical disector. *J Comp Neurol.* **408(4)**, 560-6.

Aggerbeck, L.P., Wetterau, J.R., Weisgraber, K.H., Wu, C.S., Lindgren, F.T. (1988). Human apolipoprotein E3 in aqueous solution. II. Properties of the amino- and carboxyl-terminal domains. *J Biol Chem.* **263(13)**, 6249-58.

Al Nimer, F., Wennersten, A., Holmin, S., Meijer, X., Wahlberg, L., Mathiesen, T. (2004). MHC expression after human neural stem cell transplantation to brain contused rats. *Neuroreport.* **15(12)**, 1871-5.

Alberts, M.J., Graffagnino, C., McClenny, C., DeLong, D., Strittmatter, W., Saunders, A.M., Roses, A.D. (1995). ApoE genotype and survival from intracerebral haemorrhage. *Lancet.* **346(8974)**, 575.

Alexson, T.O., Hitoshi, S., Coles, B.L., Bernstein, A., van der Kooy, D. (2006). Notch signaling is required to maintain all neural stem cell populations--irrespective of spatial or temporal niche. *Dev Neurosci.* **28(1-2)**, 34-48.

Ali, S.M., Dunn, E., Oostveen, J.A., Hall, E.D., Carter, D.B. (1996). Induction of apolipoprotein E mRNA in the hippocampus of the gerbil after transient global ischemia. *Brain Res Mol Brain Res.* **38(1)**, 37-44.

Altman, J. (1963). Autoradiographic investigation of cell proliferation in the brains of rats and cats. *Anat Rec.* **145**, 573-91.

Altman, J. (1969). Autoradiographic and histological studies of postnatal neurogenesis. IV. Cell proliferation and migration in the anterior forebrain, with special reference to persisting neurogenesis in the olfactory bulb. *J Comp Neurol.* **137(4)**, 433-57.

Alzheimer, A. (1907). Über eine eigenartige Erkrankung der Hirnrinde. *Allg. Zeitschr. Psychiat. Psych.-Gericht. Med.* **64**, 146-8.

Anderson, R., Barnes, J.C., Bliss, T.V., Cain, D.P., Cambon, K., Davies, H.A., Errington, M.L., Fellows, L.A., Gray, R.A., Hoh, T., Stewart, M., Large, C.H.,

Higgins, G.A. (1998). Behavioural, physiological and morphological analysis of a line of apolipoprotein E knockout mouse. *Neuroscience.* **85(1)**, 93-110.

Andrews, P.W., Damjanov, I., Simon, D., Banting, G.S., Carlin, C., Dracopoli, N.C., Fogh, J. (1984). Pluripotent embryonal carcinoma clones derived from the human teratocarcinoma cell line Tera-2. Differentiation in vivo and in vitro. *Lab Invest.* **50(2)**, 147-62.

Androutsellis-Theotokis, A., Leker, R.R., Soldner, F., Hoeppner, D.J., Ravin, R., Poser, S.W., Rueger, M.A., Bae, S.K., Kittappa, R., McKay, R.D. (2006). Notch signalling regulates stem cell numbers in vitro and in vivo. *Nature.* **442(7104)**, 823-6.

Andsberg, G., Kokaia, Z., Bjorklund, A., Lindvall, O., Martinez-Serrano, A. Amelioration of ischaemia-induced neuronal death in the rat striatum by NGF-secreting neural stem cells. *Eur J Neurosci.* **10(6)**, 2026-36.

Aono, M., Bennett, E.R., Kim, K.S., Lynch, J.R., Myers, J., Pearlstein, R.D., Warner, D.S., Laskowitz, D.T. (2003). Protective effect of apolipoprotein E-mimetic peptides on N-methyl-D-aspartate excitotoxicity in primary rat neuronal-glial cell cultures. *Neuroscience.* **116(2)**, 437-45.

Aono, M., Lee, Y., Grant, E.R., Zivin, R.A., Pearlstein, R.D., Warner, D.S., Bennett, E.R., Laskowitz, D.T. (2002). Apolipoprotein E protects against NMDA excitotoxicity. *Neurobiol Dis.* **11(1)**, 214-20.

Ariza, M., Pueyo, R., Matarin, M.D., Junque, C., Mataro, M., Clemente, I., Moral, P., Poca, M.A., Garnacho, A., Sahuquillo, J. (2006). Influence of APOE polymorphism on cognitive and behavioural outcome in moderate and severe traumatic brain injury. *J Neurol Neurosurg Psychiatry.* **77(10)**, 1191-3.

Arnhold, S., Klein, H., Semkova, I., Addicks, K., Schraermeyer, U. (2004). Neurally selected embryonic stem cells induce tumor formation after long-term survival following engraftment into the subretinal space. *Invest Ophthalmol Vis Sci.* **45(12)**, 4251-5.

Arvidsson, A., Collin, T., Kirik, D., Kokaia, Z., Lindvall, O. (2002). Neuronal replacement from endogenous precursors in the adult brain after stroke. *Nat Med.* **8(9)**, 963-70.

Asahi, M., Hoshimaru, M., Uemura, Y., Tokime, T., Kojima, M., Ohtsuka, T., Matsuura, N., Aoki, T., Shibahara, K., Kikuchi, H. (1997). Expression of interleukin-1 beta converting enzyme gene family and bcl-2 gene family in the rat brain following permanent occlusion of the middle cerebral artery. *J Cereb Blood Flow Metab.* **17(1)**, 11-8.

Auer, R.N. & Sutherland, G.R. (2002). Hypoxic brain damage, in *Greenfield's Neuropathology, 7th ed.* (Graham, D.I. & Lantos, P.L.). Hodder Arnold.

Bachoud-Levi, A.C., Gaura, V., Brugieres, P., Lefaucheur, J.P., Boisse, M.F., Maison, P., Baudic, S., Ribeiro, M.J., Bourdet, C., Remy, P., Cesaro, P., Hantraye, P., Peschanski, M. (2006). Effect of fetal neural transplants in patients with Huntington's disease 6 years after surgery, a long-term follow-up study. *Lancet Neurol.* **5(4)**, 303-9.

Bachoud-Levi, A.C., Remy, P., Nguyen, J.P., Brugieres, P., Lefaucheur, J.P., Bourdet, C., Baudic, S., Gaura, V., Maison, P., Haddad, B., Boisse, M.F., Grandmougin, T., Jeny, R., Bartolomeo, P., Dalla Barba, G., Degos, J.D., Lisovoski, F., Ergis, A.M., Pailhous, E., Cesaro, P., Hantraye, P., Peschanski, M. (2000). Motor and cognitive improvements in patients with Huntington's disease after neural transplantation. *Lancet.* **356(9246)**, 1975-9.

Bacskai, B.J., Xia, M.Q., Strickland, D.K., Rebeck, G.W., Hyman, B.T. (2000). The endocytic receptor protein LRP also mediates neuronal calcium signaling via N-methyl-D-aspartate receptors. *Proc Natl Acad Sci USA.* **97(21)**, 11551-6.

Baker, K.A., Hong, M., Sadi, D., Mendez, I. (2000). Intrastriatal and intranigral grafting of hNT neurons in the 6-OHDA rat model of Parkinson's disease. *Exp Neurol.* **162(2)**, 350-60.

Bakshi, A., Shimizu, S., Keck, C.A., Cho, S., LeBold, D.G., Morales, D., Arenas, E., Snyder, E.Y., Watson, D.J., McIntosh, T.K. (2006). Neural progenitor cells engineered to secrete GDNF show enhanced survival, neuronal differentiation and improve cognitive function following traumatic brain injury. *Eur J Neurosci.* **23(8)**, 2119-34.

Barbier, A., Clement-Collin, V., Dergunov, A.D., Visvikis, A., Siest, G., Aggerbeck, L.P. (2006). The structure of human apolipoprotein E2, E3 and E4 in solution 1. Tertiary and quaternary structure. *Biophys Chem.* **119(2)**, 158-69.

Barone, F.C., Arvin, B., White, R.F., Miller, A., Webb, C.L., Willette, R.N., Lysko, P.G., Feuerstein, G.Z. (1997). Tumor necrosis factor-α. A mediator of focal ischemic brain injury. *Stroke.* **28(6)**, 1233-44

Basu, S.K., Brown, M.S., Ho, Y.K., Havel, R.J., Goldstein, J.L. (1981). Mouse macrophages synthesize and secrete a protein resembling apolipoprotein E. *Proc Natl Acad Sci USA.* **78(12)**, 7545-9.

Basu, S.K., Ho, Y.K., Brown, M.S., Bilheimer, D.W., Anderson, R.G., Goldstein, J.L. (1982). Biochemical and genetic studies of the apoprotein E secreted by mouse macrophages and human monocytes. *J Biol Chem.* **257(16)**, 9788-95.

Basun, H., Corder, E.H., Guo, Z., Lannfelt, L., Corder, L.S., Manton, K.G., Winblad, B., Viitanen, M. (1996). Apolipoprotein E polymorphism and stroke in a population sample aged 75 years or more. *Stroke.* **27(8)**, 1310-5.

Beffert, U., Morfini, G., Bock, H.H., Reyna, H., Brady, S.T., Herz, J. (2002). Reelin-mediated signaling locally regulates protein kinase B/Akt and glycogen synthase kinase 3beta. *J Biol Chem.* **277(51)**, 49958-64.

Beffert, U., Weeber, E.J., Morfini, G., Ko, J., Brady, S.T., Tsai, L.H., Sweatt, J.D., Herz, J. (2004). Reelin and cyclin-dependent kinase 5-dependent signals cooperate in regulating neuronal migration and synaptic transmission. *J Neurosci.* **24(8)**, 1897-906.

Beffert, U., Weeber, E.J., Durudas, A., Qiu, S., Masiulis, I., Sweatt, J.D., Li, W.P., Adelmann, G., Frotscher, M., Hammer, R.E., Herz, J. (2005). Modulation of synaptic plasticity and memory by Reelin involves differential splicing of the lipoprotein receptor Apoer2. *Neuron.* **47(4)**, 567-79.

Belloni, E., Muenke, M., Roessler, E., Traverso, G., Siegel-Bartelt, J., Frumkin, A., Mitchell, H.F., Donis-Keller, H., Helms, C., Hing, A.V., Heng, H.H., Koop, B., Martindale, D., Rommens, J.M., Tsui, L.C., Scherer, S.W. (1996). Identification of Sonic hedgehog as a candidate gene responsible for holoprosencephaly. *Nat Genet.* **14(3)**, 353-6.

Bellosta, S., Nathan, B.P., Orth, M., Dong, L.M., Mahley, R.W., Pitas, R.E. (1995). Stable expression and secretion of apolipoproteins E3 and E4 in mouse neuroblastoma cells produces differential effects on neurite outgrowth. *J Biol Chem.* **270(45)**, 27063-71.

Belmadani, A., Tran, P.B., Ren, D., Assimacopoulos, S., Grove, E.A., Miller, R.J. (2005). The chemokine stromal cell-derived factor-1 regulates the migration of sensory neuron progenitors. *J Neurosci.* **25(16)**, 3995-4003.

Benzing, W.C., Mufson, E.J. (1995). Apolipoprotein E immunoreactivity within neurofibrillary tangles, relationship to Tau and PHF in Alzheimer's disease. *Exp Neurol.* **132(2)**, 162-71.

Bernabeu, R. & Sharp, F.R. (2000). NMDA and AMPA/kainate glutamate receptors modulate dentate neurogenesis and CA3 synapsin-I in normal and ischemic hippocampus. *J Cereb Blood Flow Metab.* **20(12)**, 1669-80.

Birmingham, K. (2002). Future of neuroprotective drugs in doubt. *Nat Med.* **8(1)**, 5.

Bjorklund, A., Dunnett, S.B., Brundin, P., Stoessl, A.J., Freed, C.R., Breeze, R.E., Levivier, M., Peschanski, M., Studer, L., Barker, R. (2003). Neural transplantation for the treatment of Parkinson's disease. *Lancet Neurol.* **2(7)**, 437-45.

Bjorklund, A. (2005). Cell therapy for Parkinson's disease, problems and prospects. *Novartis Found Symp.* **265**, 174-86

Bock, H.H., Jossin, Y., Liu, P., Forster, E., May, P., Goffinet, A.M., Herz, J. (2003). Phosphatidylinositol 3-kinase interacts with the adaptor protein Dab1 in response to

Reelin signaling and is required for normal cortical lamination. *J Biol Chem.* **278(40)**, 38772-9.

Borlongan, C.V., Tajima, Y., Trojanowski, J.Q., Lee, V.M., Sanberg, P.R. (1998). Transplantation of cryopreserved human embryonal carcinoma-derived neurons (NT2N cells) promotes functional recovery in ischemic rats. *Exp Neurol.* **149(2)**, 310-21.

Boschert, U., Merlo-Pich, E., Higgins, G., Roses, A.D., Catsicas, S. (1999). Apolipoprotein E expression by neurons surviving excitotoxic stress. *Neurobiol Dis.* **6(6)**, 508-14.

Boyles, J.K., Pitas, R.E., Wilson, E., Mahley, R.W., Taylor, J.M. (1985). Apolipoprotein E associated with astrocytic glia of the central nervous system and with nonmyelinating glia of the peripheral nervous system. *J Clin Invest.* **76(4)**, 1501-13.

Boyles, J.K., Zoellner, C.D., Anderson, L.J., Kosik, L.M., Pitas, R.E., Weisgraber, K.H., Hui, D.Y., Mahley, R.W., Gebicke-Haerter, P.J., Ignatius, M.J, et al. (1989). A role for apolipoprotein E, apolipoprotein A-I, and low density lipoprotein receptors in cholesterol transport during regeneration and remyelination of the rat sciatic nerve. *J Clin Invest.* **83(3)**, 1015-31.

Brecht, W.J., Harris, F.M., Chang, S., Tesseur, I., Yu, G.Q., Xu, Q., Dee Fish, J., Wyss-Coray, T., Buttini, M., Mucke, L., Mahley, R.W., Huang, Y. (2004). Neuron-specific apolipoprotein e4 proteolysis is associated with increased tau phosphorylation in brains of transgenic mice. *J Neurosci.* **24(10)**, 2527-34.

Brown, M.S., Goldstein, J.L. (1986). A receptor-mediated pathway for cholesterol homeostasis. *Science.* **232(4746)**, 34-47.

Buckner, C.D., Epstein, R.B., Rudolph, R.H., Clift, R.A., Storb, R., Thomas, E.D. (1970). Allogeneic marrow engraftment following whole body irradiation in a patient with leukemia. *Blood.* **35(6)**, 741-50.

Burd, G.D. & Nottebohm, F. (1985). Ultrastructural characterization of synaptic terminals formed on newly generated neurons in a song control nucleus of the adult canary forebrain. *J Comp Neurol.* **240(2)**, 143-52.

Buttery, L.D., Bourne, S., Xynos, J.D., Wood, H., Hughes, F.J., Hughes, S.P., Episkopou, V., Polak, J.M. (2001). Differentiation of osteoblasts and in vitro bone formation from murine embryonic stem cells. *Tissue Eng.* **7(1)**, 89-99.

Buttini, M., Orth, M., Bellosta, S., Akeefe, H., Pitas, R.E., Wyss-Coray, T., Mucke, L., Mahley, R.W. (1999). Expression of human apolipoprotein E3 or E4 in the brains of Apoe-/- mice, isoform-specific effects on neurodegeneration. *J Neurosci.* **19(12)**, 4867-80.

Callis, G. (2004). Preparation and snap freezing of murine tissues for research immunohistochemistry and routine hematoxylin and eosin staining. *Sakura Histologic.* 37(1), 4-7.

Callis, G. (2004). Cryomicrotomy of murine tissues for research immunohistochemistry and routine hematoxylin and eosin staining. Part II. *Sakura Histologic.* 37(2), 9-13.

Caruso, A., Motolese, M., Iacovelli, L., Caraci, F., Copani, A., Nicoletti, F., Terstappen, G.C., Gaviraghi, G., Caricasole, A. (2006). Inhibition of the canonical Wnt signaling pathway by apolipoprotein E4 in PC12 cells. *J Neurochem.* **98(2)**, 364-71.

Castelo-Branco, G., Wagner, J., Rodriguez, F.J., Kele, J., Sousa, K., Rawal, N., Pasolli, H.A., Fuchs, E., Kitajewski, J., Arenas, E. (2003). Differential regulation of midbrain dopaminergic neuron development by Wnt-1, Wnt-3a, and Wnt-5a. *Proc Natl Acad Sci USA.* **100(22)**, 12747-52.

Castelo-Branco, G., Arenas, E. (2006). Function of Wnts in dopaminergic neuron development. *Neurodegener Dis.* **3(1-2)**, 5-11.

Catto, A.J., McCormack, L.J., Mansfield, M.W., Carter, A.M., Bamford, J.M., Robinson, P., Grant, P.J. (2000). Apolipoprotein E polymorphism in cerebrovascular disease. *Acta Neurol Scand.* **101(6)**, 399-404.

Champagne, D., Rochford, J., Poirier, J. (2005). Effect of apolipoprotein E deficiency on reactive sprouting in the dentate gyrus of the hippocampus following entorhinal cortex lesion, role of the astroglial response. *Exp Neurol.* **194(1)**, 31-42.

Chen, H.H., Liu, H.M. (1996). A new fluorescent histological marker for ischemic neurons, EA 50, correlated with Fos and Jun/AP-1 immunoreactivity. *Histochem Cell Biol.* **105(5)**, 375-82.

Chen, J., Graham, S.H., Nakayama, M., Zhu, R.L., Jin, K., Stetler, R.A., Simon, R.P. (1997). Apoptosis repressor genes Bcl-2 and Bcl-x-long are expressed in the rat brain following global ischemia. *J Cereb Blood Flow Metab.* **17(1)**, 2-10.

Chen, J., Li, Y., Wang, L., Lu, M., Zhang, X., Chopp, M. (2001). Therapeutic benefit of intracerebral transplantation of bone marrow stromal cells after cerebral ischemia in rats. *J Neurol Sci.* **189(1-2)**, 49-57.

Chen, J., Bernreuther, C., Dihne, M., Schachner, M. (2005). Cell adhesion molecule L1-transfected embryonic stem cells with enhanced survival support regrowth of corticospinal tract axons in mice after spinal cord injury. *J Neurotrauma.* **22(8)**, 896-906.

Chen, Y., Lomnitski, L., Michaelson, D.M., Shohami, E. (1997). Motor and cognitive deficits in apolipoprotein E-deficient mice after closed head injury. *Neuroscience.* **80(4)**, 1255-62.

Chiang, M.F., Chang, J.G., Hu, C.J. (2003). Association between apolipoprotein E genotype and outcome of traumatic brain injury. *Acta Neurochir (Wien).* **145(8)**, 649-53.

Chu, K., Kim, M., Jeong, S.W., Kim, S.U., Yoon, B.W. (2003). Human neural stem cells can migrate, differentiate, and integrate after intravenous transplantation in adult rats with transient forebrain ischemia. *Neurosci Lett.* **343(2)**, 129-33.

Clark, D. D. & Sokoloff, L. (1999). Circulation and Energy Metabolism of the Brain, in *Basic Neurochemistry, Molecular, Cellular and Medical Aspects, 6th ed.* (Siegel, G. J., Agranoff, B. W., Albers, R. W., Fisher, S. K. & Uhler, M. D.). Philadelphia, Lippincott Williams & Wilkins.

Clark, R.S., Chen, J., Watkins, S.C., Kochanek, P.M., Chen, M., Stetler, R.A., Loeffert, J.E., Graham, S.H. (1997). Apoptosis-suppressor gene bcl-2 expression after traumatic brain injury in rats. *J Neurosci.* **17(23)**, 9172-82.

Clark, W.M., Lauten, J.D., Lessov, N., Woodward, W., Coull, B.M. (1995). Time course of ICAM-1 expression and leukocyte subset infiltration in rat forebrain ischemia. *Mol Chem Neuropathol.* **26(3)**, 213-30.

Clement-Collin, V., Barbier, A., Dergunov, A.D., Visvikis, A., Siest, G., Desmadril, M., Takahashi, M., Aggerbeck, L.P. (2006). The structure of human apolipoprotein E2, E3 and E4 in solution. 2. Multidomain organization correlates with the stability of apoE structure. *Biophys Chem.* **119(2)**, 170-85.

Collins, R.C., Dobkin, B.H., Choi, D.W. (1989). Selective vulnerability of the brain, new insights into the pathophysiology of stroke. *Ann Intern Med.* **110(12)**, 992-1000.

Corder, E.H., Saunders, A.M., Strittmatter, W.J., Schmechel, D.E., Gaskell, P.C., Small, G.W., Roses, A.D., Haines, J.L., Pericak-Vance, M.A. (1993). Gene dose of apolipoprotein E type 4 allele and the risk of Alzheimer's disease in late onset families. *Science.* **261(5123)**, 921-3.

Corder, E.H., Saunders, A.M., Risch, N.J., Strittmatter,W.J., Schmechel, D.E., Gaskell, P.C. Jr., Rimmler, J.B., Locke, P.A., Conneally, P.M., Schmader, K.E., et al. (1994). Protective effect of apolipoprotein E type 2 allele for late onset Alzheimer disease. *Nat Genet.* **7(2)**, 180-4.

Couderc, R., Mahieux, F., Bailleul, S., Fenelon, G., Mary, R., Fermanian, J. (1993). Prevalence of apolipoprotein E phenotypes in ischemic cerebrovascular disease. A case-control study. *Stroke.* **24(5)**, 661-4.

Crawford, F.C., Vanderploeg, R.D., Freeman, M.J., Singh, S., Waisman, M., Michaels, L., Abdullah, L., Warden, D., Lipsky, R., Salazar, A., Mullan, M.J. (2002). APOE genotype influences acquisition and recall following traumatic brain injury. *Neurology.* **58(7)**, 1115-8.

Crockard, A., Iannotti, F., Hunstock, A.T., Smith, R.D., Harris, R.J., Symon, L. (1980). Cerebral blood flow and edema following carotid occlusion in the gerbil. *Stroke.* **11(5)**, 494-8.

Dani, C. Embryonic stem cell-derived adipogenesis. (1999). *Cells Tissues Organs*. **165(3-4)**, 173-80.

D'Arcangelo, G., Miao, G.G., Chen, S.C., Soares, H.D., Morgan, J.I., Curran, T. (1995). A protein related to extracellular matrix proteins deleted in the mouse mutant reeler. *Nature.* **374(6524)**, 719-23.

D'Arcangelo, G., Homayouni, R., Keshvara, L., Rice, D.S., Sheldon, M., Curran, T. (1999). Reelin is a ligand for lipoprotein receptors. *Neuron.* **24(2)**, 471-9.

Davignon, J., Gregg, R.E., Sing, C.F. (1988). Apolipoprotein E polymorphism and atherosclerosis. *Arteriosclerosis.* **8(1)**, 1-21.

de Bont, N., Netea, M.G., Demacker, P.N., Verschueren, I., Kullberg, B.J., van Dijk, K.W., van der Meer, J.W., Stalenhoef, A.F. (1999). Apolipoprotein E knock-out mice are highly susceptible to endotoxemia and Klebsiella pneumoniae infection. *J Lipid Res.* **40(4)**, 680-5.

Deisseroth, K., Bito, H., Tsien, R.W. (1996). Signaling from synapse to nucleus, postsynaptic CREB phosphorylation during multiple forms of hippocampal synaptic plasticity. *Neuron.* **16(1)**, 89-101.

Della Fazia, M.A., Servillo, G., Sassone-Corsi, P. (1997). Cyclic AMP signalling and cellular proliferation, regulation of CREB and CREM. *FEBS Lett.* **410(1)**, 22-4.

DeMattos, R.B., Curtiss, L.K., Williams, D.L. (1998). A minimally lipidated form of cell-derived apolipoprotein E exhibits isoform-specific stimulation of neurite outgrowth in the absence of exogenous lipids or lipoproteins. *J Biol Chem.* **273(7)**, 4206-12.

DeMattos, R.B., Thorngate, F.E., Williams, D.L. (1999). A test of the cytosolic apolipoprotein E hypothesis fails to detect the escape of apolipoprotein E from the endocytic pathway into the cytosol and shows that direct expression of apolipoprotein E in the cytosol is cytotoxic. *J Neurosci.* **19(7)**, 2464-73.

Dik, M.G., Deeg, D.J., Bouter, L.M., Corder, E.H., Kok, A., Jonker, C. (2000). Stroke and apolipoprotein E epsilon4 are independent risk factors for cognitive decline, A population-based study. *Stroke.* **31(10)**, 2431-6.

Dinsmore, J., Ratliff, J., Deacon, T., Pakzaban, P., Jacoby, D., Galpern, W., Isacson, O. (1996). Embryonic stem cells differentiated in vitro as a novel source of cells for transplantation. *Cell Transplant.* **5(2)**, 131-43.

Duan, W.M., Widner, H., Brundin, P. (1995). Temporal pattern of host responses against intrastriatal grafts of syngeneic, allogeneic or xenogeneic embryonic neuronal tissue in rats. *Exp Brain Res.* **104(2)**, 227-42.

Dulabon, L., Olson, E.C., Taglienti, M.G., Eisenhuth, S., McGrath, B., Walsh, C.A., Kreidberg, J.A., Anton, E.S. (2000). Reelin binds alpha3beta1 integrin and inhibits neuronal migration. *Neuron.* **27(1)**, 33-44.

Dunn, E.H. (1917). Primary and secondary findings in a series of attempts to transplant cerebral cortex in the albino rat. *J. Comp. Neurol.* **27**, 565-582.

Dunn, L.T., Stewart, E., Murray, G.D., Nicoll, J.A., Teasdale, G.M. (2001). The influence of apolipoprotein E genotype on outcome after spontaneous subarachnoid hemorrhage, a preliminary study. *Neurosurgery.* **48(5)**, 1006-10.

Dupont-Wallois, L., Soulié, C., Sergeant, N., Wavrant-de Wrieze, N., Chartier-Harlin, M.C., Delacourte, A., Caillet-Boudin, M.L. (1997). ApoE synthesis in human neuroblastoma cells. *Neurobiol Dis.* **4(5)**, 356-64.

Ekdahl, C.T., Claasen, J.H., Bonde, S., Kokaia, Z., Lindvall, O. (2003). Inflammation is detrimental for neurogenesis in adult brain. *Proc Natl Acad Sci USA. 2003* **100(23)**, 13632-7.

Eklof, B. & Siesjo, B.K. (1972). The effect of bilateral carotid artery ligation upon the blood flow and the energy state of the rat brain. *Acta Physiol Scand.* **86(2)**, 155-65.

Eklof, B. & Siesjo, B.K. (1973). Cerebral blood flow in ischemia caused by carotid artery ligation in the rat. *Acta Physiol Scand.* **87(1)**, 69-77.

Elshourbagy, N.A., Liao, W.S., Mahley, R.W., Taylor, J.M. (1985). Apolipoprotein E mRNA is abundant in the brain and adrenals, as well as in the liver, and is present in other peripheral tissues of rats and marmosets. *Proc Natl Acad Sci USA*. **82(1)**, 203-7.

Endoh, M., Maiese, K., Wagner, J. Expression of the inducible form of nitric oxide synthase by reactive astrocytes after transient global ischemia. (1994). *Brain Res.* **651(1-2)**, 92-100.

Englund, U., Bjorklund, A., Wictorin, K., Lindvall, O., Kokaia, M. (2002). Grafted neural stem cells develop into functional pyramidal neurons and integrate into host cortical circuitry. *Proc Natl Acad Sci USA*. **99(26)**, 17089-94.

Eriksson, P.S., Perfilieva, E., Bjork-Eriksson, T., Alborn, A.M., Nordborg, C., Peterson, D.A., Gage, F.H. (1998). Neurogenesis in the adult human hippocampus. *Nat Med.* **4(11)**, 1313-7.

Evans, M.J. & Kaufman, M.H. (1981). Establishment in culture of pluripotential cells from mouse embryos. *Nature.* **292(5819)**, 154-6.

Fagan, A.M., Holtzman, D.M., Munson, G., Mathur, T., Schneider, D., Chang, L.K., Getz, G.S., Reardon, C.A., Lukens, J., Shah, J.A., LaDu, M.J. (1999). Unique lipoproteins secreted by primary astrocytes from wild type, apoE (-/-), and human apoE transgenic mice. *J Biol Chem.* **274(42)**, 30001-7.

Falconer, D.S. (1951) 2 new mutants, trembler and reeler, with neurological actions in the house mouse (mus-musculus l). *Journal of Genetics.* **50(2)**, 192-201

Ferreira, S., Dupire, M.J., Delacourte, A., Najib, J., Caillet-Boudin, M.L. (2000). Synthesis and regulation of apolipoprotein E during the differentiation of human neuronal precursor NT2/D1 cells into postmitotic neurons. *Exp Neurol.* **166(2)**, 415-21.

Ferrucci, L., Guralnik, J.M., Pahor, M., Harris, T., Corti, M.C., Hyman, B.T., Wallace, R.B., Havlik, R.J. (1997). Apolipoprotein E epsilon 2 allele and risk of stroke in the older population. *Stroke.* **28(12**), 2410-6.

Fleming, L.M., Weisgraber, K.H., Strittmatter, W.J., Troncoso, J.C., Johnson, G.V. (1996). Differential binding of apolipoprotein E isoforms to tau and other cytoskeletal proteins. *Exp Neurol.* **138(2)**, 252-60.

Francis, A. & Pulsinelli, W. (1982). The response of GABAergic and cholinergic neurons to transient cerebral ischemia. *Brain Res.* **243(2)**, 271-8.

Franklin, R.J., Blaschuk, K.L., Bearchell, M.C., Prestoz, L.L., Setzu, A., Brindle, K.M., ffrench-Constant, C. (1999). Magnetic resonance imaging of transplanted oligodendrocyte precursors in the rat brain. *Neuroreport.* **10(18)**, 3961-5.

Freed, C.R., Greene, P.E., Breeze, R.E., Tsai, W.Y., DuMouchel, W., Kao, R., Dillon, S., Winfield, H., Culver, S., Trojanowski, J.Q., Eidelberg, D., Fahn, S. (2001). Transplantation of embryonic dopamine neurons for severe Parkinson's disease. *N Engl J Med.* **344(10)**, 710-9.

Fricker-Gates, R.A., Muir, J.A., Dunnett, S.B. (2004). Transplanted hNT cells ("LBS neurons") in a rat model of huntington's disease, good survival, incomplete differentiation, and limited functional recovery. *Cell Transplant.* **13(2)**, 123-36.

Friedman, G., Froom, P., Sazbon, L., Grinblatt, I., Shochina, M., Tsenter, J., Babaey, S., Yehuda, B., Groswasser, Z. (1999). Apolipoprotein E-epsilon4 genotype predicts a poor outcome in survivors of traumatic brain injury. *Neurology.* **52(2)**, 244-8.

Fryd Johansen, F., Balslev Jorgensen, M., Diemer, N.H. (1983). Resistance of hippocampal CA-1 interneurons to 20 min of transient cerebral ischemia in the rat. *Acta Neuropathol (Berl).* **61(2)**, 135-40.

Frykman, P.K., Brown, M.S., Yamamoto, T., Goldstein, J.L., Herz, J. (1995). Normal plasma lipoproteins and fertility in gene-targeted mice homozygous for a disruption in the gene encoding very low density lipoprotein receptor. *Proc Natl Acad Sci USA.* **92(18)**, 8453-7.

Fujii, M., Hara, H., Meng, W., Vonsattel, J.P., Huang, Z., Moskowitz, M.A. (1997). Strain-related differences in susceptibility to transient forebrain ischemia in SV-129 and C57black/6 mice. *Stroke.* **28(9)**, 1805-10.

Fujikawa, T., Oh, S.H., Pi, L., Hatch, H.M., Shupe, T., Petersen, B.E. (2005). Teratoma formation leads to failure of treatment for type I diabetes using embryonic stem cell-derived insulin-producing cells. *Am J Pathol.* **166(6)**, 1781-91.

Gage, F.H. (2000). Mammalian neural stem cells. *Science.* **287(5457)**, 1433-8.

Garcia-Verdugo, J.M., Doetsch, F., Wichterle, H., Lim, D.A., Alvarez-Buylla, A. (1998). Architecture and cell types of the adult subventricular zone, in search of the stem cells. *J Neurobiol.* **36(2)**, 234-48.

Gaura, V., Bachoud-Levi, A.C., Ribeiro, M.J., Nguyen, J.P., Frouin, V., Baudic, S., Brugieres, P., Mangin, J.F., Boisse, M.F., Palfi, S., Cesaro, P., Samson, Y., Hantraye, P., Peschanski, M., Remy, P. (2004). Striatal neural grafting improves cortical metabolism in Huntington's disease patients. *Brain.* **127(Pt 1)**, 65-72.

Gillingwater, T.H., Haley, J.E., Ribchester, R.R., Horsburgh, K. (2004). Neuroprotection after transient global cerebral ischemia in Wld(s) mutant mice. *J Cereb Blood Flow Metab.* **24(1)**, 62-6.

Goldman, S.A. & Nottebohm, F. (1983). Neuronal production, migration, and differentiation in a vocal control nucleus of the adult female canary brain. *Proc Natl Acad Sci USA.* **80(8)**, 2390-4.

Goldstein, L.B., Vitek, M.P., Dawson, H., Bullman, S. (2000). Expression of the apolipoprotein E gene does not affect motor recovery after sensorimotor cortex injury in the mouse. *Neuroscience.* **99(4)**, 705-10.

Gong, X., He, X., Qi, L., Zuo, H., Xie, Z. (2006). Stromal cell derived factor-1 acutely promotes neural progenitor cell proliferation in vitro by a mechanism involving the ERK1/2 and PI-3K signal pathways. *Cell Biol Int.* **30(5)**, 466-71.

Gorba, T., Bradoo, P., Antonic, A., Marvin, K., Liu, D.X., Lobie, P.E., Reymann, K.G., Gluckman, P.D., Sieg, F. (2006). Neural regeneration protein is a novel chemoattractive and neuronal survival-promoting factor. *Exp Cell Res.* **312(16)**, 3060-74.

Gordon, I., Grauer, E., Genis, I., Sehayek, E., Michaelson, D.M. (1995). Memory deficits and cholinergic impairments in apolipoprotein E-deficient mice. *Neurosci Lett.* **199(1)**, 1-4.

Gould, E. & Tanapat, P. (1999). Stress and hippocampal neurogenesis. *Biol Psychiatry.* **46(11)**, 1472-9.

Gould, E., Beylin, A., Tanapat, P., Reeves, A., Shors, T.J. (1999). Learning enhances adult neurogenesis in the hippocampal formation. *Nat Neurosci.* **2(3)**, 260-5.

Greenamyre, J.T., Olson, J.M., Penney, J.B. Jr, Young, A.B. (1985). Autoradiographic characterization of N-methyl-D-aspartate-, quisqualate- and kainate-sensitive glutamate binding sites. *J Pharmacol Exp Ther.* **233(1)**, 254-63.

Greenberg, S.M., Rebeck, G.W., Vonsattel, J.P., Gomez-Isla, T., Hyman, B.T. (1995). Apolipoprotein E epsilon 4 and cerebral hemorrhage associated with amyloid angiopathy. *Ann Neurol.* **38(2)**, 254-9.

Greenberg, S.M., Vonsattel, J.P., Segal, A.Z., Chiu, R.I., Clatworthy, A.E., Liao, A., Hyman, B.T., Rebeck, G.W. (1998). Association of apolipoprotein E epsilon2 and vasculopathy in cerebral amyloid angiopathy. *Neurology.* **50(4)**, 961-5.

Grigoryan, G.A., Gray, J.A., Rashid, T., Chadwick, A., Hodges, H. (2000). Conditionally immortal neuroepithelial stem cell grafts restore spatial learning in rats with lesions at the source of cholinergic forebrain projections cholinergic forebrain projections Conditionally immortal neuroepithelial stem cell grafts restore spatial leaming in rats with lesions at the source of cholinergic forebrain projections. *Restor Neurol Neurosci.* **17(4)**, 1.

Grootendorst, J., de Kloet, E.R., Dalm, S., Oitzl, M.S. (2001). Reversal of cognitive deficit of apolipoprotein E knockout mice after repeated exposure to a common environmental experience. *Neuroscience.* **108(2)**, 237-47.

Grootendorst, J., Bour, A., Vogel, E., Kelche, C., Sullivan, P.M., Dodart, J.C., Bales, K., Mathis, C. (2005). Human apoE targeted replacement mouse lines, h-apoE4 and h-apoE3 mice differ on spatial memory performance and avoidance behavior. *Behav Brain Res.* **159(1)**, 1-14.

Guo, Y., Hangoc, G., Bian, H., Pelus, L.M., Broxmeyer, H.E. (2005). SDF-1/CXCL12 enhances survival and chemotaxis of murine embryonic stem cells and production of primitive and definitive hematopoietic progenitor cells. *Stem Cells.* **23(9)**, 1324-32.

Haegele, L., Ingold, B., Naumann, H., Tabatabai, G., Ledermann, B., Brandner, S. (2003). Wnt signalling inhibits neural differentiation of embryonic stem cells by controlling bone morphogenetic protein expression. *Mol Cell Neurosci.* **24(3)**, 696-708.

Hall, E.D., Oostveen, J.A., Dunn, E., Carter, D.B. (1995). Increased amyloid protein precursor and apolipoprotein E immunoreactivity in the selectively vulnerable hippocampus following transient forebrain ischemia in gerbils. *Exp Neurol.* **135(1)**, 17-27.

Han, S.H., Chung, S.Y. (2000). Marked hippocampal neuronal damage without motor deficits after mild concussive-like brain injury in apolipoprotein E-deficient mice. *Ann N Y Acad Sci.* **903**, 357-65.

Handelmann, G.E., Boyles, J.K., Weisgraber, K.H., Mahley, R.W., Pitas, R.E. (1992). Effects of apolipoprotein E, beta-very low density lipoproteins, and cholesterol on the extension of neurites by rabbit dorsal root ganglion neurons in vitro. *J Lipid Res.* **33(11)**, 1677-88.

Harris, F.M., Tesseur, I., Brecht, W.J., Xu, Q., Mullendorff, K., Chang, S., Wyss-Coray, T., Mahley, R.W., Huang, Y. (2004). Astroglial regulation of apolipoprotein E expression in neuronal cells. Implications for Alzheimer's disease. *J Biol Chem.* **279(5)**, 3862-8.

Harris, F.M., Brecht, W.J., Xu, Q., Mahley, R.W., Huang, Y. (2004). Increased tau phosphorylation in apolipoprotein E4 transgenic mice is associated with activation of extracellular signal-regulated kinase, modulation by zinc. *J Biol Chem.* **279(43)**, 44795-801.

Hauck, C.R., Sieg, D.J., Hsia, D.A., Loftus, J.C., Gaarde, W.A., Monia, B.P., Schlaepfer, D.D. (2001). Inhibition of focal adhesion kinase expression or activity disrupts epidermal growth factor-stimulated signaling promoting the migration of invasive human carcinoma cells. *Cancer Res.* **61(19)**, 7079-90.

Hayek, T., Oiknine, J., Brook, J.G., Aviram, M. (1994). Increased plasma and lipoprotein lipid peroxidation in apo E-deficient mice. *Biochem Biophys Res Commun.* **201(3)**, 1567-74.

Herdegen, T., Skene, P., Bahr, M. (1997). The c-Jun transcription factor--bipotential mediator of neuronal death, survival and regeneration. *Trends Neurosci.* **20(5)**, 227-31.

Herdegen, T., Claret, F.X., Kallunki, T., Martin-Villalba, A., Winter, C., Hunter, T., Karin, M. (1998). Lasting N-terminal phosphorylation of c-Jun and activation of c-Jun N-terminal kinases after neuronal injury. *J Neurosci.* **18(14)**, 5124-35.

Herz, J., Clouthier, D.E., Hammer, R.E. (1992). LDL receptor-related protein internalizes and degrades uPA-PAI-1 complexes and is essential for embryo implantation. *Cell.* **71(3)**, 411-21.

Herz, J. & Beffert, U. (2000). Apolipoprotein E receptors, linking brain development and Alzheimer's disease. *Nat Rev Neurosci.* **1(1)**, 51-8.

Herz, J., Strickland, D.K. (2001). LRP, a multifunctional scavenger and signaling receptor. *J Clin Invest.* **108(6)**, 779-84.

Hiesberger, T., Trommsdorff, M., Howell, B.W., Goffinet, A., Mumby, M.C., Cooper, J.A., Herz, J. (1999). Direct binding of Reelin to VLDL receptor and ApoE receptor 2 induces tyrosine phosphorylation of disabled-1 and modulates tau phosphorylation. *Neuron.* **24(2)**, 481-9.

Hirabayashi, Y., Itoh, Y., Tabata, H., Nakajima, K., Akiyama, T., Masuyama, N., Gotoh, Y. (2004). The Wnt/beta-catenin pathway directs neuronal differentiation of cortical neural precursor cells. *Development.* **131(12)**, 2791-801.

Hitoshi, S., Alexson, T., Tropepe, V., Donoviel, D., Elia, A.J., Nye, J.S., Conlon, R.A., Mak, T.W., Bernstein, A., van der Kooy, D. (2002). Notch pathway molecules are essential for the maintenance, but not the generation, of mammalian neural stem cells. *Genes Dev.* **16(7)**, 846-58.

Hodges, H., Veizovic, T., Bray, N., French, S.J., Rashid, T.P., Chadwick, A., Patel, S., Gray, J.A. (2000). Conditionally immortal neuroepithelial stem cell grafts reverse age-associated memory impairments in rats. *Neuroscience.* **101(4)**, 945-55.

Hodges, H., Sowinski, P., Virley, D., Nelson, A., Kershaw, T.R., Watson, W.P., Veizovic, T., Patel, S., Mora, A., Rashid, T., French, S.J., Chadwick, A., Gray, J.A., Sinden, J.D. (2000). Functional reconstruction of the hippocampus: fetal versus conditionally immortal neuroepithelial stem cell grafts. *Novartis Found Symp.* **231**, 53-65

Hoe, H.S., Harris, D.C., Rebeck, G.W. (2005). Multiple pathways of apolipoprotein E signaling in primary neurons. *J Neurochem.* **93(1)**, 145-55.

Hoe, H.S., Pocivavsek, A., Chakraborty, G., Fu, Z., Vicini, S., Ehlers, M.D., Rebeck, G.W. (2006). Apolipoprotein E receptor 2 interactions with the N-methyl-D-aspartate receptor. *J Biol Chem.* **281(6)**, 3425-31.

Hoffer, B.J., Olson, L. (1991). Ethical issues in brain-cell transplantation. *Trends Neurosci.* 1991 **14(8)**, 384-8.

Honkaniemi, J., Massa, S.M., Breckinridge, M., Sharp, F.R. (1996). Global ischemia induces apoptosis-associated genes in hippocampus. *Brain Res Mol Brain Res.* **42(1)**, 79-88.

Horn, M. & Scholte, W. (1992). Delayed neuronal death and delayed neuronal recovery in the human brain following global ischemia. *Acta Neuropathol (Berl).* **85**, 79–87

Horsburgh, K. & Nicoll, J.A. (1996). Selective alterations in the cellular distribution of apolipoprotein E immunoreactivity following transient cerebral ischaemia in the rat. *Neuropathol Appl Neurobiol.* **22(4)**, 342-9.

Horsburgh, K., Fitzpatrick, M., Nilsen, M., Nicoll, J.A. (1997). Marked alterations in the cellular localisation and levels of apolipoprotein E following acute subdural haematoma in rat. *Brain Res.* **763(1)**, 103-10.

Horsburgh, K., Graham, D.I., Stewart, J., Nicoll, J.A. (1999). Influence of apolipoprotein E genotype on neuronal damage and apoE immunoreactivity in human hippocampus following global ischemia. *J Neuropathol Exp Neurol.* **58(3)**, 227-34.

Horsburgh, K., Kelly, S., McCulloch, J., Higgins, G.A., Roses, A.D., Nicoll, J.A. (1999). Increased neuronal damage in apolipoprotein E-deficient mice following global ischaemia. *Neuroreport.* **10(4)**, 837-41.

Horsburgh, K., McCulloch, J., Nilsen, M., McCracken, E., Large, C., Roses, A.D., Nicoll, J.A. (2000). Intraventricular infusion of apolipoprotein E ameliorates acute neuronal damage after global cerebral ischemia in mice. *J Cereb Blood Flow Metab.* **20(3)**, 458-62.

Horsburgh, K., McCulloch, J., Nilsen, M., Roses, A.D., Nicoll, J.A. (2000). Increased neuronal damage and apoE immunoreactivity in human apolipoprotein E, E4 isoform-specific, transgenic mice after global cerebral ischaemia. *Eur J Neurosci.* **12(12)**, 4309-17.

Hossmann, K.A. (1993). Ischemia-mediated neuronal injury. *Resuscitation.* **26(3)**, 225-35.

Hossmann, K.A. (1997). Reperfusion of the brain after global ischaemia, hemodynamic disturbances. *Shock.* **8(2)**, 95-101

Howell, B.W., Hawkes, R., Soriano, P., Cooper, J.A. (1997). Neuronal position in the developing brain is regulated by mouse disabled-1. *Nature.* **389(6652)**, 733-7.

Howell, B.W., Herrick, T.M., Hildebrand, J.D., Zhang, Y., Cooper, J.A. (2000). Dab1 tyrosine phosphorylation sites relay positional signals during mouse brain development. *Curr Biol.* **10(15)**, 877-85.

Hoyte, L., Kaur, J., Buchan, A.M. (2004). Lost in translation, taking neuroprotection from animal models to clinical trials. *Exp Neurol.* **188(2)**, 200-4.

Hsu, S.M., Raine, L., Fanger, H. (1981). The use of antiavidin antibody and avidin-biotin-peroxidase complex in immunoperoxidase technics. *Am J Clin Pathol.* **75(6)**, 816-21.

Hsu, S.M., Raine, L., Fanger, H. (1981). Use of avidin-biotin-peroxidase complex (ABC) in immunoperoxidase techniques: a comparison between ABC and unlabeled antibody (PAP) procedures. *J Histochem Cytochem.* **29(4)**, 577-80.

Hu, J., LaDu, M.J., Van Eldik, L.J. (1998). Apolipoprotein E attenuates beta-amyloid-induced astrocyte activation. *J Neurochem.* **71(4)**, 1626-34.

Huang, C., Rajfur, Z., Borchers, C., Schaller, M.D., Jacobson, K. (2003). JNK phosphorylates paxillin and regulates cell migration. *Nature.* **424(6945)**, 219-23.

Huang, D.Y., Goedert, M., Jakes, R., Weisgraber, K.H., Garner, C.C., Saunders, A.M., Pericak-Vance, M.A., Schmechel, D.E., Roses, A.D., Strittmatter, W.J. (1994). Isoform-specific interactions of apolipoprotein E with the microtubule-associated protein MAP2c, implications for Alzheimer's disease. *Neurosci Lett.* **182(1)**, 55-8.

Hudson, J.L., Hoffman, A., Stromberg, I., Hoffer, B.J., Moorhead, J.W. (1994). Allogeneic grafts of fetal dopamine neurons, behavioral indices of immunological interactions. *Neurosci Lett.* **171(1-2)**, 32-6.

Hui, D.Y., Basford, J.E. (2005). Distinct signaling mechanisms for apoE inhibition of cell migration and proliferation. *Neurobiol Aging.* **26(3)**, 317-23.

Huntington, G. (1872). On chorea. *Medical and Surgical Reporter.* **26**, 320-321.

Hurlbert, M.S., Gianani, R.I., Hutt, C., Freed, C.R., Kaddis, F.G. (1999). Neural transplantation of hNT neurons for Huntington's disease. *Cell Transplant.* **8(1)**, 143-51.

Ignatius, M.J., Gebicke-Harter, P.J., Skene, J.H., Schilling, J.W., Weisgraber, K.H., Mahley, R.W., Shooter, E.M. (1986). Expression of apolipoprotein E during nerve degeneration and regeneration. *Proc Natl Acad Sci USA.* **83(4)**, 1125-9.

Ikonomidou, C., Turski, L., (2002). Why did NMDA receptor antagonists fail clinical trials for stroke and traumatic brain injury? *Lancet Neurol.* **1(6)**, 383-6.

Imitola, J., Raddassi, K., Park, K.I., Mueller, F.J., Nieto, M., Teng, Y.D., Frenkel, D., Li, J., Sidman, R.L., Walsh, C.A., Snyder, E.Y., Khoury, S.J. (2004). Directed migration of neural stem cells to sites of CNS injury by the stromal cell-derived factor 1alpha/CXC chemokine receptor 4 pathway. *Proc Natl Acad Sci USA.* **101(52)**, 18117-22.

Ishibashi, S., Brown, M.S., Goldstein, J.L., Gerard, R.D., Hammer, R.E., Herz, J. (1993). Hypercholesterolemia in low density lipoprotein receptor knockout mice and its reversal by adenovirus-mediated gene delivery. *J Clin Invest.* **92(2)**, 883-93.

Ishigami, M., Swertfeger, D.K., Granholm, N.A., Hui, D.Y. (1998). Apolipoprotein E inhibits platelet-derived growth factor-induced vascular smooth muscle cell

migration and proliferation by suppressing signal transduction and preventing cell entry to G1 phase. *J Biol Chem.* **273(32)**, 20156-61.

Ishigami, M., Swertfeger, D.K., Hui, M.S., Granholm, N.A., Hui, D.Y. (2000). Apolipoprotein E inhibition of vascular smooth muscle cell proliferation but not the inhibition of migration is mediated through activation of inducible nitric oxide synthase. *Arterioscler Thromb Vasc Biol.* **20(4)**, 1020-6.

Ishimaru, H., Ishikawa, K., Haga, S., Shoji, M., Ohe, Y., Haga, C., Sasaki, A., Takashashi, A., Maruyama, Y. (1996). Accumulation of apolipoprotein E and beta-amyloid-like protein in a trace of the hippocampal CA1 pyramidal cell layer after ischaemic delayed neuronal death. *Neuroreport.* **7(18)**, 3063-7.

Iwai, M., Sato, K., Kamada, H., Omori, N., Nagano, I., Shoji, M., Abe, K. (2003). Temporal profile of stem cell division, migration, and differentiation from subventricular zone to olfactory bulb after transient forebrain ischemia in gerbils. *J Cereb Blood Flow Metab.* **23(3)**, 331-41.

Iwata, A., Browne, K.D., Chen, X.H., Yuguchi, T., Smith, D.H. (2005). Traumatic brain injury induces biphasic upregulation of ApoE and ApoJ protein in rats. *J Neurosci Res.* **82(1)**, 103-14.

Jat, P.S., Noble, M.D., Ataliotis, P., Tanaka, Y., Yannoutsos, N., Larsen, L., Kioussis, D. (1991). Direct derivation of conditionally immortal cell lines from an H-2Kb-tsA58 transgenic mouse. *Proc Natl Acad Sci USA.* **88(12)**, 5096-100.

Jin, K., Minami, M., Lan, J.Q., Mao, X.O., Batteur, S., Simon, R.P., Greenberg, D.A. (2001). Neurogenesis in dentate subgranular zone and rostral subventricular zone after focal cerebral ischemia in the rat. *Proc Natl Acad Sci USA.* **98(8)**, 4710-5.

Jin, K., Mao, X.O., Sun, Y., Xie, L., Greenberg, D.A. (2002). Stem cell factor stimulates neurogenesis in vitro and in vivo. *J Clin Invest.* **110(3)**, 311-9.

Johnson, G.L., Lapadat, R. (2002). Mitogen-activated protein kinase pathways mediated by ERK, JNK, and p38 protein kinases. *Science.* **298(5600)**, 1911-2.

Jones, B.J. & Roberts, D.J. (1968). The quantiative measurement of motor inco-ordination in naive mice using an acelerating rotarod. *J Pharm Pharmacol.* **20(4)**, 302-4.

Jordan, B.D., Relkin, N.R., Ravdin, L.D., Jacobs, A.R., Bennett, A., Gandy, S. (1997). Apolipoprotein E epsilon4 associated with chronic traumatic brain injury in boxing. *JAMA.* **278(2)**, 136-40.

Kahan, B.W., Jacobson, L.M., Hullett, D.A., Ochoada, J.M., Oberley, T.D., Lang, K.M., Odorico, J.S. (2003). Pancreatic precursors and differentiated islet cell types from murine embryonic stem cells, an in vitro model to study islet differentiation. *Diabetes.* **52(8)**, 2016-24.

Kalaria, R.N., Cohen, D.L., Premkumar, D.R. (1996). Apolipoprotein E alleles and brain vascular pathology in Alzheimer's disease. *Ann N Y Acad Sci.* **777**, 266-70.

Kamada, H., Sato, K., Zhang, W.R., Omori, N., Nagano, I., Shoji, M., Abe, K. (2003). Spatiotemporal changes of apolipoprotein E immunoreactivity and apolipoprotein E mRNA expression after transient middle cerebral artery occlusion in rat brain. J *Neurosci Res.* **73(4)**, 545-56.

Kaplan, M.S. (1983). Proliferation of subependymal cells in the adult primate CNS, differential uptake of DNA labelled precursors. *J Hirnforsch.* **24(1)**, 23-33.

Kaplan, M.S. & Bell, D.H. (1984). Mitotic neuroblasts in the 9-day-old and 11-month-old rodent hippocampus. *J Neurosci.* **4(6)**, 1429-41.

Kaplan, M.S. (1985). Formation and turnover of neurons in young and senescent animals, an electronmicroscopic and morphometric analysis. *Ann N Y Acad Sci.* **457**, 173-92.

Katsura, K., Kristian, T., Siesjo, B.K. (1994). Energy metabolism, ion homeostasis, and cell damage in the brain. *Biochem Soc Trans.* **22(4)**, 991-6.

Kavurma, M.M., Khachigian, L.M. (2003). ERK, JNK, and p38 MAP kinases differentially regulate proliferation and migration of phenotypically distinct smooth muscle cell subtypes. *J Cell Biochem.* **89(2)**, 289-300.

Kawauchi, T., Chihama, K., Nabeshima, Y., Hoshino, M. (2003). The in vivo roles of STEF/Tiam1, Rac1 and JNK in cortical neuronal migration. *EMBO J.* **22(16)**, 4190-201.

Kay, A., Petzold, A., Kerr, M., Keir, G., Thompson, E., Nicoll, J. (2003). Decreased cerebrospinal fluid apolipoprotein E after subarachnoid hemorrhage, correlation with injury severity and clinical outcome. *Stroke.* **34(3)**, 637-42.

Kay, A., Petzold, A., Kerr, M., Keir, G., Thompson, E., Nicoll, J. (2003). Temporal alterations in cerebrospinal fluid amyloid beta-protein and apolipoprotein E after subarachnoid hemorrhage. *Stroke.* **34(12)**, 240-3.

Kee, N.J., Preston, E., Wojtowicz, J.M. (2001). Enhanced neurogenesis after transient global ischemia in the dentate gyrus of the rat. *Exp Brain Res.* **136(3)**, 313-20.

Kelly, M.E., Clay, M.A., Mistry, M.J., Hsieh-Li, H.M., Harmony, J.A. (1994). Apolipoprotein E inhibition of proliferation of mitogen-activated T lymphocytes, production of interleukin 2 with reduced biological activity. *Cell Immunol.* **159(2)**, 124-39.

Kelly, S., McCulloch, J., Horsburgh, K. (2001). Minimal ischaemic neuronal damage and HSP70 expression in MF1 strain mice following bilateral common carotid artery occlusion. *Brain Res.* **914(1-2)**, 185-95.

Kelly, S., Bliss, T.M., Shah, A.K., Sun, G.H., Ma, M., Foo, W.C., Masel, J., Yenari, M.A., Weissman, I.L., Uchida, N., Palmer, T., Steinberg, G.K. (2004). Transplanted human fetal neural stem cells survive, migrate, and differentiate in ischemic rat cerebral cortex. *Proc Natl Acad Sci USA.* **101(32)**, 11839-44.

Kempermann, G., Kuhn, H.G., Gage, F.H. (1997). Genetic influence on neurogenesis in the dentate gyrus of adult mice. *Proc Natl Acad Sci USA.* **94(19)**, 10409-14.

Kida, E., Pluta, R., Lossinsky, A.S., Golabek, A.A., Choi-Miura, N.H., Wisniewski, H.M., Mossakowski, M.J. (1995). Complete cerebral ischemia with short-term survival in rat induced by cardiac arrest. II. Extracellular and intracellular accumulation of apolipoproteins E and J in the brain. *Brain Res.* **674(2)**, 341-6.

Kiessling, M., Stumm, G., Xie, Y., Herdegen, T., Aguzzi, A., Bravo, R., Gass, P. (1993). Differential transcription and translation of immediate early genes in the gerbil hippocampus after transient global ischemia. *J Cereb Blood Flow Metab.* **13(6)**, 914-24.

Kihara, S., Shiraishi, T., Nakagawa, S., Toda, K., Tabuchi, K. (1994). Visualization of DNA double strand breaks in the gerbil hippocampal CA1 following transient ischemia. *Neurosci Lett.* **175(1-2)**, 133-6.

Kim, D.E., Schellingerhout, D., Ishii, K., Shah, K., Weissleder, R. (2004). Imaging of stem cell recruitment to ischemic infarcts in a murine model. *Stroke.* **35(4)**, 952-7.

Kim, D.H., Inagaki, Y., Suzuki, T., Ioka, R.X., Yoshioka, S.Z., Magoori, K., Kang, M.J., Cho, Y., Nakano, A.Z., Liu, Q., Fujino, T., Suzuki, H., Sasano, H., Yamamoto, T.T. (1998). A new low density lipoprotein receptor related protein, LRP5, is expressed in hepatocytes and adrenal cortex, and recognizes apolipoprotein E. *J Biochem (Tokyo).* **124(6)**, 1072-6.

Kirik, D., Breysse, N., Bjorklund, T., Besret, L., Hantraye, P. (2005). Imaging in cell-based therapy for neurodegenerative diseases. *Eur J Nucl Med Mol Imaging.* **32 Suppl 2**, S417-34.

Kirino, T. (1982). Delayed neuronal death in the gerbil hippocampus following ischemia. *Brain Res.* **239(1)**, 57-69.

Kirino, T. & Sano, K. (1984). Selective vulnerability in the gerbil hippocampus following transient ischemia. *Acta Neuropathol (Berl).* **62(3)**, 201-8.

Kita, T., Brown, M.S., Bilheimer, D.W., Goldstein, J.L. (1982). Delayed clearance of very low density and intermediate density lipoproteins with enhanced conversion to low density lipoprotein in WHHL rabbits. *Proc Natl Acad Sci USA.* **79(18)**, 5693-7.

Kitagawa, K., Matsumoto, M., Kuwabara, K., Ohtsuki, T., Hori, M. (2001). Delayed, but marked, expression of apolipoprotein E is involved in tissue clearance after cerebral infarction. *J Cereb Blood Flow Metab.* **21(10)**, 1199-207.

Kitagawa, K., Matsumoto, M., Hori, M., Yanagihara, T. (2002). Neuroprotective effect of apolipoprotein E against ischemia. *Ann N Y Acad Sci.* **977**, 468-75.

Kitchens, D.L., Snyder, E.Y., Gottlieb, D.I. (1994). FGF and EGF are mitogens for immortalized neural progenitors. *J Neurobiol.* **25(7)**, 797-807.

Kleppner, S.R., Robinson, K.A., Trojanowski, J.Q., Lee, V.M. (1995). Transplanted human neurons derived from a teratocarcinoma cell line (NTera-2) mature, integrate, and survive for over 1 year in the nude mouse brain. *J Comp Neurol.* **357(4)**, 618-32.

Kondziolka, D., Wechsler, L., Goldstein, S., Meltzer, C., Thulborn, K.R., Gebel, J., Jannetta, P., DeCesare, S., Elder, E.M., McGrogan, M., Reitman, M.A., Bynum, L. (2000). Transplantation of cultured human neuronal cells for patients with stroke. *Neurology.* **55(4)**, 565-9.

Kondziolka, D., Steinberg,G.K., Wechsler, L., Meltzer, C.C., Elder, E., Gebel, J., Decesare, S., Jovin, T., Zafonte, R., Lebowitz, J., Flickinger, J.C., Tong, D., Marks, M.P., Jamieson, C., Luu, D., Bell-Stephens, T., Teraoka, J. (2005). Neurotransplantation for patients with subcortical motor stroke, a phase 2 randomized trial. *J Neurosurg.* **103(1)**, 38-45.

Kordower, J.H., Freeman, T.B., Snow, B.J., Vingerhoets, F.J., Mufson, E.J., Sanberg, P.R., Hauser, R.A., Smith, D.A., Nauert, G.M., Perl, D.P., et al. (1995). Neuropathological evidence of graft survival and striatal reinnervation after the transplantation of fetal mesencephalic tissue in a patient with Parkinson's disease. *N Engl J Med.* **332(17)**, 1118-24.

Kramer, J., Hargus, G., Rohwedel, J. (2006). Derivation and characterization of chondrocytes from embryonic stem cells in vitro. *Methods Mol Biol.* **330**, 171-90.

Krathwohl, M.D., Kaiser, J.L. (2004). Chemokines promote quiescence and survival of human neural progenitor cells. *Stem Cells.* **22(1)**, 109-18.

Kristian, T., & Siesjo, B.K. (1998). Calcium in ischemic cell death. *Stroke.* **29(3)**, 705-18.

Krugers, H.J., Mulder, M., Korf, J., Havekes, L., de Kloet, E.R., Joels, M. (1997). Altered synaptic plasticity in hippocampal CA1 area of apolipoprotein E deficient mice. *Neuroreport.* **8(11)**, 2505-10.

Krzywkowski, P., Ghribi, O., Gagne, J., Chabot, C., Kar, S., Rochford, J., Massicotte, G., Poirier, J. (1999). Cholinergic systems and long-term potentiation in memory-impaired apolipoprotein E-deficient mice. *Neuroscience.* **92(4)**, 1273-86.

Kuhn, H.G., Dickinson-Anson, H., Gage, F.H. (1996). Neurogenesis in the dentate gyrus of the adult rat, age-related decrease of neuronal progenitor proliferation. *J Neurosci.* **16(6)**, 2027-33.

Kutner, K.C., Erlanger, D.M., Tsai, J., Jordan, B., Relkin, N.R. (2000). Lower cognitive performance of older football players possessing apolipoprotein E epsilon4. *Neurosurgery.* **47(3)**, 651-7.

Kuusisto, J., Mykkanen, L., Kervinen, K., Kesaniemi, Y.A., Laakso, M. (1995). Apolipoprotein E4 phenotype is not an important risk factor for coronary heart disease or stroke in elderly subjects. *Arterioscler Thromb Vasc Biol.* **15(9)**, 1280-6.

Lanterna, L.A., Rigoldi, M., Tredici, G., Biroli, F., Cesana, C., Gaini, S.M., Dalpra, L. (2005). APOE influences vasospasm and cognition of noncomatose patients with subarachnoid hemorrhage. *Neurology.* **64(7)**, 1238-44.

Larsson, E., Mandel, R.J., Klein, R.L., Muzyczka, N., Lindvall, O., Kokaia, Z. (2002). Suppression of insult-induced neurogenesis in adult rat brain by brain-derived neurotrophic factor. *Exp Neurol.* **177(1)**, 1-8.

Laskowitz, D.T., Goel, S., Bennett, E.R., Matthew, W.D. (1997). Apolipoprotein E suppresses glial cell secretion of TNF alpha. *J Neuroimmunol.* **76(1-2)**, 70-4.

Laskowitz, D.T., Sheng, H., Bart, R.D., Joyner, K.A., Roses, A.D., Warner, D.S. (1997). Apolipoprotein E-deficient mice have increased susceptibility to focal cerebral ischemia. *J Cereb Blood Flow Metab.* **17(7)**, 753-8.

Laskowitz, D.T., Lee, D.M., Schmechel, D., Staats, H.F. (2000). Altered immune responses in apolipoprotein E-deficient mice. *J Lipid Res.* **41(4)**, 613-20.

Laskowitz, D.T., Thekdi, A.D., Thekdi, S.D., Han, S.K., Myers, J.K., Pizzo, S.V., Bennett, E.R. (2001). Downregulation of microglial activation by apolipoprotein E and apoE-mimetic peptides. *Exp Neurol.* **167(1)**, 74-85.

Lauderback, C.M., Kanski, J., Hackett, J.M., Maeda, N., Kindy, M.S., Butterfield, D.A. (2002). Apolipoprotein E modulates Alzheimer's Abeta(1-42)-induced oxidative damage to synaptosomes in an allele-specific manner. *Brain Res.* **924(1)**, 90-7.

Le Gros Clark, W.E. (1940). Neuronal differentiation in implanted foetal cortical tissue. *J. Neurol. Psychiatry.* **3**, 263-284.

Leclercq, P.D., Murray, L.S., Smith, C., Graham, D.I., Nicoll, J.A., Gentleman, S.M. (2005). Cerebral amyloid angiopathy in traumatic brain injury, association with apolipoprotein E genotype. *J Neurol Neurosurg Psychiatry.* **76(2)**, 229-33.

Lee, Y., Aono, M., Laskowitz, D., Warner, D.S., Pearlstein, R.D. (2004). Apolipoprotein E protects against oxidative stress in mixed neuronal-glial cell cultures by reducing glutamate toxicity. *Neurochem Int.* **44(2)**, 107-18.

Leung, C.H., Poon, W.S., Yu, L.M., Wong, G.K., Ng, H.K. (2002). Apolipoprotein e genotype and outcome in aneurysmal subarachnoid hemorrhage. *Stroke.* **33(2)**, 548-52.

Levi, O., Jongen-Relo, A.L., Feldon, J., Roses, A.D., Michaelson, D.M. (2003). ApoE4 impairs hippocampal plasticity isoform-specifically and blocks the environmental stimulation of synaptogenesis and memory. *Neurobiol Dis.* **13(3)**, 273-82.

Levine, S. & Sohn, D. (1969). Cerebral ischemia in infant and adult gerbils. Relation to incomplete circle of Willis. *Arch Pathol.* **87(3)**, 315-7.

Lewis, J. (1998). Notch signalling and the control of cell fate choices in vertebrates. *Semin Cell Dev Biol.* **9(6)**, 583-9.

Liberman, J.N., Stewart, W.F., Wesnes, K., Troncoso, J. (2002). Apolipoprotein E epsilon 4 and short-term recovery from predominantly mild brain injury. *Neurology.* **58(7)**, 1038-44.

Lichtman, S.W., Seliger, G., Tycko, B., Marder, K. (2000). Apolipoprotein E and functional recovery from brain injury following postacute rehabilitation. *Neurology.* **55(10)**, 1536-9.

Liestol, K., Kvittingen, E.A., Rootwelt, H., Dunlop, O., Goplen, A.K., Pedersen, J.C., Brorson, S.H., Borresen-Dale, A.L., Myrvang, B., Maehlen, J. (2000). Association between apolipoprotein E genotypes and cancer risk in patients with acquired immunodeficiency syndrome. *Cancer Detect Prev.* **24(5)**, 496-9.

Lindvall, O. (2000). Neural transplantation in Parkinson's disease. *Novartis Found Symp.* **231**, 110-23.

Lipton, P. (1999). Ischemic cell death in brain neurons. *Physiol Rev.* **79(4)**, 1431-568.

Liu, J., Solway, K., Messing, R.O., Sharp, F.R. (1998). Increased neurogenesis in the dentate gyrus after transient global ischemia in gerbils. *J Neurosci.* **18(19)**, 7768-78.

Liu, N.K. & Xu, X.M. (2006). beta-tubulin is a more suitable internal control than beta-actin in western blot analysis of spinal cord tissues after traumatic injury. *J Neurotrauma.* **23(12)**, 1794-801.

Liu, Y., Laakso, M.P., Karonen, J.O., Vanninen, R.L., Nuutinen, J., Soimakallio, S., Aronen, H.J. (2002). Apolipoprotein E polymorphism and acute ischemic stroke, a

diffusion- and perfusion-weighted magnetic resonance imaging study. *J Cereb Blood Flow Metab.* **22(11)**, 1336-42.

Lominska, C., Levin, J.A., Wang, J., Sikes, J., Kao, C., Smith, J.D. (2001). Apolipoprotein E deficiency effects on learning in mice are dependent upon the background strain. *Behav Brain Res.* **120(1)**, 23-34.

Lomnitski, L., Kohen, R., Chen, Y., Shohami, E., Trembovler, V., Vogel, T., Michaelson, D.M. (1997). Reduced levels of antioxidants in brains of apolipoprotein E-deficient mice following closed head injury. *Pharmacol Biochem Behav.* **56(4)**, 669-73.

Lomnitski, L., Chapman, S., Hochman, A., Kohen, R., Shohami, E., Chen, Y., Trembovler, V., Michaelson, D.M. (1999). Antioxidant mechanisms in apolipoprotein E deficient mice prior to and following closed head injury. *Biochim Biophys Acta.* **1453(3)**, 359-68.

Longstreth, W.T. Jr, Schellenberg, G.D., Fahrenbruch, C.E., Cobb, L.A., Copass, M.K., Siscovick, D.S. (2003). Apolipoprotein E genotypes and outcome from out of hospital cardiac arrest. *J Neurol Neurosurg Psychiatry.* **74(10)**, 1441-3.

Luine, V. & Hearns, M. (1990). Spatial memory deficits in aged rats, contributions of the cholinergic system assessed by ChAT. *Brain Res.* **523(2)**, 321-4.

Lund, R.D. & Hauschka, S.D. (1976). Transplanted neural tissue develops connections with host rat brain. *Science.* 193(4253), 582-4.

Lundberg, C., Winkler, C., Whittemore, S.R., Bjorklund, A. (1996). Conditionally immortalized neural progenitor cells grafted to the striatum exhibit site-specific neuronal differentiation and establish connections with the host globus pallidus. *Neurobiol Dis.* **3(1)**, 33-50.

Lundberg, C., Martinez-Serrano, A., Cattaneo, E., McKay, R.D., Bjorklund, A. (1997). Survival, integration, and differentiation of neural stem cell lines after transplantation to the adult rat striatum. *Exp Neurol.* **145(2 Pt 1)**, 342-60.

Lynch, J.R., Morgan, D., Mance, J., Matthew, W.D., Laskowitz, D.T. (2001). Apolipoprotein E modulates glial activation and the endogenous central nervous system inflammatory response. *J Neuroimmunol.* **114(1-2)**, 107-13.

Lynch, J.R., Pineda, J.A., Morgan, D., Zhang, L., Warner, D.S., Benveniste, H., Laskowitz, D.T. (2002). Apolipoprotein E affects the central nervous system response to injury and the development of cerebral edema. *Ann Neurol.* **51(1)**, 113-7.

Lythgoe, M.F., Thomas, D.L., King, M.D., Pell, G.S., van der Weerd, L., Ordidge, R.J., Gadian, D.G. (2005). Gradual changes in the apparent diffusion coefficient of water in selectively vulnerable brain regions following brief ischemia in the gerbil. *Magn Reson Med.* **53(3)**, 593-600.

MacLeod, M.J., De Lange, R.P., Breen, G., Meiklejohn, D., Lemmon, H., Clair, D.S. (2001). Lack of association between apolipoprotein E genoype and ischaemic stroke in a Scottish population. *Eur J Clin Invest.* **31(7)**, 570-3.

Mahley, R.W. (1988). Apolipoprotein E, cholesterol transport protein with expanding role in cell biology. *Science.* **240(4852)**, 622-30.

Mahley, R.W., Huang, Y. (1999). Apolipoprotein E, from atherosclerosis to Alzheimer's disease and beyond. *Curr Opin Lipidol.* **10(3)**, 207-17.

Mahley, R.W., Huang, Y., Rall, S.C. Jr. (1999). Pathogenesis of type III hyperlipoproteinemia (dysbetalipoproteinemia). Questions, quandaries, and paradoxes. *J Lipid Res.* **40(11)**, 1933-49.

Maltsev, V.A., Wobus, A.M., Rohwedel, J., Bader, M., Hescheler, J. (1994). Cardiomyocytes differentiated in vitro from embryonic stem cells developmentally express cardiac-specific genes and ionic currents. *Circ Res.* **75(2)**, 233-44.

Mantamadiotis, T., Lemberger, T., Bleckmann, S.C., Kern, H., Kretz, O., Martin Villalba, A., Tronche, F., Kellendonk, C., Gau, D., Kapfhammer, J., Otto, C., Schmid, W., Schutz, G. (2002). Disruption of CREB function in brain leads to neurodegeneration. *Nat Genet.* **31(1)**, 47-54.

Margaglione, M., Seripa, D., Gravina, C., Grandone, E., Vecchione, G., Cappucci, G., Merla, G., Papa, S., Postiglione, A., Di Minno, G., Fazio, V.M. (1998). Prevalence of apolipoprotein E alleles in healthy subjects and survivors of ischemic stroke, an Italian Case-Control Study. *Stroke.* **29(2)**, 399-403.

Martin, G.R. (1981). Isolation of a pluripotent cell line from early mouse embryos cultured in medium conditioned by teratocarcinoma stem cells. *Proc Natl Acad Sci USA.* **78(12)**, 7634-8.

Martin, R.L., Lloyd, H.G., Cowan, A.I. (1994). The early events of oxygen and glucose deprivation, setting the scene for neuronal death? *Trends Neurosci.* **17(6)**, 251-7.

Martin-Blanco, E., Pastor-Pareja, J.C., Garcia-Bellido, A. (2000). JNK and decapentaplegic signaling control adhesiveness and cytoskeleton dynamics during thorax closure in Drosophila. *Proc Natl Acad Sci USA.* **97(14)**, 7888-93.

Martinez-Serrano, A., Lundberg, C., Horellou, P., Fischer, W., Bentlage, C., Campbell, K., McKay, R.D., Mallet, J., Bjorklund, A. (1995). CNS-derived neural progenitor cells for gene transfer of nerve growth factor to the adult rat brain, complete rescue of axotomized cholinergic neurons after transplantation into the septum. *J Neurosci.* **15(8)**, 5668-80.

Masliah, E., Mallory, M., Ge, N., Alford, M., Veinbergs, I., Roses, A.D. (1995). Neurodegeneration in the central nervous system of apoE-deficient mice. *Exp Neurol.* **136(2)**, 107-22.

Masliah, E., Mallory, M., Veinbergs, I., Miller, A., Samuel, W. (1996). Alterations in apolipoprotein E expression during aging and neurodegeneration. *Prog Neurobiol.* **50(5-6)**, 493-503.

Masliah, E., Samuel, W., Veinbergs, I., Mallory, M., Mante, M., Saitoh, T. (1997). Neurodegeneration and cognitive impairment in apoE-deficient mice is ameliorated by infusion of recombinant apoE. *Brain Res.* **751(2)**, 307-14.

Mason, H.A., Rakowiecki, S.M., Gridley, T., Fishell, G. (2006). Loss of notch activity in the developing central nervous system leads to increased cell death. *Dev Neurosci.* **28(1-2)**, 49-57.

Matsuoka, N., Nozaki, K., Takagi, Y., Nishimura, M., Hayashi, J., Miyatake, S., Hashimoto, N. (2003). Adenovirus-mediated gene transfer of fibroblast growth factor-2 increases BrdU-positive cells after forebrain ischemia in gerbils. *Stroke.* **34(6)**, 1519-25.

May, P., Bock, H.H., Nimpf, J., Herz, J. (2003). Differential glycosylation regulates processing of lipoprotein receptors by gamma-secretase. *J Biol Chem.* **278(39)**, 37386-92.

May, P., Rohlmann, A., Bock, H.H., Zurhove, K., Marth, J.D., Schomburg, E.D., Noebels, J.L., Beffert, U., Sweatt, J.D., Weeber, E.J., Herz, J. (2004). Neuronal LRP1 functionally associates with postsynaptic proteins and is required for normal motor function in mice. *Mol Cell Biol.* **24(20)**, 8872-83.

McCarron, M.O., Nicoll, J.A. (1998). High frequency of apolipoprotein E epsilon 2 allele is specific for patients with cerebral amyloid angiopathy-related haemorrhage. *Neurosci Lett.* **247(1)**, 45-8.

McCarron, M.O., Nicoll, J.A., Graham, D.I. (1998). A quartet of Down's syndrome, Alzheimer's disease, cerebral amyloid angiopathy, and cerebral haemorrhage, interacting genetic risk factors. *J Neurol Neurosurg Psychiatry.* **65(3)**, 405-6

McCarron, M.O., Delong, D., Alberts, M.J. (1999). APOE genotype as a risk factor for ischemic cerebrovascular disease, a meta-analysis. *Neurology.* **53(6)**, 1308-11.

McCarron, M.O., Hoffmann, K.L., DeLong, D.M., Gray, L., Saunders, A.M., Alberts, M.J. (1999). Intracerebral hemorrhage outcome, apolipoprotein E genotype, hematoma, and edema volumes. *Neurology.* **53(9)**, 2176-9.

McCarron, M.O., Muir, K.W., Nicoll, J.A., Stewart, J., Currie, Y., Brown, K., Bone, I. (2000). Prospective study of apolipoprotein E genotype and functional outcome following ischemic stroke. *Arch Neurol.* **57(10)**, 1480-4.

McCarron, M.O., Weir, C.J., Muir, K.W., Hoffmann, K.L., Graffagnino, C., Nicoll, J.A., Lees, K.R., Alberts, M.J. (2003). Effect of apolipoprotein E genotype on in-hospital mortality following intracerebral haemorrhage. *Acta Neurol Scand.* **107(2)**, 106-9.

McKracken, E., Graham, D.I., Nilsen, M., Stewart, J., Nicoll, J.A., Horsburgh, K. (2001). 4-Hydroxynonenal immunoreactivity is increased in human hippocampus after global ischemia. *Brain Pathol.* **11(4)**, 414-21.

Mellodew, K., Suhr, R., Uwanogho, D.A., Reuter, I., Lendahl, U., Hodges, H., Price, J. (2004). Nestin expression is lost in a neural stem cell line through a mechanism involving the proteasome and Notch signalling. *Brain Res Dev Brain Res.* **151(1-2)**, 13-23.

Meltzer, C.C., Kondziolka, D., Villemagne, V.L., Wechsler, L., Goldstein, S., Thulborn, K.R., Gebel, J., Elder, E.M., DeCesare, S., Jacobs, A.. (2001). Serial [18F] fluorodeoxyglucose positron emission tomography after human neuronal implantation for stroke. *Neurosurgery.* **49(3)**, 586-91

Menzel, H.J., Kladetzky, R.G., Assmann, G. (1983). Apolipoprotein E polymorphism and coronary artery disease. *Arteriosclerosis.* **3(4)**, 310-5.

Miller, A.K., Alston, R.L., Corsellis, J.A. (1980). Variation with age in the volumes of grey and white matter in the cerebral hemispheres of man, measurements with an image analyser. *Neuropathol Appl Neurobiol.* **6(2)**, 119-32.

Miyata, M., Smith, J.D. (1996). Apolipoprotein E allele-specific antioxidant activity and effects on cytotoxicity by oxidative insults and beta-amyloid peptides. *Nat Genet.* **14(1)**, 55-61.

Miyazono, M., Nowell, P.C., Finan, J.L., Lee, V.M., Trojanowski, J.Q. (1996). Long-term integration and neuronal differentiation of human embryonal carcinoma cells (NTera-2) transplanted into the caudoputamen of nude mice. *J Comp Neurol.* **376(4)**, 603-13.

Modo, M., Rezaie, P., Heuschling, P., Patel, S., Male, D.K., Hodges, H. (2002). Transplantation of neural stem cells in a rat model of stroke, assessment of short-term graft survival and acute host immunological response. *Brain Res.* **958(1)**, 70-82.

Modo, M., Stroemer, R.P., Tang, E., Patel, S., Hodges, H. (2002). Effects of implantation site of stem cell grafts on behavioral recovery from stroke damage. *Stroke.* **33(9)**, 2270-8.

Modo, M., Hopkins, K., Virley, D., Hodges, H. (2003). Transplantation of neural stem cells modulates apolipoprotein E expression in a rat model of stroke. *Exp Neurol.* **183(2)**, 320-9.

Modo, M., Mellodew, K., Rezaie, P. (2003). In vitro expression of major histocompatibility class I and class II antigens by conditionally immortalized murine neural stem cells. *Neurosci Lett.* **337(2)**, 85-8.

Monaghan, D.T. & Cotman, C.W. (1985). Distribution of N-methyl-D-aspartate-sensitive L-[3H]glutamate-binding sites in rat brain. *J Neurosci.* **5(11)**, 2909-19.

Montoya, C.P., Campbell-Hope, L.J., Pemberton, K.D., Dunnett, S.B. (1991). The "staircase test", a measure of independent forelimb reaching and grasping abilities in rats. *J Neurosci Methods.* **36(2-3)**, 219-28.

Montpied, P., de Bock, F., Lerner-Natoli, M., Bockaert, J., Rondouin, G. (1999). Hippocampal alterations of apolipoprotein E and D mRNA levels in vivo and in vitro following kainate excitotoxicity. *Epilepsy Res.* **35(2)**, 135-46.

Moysich, K.B., Freudenheim, J.L., Baker, J.A., Ambrosone, C.B., Bowman, E.D., Schisterman, E.F., Vena, J.E., Shields, P.G. (2000). Apolipoprotein E genetic polymorphism, serum lipoproteins, and breast cancer risk. *Mol Carcinog.* **27(1)**, 2-9.

Muir, J.K., Raghupathi, R., Saatman, K.E., Wilson, C.A., Lee, V.M., Trojanowski, J.Q., Philips, M.F., McIntosh, T.K. (1999). Terminally differentiated human neurons survive and integrate following transplantation into the traumatically injured rat brain. *J Neurotrauma.* **16(5)**, 403-14.

Muroyama, Y., Kondoh, H., Takada, S. (2004). Wnt proteins promote neuronal differentiation in neural stem cell culture. *Biochem Biophys Res Commun.* **313(4)**, 915-21.

Nakai, M., Kawamata, T., Taniguchi, T., Maeda, K., Tanaka, C. (1996). Expression of apolipoprotein E mRNA in rat microglia. *Neurosci Lett.* **211(1)**, 41-4.

Nakatomi, H., Kuriu, T., Okabe, S., Yamamoto, S., Hatano, O., Kawahara, N., Tamura, A., Kirino, T., Nakafuku, M. (2002). Regeneration of hippocampal pyramidal neurons after ischemic brain injury by recruitment of endogenous neural progenitors. *Cell.* **110(4)**, 429-41.

Namba, Y., Tomonaga, M., Kawasaki, H., Otomo, E., Ikeda, K. (1991). Apolipoprotein E immunoreactivity in cerebral amyloid deposits and neurofibrillary tangles in Alzheimer's disease and kuru plaque amyloid in Creutzfeldt-Jakob disease. *Brain Res.* **541(1)**, 163-6.

Namura, S., Zhu, J., Fink, K., Endres, M., Srinivasan, A., Tomaselli, K.J., Yuan, J., Moskowitz, M.A. (1998). Activation and cleavage of caspase-3 in apoptosis induced by experimental cerebral ischemia. *J Neurosci.* **18(10)**, 3659-68.

Nathan, B.P., Bellosta, S., Sanan, D.A., Weisgraber, K.H., Mahley, R.W., Pitas, R.E. (1994). Differential effects of apolipoproteins E3 and E4 on neuronal growth in vitro. *Science.* **264(5160)**, 850-2.

Nathan, B.P., Chang, K.C., Bellosta, S., Brisch, E., Ge, N., Mahley, R.W., Pitas, R.E. (1995). The inhibitory effect of apolipoprotein E4 on neurite outgrowth is associated with microtubule depolymerization. *J Biol Chem.* **270(34)**, 19791-9.

Nathan, B.P., Jiang, Y., Wong, G.K., Shen, F., Brewer, G.J., Struble, R.G. (2002). Apolipoprotein E4 inhibits, and apolipoprotein E3 promotes neurite outgrowth in cultured adult mouse cortical neurons through the low-density lipoprotein receptor-related protein. *Brain Res.* **928(1-2)**, 96-105.

Nelson, P.T., Kondziolka, D., Wechsler, L., Goldstein, S., Gebel, J., DeCesare, S., Elder, E.M., Zhang, P.J., Jacobs, A., McGrogan, M., Lee, V.M., Trojanowski, J.Q. (2002). Clonal human (hNT) neuron grafts for stroke therapy, neuropathology in a patient 27 months after implantation. *Am J Pathol.* **160(4)**, 1201-6.

Nicoll, J.A., Roberts, G.W., Graham, D.I. (1995). Apolipoprotein E epsilon 4 allele is associated with deposition of amyloid beta-protein following head injury. *Nat Med.* **1(2)**, 135-7.

Nicoll, J.A., Roberts, G.W., Graham, D.I. (1996). Amyloid beta-protein, APOE genotype and head injury. *Ann. N Y Acad Sci.* **777**, 271-5.

Nicoll, J.A., Burnett, C., Love, S., Graham, D.I., Dewar, D., Ironside, J.W., Stewart, J., Vinters, H.V. (1997). High frequency of apolipoprotein E epsilon 2 allele in hemorrhage due to cerebral amyloid angiopathy. *Ann Neurol.* **41(6)**, 716-21.

Nishio, M., Kohmura, E., Yuguchi, T., Nakajima, Y., Fujinaka, T., Akiyama, C., Iwata, A., Yoshimine, T. (2003). Neuronal apolipoprotein E is not synthesized in neuron after focal ischemia in rat brain. *Neurol Res.* **25(4)**, 390-4.

Niskakangas, T., Ohman, J., Niemela, M., Ilveskoski, E., Kunnas, T.A., Karhunen, P.J. (2001). Association of apolipoprotein E polymorphism with outcome after aneurysmal subarachnoid hemorrhage, a preliminary study. *Stroke.* **32(5)**, 1181-4.

Novak, S., Hiesberger, T., Schneider, W.J., Nimpf, J. (1996). A new low density lipoprotein receptor homologue with 8 ligand binding repeats in brain of chicken and mouse. *J Biol Chem.* **271(20)**, 11732-6.

Nunn, J. & Hodges, H. (1994). Cognitive deficits induced by global cerebral ischaemia, relationship to brain damage and reversal by transplants. *Behav Brain Res.* **65(1)**, 1-31.

Nykjaer, A., Dragun, D., Walther, D., Vorum, H., Jacobsen, C., Herz, J., Melsen, F., Christensen, E.I., Willnow, T.E. (1999). An endocytic pathway essential for renal uptake and activation of the steroid 25-(OH) vitamin D3. *Cell.* **96(4)**, 507-15.

O'Donnell, H.C., Rosand, J., Knudsen, K.A., Furie, K.L., Segal, A.Z., Chiu, R.I., Ikeda, D., Greenberg, S.M. (2000). Apolipoprotein E genotype and the risk of recurrent lobar intracerebral hemorrhage. *N Engl J Med.* **342(4)**, 240-5.

Ohkubo, N., Mitsuda, N., Tamatani, M., Yamaguchi, A., Lee, Y.D., Ogihara, T., Vitek, M.P., Tohyama, M. (2001). Apolipoprotein E4 stimulates cAMP response element-binding protein transcriptional activity through the extracellular signal-regulated kinase pathway. *J Biol Chem.* **276(5)**, 3046-53.

Ohkubo, N., Lee, Y.D., Morishima, A., Terashima, T., Kikkawa, S., Tohyama, M., Sakanaka, M., Tanaka, J., Maeda, N., Vitek, M.P., Mitsuda, N. (2003). Apolipoprotein E and Reelin ligands modulate tau phosphorylation through an apolipoprotein E receptor/disabled-1/glycogen synthase kinase-3beta cascade. *FASEB J.* **17(2)**, 295-7.

Ohshima, T., Ogawa, M., Veeranna Hirasawa, M., Longenecker, G., Ishiguro, K., Pant, H.C., Brady, R.O., Kulkarni, A.B., Mikoshiba, K. (2001). Synergistic contributions of cyclin-dependant kinase 5/p35 and Reelin/Dab1 to the positioning of cortical neurons in the developing mouse brain. *Proc Natl Acad Sci USA.* **98(5)**, 2764-9.

Oishi, K., Kamakura, S., Isazawa, Y., Yoshimatsu, T., Kuida, K., Nakafuku, M., Masuyama, N., Gotoh, Y. (2004). Notch promotes survival of neural precursor cells via mechanisms distinct from those regulating neurogenesis. *Dev Biol.* **276(1)**, 172-84.

Oitzl, M.S., Mulder, M., Lucassen, P.J., Havekes, L.M., Grootendorst, J., de Kloet, E.R. (1997). Severe learning deficits in apolipoprotein E-knockout mice in a water maze task. *Brain Res.* **752(1-2)**, 189-96.

Olanow, C.W., Goetz, C.G., Kordower, J.H., Stoessl, A.J., Sossi, V., Brin, M.F., Shannon, K.M., Nauert, G.M., Perl, D.P., Godbold, J., Freeman, T.B. (2003). A double-blind controlled trial of bilateral fetal nigral transplantation in Parkinson's disease. *Ann Neurol.* **54(3)**, 403-14.

Olichney, J.M., Hansen, L.A., Galasko, D., Saitoh, T., Hofstetter, C.R., Katzman, R., Thal, L.J. (1996). The apolipoprotein E epsilon 4 allele is associated with increased neuritic plaques and cerebral amyloid angiopathy in Alzheimer's disease and Lewy body variant. *Neurology.* **47(1)**, 190-6.

Otero, J.J., Fu, W., Kan, L., Cuadra, A.E., Kessler, J.A. (2004). Beta-catenin signaling is required for neural differentiation of embryonic stem cells. *Development.* **131(15)**, 3545-57.

Parent, J.M., Yu, T.W., Leibowitz, R.T., Geschwind, D.H., Sloviter, R.S., Lowenstein, D.H. (1997). Dentate granule cell neurogenesis is increased by seizures and contributes to aberrant network reorganization in the adult rat hippocampus. *J Neurosci.* **17(10)**, 3727-38.

Parent, J.M., Valentin, V.V., Lowenstein, D.H. (2002). Prolonged seizures increase proliferating neuroblasts in the adult rat subventricular zone-olfactory bulb pathway. *J Neurosci.* **22(8)**, 3174-88.

Park, K.I. (2000). Transplantation of neural stem cells, cellular & gene therapy for hypoxic-ischemic brain injury. *Yonsei Med J.* **41(6)**, 825-35.

Park, K.I., Teng, Y.D., Snyder, E.Y. (2002). The injured brain interacts reciprocally with neural stem cells supported by scaffolds to reconstitute lost tissue. *Nat. Biotechnol.* **20(11)**, 1111-7.

Paton, J.A. & Nottebohm, F.N. (1984). Neurons generated in the adult brain are recruited into functional circuits. *Science.* **225(4666)**, 1046-8.

Paxinos, G. and Franklin, K.B.J., (2001). *The Mouse Brain in Stereotaxic Coordinates, Second Edition,* Academic Press, San Diego.

Pedersen, E.B., Poulsen, F.R., Zimmer, J., Finsen, B. (1995). Prevention of mouse-rat brain xenograft rejection by a combination therapy of cyclosporin A, prednisolone and azathioprine. *Exp Brain Res.* **106(2)**, 181-6.

Pedersen, E.B., Zimmer, J., Finsen, B. (1997). Triple immunosuppression protects murine intracerebral, hippocampal xenografts in adult rat hosts: effects on cellular infiltration, major histocompatibility complex antigen induction and blood-brain barrier leakage. *Neuroscience.* **78(3)**, 685-701.

Peled, A., Petit, I., Kollet, O., Magid, M., Ponomaryov, T., Byk, T., Nagler, A., Ben-Hur, H., Many, A., Shultz, L., Lider, O., Alon, R., Zipori, D., Lapidot, T. (1999). Dependence of human stem cell engraftment and repopulation of NOD/SCID mice on CXCR4. *Science.* **283(5403)**, 845-8.

Peng, D.Q., Zhao, S.P., Wang, J.L. (1999). Lipoprotein (a) and apolipoprotein E epsilon 4 as independent risk factors for ischemic stroke. *J Cardiovasc Risk.* **6(1)**, 1-6.

Perlow, M.J., Freed, W.J., Hoffer, B.J., Seiger, A., Olson, L., Wyatt, R.J. (1979). Brain grafts reduce motor abnormalities produced by destruction of nigrostriatal dopamine system. *Science.* **204(4393)**, 643-7.

Peterson, D.A. (2002). Stem cells in brain plasticity and repair. *Curr Opin Pharmacol.* **2(1)**, 34-42.

Petito, C.K., Feldmann, E., Pulsinelli, W.A., Plum, F. (1987). Delayed hippocampal damage in humans following cardiorespiratory arrest. *Neurology.* **37(8)**, 1281-6.

Petito, C.K., Morgello, S., Felix, J.C., Lesser, M.L. (1990). The two patterns of reactive astrocytosis in postischemic rat brain. *J Cereb Blood Flow Metab.* **10(6)**, 850-9.

Petit-Turcotte, C., Aumont, N., Beffert, U., Dea, D., Herz, J., Poirier, J. (2005). The apoE receptor apoER2 is involved in the maintenance of efficient synaptic plasticity. *Neurobiol Aging.* **26(2)**, 195-206.

Philips, M.F., Muir, J.K., Saatman, K.E., Raghupathi, R., Lee, V.M., Trojanowski, J.Q., McIntosh, T.K. (1999). Survival and integration of transplanted postmitotic human neurons following experimental brain injury in immunocompetent rats. *J Neurosurg.* **90(1)**, 116-24.

Piedrahita, J.A., Zhang, S.H., Hagaman, J.R., Oliver, P.M., Maeda, N. (1992). Generation of mice carrying a mutant apolipoprotein E gene inactivated by gene targeting in embryonic stem cells. *Proc Natl Acad Sci USA.* **89(10)**, 4471-5.

Pietrzik, C.U., Busse, T., Merriam, D.E., Weggen, S., Koo, E.H. (2002). The cytoplasmic domain of the LDL receptor-related protein regulates multiple steps in APP processing. *EMBO J.* 21(21), 5691-700.

Pitas, R.E., Boyles, J.K., Lee, S.H., Foss, D., Mahley, R.W. (1987). Astrocytes synthesize apolipoprotein E and metabolize apolipoprotein E-containing lipoproteins. *Biochim Biophys Acta.* **917(1)**, 148-61.

Pleasure, S.J., Page, C., Lee, V.M. (1992). Pure, postmitotic, polarized human neurons derived from NTera 2 cells provide a system for expressing exogenous proteins in terminally differentiated neurons. *J Neurosci.* **12(5)**, 1802-15.

Plump, A.S., Smith, J.D., Hayek, T., Aalto-Setala, K., Walsh, A., Verstuyft, J.G., Rubin, E.M., Breslow, J.L. (1992). Severe hypercholesterolemia and atherosclerosis in apolipoprotein E-deficient mice created by homologous recombination in ES cells. *Cell.* **71(2)**, 343-53.

Poirier, J., Baccichet, A., Dea, D., Gauthier, S. (1993). Cholesterol synthesis and lipoprotein reuptake during synaptic remodelling in hippocampus in adult rats. *Neuroscience.* **55(1)**, 81-90.

Pollock, K., Stroemer, P., Patel, S., Stevanato, L., Hope, A., Miljan, E., Dong, Z., Hodges, H., Price, J., Sinden, J.D. (2006). A conditionally immortal clonal stem cell line from human cortical neuroepithelium for the treatment of ischemic stroke. *Exp Neurol.* **199(1)**, 143-55.

Ponomaryov, T., Peled, A., Petit, I., Taichman, R.S., Habler, L., Sandbank, J., Arenzana-Seisdedos, F., Magerus, A., Caruz, A., Fujii, N., Nagler, A., Lahav, M., Szyper-Kravitz, M., Zipori, D., Lapidot, T. (2000). Induction of the chemokine stromal-derived factor-1 following DNA damage improves human stem cell function. *J Clin Invest.* **106(11)**, 1331-9.

Premkumar, D.R., Cohen, D.L., Hedera, P., Friedland, R.P., Kalaria, R.N. (1996). Apolipoprotein E-epsilon4 alleles in cerebral amyloid angiopathy and cerebrovascular pathology associated with Alzheimer's disease. *Am J Pathol.* **148(6)**, 2083-95.

Pulsinelli, W.A. & Brierley, J.B. (1979). A new model of bilateral hemispheric ischemia in the unanesthetized rat. *Stroke.* **10(3)**, 267-72.

Pulsinelli, W.A., Brierley, J.B., Plum, F. (1982). Temporal profile of neuronal damage in a model of transient forebrain ischemia. *Ann Neurol.* **11(5)**, 491-8.

Pulsinelli, W.A. (1985). Selective neuronal vulnerability, morphological and molecular characteristics. *Prog Brain Res.* **63**, 29-37.

Qiu, Z., Strickland, D.K., Hyman, B.T., Rebeck, G.W. (2002). alpha 2-Macroglobulin exposure reduces calcium responses to N-methyl-D-aspartate via low density lipoprotein receptor-related protein in cultured hippocampal neurons. *J Biol Chem.* **277(17)**, 14458-66.

Qiu, Z., Crutcher, K.A., Hyman, B.T., Rebeck, G.W. (2003). ApoE isoforms affect neuronal N-methyl-D-aspartate calcium responses and toxicity via receptor-mediated processes. *Neuroscience.* **122(2)**, 291-303.

Qiu, Z., Hyman, B.T., Rebeck, G.W. (2004). Apolipoprotein E receptors mediate neurite outgrowth through activation of p44/42 mitogen-activated protein kinase in primary neurons. *J Biol Chem.* **279(33)**, 34948-56.

Raballo, R., Rhee, J., Lyn-Cook, R., Leckman, J.F., Schwartz, M.L., Vaccarino, F.M. (2000). Basic fibroblast growth factor (FGF2) is necessary for cell proliferation and neurogenesis in the developing cerebral cortex. *J Neurosci.* **20(13)**, 5012-23.

Raber, J., Wong, D., Buttini, M., Orth, M., Bellosta, S., Pitas, R.E., Mahley, R.W., Mucke, L. (1998). Isoform-specific effects of human apolipoprotein E on brain function revealed in ApoE knockout mice, increased susceptibility of females. *Proc Natl Acad Sci USA.* **95(18)**, 10914-9.

Raffai, R.L., Dong, L.M., Farese, R.V. Jr., Weisgraber, K.H. (2001). Introduction of human apolipoprotein E4 "domain interaction" into mouse apolipoprotein E. *Proc Natl Acad Sci USA.* **98(20)**, 11587-91.

Raisman, G. (1969). Neuronal plasticity in the septal nuclei of the adult rat. *Brain Res.* **14(1)**, 25-48.

Rajavashisth, T.B., Kaptein, J.S., Reue, K.L., Lusis, A.J. (1985). Evolution of apolipoprotein E, mouse sequence and evidence for an 11-nucleotide ancestral unit. *Proc Natl Acad Sci USA.* **82(23)**, 8085-9.

Ramassamy, C., Krzywkowski, P., Averill, D., Lussier-Cacan, S., Theroux, L., Christen, Y., Davignon, J., Poirier, J. (2001). Impact of apoE deficiency on oxidative insults and antioxidant levels in the brain. *Brain Res Mol Brain Res.* **86(1-2)**, 76-83.

Ramon y Cajal, S. (1928). Degeneration and regeneration of the nervous system. Volume 2. New York, Haffner Publishing Co.

Rebeck, G.W., Reiter, J.S., Strickland, D.K., Hyman, B.T. (1993). Apolipoprotein E in sporadic Alzheimer's disease, allelic variation and receptor interactions. *Neuron.* **11(4)**, 575-80.

Reynolds, B.A. & Weiss, S. (1992). Generation of neurons and astrocytes from isolated cells of the adult mammalian central nervous system. *Science.* **255(5052)**, 1707-10.

Riess, P., Zhang, C., Saatman, K.E., Laurer, H.L., Longhi, L.G., Raghupathi, R., Lenzlinger, P.M., Lifshitz, J., Boockvar, J., Neugebauer, E., Snyder, E.Y., McIntosh, T.K. (2002). Transplanted neural stem cells survive, differentiate, and improve neurological motor function after experimental traumatic brain injury. *Neurosurgery.* **51(4)**, 1043-52.

Roberts, T.J., Price, J., Williams, S.C., Modo, M. (2006). Preservation of striatal tissue and behavioral function after neural stem cell transplantation in a rat model of Huntington's disease. *Neuroscience.* **139(4)**, 1187-99.

Robin, A.M., Zhang, Z.G., Wang, L., Zhang, R.L., Katakowski, M., Zhang, L., Wang, Y., Zhang, C., Chopp, M. (2006). Stromal cell-derived factor 1alpha mediates neural progenitor cell motility after focal cerebral ischemia. *J Cereb Blood Flow Metab.* **26(1)**, 125-34.

Roessler, E., Belloni, E., Gaudenz, K., Jay, P., Berta, P., Scherer, S.W., Tsui, L.C., Muenke, M. (1996). Mutations in the human Sonic Hedgehog gene cause holoprosencephaly. *Nat Genet.* **14(3)**, 357-60.

Roselaar, S.E., Daugherty, A. (1998). Apolipoprotein E-deficient mice have impaired innate immune responses to Listeria monocytogenes in vivo. *J Lipid Res.* **39(9)**, 1740-3.

Rosen, G.D., Williams, R.W. (2001). Complex trait analysis of the mouse striatum, independent QTLs modulate volume and neuron number. *BMC Neurosci.* **2** ,5.

Roses, A.D., Einstein, G., Gilbert, J., Goedert, M., Han, S.H., Huang, D., Hulette, C., Masliah, E., Pericak-Vance, M.A., Saunders, A.M., Schmechel, D.E., Strittmatter, W.J., Weisgraber, K.H., Xi, P.T. (1996). Morphological, biochemical, and genetic support for an apolipoprotein E effect on microtubular metabolism. *Ann N Y Acad Sci.* **777**, 146-57.

Ross, D.T. & Duhaime, A.C. (1989). Degeneration of neurons in the thalamic reticular nucleus following transient ischemia due to raised intracranial pressure, excitotoxic degeneration mediated via non-NMDA receptors? *Brain Res.* **501(1)**, 129-43.

Rothman, S.M. & Olney, J.W. (1986). Glutamate and the pathophysiology of hypoxic--ischemic brain damage. *Ann Neurol.* **19(2)**, 105-11.

Ryder, E.F., Snyder, E.Y., Cepko, C.L. (1990). Establishment and characterization of multipotent neural cell lines using retrovirus vector-mediated oncogene transfer. *J Neurobiol.* **21(2)**, 356-75.

Sabo, T., Lomnitski, L., Nyska, A., Beni, S., Maronpot, R.R., Shohami, E., Roses, A.D., Michaelson, D.M. (2000). Susceptibility of transgenic mice expressing human apolipoprotein E to closed head injury, the allele E3 is neuroprotective whereas E4 increases fatalities. *Neuroscience.* **101(4)**, 879-84.

Sairanen, T.R., Lindsberg, P.J., Brenner, M., Sirén, A.L. (1997). Global forebrain ischemia results in differential cellular expression of interleukin-1beta (IL-1β) and its receptor at mRNA and protein level. *J Cereb Blood Flow Metab.* **17(10)**, 1107-20.

Saito, K., Suyama, K., Nishida, K., Sei, Y., Basile, A.S. (1996). Early increases in TNF-alpha, IL-6 and IL-1 beta levels following transient cerebral ischemia in gerbil brain. *Neurosci Lett.* **206(2-3)**, 149-52.

Sakata, A., Tamai, I., Kawazu, K., Deguchi, Y., Ohnishi, T., Saheki, A., Tsuji, A. (1994). In vivo evidence for ATP-dependent and P-glycoprotein-mediated transport of cyclosporin A at the blood-brain barrier. *Biochem Pharmacol.* **48(10)**, 1989-92.

Saporta, S., Borlongan, C.V., Sanberg, P.R. (1999). Neural transplantation of human neuroteratocarcinoma (hNT) neurons into ischemic rats. A quantitative dose-response analysis of cell survival and behavioral recovery. *Neuroscience.* **91(2)**, 519-25.

Saunders, A.M., Strittmatter, W.J., Schmechel, D., George-Hyslop, P.H., Pericak-Vance, M.A., Joo, S.H., Rosi, B.L., Gusella, J.F., Crapper-MacLachlan, D.R., Alberts, M.J. (1993). Association of apolipoprotein E allele epsilon 4 with late-onset familial and sporadic Alzheimer's disease. *Neurology.* **43(8)**, 1467-72.

Schiefermeier, M., Kollegger, H., Madl, C., Schwarz, C., Holzer, M., Kofler, J., Sterz, F. (2000). Apolipoprotein E polymorphism, survival and neurological outcome after cardiopulmonary resuscitation. *Stroke.* **31(9)**, 2068-73.

Schmechel, D.E., Saunders, A.M., Strittmatter, W.J., Crain, B.J., Hulette, C.M., Joo, S.H., Pericak-Vance, M.A., Goldgaber, D., Roses, A.D. (1993). Increased amyloid beta-peptide deposition in cerebral cortex as a consequence of apolipoprotein E genotype in late-onset Alzheimer disease. *Proc Natl Acad Sci USA.* **90(20)**, 9649-53.

Selkoe, D.J. (2002). Deciphering the genesis and fate of amyloid beta-protein yields novel therapies for Alzheimer disease. *J Clin Invest.* **110(10)**, 1375-81.

Shea, T.B., Rogers, E., Ashline, D., Ortiz, D., Sheu, M.S. (2002). Apolipoprotein E deficiency promotes increased oxidative stress and compensatory increases in antioxidants in brain tissue. *Free Radic Biol Med.* **33(8)**, 1115-20.

Sheldon, M, Rice, D.S., D'Arcangelo, G., Yoneshima, H., Nakajima, K., Mikoshiba, K., Howell, B.W., Cooper, J.A., Goldowitz, D., Curran, T. (1997). Scrambler and yotari disrupt the disabled gene and produce a reeler-like phenotype in mice. *Nature.* **389(6652)**, 730-3.

Sheng, H., Laskowitz, D.T., Bennett, E., Schmechel, D.E., Bart, R.D., Saunders, A.M., Pearlstein, R.D., Roses, A.D., Warner, D.S. (1998). Apolipoprotein E isoform-specific differences in outcome from focal ischemia in transgenic mice. *J Cereb Blood Flow Metab.* **18(4)**, 361-6.

Sheng, H., Laskowitz, D.T., Mackensen, G.B., Kudo, M., Pearlstein, R.D., Warner, D.S. (1999). Apolipoprotein E deficiency worsens outcome from global cerebral ischemia in the mouse. *Stroke.* **30(5)**, 1118-24.

Shihabuddin, L.S., Hertz, J.A., Holets, V.R., Whittemore, S.R. (1995). The adult CNS retains the potential to direct region-specific differentiation of a transplanted neuronal precursor cell line. *J Neurosci.* **15(10)**, 6666-78.

Shihabuddin, L.S., Brunschwig, J.P., Holets, V.R., Bunge, M.B., Whittemore, S.R. (1996). Induction of mature neuronal properties in immortalized neuronal precursor cells following grafting into the neonatal CNS. *J Neurocytol.* **25(2)**, 101-11.

Shihabuddin, L.S., Holets, V.R., Whittemore, S.R. (1996). Selective hippocampal lesions differentially affect the phenotypic fate of transplanted neuronal precursor cells. *Exp Neurol.* **139(1)**, 61-72.

Shin, E.Y., Kim, S.Y., Kim, E.G. (2001). c-Jun N-terminal kinase is involved in motility of endothelial cell. *Exp Mol Med.* **33(4)**, 276-83.

Shinoda, M., Hudson, J.L., Stromberg, I., Hoffer, B.J., Moorhead, J.W., Olson, L. (1995). Allogeneic grafts of fetal dopamine neurons, immunological reactions following active and adoptive immunizations. *Brain Res.* **680(1-2)**, 180-95.

Shore, V.G. & Shore, B. (1973). Heterogeneity of human plasma very low density lipoproteins. Separation of species differing in protein components. *Biochemistry.* **12(3)**, 502-7.

Siesjo, B.K., Agardh, C.D., Bengtsson, F. (1989). Free radicals and brain damage. *Cerebrovasc Brain Metab Rev.* **1(3)**, 165-211.

Siesjo, B.K. (1992). Pathophysiology and treatment of focal cerebral ischemia. Part I, Pathophysiology. *J Neurosurg.* **77(2)**, 169-84.

Siesjo, B.K. (1992). Pathophysiology and treatment of focal cerebral ischemia. Part II, Mechanisms of damage and treatment. *J Neurosurg.* **77(3)**, 337-54.

Sinden, J.D., Rashid-Doubell, F., Kershaw, T.R., Nelson, A., Chadwick, A., Jat, P.S., Noble, M.D., Hodges, H., Gray, J.A. (1997). Recovery of spatial learning by grafts of a conditionally immortalized hippocampal neuroepithelial cell line into the ischaemia-lesioned hippocampus. *Neuroscience.* **81(3)**, 599-608.

Slooter, A.J., Tang, M.X., van Duijn, C.M., Stern, Y., Ott, A., Bell, K., Breteler, M.M., Van Broeckhoven, C., Tatemichi, T.K., Tycko, B., Hofman, A., Mayeux, R. (1997). Apolipoprotein E epsilon4 and the risk of dementia with stroke. A population-based investigation. *JAMA.* **277(10)**, 818-21.

Slooter, A.J., Cruts, M., Hofman, A., Koudstaal, P.J., van der Kuip, D., de Ridder, M.A., Witteman, J.C., Breteler, M.M., Van Broeckhoven, C., van Duijn, C.M. (2004). The impact of APOE on myocardial infarction, stroke, and dementia, the Rotterdam Study. *Neurology.* **62(7)**, 1196-8.

Smith, C., Graham, D.I., Murray, L.S., Stewart, J., Nicoll, J.A. (2006). Association of APOE e4 and cerebrovascular pathology in traumatic brain injury. *J Neurol Neurosurg Psychiatry.* **77(3)**, 363-6.

Smith, M.L., Auer, R.N., Siesjo, B.K. (1984). The density and distribution of ischemic brain injury in the rat following 2-10 min of forebrain ischemia. *Acta Neuropathol (Berl).* **64(4)**, 319-32.

Snipes, G.J., McGuire, C.B., Norden, J.J., Freeman, J.A. (1986). Nerve injury stimulates the secretion of apolipoprotein E by nonneuronal cells. *Proc Natl Acad Sci USA.* **83(4)**, 1130-4.

Snyder, E.Y., Deitcher, D.L., Walsh, C., Arnold-Aldea, S., Hartwieg, E.A., Cepko, C.L. (1992). Multipotent neural cell lines can engraft and participate in development of mouse cerebellum. *Cell.* **68(1)**, 33-51.

Soulié, C., Mitchell, V., Dupont-Wallois, L., Chartier-Harlin, M.C., Beauvillain, J.C., Delacourte, A., Caillet-Boudin, M.L. (1999). Synthesis of apolipoprotein E (ApoE) mRNA by human neuronal-type SK N SH-SY 5Y cells and its regulation by nerve growth factor and ApoE. *Neurosci Lett.* **265(2)**, 147-50.

Spoelgen, R., Hammes, A., Anzenberger, U., Zechner, D., Andersen, O.M., Jerchow, B., Willnow, T.E. (2005). LRP2/megalin is required for patterning of the ventral telencephalon. *Development.* **132(2)**, 405-14.

Stenevi, U., Bjorklund, A., Svendgaard, N.A. (1976). Transplantation of central and peripheral monoamine neurons to the adult rat brain, techniques and conditions for survival. *Brain Res.* **114(1)**, 1-20.

Stockinger, W., Hengstschlager-Ottnad, E., Novak, S., Matus, A., Huttinger, M., Bauer, J., Lassmann, H., Schneider, W.J., Nimpf, J. (1998). The low density lipoprotein receptor gene family. Differential expression of two alpha2-macroglobulin receptors in the brain. *J Biol Chem.* **273(48)**, 32213-21.

Stoll, G. & Muller, H.W. (1986). Macrophages in the peripheral nervous system and astroglia in the central nervous system of rat commonly express apolipoprotein E during development but differ in their response to injury. *Neurosci Lett.* **72(3)**, 233-8.

Stone, D.J., Rozovsky, I., Morgan, T.E., Anderson, C.P., Hajian, H., Finch, C.E. (1997). Astrocytes and microglia respond to estrogen with increased apoE mRNA in vivo and in vitro. *Exp Neurol.* **143(2)**, 313-8.

Strittmatter, W.J., Saunders, A.M., Schmechel, D., Pericak-Vance, M., Enghild, J., Salvesen, G.S., Roses, A.D. (1993). Apolipoprotein E, high-avidity binding to beta-amyloid and increased frequency of type 4 allele in late-onset familial Alzheimer disease. *Proc Natl Acad Sci USA.* **90(5)**, 1977-81.

Strittmatter, W.J., Weisgraber, K.H., Huang, D.Y., Dong, L.M., Salvesen, G.S., Pericak-Vance, M., Schmechel, D., Saunders, A.M., Goldgaber, D., Roses, A.D. (1993). Binding of human apolipoprotein E to synthetic amyloid beta peptide, isoform-specific effects and implications for late-onset Alzheimer disease. *Proc Natl Acad Sci USA.* **90(17)**, 8098-102.

Strittmatter, W.J., Saunders, A.M., Goedert, M., Weisgraber, K.H., Dong, L.M., Jakes, R., Huang, D.Y., Pericak-Vance, M., Schmechel, D., Roses, A.D. (1994). Isoform-specific interactions of apolipoprotein E with microtubule-associated protein tau, implications for Alzheimer disease. *Proc Natl Acad Sci USA.* **91(23)**, 11183-6.

Sudlow, C., Martinez Gonzalez, N.A., Kim, J., Clark, C. (2006). Does apolipoprotein E genotype influence the risk of ischemic stroke, intracerebral hemorrhage, or subarachnoid hemorrhage? Systematic review and meta-analyses of 31 studies among 5961 cases and 17,965 controls. *Stroke.* **37(2)**, 364-70.

Sun, Y., Wu, S., Bu, G., Onifade, M.K., Patel, S.N., LaDu, M.J., Fagan, A.M., Holtzman, D.M. (1998). Glial fibrillary acidic protein-apolipoprotein E (apoE) transgenic mice, astrocyte-specific expression and differing biological effects of astrocyte-secreted apoE3 and apoE4 lipoproteins. *J Neurosci.* **18(9)**, 3261-72.

Sun, Y.X., Wang, J., Shelburne, C.E., Lopatin, D.E., Chinnaiyan, A.M., Rubin, M.A., Pienta, K.J., Taichman, R.S. (2003). Expression of CXCR4 and CXCL12 (SDF-1) in human prostate cancers (PCa) in vivo. *J Cell Biochem.* **89(3)**, 462-73.

Suzuki, R., Yamaguchi, T., Kirino, T., Orzi, F., Klatzo, I. (1983). The effects of 5-minute ischemia in Mongolian gerbils, I. Blood-brain barrier, cerebral blood flow, and local cerebral glucose utilization changes. *Acta Neuropathol (Berl).* **60(3-4)**, 207-16.

Suzuki, R., Yamaguchi, T., Li, C.L., Klatzo, I. (1983). The effects of 5-minute ischemia in Mongolian gerbils, II. Changes of spontaneous neuronal activity in cerebral cortex and CA1 sector of hippocampus. *Acta Neuropathol (Berl).* **60(3-4)**, 217-22.

Swertfeger, D.K., Hui, D.Y. (2001). Apolipoprotein E receptor binding versus heparan sulfate proteoglycan binding in its regulation of smooth muscle cell migration and proliferation. *J Biol Chem.* **276(27)**, 25043-8.

Swertfeger, D.K., Bu, G., Hui, D.Y. (2002). Low density lipoprotein receptor-related protein mediates apolipoprotein E inhibition of smooth muscle cell migration. *J Biol Chem.* **277(6)**, 4141-6.

Takagi, Y., Nozaki, K., Takahashi, J., Yodoi, J., Ishikawa, M., Hashimoto, N. (1999). Proliferation of neuronal precursor cells in the dentate gyrus is accelerated after transient forebrain ischemia in mice. *Brain Res.* **831(1-2)**, 283-7.

Tang, J., Zhao, J., Zhao, Y., Wang, S., Chen, B., Zeng, W. (2003). Apolipoprotein E epsilon4 and the risk of unfavorable outcome after aneurysmal subarachnoid hemorrhage. *Surg Neurol.* **60(5)**, 391-6.

Tavor, S., Petit, I., Porozov, S., Avigdor, A., Dar, A., Leider-Trejo, L., Shemtov, N., Deutsch, V., Naparstek, E., Nagler, A., Lapidot, T. (2004). CXCR4 regulates migration and development of human acute myelogenous leukemia stem cells in transplanted NOD/SCID mice. *Cancer Res.* **64(8)**, 2817-24.

Teasdale, G.M., Nicoll, J.A., Murray, G., Fiddes, M. (1997). Association of apolipoprotein E polymorphism with outcome after head injury. *Lancet.* **350(9084)**, 1069-71.

Teramoto, T., Qiu, J., Plumier, J.C., Moskowitz, M.A. (2003). EGF amplifies the replacement of parvalbumin-expressing striatal interneurons after ischemia. *J Clin Invest.* **111(8)**, 1125-32.

Tesseur, I., Van Dorpe, J., Spittaels, K., Van den Haute, C., Moechars, D., Van Leuven, F. (2000). Expression of human apolipoprotein E4 in neurons causes hyperphosphorylation of protein tau in the brains of transgenic mice. *Am J Pathol.* **156(3)**, 951-64.

Teter, B., Xu, P.T., Gilbert, J.R., Roses, A.D., Galasko, D., Cole, G.M. (1999). Human apolipoprotein E isoform-specific differences in neuronal sprouting in organotypic hippocampal culture. *J Neurochem.* **73(6)**, 2613-6.

Thaker, U., McDonagh, A.M., Iwatsubo, T., Lendon, C.L., Pickering-Brown, S.M., Mann, D.M. (2003). Tau load is associated with apolipoprotein E genotype and the amount of amyloid beta protein, Abeta40, in sporadic and familial Alzheimer's disease. *Neuropathol Appl Neurobiol.* **29(1)**, 35-44.

Thilmann, R., Xie, Y., Kleihues, P., Kiessling, M. (1986). Persistent inhibition of protein synthesis precedes delayed neuronal death in postischemic gerbil hippocampus. *Acta Neuropathol (Berl).* **71(1-2)**, 88-93.

Thompson, W.G. (1890). Successful brain grafting. *NY. Med. J.* **51**, 701-702.

Thomson, J.A., Itskovitz-Eldor, J., Shapiro, S.S., Waknitz, M.A., Swiergiel, J.J., Marshall, V.S., Jones, J.M. (1998). Embryonic stem cell lines derived from human blastocysts. *Science.* **282(5391)**, 1145-7.

Toda, H., Takahashi, J., Iwakami, N., Kimura, T., Hoki, S., Mozumi-Kitamura, K., Ono, S., Hashimoto, N. (2001). Grafting neural stem cells improved the impaired spatial recognition in ischemic rats. *Neurosci Lett.* **316(1)**, 9-12.

Tonchev, A.B., Yamashima, T., Sawamoto, K., Okano, H. (2005). Enhanced proliferation of progenitor cells in the subventricular zone and limited neuronal production in the striatum and neocortex of adult macaque monkeys after global cerebral ischemia. *J Neurosci Res.* **81(6)**, 776-88.

Tran, P.B., Ren, D., Veldhouse, T.J., Miller, R.J. (2004). Chemokine receptors are expressed widely by embryonic and adult neural progenitor cells. *J Neurosci Res.* **76(1)**, 20-34.

Treger, I., Froom, P., Ring, H., Friedman, G. (2003). Association between apolipoprotein E4 and rehabilitation outcome in hospitalized ischemic stroke patients. *Arch Phys Med Rehabil.* **84(7)**, 973-6.

Trommer, B.L., Shah, C., Yun, S.H., Gamkrelidze, G., Pasternak, E.S., Ye, G.L., Sotak, M., Sullivan, P.M., Pasternak, J.F., LaDu, M.J. (2004). ApoE isoform affects LTP in human targeted replacement mice. *Neuroreport.* **15(17)**, 2655-8.

Trommsdorff, M., Gotthardt, M., Hiesberger, T., Shelton, J., Stockinger, W., Nimpf, J., Hammer, R.E., Richardson, J.A., Herz, J. (1999). Reeler/Disabled-like disruption of neuronal migration in knockout mice lacking the VLDL receptor and ApoE receptor 2. *Cell.* **97(6)**, 689-701.

Uchino, H., Elmer, E., Uchino, K., Lindvall, O., Siesjo, B.K. (1995). Cyclosporin A dramatically ameliorates CA1 hippocampal damage following transient forebrain ischaemia in the rat. *Acta Physiol Scand.* **155(4)**, 469-71.

Utermann, G., Hees, M., Steinmetz, A. (1977). Polymorphism of apolipoprotein E and occurrence of dysbetalipoproteinaemia in man. *Nature.* **269(5629)**, 604-7.

van Praag, H., Kempermann, G., Gage, F.H. (1999). Running increases cell proliferation and neurogenesis in the adult mouse dentate gyrus. *Nat Neurosci.* **2(3)**, 266-70.

van Praag, H., Shubert, T., Zhao, C., Gage, F.H. (2005). Exercise enhances learning and hippocampal neurogenesis in aged mice. *J Neurosci.* **25(38)**, 8680-5.

van Ree, J.H., van den Broek, W.J., Dahlmans, V.E., Groot, P.H., Vidgeon-Hart, M., Frants, R.R., Wieringa, B., Havekes, L.M., Hofker, M.H. (1994). Diet-induced hypercholesterolemia and atherosclerosis in heterozygous apolipoprotein E-deficient mice. *Atherosclerosis.* **111(1)**, 25-37.

Veinbergs, I., Jung, M.W., Young, S.J., Van Uden, E., Groves, P.M., Masliah, E. (1998). Altered long-term potentiation in the hippocampus of apolipoprotein E-deficient mice. *Neurosci Lett.* **249(2-3)**, 71-4.

Veizovic, T., Beech, J.S., Stroemer, R.P., Watson, W.P., Hodges, H. (2001). Resolution of stroke deficits following contralateral grafts of conditionally immortal neuroepithelial stem cells. *Stroke.* **32(4)**, 1012-9.

Vilhardt, F. (2005). Microglia: phagocyte and glia cell. *Int J Biochem Cell Biol.* **37(1)**, 17-21.

Virley, D., Ridley, R.M., Sinden, J.D., Kershaw, T.R., Harland, S., Rashid, T., French, S., Sowinski, P., Gray, J.A., Lantos, P.L., Hodges, H. (1999). Primary CA1 and conditionally immortal MHP36 cell grafts restore conditional discrimination learning and recall in marmosets after excitotoxic lesions of the hippocampal CA1 field. *Brain.* **122 (Pt 12)**, 2321-35.

Vogel, T., Guo, N.H., Guy, R., Drezlich, N., Krutzsch, H.C., Blake, D.A., Panet, A., Roberts, D.D. (1994). Apolipoprotein E, a potent inhibitor of endothelial and tumor cell proliferation. *J Cell Biochem.* **54(3)**, 299-308.

Ware, M.L., Fox, J.W., Gonzalez, J.L., Davis, N.M., Lambert de Rouvroit, C., Russo, C.J., Chua, S.C. Jr., Goffinet, A.M., Walsh, C.A. (1997). Aberrant splicing of a mouse disabled homolog, mdab1, in the scrambler mouse. *Neuron.* **19(2)**, 239-49.

Watson, D.J., Longhi, L., Lee, E.B., Fulp, C.T., Fujimoto, S., Royo, N.C., Passini, M.A., Trojanowski, J.Q., Lee, V.M., McIntosh, T.K., Wolfe, J.H. (2003). Genetically modified NT2N human neuronal cells mediate long-term gene expression as CNS grafts in vivo and improve functional cognitive outcome following experimental traumatic brain injury. *J Neuropathol Exp Neurol.* **62(4)**, 368-80.

Weeber, E.J., Beffert, U., Jones, C., Christian, J.M., Forster, E., Sweatt, J.D., Herz, J. (2002). Reelin and ApoE receptors cooperate to enhance hippocampal synaptic plasticity and learning. *J Biol Chem.* **277(42)**, 39944-52.

Wei, L., Cui, L., Snider, B.J., Rivkin, M., Yu, S.S., Lee, C.S., Adams, L.D., Gottlieb, D.I., Johnson, E.M. Jr, Yu, S.P., Choi, D.W. (2005). Transplantation of embryonic stem cells overexpressing Bcl-2 promotes functional recovery after transient cerebral ischemia. *Neurobiol Dis.* **19(1-2)**, 183-93.

Weigl, M., Tenze, G., Steinlechner, B., Skhirtladze, K., Reining, G., Bernardo, M., Pedicelli, E., Dworschak, M. (2005). A systematic review of currently available pharmacological neuroprotective agents as a sole intervention before anticipated or induced cardiac arrest. *Resuscitation.* **65(1)**, 21-39.

Weiss, M.L., Mitchell, K.E., Hix, J.E., Medicetty, S., El-Zarkouny, S.Z., Grieger, D., Troyer, D.L. (2003). Transplantation of porcine umbilical cord matrix cells into the rat brain. *Exp Neurol.* **182(2)**, 288-99.

Wennersten, A., Holmin, S., Al Nimer, F., Meijer, X., Wahlberg, L.U., Mathiesen, T. (2006). Sustained survival of xenografted human neural stem/progenitor cells in experimental brain trauma despite discontinuation of immunosuppression. *Exp Neurol.* **199(2)**, 339-47.

Wenning, G.K., Odin, P., Morrish, P., Rehncrona, S., Widner, H., Brundin, P., Rothwell, J.C., Brown, R., Gustavii, B., Hagell, P., Jahanshahi, M., Sawle, G., Bjorklund, A., Brooks, D.J., Marsden, C.D., Quinn, N.P., Lindvall, O. (1997). Short- and long-term survival and function of unilateral intrastriatal dopaminergic grafts in Parkinson's disease. *Ann Neurol.* **42(1)**, 95-107.

Wetterau, J.R., Aggerbeck, L.P., Rall, S.C. Jr, Weisgraber, K.H. (1988). Human apolipoprotein E3 in aqueous solution. I. Evidence for two structural domains. *J Biol Chem.* **263(13)**, 6240-8.

White, F., Nicoll, J.A., Roses, A.D., Horsburgh, K. (2001). Impaired neuronal plasticity in transgenic mice expressing human apolipoprotein E4 compared to E3 in a model of entorhinal cortex lesion. *Neurobiol Dis.* **8(4)**, 611-25.

Whittemore, S.R. & White, L.A. (1993). Target regulation of neuronal differentiation in a temperature-sensitive cell line derived from medullary raphe. *Brain Res.* **615(1)**, 27-40.

Whittemore, S.R., Onifer, S.M. (2000). Immortalized neural cell lines for CNS transplantation. *Prog Brain Res.* **127**, 49-65.

Widner, H., Brundin, P. (1988). Immunological aspects of grafting in the mammalian central nervous system. A review and speculative synthesis. *Brain Res.* **472(3)**, 287-324.

Wiles, M.V., Keller, G. (1991). Multiple hematopoietic lineages develop from embryonic stem (ES) cells in culture. *Development.* **111(2)**, 259-67.

Willnow, T.E., Hilpert, J., Armstrong, S.A., Rohlmann, A., Hammer, R.E., Burns, D.K., Herz, J. (1996). Defective forebrain development in mice lacking gp330/megalin. *Proc Natl Acad Sci USA.* **93(16)**, 8460-4.

Wilson, C., Wardell, M.R., Weisgraber, K.H., Mahley, R.W., Agard, D.A. (1991). Three-dimensional structure of the LDL receptor-binding domain of human apolipoprotein E. *Science.* **252(5014)**, 1817-22.

Wisniewski, T., Frangione, B. (1992). Apolipoprotein E, a pathological chaperone protein in patients with cerebral and systemic amyloid. *Neurosci Lett.* **135(2)**, 235-8.

Wolf, B.B., Lopes, M.B., VandenBerg, S.R., Gonias, S.L. (1992). Characterization and immunohistochemical localization of alpha 2-macroglobulin receptor (low-density lipoprotein receptor-related protein) in human brain. *Am J Pathol.* **141(1)**, 37-42.

Wong, A.M., Hodges, H., Horsburgh, K. (2005). Neural stem cell grafts reduce the extent of neuronal damage in a mouse model of global ischaemia. *Brain Res.* **1063(2)**, 140-50.

Woo, D., Sauerbeck, L.R., Kissela, B.M., Khoury, J.C., Szaflarski, J.P., Gebel, J., Shukla, R., Pancioli, A.M., Jauch, E.C., Menon, A.G., Deka, R., Carrozzella, J.A., Moomaw, C.J., Fontaine, R.N., Broderick, J.P. (2002). Genetic and environmental risk factors for intracerebral hemorrhage, preliminary results of a population-based study. *Stroke.* **33(5)**, 1190-5.

Woo, D., Kaushal, R., Chakraborty, R., Woo, J., Haverbusch, M., Sekar, P., Kissela, B., Pancioli, A., Jauch, E., Kleindorfer, D., Flaherty, M., Schneider, A., Khatri, P., Sauerbeck, L., Khoury, J., Deka, R., Broderick, J. (2005). Association of apolipoprotein E4 and haplotypes of the apolipoprotein E gene with lobar intracerebral hemorrhage. *Stroke.* **36(9)**, 1874-9.

Xia, Z., Dickens, M., Raingeaud, J., Davis, R.J., Greenberg, M.E. (1995). Opposing effects of ERK and JNK-p38 MAP kinases on apoptosis. *Science.* **270(5240)**, 1326-31.

Xu, P.T., Schmechel, D., Rothrock-Christian, T., Burkhart, D.S., Qiu, H.L., Popko, B., Sullivan, P., Maeda, N., Saunders, A.M., Roses, A.D., Gilbert, J.R. (1996). Human apolipoprotein E2, E3, and E4 isoform-specific transgenic mice, human-like pattern of glial and neuronal immunoreactivity in central nervous system not observed in wild-type mice. *Neurobiol Dis.* **3(3)**, 229-45.

Xu, P.T., Gilbert, J.R., Qiu, H.L., Rothrock-Christian, T., Settles, D.L., Roses, A.D., Schmechel, D.E. (1998). Regionally specific neuronal expression of human APOE gene in transgenic mice. *Neurosci Lett.* **246(2)**, 65-8.

Xu, P.T., Gilbert, J.R., Qiu, H.L., Ervin, J., Rothrock-Christian, T.R., Hulette, C., Schmechel, D.E. (1999). Specific regional transcription of apolipoprotein E in human brain neurons. *Am J Pathol.* **154(2)**, 601-11.

Yamauchi, J., Chan, J.R., Shooter, E.M. (2003). Neurotrophin 3 activation of TrkC induces Schwann cell migration through the c-Jun N-terminal kinase pathway. *Proc Natl Acad Sci USA.* **100(24)**, 14421-6.

Yan, J., Xu, L., Welsh, A.M., Chen, D., Hazel, T., Johe, K., Koliatsos, V.E. (2006). Combined immunosuppressive agents or CD4 antibodies prolong survival of human neural stem cell grafts and improve disease outcomes in amyotrophic lateral sclerosis transgenic mice. *Stem Cells.* **24(8)**, 1976-85.

Yang, G., Kitagawa, K., Ohtsuki, T., Kuwabara, K., Mabuchi, T., Yagita, Y., Takazawa, K., Tanaka, S., Yanagihara, T., Hori, M., Matsumoto, M. (2000). Regional difference of neuronal vulnerability in the murine hippocampus after transient forebrain ischemia. *Brain Res.* **870(1-2)**, 195-8.

Yang, M., Stull, N.D., Berk, M.A., Snyder, E.Y., Iacovitti, L. (2002). Neural stem cells spontaneously express dopaminergic traits after transplantation into the intact or 6-hydroxydopamine-lesioned rat. *Exp Neurol.* **177(1)**, 50-60.

Zannis, V.I. & Breslow, J.L. (1981). Human very low density lipoprotein apolipoprotein E isoprotein polymorphism is explained by genetic variation and posttranslational modification. *Biochemistry.* **20(4)**, 1033-41.

Zannis,V.I., Just, P.W., Breslow, J.L. (1981). Human apolipoprotein E isoprotein subclasses are genetically determined. *Am J Hum Genet.* **33(1)**, 11-24.

Zeleny, M., Swertfeger, D.K., Weisgraber, K.H., Hui, D.Y. (2002). Distinct apolipoprotein E isoform preference for inhibition of smooth muscle cell migration and proliferation. *Biochemistry.* **41(39)**, 11820-3.

Zhang, R.L., Zhang, Z.G., Zhang, L., Chopp, M. (2001). Proliferation and differentiation of progenitor cells in the cortex and the subventricular zone in the adult rat after focal cerebral ischemia. *Neuroscience.* **105(1)**, 33-41.

Zhang, S.H., Reddick, R.L., Burkey, B., Maeda, N. (1994). Diet-induced atherosclerosis in mice heterozygous and homozygous for apolipoprotein E gene disruption. *J Clin Invest.* **94(3)**, 937-45.

Zhou, Y., Larsen, P.H., Hao, C., Yong, V.W. (2002). CXCR4 is a major chemokine receptor on glioma cells and mediates their survival. *J Biol Chem.* **277(51)**, 49481-7.

Zhu, Y., Hui, D.Y. (2003). Apolipoprotein E binding to low density lipoprotein receptor-related protein-1 inhibits cell migration via activation of cAMP-dependent protein kinase A. *J Biol Chem.* **278(38)**, 36257-63.

Publications

Wong, A.M., Hodges, H., Horsburgh, K. (2004). Characterisation of neural stem cell grafts in a mouse model of global ischaemia. *Society for Neuroscience Abstract 34th Annual Meeting*.

McColl, B.W., **Wong, A.M.,** McGregor, A., Harris, J.D., Dickson, G., Amalfitano, A., Magnoni, S., Baker, A., Horsburgh, K. (2004). Adenoviral overexpression of apolipoprotein E3 protects against neuronal injury following focal cerebral ischaemia in mice. *Society for Neuroscience Abstract 34th Annual Meeting*.

Wong, A.M., Hodges, H., Horsburgh, K. (2005). Influences of apolipoprotein E on neural stem cell grafts in a mouse model of global ischaemia. *British Neuroscience Association Abstract 18th National Meeting.*

Wong, A.M., Hodges, H., Horsburgh, K. (2005). Neural stem cell grafts reduce the extent of neuronal damage in a mouse model of global ischaemia. *Brain Res.* **1063(2)**, 140-50.

McColl, B.W., McGregor, A.L., **Wong, A.,** Harris, J.D., Amalfitano, A., Magnoni, S., Baker, A.H., Dickson, G., Horsburgh, K. (2006). APOE varepsilon3 gene transfer attenuates brain damage after experimental stroke. *J Cereb Blood Flow Metab.* **27(3)**, 477-87.

Appendix: Solutions and recipes

Poly-L-lysine Slides

Slides were placed in racks and soaked in poly-L-Lysine (0.1% solution, Sigma, UK) for 5 minutes. Slides were then dried overnight at room temperature or in an oven at 60^{o}C for 2 hours. The poly-L-Lysine solution was stored in a sealed container at 4^{o}C and used to coat up to 1000 glass slides.

10x Phosphate Buffer (PB)

2.57g of NaH_2PO_4 and 11.95g of Na_2HPO_4 were dissolved and made up to 1L with distilled water. For 10X Phosphate Buffered Saline (PBS) 86.67g of NaCl was added and the solution pH adjusted to 7.4. Both 10X Solutions were filtered prior to storage. 10X PB was stored at 4^{o}C, whilst 10X PBS was stored at room temperature.

Paraformaldehyde Fixative 4% (PAM)

40g of paraformaldehyde (weighed in the fumehood) was added to 900ml of 1xPB which had been heated to 60-65^{o}C. The temperature was maintained between 60^{o}C and 65^{o}C until the paraformaldehyde dissolved. The solution was allowed to cool, made up to 1L with PB and filtered for purity.

Citric Acid Buffer

2.1g of citric acid was dissolved in 1L of distilled water. The pH was adjusted to 6.0 by the addition of 1M NaOH.

Acrylamide Gel Solutions
(To make 2 gels for a Mini PROTEAN-II system):

	Resolving Gel (10%)	Stacking Gel (4%)
Distilled Water	9.1 ml	7.1 ml
1.5mM Tris pH 8.8	5 ml	-
0.5mM Tris pH 6.8	-	2.5 ml
10% SDS	200 μl	100 μl
30% Acrylamide	6.6 ml	1.3 ml
10% APS	100 μl	50 μl
TEMED	10 μl	10 μl

10x SDS-PAGE Running Buffer

30g of Tris-Base, 144g of glycine, and 10g of SDS were fully dissolved in 1L of distilled water. The final solution was adjusted to pH 8.3.

Western Transfer Buffer

16.66g of Tris-Base and 79.2g of glycine were fully dissolved in 4.4L of distilled water. Immediately prior to use 1.1L of methanol was added to the solution, to give a final volume of 5.5L.

Modified RIPA Buffer

790 mg of Tris-Base was added to 75 ml distilled water. 900 mg of NaCl was then added and the solution stirred until all solids were dissolved. The pH was adjusted to 7.4 with HCL. 10ml of 10% NP-40 was then added to the solution, followed by 2.5ml of 10% Na-deoxycholate and the solution stirred until it became clear. 1ml of 100mM EDTA was then added to the solution and the total volume of the solution adjusted to 100ml with distilled water. This modified RIPA buffer was stored at $4^{o}C$ until ready for use. Immediately prior to use, one Complete protease inhibitor tablet (Roche) was dissolved to 25ml of ice-cold modified RIPA buffer.